Roman Lucrezi, BSc

Equation of Motion for Non-Equilibrium Green's Functions in the Interacting Resonant Level Model

MASTER'S THESIS

to achieve the academic degree of
Diplom-Ingenieur

Master's degree programme: Technical Physics

submitted to
Graz University of Technology

Supervisor
Univ.-Prof. Dipl.-Phys. Dr.rer.nat. Wolfgang von der Linden

Institute of Theoretical and Computational Physics

Graz, September 2019

Affidavit

I declare that I have authored this thesis independently, that I have not used other than the declared sources/resources, and that I have explicitly indicated all material which has been quoted either literally or by content from the sources used. The text document uploaded to TUGRAZonline is identical to the present master's thesis.

Date	Signature

Eidesstattliche Erklärung

Ich erkläre an Eides statt, dass ich die vorliegende Arbeit selbstständig verfasst, andere als die angegebenen Quellen/Hilfsmittel nicht benutzt, und die den benutzten Quellen wörtlich und inhaltlich entnommenen Stellen als solche kenntlich gemacht habe. Das in TUGRAZonline hochgeladene Textdokument ist mit der vorliegenden Masterarbeit identisch.

Datum	Unterschrift

Abstract

The equation-of-motion technique for Green's functions has been used widely and successfully in quantum-mechanical systems in equilibrium. With the ever decreasing size of electronic devices, though, the importance of non-equilibrium properties, such as current-voltage characteristics, of strongly correlated molecular electronic devices increases.

The aim of this thesis is to examine the method in its non-equilibrium formulation in order to gain a better understanding for future research on this topic.

Therefore, the equation of motion for non-equilibrium Green's functions is derived in detail in the framework of path-ordering for both the two-time domain and, for steady-state solutions, the frequency domain. In addition to the usual form, an alternative expression is presented.

The steady-state equations are then applied to a benchmark model out of equilibrium, namely the interacting resonant level model (IRLM), where first self-consistent analytical solutions are obtained within a mean-field approximation. Numerical results for different parameter sets are achieved in good agreement with the literature.

Eventually, the examination is extended to include higher correlations of distinct orders and alternative approximation schemes. Special attention is paid to the intricacies of arising symmetry violations as well as to their restoration. Numerical results are shown for each approach.

Kurzfassung

Der Bewegungsgleichungsformalismus für Green-Funktionen hat bisher bei quantenmechanischen Systemen im Gleichgewicht erfolgreich Anwendung gefunden. Durch immer kleiner werdende elektronische Geräte werden allerdings Nichtgleichgewichtseigenschaften wie Strom-Spannungskurven stark korrelierter molekularer Systeme immer wichtiger.

Ziel dieser Arbeit ist es daher, die Methode in der entsprechenden Nichtgleichgewichtsformulierung zu untersuchen, um für zukünftige Forschung zu diesem Thema ein besseres Verständnis zu erlangen.

Dazu wird erst im Rahmen der Pfadordnung die Bewegungsgleichung für Green-Funktionen im Nichtgleichgewicht sowohl im Zweizeitbereich als auch für Steady-State-Lösungen im Frequenzbereich detailliert hergeleitet. Zusätzlich zu der üblichen Form wird ein alternativer Ausdruck präsentiert.

Die Steady-State-Gleichungen werden dann auf das Interacting-Resonant-Level-Modell (IRLM) als Benchmark-Modell im Nichtgleichgewicht angewandt, wobei erste selbstkonsistente analytische Lösungen durch eine Mean-Field-Näherung erhalten werden. Für verschiedene Parametersätze werden in guter Übereinstimmung mit Literaturwerten numerische Ergebnisse erzielt.

Schließlich wird die Analyse um höhere Korrelationen verschiedener Ordnungen und alternative Näherungsschemata erweitert. Besonderes Augenmerk wird auf die Komplikationen auftretender Symmetrieverletzungen sowie deren Wiederherstellung gelegt. Ausgewählte numerische Ergebnisse werden für jeden Ansatz präsentiert.

Ἀλλὰ τἀληθὲς λέγεις, ἦ δ᾽ ὃς ὁ Διμπλόδωρος ἀναπνεύσας τι. καλὸν γάρ τοί ἐστι δεινὸν δ᾽ ἅμα· δεῖ οὖν χρῆσθαι αὐτῷ πολλῆς μετ᾽ εὐλαβείας.

— Τζόαν Κ. Ῥόουλινγκ,
Ἄρειος Ποτὴρ καὶ ἡ τοῦ φιλοσόφου λίθος

Acknowledgement

To begin with, I would like to thank my supervisor Wolfgang von der Linden for giving me the opportunity to investigate an exciting topic in the realm of non-equilibrium quantum mechanics. I was free to pursue my own strategies and received the right food for thought where it was needed.

An important aspect of scientific work is certainly the common exchange of thoughts, for which I wish to present my special thanks to my colleagues Gerhard Dorn, Delia Fugger, Andrei Man, Richard Meister, Alexander Schossmann, Irakli Titvinidze, and further Patrick Lainer, who can solve even the most intricate typesetting problems, and Max Sorantin, who encouraged me to publish part of my work together with him.

I want to express my sincere appreciation to my friends and deskmates Sebastian Gotthardt, Michael Seidl and René Vötter. Our conversations and discussions over the past few years went far beyond our courses, opened up unsolvable questions, but also led to big epiphanies.

My profound gratitude goes to my parents, who always supported me in my decisions and who sometimes enjoyed my achievements even more than I did.

Writing a thesis can be a very intense process that does not necessarily stop – at least mentally – when you leave the desk and call it a day. My deeply felt thanks therefore go to Michi. She probably perceived this the most, but still supported me in every possible way.

Preliminary Remarks

Units

Throughout this thesis, the reduced Planck constant $\hbar$ and the Boltzmann constant k_B equal

$$\hbar = k_\mathrm{B} = 1.$$

As a consequence, the dimension[I] of the angular frequency ω used in the Fourier transform and the dimension of temperature become both equal to energy, i.e.

$$[T] \leftarrow [k_\mathrm{B} T] = \mathsf{E} = [\hbar\omega] \rightarrow [\omega]\,,$$

the dimension of time becomes equal to an inverse energy

$$\mathsf{E}^{-1} = \left[t\hbar^{-1}\right] \rightarrow [t]\,,$$

and so especially the dimension of electric current becomes equal to charge times energy

$$[I] = \mathsf{Q}\,[t]^{-1} \rightarrow \mathsf{QE}.$$

Nomenclature

$\langle\langle A;B\rangle\rangle$ without a superscript refers always to a retarded or advanced Green's function, where the argumentation or equation is valid for both. Operator hats for A and B are only used in the opening sections to familiarize the reader with the symbols.

$\langle\langle A;B\rangle\rangle^{\varkappa}$ with any superscript $\varkappa$ but no direct variable dependence in the operators, which would be shown in brackets like in $A(t)$, refers to the Fourier-transform with respect to ω.

G is used for Green's functions in general, superscripts and variable dependence is indicated if needed.

Some technical terms are shown in italics (mostly) on first appearance.

Abbreviations

NEGF:	Non-equilibrium Green's function
(N)EQ:	(Non)-equilibrium
TB:	Tight-binding
WBL(*):	Wide-band limit (in higher truncation levels)
HF:	Hartree-Fock
IRLM:	Interacting Resonant Level Model
EoM:	Equation of motion

[I] *Dimension* denotes here the dimension of the physical quantity and is represented by sans-serif letters.

Contents

List of Figures

1. Introduction

In many-body physics, Green's functions are a very general and powerful tool for the calculation of observables in a quantum mechanical system. More precisely, different types of *two-point*[I] Green's functions G are used throughout this thesis, which are proportional to quantum mechanical correlation functions of two general operators $\hat{A}$ and $\hat{B}$ at times t_1 and t_2, so

$$G_{AB}(t_1, t_2) \propto \left\langle \hat{A}(t_1)\hat{B}(t_2) \right\rangle ,$$

and thus grant access to measurable quantities of the system under investigation, such as a density of states or general expectation values.

The calculation of such Green's functions is often performed with the help of the self-energy in the *Dyson*-equation framework (cf. section 4.3 in [1]), but another approach shall be considered here, which has brought success in equilibrium situations: The equation-of-motion method, which can easily provide exact solutions to quadratic Hamiltonians (cf. section 3.2 in [2]) and which has been successful especially in the treatment of the Kondo effect (e.g. [3], [4], [5]).

Inspired by the equilibrium results, the aim of this thesis is to investigate the equation-of-motion method in its non-equilibrium formulation in order to investigate dynamic quantities of a quantum mechanical system, such as the current, and to gain a better understanding for future research on this topic. This formulation allows for a direct calculation of the type of Green's functions that determines steady-state expectation values, namely the so-called *lesser* Green's function:

$$\left\langle \hat{B}\hat{A} \right\rangle \propto G^{<}_{AB}(t_1 - t_2) = G^{<}_{AB}(0)$$

An essential steady-state observable in non-equilibrium physics is the current flowing in a system, i.e. the transport of charge carriers from one region of the system to another. Quantitatively, this can be described by the change in total electron number in a region x,

$$I_x = -e \left\langle \frac{\mathrm{d}\hat{N}_x}{\mathrm{d}t} \right\rangle , \tag{1.0.1}$$

where an electron carries the charge of $-e$, resulting in an outgoing current (negative change in total electron number) to be positive.

After this brief motivation, the interested reader should bring a basic understanding for the second-quantization formalism[II] from here on, but will further be guided through this thesis step-by-step with the following structure and will hopefully be motivated to try it out for themself.

[I] n-point generalizations are especially used in relativistic quantum field theory.

[II] In many-body physics, Green's functions may also be used to describe spin systems, where themselves are described by spin operators, (see e.g. [6]), however, this thesis is completely restricted to the formalism of second quantization. Hence, all occurring operators are products of creation- and annihilation operators.

In the beginning, a short overview of the equation-of-motion technique and its limitations to the equilibrium case are given. Starting from a very general definition for expectation values, an expression for a time-ordered Green's function is found which is the basis for the derivation of the equation of motion. The resulting equation is represented as a set of integral equations that are further transformed to algebraic equations for steady-state solutions.

The application of these equations is shown throughout the thesis using the *interacting resonant level model* which is introduced including its symmetries, possible current definitions, coupling to different environments, and the basic equations resulting from the equation of motion.

The interaction – which is the hard part in first place – is treated in a first mean-field approximation, leading to closed solutions that are evaluated analytically and numerically for two different environments in order to obtain quantitative results.

Finally, the equations are extended to include higher Green's functions, where special attention is paid to arising symmetry violations that lead to unphysical results. A symmetry restoration is discussed and applied, which ultimately leads to reasonable numerical results for different orders.

2. Equation of Motion for Non-Equilibrium Green's Functions

In this chapter, the framework of non-equilibrium Green's functions is set up in the detailed derivation of their equation of motion. Its Fourier transform as well as more convenient forms are presented.

However, before plunging into the non-equilibrium formalism it seems reasonable to recap the equation-of-motion technique for equilibrium systems. The central objects are the fermionic[I] two-time *retarded* (R) and *advanced* (A) Green's functions

$$\begin{aligned} G^{\mathrm{R}}_{AB}(t_a, t_b) &\equiv \langle\langle A(t_a); B(t_b)\rangle\rangle^{\mathrm{R}} := -i\Theta\left(t_a - t_b\right)\left\langle\left\{\hat{A}(t_a), \hat{B}(t_b)\right\}\right\rangle \\ G^{\mathrm{A}}_{AB}(t_a, t_b) &\equiv \langle\langle A(t_a); B(t_b)\rangle\rangle^{\mathrm{A}} := +i\Theta\left(t_b - t_a\right)\left\langle\left\{\hat{A}(t_a), \hat{B}(t_b)\right\}\right\rangle, \end{aligned} \tag{2.0.1}$$

where $\hat{A}(t_a)$ and $\hat{B}(t_b)$ are some general operators in second quantization, $\Theta(t)$ is the Heaviside step function, $\langle \ldots \rangle$ denotes the expectation value with respect to some general ensemble, and the curly braces denote the anticommutator

$$\left\{\hat{A}, \hat{B}\right\} := \hat{A}\hat{B} + \hat{B}\hat{A}.$$

The functional dependence of a Green's function $G(t_a, t_b)$ is in general of two independent time variables t_a and t_b, but in equilibrium this simplifies to a single-variable function in time difference $t_a - t_b$, so

$$G(t_a, t_b) \overset{\mathrm{EQ}}{\to} G(t_a - t_b).$$

As shown later (cf. equation (2.0.5)), it is convenient to work in Fourier space[II] with respect to time difference, which is obtained by

$$G(\omega) := \int_{-\infty}^{\infty} \mathrm{d}(t_a - t_b)\, \mathrm{e}^{i\omega(t_a - t_b)} G(t_a - t_b).$$

Note the convention on normalization and frequency sign. In the full notation Fourier space is indicated by a subscript, as in

$$\langle\langle A(t_a); B(t_b)\rangle\rangle \overset{\mathrm{FT}}{\to} \langle\langle A; B\rangle\rangle_{\omega},$$

or simply by the loss of explicit variable dependence in the operators. In order to obtain quantitative results from this theory, the Green's functions defined above need to be linked to measurable physical quantities (observables), which can be done via the spectral function

$$A_{AB}(\omega) := \frac{1}{2\pi i}\left(G^{\mathrm{A}}_{AB}(\omega) - G^{\mathrm{R}}_{AB}(\omega)\right)$$

[I] For bosonic systems it is more convenient to choose the commutator.

[II] Which is here equivalent to energy space as $\hbar = 1$.

that acts like a generalized density of states. As the distribution function for fermionic systems in equilibrium at temperature T and chemical potential μ is known, namely the Fermi function $f(\omega;\mu,T)$, expectation values can be obtained by the integral

$$\left\langle B^\dagger A \right\rangle = \int_{-\infty}^{\infty} \mathrm{d}\omega\, f(\omega;\mu,T) A_{AB}(\omega), \tag{2.0.2}$$

where

$$f(\omega;\mu,T) := \frac{1}{\mathrm{e}^{\beta(\omega-\mu)}+1}$$

and $\beta = T^{-1}$ is the inverse temperature as $k_\mathrm{B} = 1$.

The well-known equation of motion for retarded and advanced Green's functions is now easily obtained from the *Heisenberg* equation for operators (see, e.g., chapter 3.2 in [7]). It is formally the same for both functions and reads

$$i\frac{\partial}{\partial t_a}\langle\langle A(t_a);B(t_b)\rangle\rangle^{\mathrm{R/A}} = \delta(t_a-t_b)\left\langle\left\{\hat{A}(t_a),\hat{B}(t_b)\right\}\right\rangle + \langle\langle [A,H](t_a);B(t_b)\rangle\rangle^{\mathrm{R/A}}, \tag{2.0.3}$$

where $\delta(t)$ is the Dirac delta distribution that comes from the derivative of the step function and the square-bracket term denotes the equal-time commutator

$$[A,H](t_a) \equiv \left[\hat{A}(t_a),\hat{H}(t_a)\right] := \hat{A}(t_a)\hat{H}(t_a) - \hat{H}(t_a)\hat{A}(t_a)$$

with the system Hamiltonian H. The retarded and advanced functions are explicitly obtained for the boundary conditions

$$\begin{aligned} \langle\langle A(t_a);B(t_b)\rangle\rangle^{\mathrm{R}} &= 0 \quad \text{for} \quad t_a < t_b \\ \langle\langle A(t_a);B(t_b)\rangle\rangle^{\mathrm{A}} &= 0 \quad \text{for} \quad t_a > t_b. \end{aligned} \tag{2.0.4}$$

In general, the commutator produces a linear combination of new operators, that may be higher products of creation- and annihilation operators. Thus, the second term in equation (2.0.3) produces a linear combination of new Green's functions, for which the same equation of motion can be applied. Transforming the differential equation into Fourier space reduces the problem to the algebraic equation

$$\omega\langle\langle A;B\rangle\rangle_\omega^{\mathrm{R/A}} = \left\langle\left\{\hat{A},\hat{B}\right\}\right\rangle + \langle\langle [A,H];B\rangle\rangle_\omega^{\mathrm{R/A}} \tag{2.0.5}$$

with boundary conditions

$$\omega \to \omega \pm i\eta \quad \text{for} \quad \langle\langle A(t_a);B(t_b)\rangle\rangle_\omega^{\mathrm{R/A}},$$

where the limit $\eta \to 0^+$ is intended. This algebraic form gives rise to a linear set of equations that is in principle easy to solve.

As seen later, it turns out that the equation of motion for retarded (or advanced) Green's functions are the same in a non-equilibrium situation, however, the relation to expectation values is lost as there is no general simple distribution function describing non-equilibria. Expectation values (= equal-time correlations) have to be calculated directly from correlation functions instead. They are usually defined as *lesser* ($<$) and *greater* ($>$) Green's functions:

$$\begin{aligned} \langle\langle A(t_a);B(t_b)\rangle\rangle^{<} &:= +i\left\langle\hat{B}(t_b)\hat{A}(t_a)\right\rangle \\ \langle\langle A(t_a);B(t_b)\rangle\rangle^{>} &:= -i\left\langle\hat{A}(t_a)\hat{B}(t_b)\right\rangle. \end{aligned} \tag{2.0.6}$$

A naive application of the *Heisenberg* equation in order to obtain a direct equation of motion for the correlation functions, namely

$$i\frac{\partial}{\partial t_a}\langle\langle A(t_a);B(t_b)\rangle\rangle^{\gtrless} = \langle\langle [A,H](t_a);B(t_b)\rangle\rangle^{\gtrless}, \tag{2.0.7}$$

must obviously be incomplete[III], as the equation above should ultimately determine expectation values, but it lacks statistical information. As an example, this is illustrated for a free fermion model with

$$H_{\text{free}} = \sum_k \varepsilon_k c_k^\dagger c_k \quad \text{and} \quad [c_k, H_{\text{free}}] = \varepsilon_k c_k,$$

where $c_k^{(\dagger)}$ annihilates (creates) a particle with energy ε_k. According to (2.0.7), the equation of motion for a single-particle lesser Green's function reads

$$i\frac{\partial}{\partial t}\langle\langle c_k(t);c_k^\dagger(t')\rangle\rangle^{<} = \varepsilon_k\langle\langle c_k(t);c_k^\dagger(t')\rangle\rangle^{<}, \tag{2.0.8}$$

which is solved by functions $\propto i\exp\{-i\varepsilon_k t\}$. The dependence on t' and constant prefactors remain undetermined compared to the correct solution (cf. section 12.3 in [1])

$$\langle\langle c_k(t);c_k^\dagger(t')\rangle\rangle^{<} = if(\varepsilon_k;\mu,T)\exp\{-i\varepsilon_k(t-t')\}.$$

A fully consistent equation of motion for lesser and greater Green's functions can be derived in the framework of path-ordering, which is introduced on general expectation values in the following section.

2.1. (Non-Equilibrium) Expectation Values

A non-equilibrium situation[IV] for a general quantum mechanical system can be described by the Hamiltonian

$$\hat{H}(t) = \hat{H}_0 + \Theta(t-t_0)\hat{H}_1(t), \tag{2.1.1}$$

where the time-independent operator $\hat{H}_0$ alone describes the complete system for times $t < t_0$, where at $t = t_0$ a possibly time-dependent change is introduced to the system by $\hat{H}_1(t)$, e.g. an applied voltage or hopping terms that connect subsystems. The state of the initial system, i.e. for times $t < t_0$, is given through the density operator

$$\hat{\rho}_0 \equiv \hat{\rho}(\hat{H}_0), \tag{2.1.2}$$

which may describe either one system in equilibrium or a set of disconnected subsystems each in its own equilibrium, and so observables in the initial system can be expressed as

$$\langle\hat{O}\rangle_0 := \text{tr}\{\hat{\rho}_0\hat{O}\}.$$

[III] A mathematical argumentation using Dirac delta calculus can be found in [8].
[IV] See, e.g., chapter 4 in [9].

The time evolution of the whole system can be done in different pictures – *Schrödinger* (S), *Dirac* (D) and *Heisenberg* (H) – for which the governing equations of motion and subsequently the transformations are the *von Neumann* equation for the density operator

$$+i\frac{\partial\hat{\rho}_{\mathrm{S}}}{\partial t}=\left[\hat{H},\hat{\rho}_{\mathrm{S}}\right]\qquad\Longleftrightarrow\qquad\hat{\rho}_{\mathrm{S}}(t):=\hat{\mathcal{U}}(t,t_0)\hat{\rho}_{0,\mathrm{S}}\hat{\mathcal{U}}^{\dagger}(t,t_0)\tag{2.1.3}$$

and the *Heisenberg* equation for any other operator[V]

$$-i\frac{\mathrm{d}\hat{O}_{\mathrm{H}}}{\mathrm{d}t}=\left[\hat{H},\hat{O}_{\mathrm{H}}\right]\qquad\Longleftrightarrow\qquad\hat{O}_{\mathrm{H}}(t):=\hat{\mathcal{U}}^{\dagger}(t,t_0)\hat{O}_{\mathrm{S}}\hat{\mathcal{U}}(t,t_0),\tag{2.1.4}$$

where

$$\begin{aligned}\hat{\mathcal{U}}(t,t_0)&:=\mathcal{T}\exp\left[-i\int_{t_0}^{t}\mathrm{d}t'\,\hat{H}(t')\right]\\ \hat{\mathcal{U}}^{\dagger}(t,t_0)&:=\widetilde{\mathcal{T}}\exp\left[-i\int_{t}^{t_0}\mathrm{d}t'\,\hat{H}(t')\right]\end{aligned}\tag{2.1.5}$$

defines the unitary time evolution operator[VI] and $(\widetilde{\mathcal{T}})\mathcal{T}$ is the (anti-)time-ordering operator. As the equations above suggest, in the Heisenberg picture the operator $\hat{O}_{\mathrm{H}}(t)$ carries the complete time evolution of $\hat{H}(t)$ and the states (density operator) remain constant, where in the Schrödinger picture the states evolve in time with $\hat{\rho}_{\mathrm{S}}(t)$.

The different pictures must not change physical quantities, which can be shown in fact using the cyclic invariance property of the trace, thus, an observable at time t can be written as

$$\begin{aligned}\left\langle\hat{O}(t)\right\rangle&=\mathrm{tr}\left\{\hat{\rho}_{\mathrm{S}}(t)\hat{O}_{\mathrm{S}}\right\}\\&=\mathrm{tr}\Big\{\hat{\mathcal{U}}(t,t_0)\hat{\rho}_0\hat{\mathcal{U}}^{\dagger}(t,t_0)\hat{O}_{\mathrm{S}}\Big\}\\&=\mathrm{tr}\Big\{\hat{\rho}_0\hat{\mathcal{U}}^{\dagger}(t,t_0)\hat{O}_{\mathrm{S}}\hat{\mathcal{U}}(t,t_0)\Big\}\\&=\mathrm{tr}\left\{\hat{\rho}_0\hat{O}_{\mathrm{H}}(t)\right\}.\end{aligned}\tag{2.1.6}$$

The Dirac picture takes an intermediate position, where states and operator both carry part of the time evolution. The Hamiltonian is split like in (2.1.1) and all operators carry the time evolution governed by $\hat{H}_0$, which can be integrated exactly. The operators in the Dirac picture then read

$$\begin{aligned}\hat{O}_{\mathrm{D}}(t)&:=\hat{\mathcal{U}}_0^{\dagger}(t,t_0)\hat{O}_{\mathrm{S}}\hat{\mathcal{U}}_0(t,t_0)=\mathrm{e}^{i(t-t_0)\hat{H}_0}\hat{O}_{\mathrm{S}}\mathrm{e}^{-i(t-t_0)\hat{H}_0}\\\hat{H}_{1,\mathrm{D}}(t)&:=\hat{\mathcal{U}}_0^{\dagger}(t,t_0)\hat{H}_{1,\mathrm{S}}(t)\hat{\mathcal{U}}_0(t,t_0)=\mathrm{e}^{i(t-t_0)\hat{H}_0}\hat{H}_{1,\mathrm{S}}(t)\mathrm{e}^{-i(t-t_0)\hat{H}_0},\end{aligned}\tag{2.1.7}$$

where in principle $\hat{H}_0$ is transformed as well, but as it commutes with itself, the exponentials cancel out and the operator is the same in both pictures, i.e. $\hat{H}_{0,\mathrm{D}}=\hat{H}_{0,\mathrm{S}}$. Another unitary transformation $\hat{\mathcal{V}}$ can be found, relating operators in the Heisenberg and Dirac picture via

$$\hat{O}_{\mathrm{H}}(t)=\hat{\mathcal{V}}^{\dagger}(t,t_0)\hat{O}_{\mathrm{D}}(t)\hat{\mathcal{V}}(t,t_0),\tag{2.1.8}$$

[V] With $\frac{\partial}{\partial t}\hat{O}_{\mathrm{S}}=0$.

[VI] See section A.1.1 in the appendix for the derivation.

where

$$\begin{aligned}\hat{\mathcal{V}}(t,t_0) &:= \mathcal{T}\exp\left[-i\int_{t_0}^{t}\mathrm{d}t'\,\hat{H}_{1,\mathrm{D}}(t')\right]\\ \hat{\mathcal{V}}^{\dagger}(t,t_0) &:= \widetilde{\mathcal{T}}\exp\left[-i\int_{t}^{t_0}\mathrm{d}t'\,\hat{H}_{1,\mathrm{D}}(t')\right].\end{aligned} \tag{2.1.9}$$

Equation (2.1.8) implies the special time-ordering $t_0 \xrightarrow{\mathcal{T}} t \xrightarrow{\widetilde{\mathcal{T}}} t_0$, i.e. regular time-ordering from t_0 to t and anti-time ordering from t back to t_0, that can be combined to a new time-ordering for a variable τ along a contour C_t[VII]. With the help of the corresponding time-ordering operator $\mathcal{T}_{C_t}$ the operator in the Heisenberg picture can finally be written as

$$\begin{aligned}\hat{O}_{\mathrm{H}}(t) &= \mathcal{T}_{C_t}\left\{\hat{O}_{\mathrm{D}}(t)\exp\left[-i\int_{C_t}\mathrm{d}\tau\,\hat{H}_{1,D}(\tau)\right]\right\}\\ &:= \sum_{n=0}^{\infty}\frac{(-i)^n}{n!}\int_{C_t}\mathrm{d}t_1\ldots\int_{C_t}\mathrm{d}t_n\,\mathcal{T}_{C_t}\left[\hat{O}_{\mathrm{D}}(t)\hat{H}_{1,D}(t_1)\ldots\hat{H}_{1,D}(t_n)\right]\\ &:= \hat{\mathbb{1}}\hat{O}_{\mathrm{D}}(t) + \sum_{n=1}^{\infty}\frac{(-i)^n}{n!}\int_{C_t}\mathrm{d}t_1\ldots\int_{C_t}\mathrm{d}t_n\,\mathcal{T}_{C_t}\left[\hat{O}_{\mathrm{D}}(t)\hat{H}_{1,D}(t_1)\ldots\hat{H}_{1,D}(t_n)\right],\end{aligned} \tag{2.1.10}$$

where the last two lines define the explicit form of the *ordered operator exponentials* occurring in this section. Note that the integration variables t_i in (2.1.10) are derived from the contour variable τ and already appear in the correct order, i.e. the time-ordering only affects the position of $\hat{O}_{\mathrm{D}}(t)$. This can be seen in the derivation of the time evolution operator in section A.1.1 in the appendix, with the only difference that the integration variables are related to t' in the regular time-ordering.

The expressions from the last two lines in (2.1.10) will be the starting point for the derivation of the desired equation of motion. For that purpose, a similar representation[VIII] for a Green's function is needed, and can be achieved with the additional time-ordered two-times Green's function that is later used to construct the retarded, advanced, lesser and greater functions:

$$\begin{aligned}i\langle\!\langle A(t_a);B(t_b)\rangle\!\rangle &:= \langle\mathcal{T}\left[A(t_a)B(t_b)\right]\rangle\\ &= \mathrm{tr}\{\hat{\rho}_0\mathcal{T}\left[A_{\mathrm{H}}(t_a)B_{\mathrm{H}}(t_b)\right]\}\\ &= \mathrm{tr}\{\hat{\rho}_0\left[\Theta(t_a-t_b)A_{\mathrm{H}}(t_a)B_{\mathrm{H}}(t_b)-\Theta(t_b-t_a)B_{\mathrm{H}}(t_b)A_{\mathrm{H}}(t_a)\right]\}\end{aligned} \tag{2.1.11}$$

Using the propagator property of the time-evolution operator, $\mathcal{V}(t,t_0)=\mathcal{V}(t,t')\mathcal{V}(t',t_0)$, and relation (2.1.8) the product for $t_a > t_b$ can be written as

$$\begin{aligned}A_{\mathrm{H}}(t_a)B_{\mathrm{H}}(t_b) &= \mathcal{V}^{\dagger}(t_a,t_0)A_{\mathrm{D}}(t_a)\mathcal{V}(t_a,t_0)\mathcal{V}^{\dagger}(t_b,t_0)B_{\mathrm{D}}(t_b)\mathcal{V}(t_b,t_0)\\ &= \mathcal{V}^{\dagger}(t_a,t_0)A_{\mathrm{D}}(t_a)\mathcal{V}(t_a,t_b)\underbrace{\mathcal{V}(t_b,t_0)\mathcal{V}^{\dagger}(t_b,t_0)}_{=\mathbb{1}}B_{\mathrm{D}}(t_b)\mathcal{V}(t_b,t_0)\\ &= \mathcal{V}^{\dagger}(t_a,t_0)A_{\mathrm{D}}(t_a)\mathcal{V}(t_a,t_b)B_{\mathrm{D}}(t_b)\mathcal{V}(t_b,t_0)\end{aligned} \tag{2.1.12}$$

[VII] In literature, this is referred to as either the *Schwinger-Keldysh* closed time path or real-time closed contour. It coincides with the contour C if $t = t_a = t_b$ (cf. (2.1.14)), which is depicted in figure 2.1.

[VIII] From here on, it is assumed that the reader is familiar with the defined symbols, and hats are dropped on most operators for the sake of simplicity. They may still occur in some places for traditional reasons or to prevent misunderstandings

and analogously for $t_a < t_b$

$$\begin{aligned} B_{\mathrm{H}}(t_b)A_{\mathrm{H}}(t_a) &= \mathcal{V}^\dagger(t_b,t_0)B_{\mathrm{D}}(t_b)\mathcal{V}(t_b,t_0)\mathcal{V}^\dagger(t_a,t_0)A_{\mathrm{D}}(t_a)\mathcal{V}(t_a,t_0) \\ &= \mathcal{V}^\dagger(t_b,t_0)B_{\mathrm{D}}(t_b)\mathcal{V}(t_b,t_a)A_{\mathrm{D}}(t_a)\mathcal{V}(t_a,t_0) \end{aligned} \tag{2.1.13}$$

is obtained. So the new time-ordering can be identified as $t_0 \xrightarrow{\mathcal{T}} t_{a,b} \xrightarrow{\mathcal{T}} t_{b,a} \xrightarrow{\tilde{\mathcal{T}}} t_0$ and in analogy to equation (2.1.10) the contour C can be defined as

$$C = \begin{cases} C^< & \text{for } t_a < t_b \\ C^> & \text{for } t_a > t_b \end{cases} \tag{2.1.14}$$

and is shown in figure 2.1.

(a) $C^<$ (b) $C^>$

Figure 2.1.: Schematics for the two cases of contour C for $t_0 \to -\infty$.

And finally the time-ordered Green's functions can be written in the Dirac picture as

$$\begin{aligned} i\langle\langle A(t_a);B(t_b)\rangle\rangle &= \mathrm{tr}\Big\{\hat{\rho}_0\mathcal{T}_C\left[A_{\mathrm{D}}(t_a)B_{\mathrm{D}}(t_b)\mathrm{e}^{-i\int_C \mathrm{d}t H_{1\mathrm{D}}(t)}\right]\Big\} \\ &= \mathrm{tr}\{\hat{\rho}_0\mathcal{T}_C\left[A_{\mathrm{D}}(t_a)B_{\mathrm{D}}(t_b)\right]\} \\ &+ \sum_{n=1}^{\infty}\frac{(-i)^n}{n!}\int_C \mathrm{d}t_1\ldots\int_C \mathrm{d}t_n\,\mathrm{tr}\{\hat{\rho}_0\mathcal{T}_C\left[A_{\mathrm{D}}(t_a)B_{\mathrm{D}}(t_b)H_{1,D}(t_1)\ldots H_{1,D}(t_n)\right]\}. \end{aligned} \tag{2.1.15}$$

In the following, a derivation for the equation of motion for the above non-equilibrium Green's function is presented according to [8].

2.2. Derivation of the Equation of Motion for Non-Equilibrium Green's Functions

The equation of motion is derived for an initial state in the grand-canonical ensemble that consists of disconnected subsystems, which correspond to sites, orbitals or isolated clusters in many-body models. The Hamiltonian

$$H = H_0 + H_1$$

is therefore split in a way that H_0 contains only free fermions, so

$$H_0 = \sum_\zeta \varepsilon_\zeta \hat{n}_\zeta = \sum_\zeta \varepsilon_\zeta a_\zeta^\dagger a_\zeta, \tag{2.2.1}$$

where $\hat{n}_\zeta = a_\zeta^\dagger a_\zeta$ denotes the number operator for subsystem ζ, respectively creation- and annihilation operator, ε_ζ is the corresponding (on-site) energy, and ζ runs over each subsystem. All other terms like hoppings, that eventually connect the subsystems, and interactions are contained in H_1. The subsystems in the initial state are all in their own equilibrium characterized by chemical potentials μ_ζ and inverse temperatures $\beta_\zeta = T_\zeta^{-1}$, and so, using the formal definition in (2.1.2), the grand-canonical density operator reads

$$\hat{\rho}_0 = \frac{\exp\left[-\sum_\zeta \beta_\zeta \left(\varepsilon_\zeta - \mu_\zeta\right) \hat{n}_\zeta\right]}{\mathrm{tr}\left\{\exp\left[-\sum_\zeta \beta_\zeta \left(\varepsilon_\zeta - \mu_\zeta\right) \hat{n}_\zeta\right]\right\}}. \tag{2.2.2}$$

With the choice of H_0 the Dirac representation for the operators A and B in the Green's function can be worked out explicitly. Focussing on arbitrary odd[IX] products of creation- and annihilation operators α_i in the Schrödinger picture, i.e.

$$A_\mathrm{D}(0) = A_\mathrm{S} = \prod_{i=1}^{2m+1} \alpha_i,$$

and H_0 containing only number operators, the commutators reproduce just the operator with some constant γ. The equation of motion for the operator in the Dirac picture reads

$$\frac{\mathrm{d}A_\mathrm{D}(t)}{\mathrm{d}t} = -i[A_\mathrm{D}(t), H_0] = -iA_\mathrm{D}(t) \sum_i \lambda_i \varepsilon_i =: -iA_\mathrm{D}(t)\gamma_a, \tag{2.2.3}$$

where[X]

$$\lambda_i = \begin{cases} +1 & \text{if } \alpha_i \text{ is an annihilation operator} \\ -1 & \text{if } \alpha_i \text{ is a creation operator.} \end{cases} \tag{2.2.4}$$

The differential equation is solved by

$$A_\mathrm{D}(t) = A_\mathrm{D}(0)\mathrm{e}^{-it\gamma_a} =: A_\mathrm{D}(0) f_a(t),$$

which has the property

$$A_\mathrm{D}(t) f_a(t' - t) = A_\mathrm{D}(0)\mathrm{e}^{-it\gamma_a}\mathrm{e}^{-i(t'-t)\gamma_a} = A_\mathrm{D}(0) f_a(t') = A_\mathrm{D}(t'). \tag{2.2.5}$$

The result for B is obviously obtained analogously.

The sum in the equation defining γ_a (cf. equation (2.2.3)) runs formally over all operator indices in A_S, but practically it is enough to count the signed factors $\lambda_i \varepsilon_i$ only for operators that are not paired with their Hermitian conjugate, as pairs cancel out. Consider, e.g., the following operator, composed by annihilation (creation) operators $x_i^{(\dagger)}$,

$$X_\mathrm{S} = x_1 x_2^\dagger x_2 x_3^\dagger x_4$$

[IX] With A and B being odd, the total Green's function describes correlations of an even number of operators, which is needed in total particle-number conserving fermionic systems. Even products of operators for A and B are excluded, as with the chosen H_0 the Dirac form of, e.g., number operators $\hat{n}$ coincides with their Schrödinger form and therefore the later defined $\gamma_{\hat{n}} = 0$ and $f_{\hat{n}} = F_{\hat{n}} = 1$, which does not allow a closed solution in turn. Products of terms $a_i^\dagger a_j$ work out using commutator instead of anticommutator relations in a first step, but produce number operator terms in further steps. Pair creation- or annihilation terms like $a_i^\dagger a_j^\dagger$ or $a_i a_j$ allow a closed solution using commutator relation that lead eventually to Bose distribution functions instead of Fermi functions, and are not treated for simplicity.

[X] Note that this definition differs from [8].

for which γ_x reads

$$\gamma_x = \varepsilon_1 - \varepsilon_2 + \varepsilon_2 - \varepsilon_3 + \varepsilon_4 = \varepsilon_1 - \varepsilon_3 + \varepsilon_4.$$

For the sake of readability and as operators only appear explicitly in the Dirac representation in the derivation, the subscript D is dropped from here on, the Hamiltonian denotes always H_1, and the time argument is indicated by a subscript, so that

$$\begin{aligned} H_i &:= H_{1,\mathrm{D}}(t_i) \\ A_i &:= A_{\mathrm{D}}(t_i) \\ B_i &:= B_{\mathrm{D}}(t_i). \end{aligned} \tag{2.2.6}$$

With these definitions equation (2.1.15) reads

$$i\langle\!\langle A(t_a); B(t_b)\rangle\!\rangle = \sum_{n=0}^{\infty} \frac{(-i)^n}{n!} \int_C \mathrm{d}t_1 \ldots \int_C \mathrm{d}t_n \,\mathrm{tr}\{\hat{\rho}_0 \mathcal{T}_C \left[A_a B_b H_1 \ldots H_n\right]\}. \tag{2.2.7}$$

The time variables t_a and t_b are now positioned[XI] on the contour C so that $t_a \succ t_b$, allowing to evaluate the time-ordering of the product in the trace explicitly. No additional sign needs to be introduced as fermionic Hamiltonians are always paired, and so the ordering for the nth term and $n \geq 1$ yields

$$W_n := \mathcal{T}_C \left[A_a B_b H_1 \ldots H_n\right] = H_1 \ldots (A_a H_i) \ldots B_b H_j \ldots H_n. \tag{2.2.8}$$

Note that eventually the same equation of motion can be obtained by following the procedure for $t_a \prec t_b$, which yields

$$\widetilde{W}_n = -H_1 \ldots B_b H_i \ldots A_a H_j \ldots H_n$$

in the beginning, as interchanging two odd products of fermionic operators gives a minus sign. The aim is now to move the operator A_a from its position $(A_a H_i)$ once through the whole contour to get back to the original expression and algebraically solve for it. Moving the operator A_a one step to the right gives

$$W_n = H_1 \ldots (H_i A_a) \ldots B_b H_j \ldots H_n + H_1 \ldots [A_a, H_i] \ldots B_b H_j \ldots H_n, \tag{2.2.9}$$

as

$$A_a H_i = H_i A_a + [A_a, H_i].$$

With (2.2.5), the time argument can be changed according to $A_a = f_a(t_a - t_i) A_i$ and the commutator in W_n can then be written as

$$\begin{aligned} [A_a, H_i] &= f_a(t_a - t_i)[A_i, H_i] \\ &=: f_a(t_a - t_i) C_i, \end{aligned} \tag{2.2.10}$$

where C_i is the equal-time commutator of A_i and H_i, that itself is again an odd product of operators, and so

$$\begin{aligned} W_n = f_a(t_a - t_i) H_1 \ldots H_{i-1} C_i H_{i+1} \ldots B_b H_j \ldots H_n \\ + H_1 \ldots H_{i-1} \left(H_i A_a\right) H_{i+1} \ldots B_b H_j \ldots H_n. \end{aligned} \tag{2.2.11}$$

[XI] Inequalities in the path-ordering are denoted by the symbols $\succ$ and $\prec$.

Each additional commutation to the right gives another summand with a factor $f_a(t_a - t_k)$ and one additional term comes from the commutation with B_b, which is expressed via their anticommutator[XII]

$$A_a B_b = \{A_a, B_b\} - B_b A_a$$

and introduces a minus sign for the succeeding summands. Similar to (2.2.10), the anticommutator from above can be written as

$$\begin{aligned} \{A_a, B_b\} &= f_a(t_a - t_b)\{A_b, B_b\} \\ &=: f_a(t_a - t_b) D_b^+, \end{aligned} \tag{2.2.12}$$

where D_b^+ is the equal-time anticommutator of A_b and B_b. Commuting A to the end of the original operator string and taking the whole trace term gives

$$\begin{aligned} \operatorname{tr}\{\hat{\rho}_0 W_n\} = {} & f_a(t_a - t_b) \operatorname{tr}\{\hat{\rho}_0 H_1 \dots D_b^+ H_j \dots H_n\} \\ & + \sum_{t_i \succeq t_k \succ t_j} f_a(t_a - t_k) \operatorname{tr}\{\hat{\rho}_0 H_1 \dots H_{i-1} \dots C_k \dots B_b H_j \dots H_n\} \\ & - \sum_{t_j \succeq t_k \succeq t_n} f_a(t_a - t_k) \operatorname{tr}\{\hat{\rho}_0 H_1 \dots H_{j-1} B_b \dots C_k \dots H_n\} \\ & - \operatorname{tr}\{\hat{\rho}_0 H_1 \dots B_b \dots (H_n A_a)\}. \end{aligned} \tag{2.2.13}$$

Notice the change in sign before the second sum due to the anticommutator. Due to cyclic invariance in the trace, the last term can be written as

$$\operatorname{tr}\{\hat{\rho}_0 H_1 \dots B_b \dots H_n A_a\} = \operatorname{tr}\{A_a \hat{\rho}_0 H_1 \dots B_b \dots H_n\}.$$

Using the series expansion of $\hat{\rho}_0$ and moving A_a to the right, the following result can be found[XIII]

$$A_a \hat{\rho}_0 = F_a \hat{\rho}_0 A_a,$$

where

$$F_a := \exp\left[- \sum_i \lambda_i \beta_i \left(\varepsilon_i - \mu_i \right) \right] =: \mathrm{e}^{-\varphi} \tag{2.2.14}$$

is similar to γ, defined in the commutation with the initial-state Hamiltonian H_0 (see (2.2.3)), but includes now statistical information. The commutations can then be continued up to the original position of A_a:

$$\begin{aligned} \operatorname{tr}\{\hat{\rho}_0 W_n\} = {} & f_a(t_a - t_b) \operatorname{tr}\{\hat{\rho}_0 H_1 \dots D_b^+ H_j \dots H_n\} \\ & + \sum_{t_i \succeq t_k \succ t_j} f_a(t_a - t_k) \operatorname{tr}\{\hat{\rho}_0 H_1 \dots C_k \dots B_b H_j \dots H_n\} \\ & - \sum_{t_j \succeq t_k \succeq t_n} f_a(t_a - t_k) \operatorname{tr}\{\hat{\rho}_0 H_1 \dots B_b \dots C_k \dots H_n\} \\ & - \sum_{t_1 \succeq t_k \succ t_i} F_a f_a(t_a - t_k) \operatorname{tr}\{\hat{\rho}_0 H_1 \dots C_k \dots H_i \dots B_b H_j \dots H_n\} \\ & - F_a \underbrace{\operatorname{tr}\{\hat{\rho}_0 H_1 \dots H_{i-1} (A_a H_i) \dots H_{j-1} B_b H_j \dots H_n\}}_{= \operatorname{tr}\{\hat{\rho}_0 W_n\}} \end{aligned} \tag{2.2.15}$$

[XII] This thesis treats only fermionic operators. For bosonic operators it is more convenient to choose the commutator. The result can be found in [8]

[XIII] See section A.1.2 in the appendix.

Solving for the left-hand side gives a global factor $(1+F_a)^{-1}$. All operator strings containing C_k in the traces can be rewritten as formally the same contour-ordered term, where the commutator takes the position of A_a in the starting definition. In the second sum an additional minus sign appears as B_b and C_k need to be interchanged, i.e.

$$-f_a(t_a-t_k)\,\mathrm{tr}\{\hat{\rho}_0 H_1\dots B_b\dots C_k\dots H_n\} = +f_a(t_a-t_k)\,\mathrm{tr}\{\hat{\rho}_0\mathcal{T}_C\,[C_k B_b H_1\dots H_n]\},$$

and so all sum terms with factor f_a occur with positive sign and the terms with factor $F_a f_a$ with negative sign. The sum indices turn out to be characterized only by t_a, namely

$$\sum_{t_i\succeq t_k\succ t_j} f_a(t_a-t_k)\dots + \sum_{t_j\succeq t_k\succeq t_n} f_a(t_a-t_k)\dots = \sum_{t_i\succeq t_k\succeq t_n} f_a(t_a-t_k)\dots = \sum_{t_a\succ t_k} f_a(t_a-t_k)\dots$$

and

$$-\sum_{t_1\succeq t_k\succ t_i} F_a f_a(t_a-t_k)\dots = -\sum_{t_k\succ t_a} F_a f_a(t_a-t_k)\dots,$$

where the for $t_a\succ t_k$ only factors $\propto f_a$ and for $t_a\prec t_k$ only factors $\propto F_a f_a$ appear, which can further be related to single-particle non-interacting Green's functions[XIV], i.e. correlations $\propto\langle c^\dagger(t_1)c(t_2)\rangle$ in a system described by H_0:

$$\begin{aligned} ig_a^{>}(t_2-t_1) &:= \frac{f_a(t_2-t_1)}{1+F_a} \\ ig_a^{<}(t_2-t_1) &:= -\frac{F_a f_a(t_2-t_1)}{1+F_a} \end{aligned} \tag{2.2.16}$$

Combining the above functions to

$$ig_a(t_2-t_1) := \begin{cases} ig_a^{>}(t_2-t_1) & \text{if } t_2\succ t_1 \\ ig_a^{<}(t_2-t_1) & \text{if } t_2\prec t_1 \end{cases} \tag{2.2.17}$$

equation (2.2.15) can be written with the single sum

$$\begin{aligned} \mathrm{tr}\{\rho_0 W_n\} = {}& ig_a(t_a-t_b)\,\mathrm{tr}\{\hat{\rho}_0\mathcal{T}_C\left[D_b^+ H_1\dots H_n\right]\} \\ & + i\sum_k g_a(t_a-t_k)\,\mathrm{tr}\{\hat{\rho}_0\mathcal{T}_C\,[C_k B_b H_1\dots H_n]\}. \end{aligned} \tag{2.2.18}$$

As noted before, the above result is valid for $n\geq 1$ and with equation (2.1.15) the result for $n=0$ is readily obtained as

$$\begin{aligned} \mathrm{tr}\{\rho_0 W_0\} :=& \,\mathrm{tr}\{\hat{\rho}_0\mathcal{T}_C A_a B_b\} \\ =& f_a(t_a-t_b)\,\mathrm{tr}\{\hat{\rho}_0 D_b^+\} - F_a\,\mathrm{tr}\{\rho_0 W_0\} \\ =& ig_a(t_a-t_b)\,\mathrm{tr}\{\hat{\rho}_0 D_b^+\}. \end{aligned} \tag{2.2.19}$$

Inserting the results for $n=0$ and $n\geq 1$ back in the definition for the Green's function (2.2.7) yields

$$\begin{aligned} i\langle\langle A(t_a);B(t_b)\rangle\rangle = {}& ig_a(t_a-t_b)\,\mathrm{tr}\{\hat{\rho}_0 D_b^+\} \\ & + ig_a(t_a-t_b)\sum_{n=1}^{\infty}\frac{(-i)^n}{n!}\int_C \mathrm{d}t_1\dots\int_C \mathrm{d}t_n\,\mathrm{tr}\{\hat{\rho}_0\mathcal{T}_C\left[D_b^+ H_1\dots H_n\right]\} \\ & + \sum_{n=1}^{\infty}\frac{(-i)^n}{n!}\int_C \mathrm{d}t_1\dots\int_C \mathrm{d}t_n\, i\sum_{k=1}^{n} g_a(t_a-t_k)\,\mathrm{tr}\{\hat{\rho}_0\mathcal{T}_C\,[C_k B_b H_1\dots H_n]\}, \end{aligned} \tag{2.2.20}$$

[XIV] Note that in equilibrium, i.e. $\mu_i=\mu=0$ and $\beta_i=\beta$, the fermionic Kubo-Martin-Schwinger boundary condition holds: $g^<(t+i\beta) = ie^{-\beta\gamma}\left(1+e^{-\beta\gamma}\right)^{-1}e^{-i\gamma(t+i\beta)} = -g^>(t)$, cf. [10].

where the expectation value for the anticommutator D_b^+ can be identified with the help of equation (2.1.10) and so

$$\begin{aligned} i\langle\langle A(t_a); B(t_b)\rangle\rangle = & \, i g_a(t_a - t_b) \left\langle D_b^+ \right\rangle \\ & + \sum_{n=1}^{\infty} \frac{(-i)^n}{n!} \int_C \mathrm{d}t_1 \ldots \int_C \mathrm{d}t_n \, i \sum_{k=1}^{n} g_a(t_a - t_k) \, \mathrm{tr}\{\hat{\rho}_0 \mathcal{T}_C \left[C_k B_b H_1 \ldots H_n\right]\}. \end{aligned} \tag{2.2.21}$$

At first glance, the new expression looks even more complicated, but analysing the nth term in the sum gives

$$\begin{aligned} & \frac{(-i)^n}{n!} \int_C \mathrm{d}t_1 \ldots \int_C \mathrm{d}t_n \, i \sum_{k=1}^{n} g_a(t_a - t_k) \, \mathrm{tr}\{\hat{\rho}_0 \mathcal{T}_C \left[C_k B_b H_1 \ldots H_n\right]\} \\ = & \frac{(-i)^n}{n!} n \int_C \mathrm{d}t_1 \ldots \int_C \mathrm{d}t_n \, i g_a(t_a - t_1) \, \mathrm{tr}\{\hat{\rho}_0 \mathcal{T}_C \left[C_1 B_b H_2 \ldots H_n\right]\} \\ = & \frac{(-i)^n}{n!} n \int_C \mathrm{d}t \, i g_a(t_a - t) \int_C \mathrm{d}t_1 \ldots \int_C \mathrm{d}t_{n-1} \, \mathrm{tr}\{\hat{\rho}_0 \mathcal{T}_C \left[C_t B_b H_1 \ldots H_{n-1}\right]\} \end{aligned}$$

as the sum over k gives just n times the same integral over different dummy variables and t_i is renamed to t_{i-1} in the last step, where t_0 is just t. The prefactor can then be rewritten in the following way

$$\frac{(-i)^n}{n!} n = \frac{(-i)^n}{(n-1)!} = \frac{1}{i} \frac{(-i)^{n-1}}{(n-1)!}$$

and so the whole sum yields

$$\begin{aligned} & \int_C \mathrm{d}t \, i g_a(t_a - t) \sum_{n=1}^{\infty} \frac{1}{i} \frac{(-i)^{n-1}}{(n-1)!} \int_C \mathrm{d}t_1 \ldots \int_C \mathrm{d}t_{n-1} \, \mathrm{tr}\{\hat{\rho}_0 \mathcal{T}_C \left[C_t B_b H_1 \ldots H_{n-1}\right]\} \\ & = \int_C \mathrm{d}t \, i g_a(t_a - t) \frac{1}{i} \underbrace{\sum_{m=0}^{\infty} \frac{(-i)^m}{m!} \int_C \mathrm{d}t_1 \ldots \int_C \mathrm{d}t_m \, \mathrm{tr}\{\hat{\rho}_0 \mathcal{T}_C \left[C_t B_b H_1 \ldots H_m\right]\}}_{i\langle\langle C_t; B_b\rangle\rangle} \\ & = i \int_C \mathrm{d}t \, g_a(t_a - t) \langle\langle C_t; B_b\rangle\rangle, \end{aligned} \tag{2.2.22}$$

where $n - 1 = m$ is renamed and the sum over m is just the initial definition for a Green's function. So in total, the equation of motion for the Green's function results in

$$\boxed{\langle\langle A(t_a); B(t_b)\rangle\rangle = g_a(t_a - t_b) \left\langle D_b^+ \right\rangle + \int_C \mathrm{d}t \, g_a(t_a - t) \langle\langle C_t; B_b\rangle\rangle.} \tag{2.2.23}$$

The single-particle Green's function g can be written in the following way

$$g_a^{\gtrless}(t_2 - t_1) = i P^{\gtrless}(\varphi_a) f_a(t_2 - t_1),$$

where with equation (2.2.14) a relation to the Fermi function $f(x)$ is found:

$$\begin{aligned} P^{<}(\varphi_a) := & \quad \frac{\mathrm{e}^{-\varphi_a}}{1 + \mathrm{e}^{-\varphi_a}} = \quad \frac{1}{1 + \mathrm{e}^{\varphi_a}} = f(\varphi_a) \\ P^{>}(\varphi_a) := & -\frac{1}{1 + \mathrm{e}^{-\varphi_a}} = -\frac{\mathrm{e}^{\varphi_a}}{1 + \mathrm{e}^{\varphi_a}} = f(\varphi_a) - 1 \end{aligned} \tag{2.2.24}$$

And so the factors can be related to each other via

$$P^{\gtrless}(-\varphi_a) = \mp\frac{1}{1+\mathrm{e}^{\pm\varphi_a}} = -P^{\lessgtr}(\varphi_a). \tag{2.2.25}$$

Notice the different superscripts $\gtrless$ and $\lessgtr$.

2.2.1. Real-Time Integrals: Langreth Path-Splitting

The derived equation of motion still involves the full Green's function containing all time information on the contour, whose direct evaluation is not straightforward. Especially for a numerical evaluation the need for regular real-axis integration is given. This is achieved by fixing the times t_a and t_b and evaluating the contour for four different Green's functions separately. In first place the two correlation functions, lesser and greater Green's functions (cf. (2.0.6)), arise, namely

$$\begin{aligned}\langle\!\langle A(t_a); B(t_b)\rangle\!\rangle^{<} &\text{ for } t_a \prec t_b\\ \langle\!\langle A(t_a); B(t_b)\rangle\!\rangle^{>} &\text{ for } t_a \succ t_b,\end{aligned}$$

as the definition from equation (2.1.11) yields

$$\begin{aligned}\langle\!\langle A(t_a); B(t_b)\rangle\!\rangle^{<} &= +i\,\mathrm{tr}\{\hat{\rho}_0 B_{\mathrm{H}}(t_b) A_{\mathrm{H}}(t_a)\} = +i\,\langle B(t_b)A(t_a)\rangle\\ \langle\!\langle A(t_a); B(t_b)\rangle\!\rangle^{>} &= -i\,\mathrm{tr}\{\hat{\rho}_0 A_{\mathrm{H}}(t_a) B_{\mathrm{H}}(t_b)\} = -i\,\langle A(t_a)B(t_b)\rangle\,.\end{aligned}$$

These functions can further be used to describe the retarded and advanced Green's functions, cf. (2.0.1):

$$\begin{aligned}\langle\!\langle A(t_a); B(t_b)\rangle\!\rangle^{\mathrm{R}} &= +\Theta(t_a - t_b)\left(\langle\!\langle A(t_a); B(t_b)\rangle\!\rangle^{>} - \langle\!\langle A(t_a); B(t_b)\rangle\!\rangle^{<}\right)\\ &= -i\Theta(t_a - t_b)\,\langle\{A(t_a), B(t_b)\}\rangle\\ \langle\!\langle A(t_a); B(t_b)\rangle\!\rangle^{\mathrm{A}} &= -\Theta(t_b - t_a)\left(\langle\!\langle A(t_a); B(t_b)\rangle\!\rangle^{>} - \langle\!\langle A(t_a); B(t_b)\rangle\!\rangle^{<}\right)\\ &= +i\Theta(t_b - t_a)\,\langle\{A(t_a), B(t_b)\}\rangle\end{aligned}$$

The main trick for the contour evaluation as introduced by Langreth in [11] consists of splitting the contour into two subcontours

$$C^{\gtrless} = C_1^{\gtrless} + C_2^{\gtrless},$$

depicted in figure 2.2, on which the following relations hold for t on the explicit four sub-contours and functions $G(t_1, t_2)$:

$$\begin{aligned}t \prec t_b \text{ for } \forall t \in C_1^{<} &\Leftrightarrow G(t, t_b) = G^{<}(t, t_b)\\ t \prec t_a \text{ for } \forall t \in C_1^{>} &\Leftrightarrow G(t_a, t) = G^{>}(t_a, t)\\ t \succ t_a \text{ for } \forall t \in C_2^{<} &\Leftrightarrow G(t_a, t) = G^{<}(t_a, t)\\ t \succ t_b \text{ for } \forall t \in C_2^{>} &\Leftrightarrow G(t, t_b) = G^{>}(t, t_b)\end{aligned} \tag{2.2.26}$$

As shown in figure 2.2, the initial time t_0 is now assumed to be in the far past, i.e. $t_0 \to -\infty$, which is a preparation for the steady-solutions presented in the next section. With the above

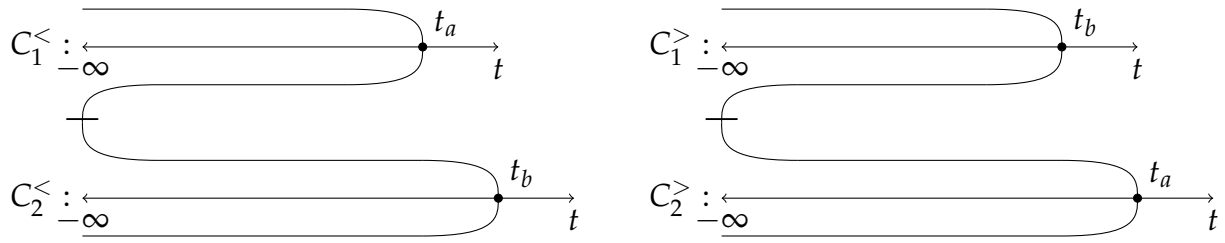

(a) $C^<$ (b) $C^>$

Figure 2.2.: Contour replacements $C^{\gtrless}$ for C

relations and the definition of the single-particle functions (2.2.16) and (2.2.17) the splitting results in

$$\begin{aligned}\int_{C^<} \mathrm{d}t\, g_a(t_a - t)\langle\!\langle C_t; B_b\rangle\!\rangle &= \int_{C_1^<} \mathrm{d}t\, g_a(t_a - t)\langle\!\langle C_t; B_b\rangle\!\rangle^< + \int_{C_2^<} \mathrm{d}t\, g_a^<(t_a - t)\langle\!\langle C_t; B_b\rangle\!\rangle \\ \int_{C^>} \mathrm{d}t\, g_a(t_a - t)\langle\!\langle C_t; B_b\rangle\!\rangle &= \int_{C_1^>} \mathrm{d}t\, g_a^>(t_a - t)\langle\!\langle C_t; B_b\rangle\!\rangle + \int_{C_2^>} \mathrm{d}t\, g_a(t_a - t)\langle\!\langle C_t; B_b\rangle\!\rangle^>.\end{aligned} \tag{2.2.27}$$

Using the same argumentation, the sub-contours $C_i^{\gtrless}$ can then be further split into regular real-time integrals over the sub-regions. For $C_1^<$ this reads explicitly

$$\begin{aligned}\int_{C_1^<} \mathrm{d}t\, g_a(t_a - t)\langle\!\langle C_t; B_b\rangle\!\rangle^< &= \int_{-\infty}^{t_a} \mathrm{d}t\, g_a^>(t_a - t)\langle\!\langle C_t; B_b\rangle\!\rangle^< + \int_{t_a}^{-\infty} \mathrm{d}t\, g_a^<(t_a - t)\langle\!\langle C_t; B_b\rangle\!\rangle^< \\ &= \int_{-\infty}^{t_a} \mathrm{d}t\, \left[g_a^>(t_a - t) - g_a^<(t_a - t)\right]\langle\!\langle C_t; B_b\rangle\!\rangle^<\end{aligned} \tag{2.2.28}$$

and for $C_1^>$

$$\begin{aligned}\int_{C_1^>} \mathrm{d}t\, g_a^>(t_a - t)\langle\!\langle C_t; B_b\rangle\!\rangle &= \int_{-\infty}^{t_b} \mathrm{d}t\, g_a^>(t_a - t)\langle\!\langle C_t; B_b\rangle\!\rangle^< + \int_{t_b}^{-\infty} \mathrm{d}t\, g_a^>(t_a - t)\langle\!\langle C_t; B_b\rangle\!\rangle^> \\ &= -\int_{-\infty}^{t_b} \mathrm{d}t\, g_a^>(t_a - t)\left[\langle\!\langle C_t; B_b\rangle\!\rangle^> - \langle\!\langle C_t; B_b\rangle\!\rangle^<\right]\end{aligned} \tag{2.2.29}$$

is obtained. The integrals can be rewritten as integrals over the whole real axis with the help of a shifted step function, namely

$$\int_{-\infty}^{t_{a,b}} \mathrm{d}t \ldots = \int_{-\infty}^{\infty} \mathrm{d}t\, \Theta(t_{a,b} - t) \ldots,$$

where the definition of a retarded (advanced) function can be identified for $C_1^<$ ($C_1^>$) and so the integration reduces to

$$\begin{aligned}\int_{C_1^<} \mathrm{d}t\, g_a(t_a - t)\langle\!\langle C_t; B_b\rangle\!\rangle^< &= \int_{-\infty}^{\infty} \mathrm{d}t\, g_a^{\mathrm{R}}(t_a - t)\langle\!\langle C_t; B_b\rangle\!\rangle^< \\ \int_{C_1^>} \mathrm{d}t\, g_a^>(t_a - t)\langle\!\langle C_t; B_b\rangle\!\rangle &= \int_{-\infty}^{\infty} \mathrm{d}t\, g_a^>(t_a - t)\langle\!\langle C_t; B_b\rangle\!\rangle^{\mathrm{A}}.\end{aligned} \tag{2.2.30}$$

An analogous splitting for $C_2^<$ leads to

$$\begin{aligned}\int_{C_2^<} \mathrm{d}t\, g_a^<(t_a-t)\langle\!\langle C_t; B_b\rangle\!\rangle &= \int_{-\infty}^{t_b} \mathrm{d}t\, g_a^<(t_a-t)\langle\!\langle C_t; B_b\rangle\!\rangle^< + \int_{t_b}^{-\infty} \mathrm{d}t\, g_a^<(t_a-t)\langle\!\langle C_t; B_b\rangle\!\rangle^> \\ &= -\int_{-\infty}^{t_b} \mathrm{d}t\, g_a^<(t_a-t)\left(\langle\!\langle C_t; B_b\rangle\!\rangle^> - \langle\!\langle C_t; B_b\rangle\!\rangle^<\right) \\ &= \int_{-\infty}^{\infty} \mathrm{d}t\, g_a^<(t_a-t)\langle\!\langle C_t; B_b\rangle\!\rangle^{\mathrm{A}}\end{aligned} \tag{2.2.31}$$

and for $C_2^>$ to

$$\begin{aligned}\int_{C_2^>} \mathrm{d}t\, g_a(t_a-t)\langle\!\langle C_t; B_b\rangle\!\rangle^> &= \int_{-\infty}^{t_a} \mathrm{d}t\, g_a^>(t_a-t)\langle\!\langle C_t; B_b\rangle\!\rangle^> + \int_{t_a}^{-\infty} \mathrm{d}t\, g_a^<(t_a-t)\langle\!\langle C_t; B_b\rangle\!\rangle^> \\ &= \int_{-\infty}^{t_a} \mathrm{d}t\, \left[g_a^>(t_a-t) - g_a^<(t_a-t)\right]\langle\!\langle C_t; B_b\rangle\!\rangle^> \\ &= \int_{-\infty}^{\infty} \mathrm{d}t\, g_a^{\mathrm{R}}(t_a-t)\langle\!\langle C_t; B_b\rangle\!\rangle^>.\end{aligned} \tag{2.2.32}$$

The whole integrals over $C^<$ and $C^>$ are formally the same and differ only in the superscript defining the lesser and greater part, so the combined results read

$$\int_{C^\gtrless} \mathrm{d}t\, g_a(t_a-t)\langle\!\langle C_t; B_b\rangle\!\rangle = \int_{-\infty}^{\infty} \mathrm{d}t\, \left[g_a^{\mathrm{R}}(t_a-t)\langle\!\langle C_t; B_b\rangle\!\rangle^\gtrless + g_a^\gtrless(t_a-t)\langle\!\langle C_t; B_b\rangle\!\rangle^{\mathrm{A}}\right]. \tag{2.2.33}$$

The explicit form of the single-particle retarded Green's function used above is obtained analogously to the full Green's function, cf. (2.0.1), and leads to the explicit form

$$\begin{aligned}g_a^{\mathrm{R}}(t_a-t) &= \Theta(t_a-t)\left[g_a^>(t_a-t) - g_a^<(t_a-t)\right] \\ &= i\Theta(t_a-t)\left(-\frac{1}{1+F_a} - \frac{F_a}{1+F_a}\right) f_a(t_a-t) \\ &= -i\Theta(t_a-t) f_a(t_a-t) \\ &= -i\Theta(t_a-t)\mathrm{e}^{-i\gamma_a(t_a-t)}\end{aligned} \tag{2.2.34}$$

and for the advanced function

$$\begin{aligned}g_a^{\mathrm{A}}(t_a-t) &= -\Theta(t-t_a)\left[g_a^>(t_a-t) - g_a^<(t_a-t)\right] \\ &= i\Theta(t-t_a)\mathrm{e}^{-i\gamma_a(t_a-t)}.\end{aligned} \tag{2.2.35}$$

The equation of motion for greater and lesser Green's functions is thus given by

$$\langle\!\langle A(t_a); B(t_b)\rangle\!\rangle^\gtrless = g_a^\gtrless(t_a-t_b)\left\langle D_b^+\right\rangle + \int_{C^\gtrless} \mathrm{d}t\, g_a(t_a-t)\langle\!\langle C_t; B_b\rangle\!\rangle \tag{2.2.36}$$

and the corresponding definitions (2.2.33)-(2.2.35).

The equation of motion for retarded and advanced Green's functions can be obtained by inserting the above equation of motion in the definition (2.0.1). The single-particle terms are

straightforward, but the integral term needs a closer look. The retarded terms yield

$$\begin{aligned}
&\Theta(t_a - t_b)\left(\int_{C^>} \mathrm{d}t\, g_a(t_a - t)\langle\!\langle C_t; B_b\rangle\!\rangle - \int_{C^<} \mathrm{d}t\, g_a(t_a - t)\langle\!\langle C_t; B_b\rangle\!\rangle\right) \\
&= \Theta(t_a - t_b)\int_{-\infty}^{\infty} \mathrm{d}t \left\{ g_a^{\mathrm{R}}(t_a - t)\left[\langle\!\langle C_t; B_b\rangle\!\rangle^{>} - \langle\!\langle C_t; B_b\rangle\!\rangle^{<}\right] \right. \\
&\qquad\qquad \left. + \left[g_a^{>}(t_a - t) - g_a^{<}(t_a - t)\right]\langle\!\langle C_t; B_b\rangle\!\rangle^{\mathrm{A}} \right\},
\end{aligned}$$

where g_a^{R} and $\langle\!\langle C_t; B_b\rangle\!\rangle^{\mathrm{A}}$ are now rewritten in terms of lesser and greater functions and the step function is incorporated in the limits, and so

$$\begin{aligned}
&= \Theta(t_a - t_b)\left\{ \int_{-\infty}^{t_a} \mathrm{d}t \left[g_a^{>}(t_a - t) - g_a^{<}(t_a - t)\right]\left[\langle\!\langle C_t; B_b\rangle\!\rangle^{>} - \langle\!\langle C_t; B_b\rangle\!\rangle^{<}\right] \right. \\
&\qquad \left. - \int_{-\infty}^{t_b} \mathrm{d}t \left[g_a^{>}(t_a - t) - g_a^{<}(t_a - t)\right]\left[\langle\!\langle C_t; B_b\rangle\!\rangle^{>} - \langle\!\langle C_t; B_b\rangle\!\rangle^{<}\right] \right\} \\
&= \Theta(t_a - t_b)\int_{t_b}^{t_a} \mathrm{d}t \left[g_a^{>}(t_a - t) - g_a^{<}(t_a - t)\right]\left[\langle\!\langle C_t; B_b\rangle\!\rangle^{>} - \langle\!\langle C_t; B_b\rangle\!\rangle^{<}\right].
\end{aligned}$$

By rewriting[XV] the expression

$$\Theta(t_a - t_b)\int_{t_b}^{t_a} \mathrm{d}t \ldots = \int_{-\infty}^{\infty} \mathrm{d}t\, \Theta(t_a - t)\Theta(t - t_b)\ldots,$$

the result for the retarded part of the integral becomes finally

$$\begin{aligned}
&= \int_{-\infty}^{\infty} \mathrm{d}t\, \Theta(t_a - t)\left[g_a^{>}(t_a - t) - g_a^{<}(t_a - t)\right] \\
&\qquad \times \Theta(t - t_b)\left[\langle\!\langle C_t; B_b\rangle\!\rangle^{>} - \langle\!\langle C_t; B_b\rangle\!\rangle^{<}\right] \\
&= \int_{-\infty}^{\infty} \mathrm{d}t\, g_a^{\mathrm{R}}(t_a - t)\langle\!\langle C_t; B_b\rangle\!\rangle^{\mathrm{R}}.
\end{aligned}$$

The procedure for the advanced part leads to an analogous expression. The results of this derivation are known as analytic continuation or *Langreth* rules (see sec. 4.3 in [1]).

So finally, the regular time integration of the equation of motion on the contour (2.2.23) can be summarized as

$$\boxed{\begin{aligned}
\langle\!\langle A(t_a); B(t_b)\rangle\!\rangle^{\gtrless} &= g_a^{\gtrless}(t_a - t_b)\,\langle\{A(t_b), B(t_b)\}\rangle \\
&\quad + \int_{-\infty}^{\infty} \mathrm{d}t\, g_a^{\mathrm{R}}(t_a - t)\langle\!\langle [A(t), H_1(t)]; B(t_b)\rangle\!\rangle^{\gtrless} \\
&\quad + \int_{-\infty}^{\infty} \mathrm{d}t\, g_a^{\gtrless}(t_a - t)\langle\!\langle [A(t), H_1(t)]; B(t_b)\rangle\!\rangle^{\mathrm{A}} \\
\langle\!\langle A(t_a); B(t_b)\rangle\!\rangle^{\mathrm{R/A}} &= g_a^{\mathrm{R/A}}(t_a - t_b)\,\langle\{A(t_b), B(t_b)\}\rangle \\
&\quad + \int_{-\infty}^{\infty} \mathrm{d}t\, g_a^{\mathrm{R/A}}(t_a - t)\langle\!\langle [A(t), H_1(t)]; B(t_b)\rangle\!\rangle^{\mathrm{R/A}}.
\end{aligned}} \tag{2.2.37}$$

[XV] See section A.1.3 in the appendix for details.

2.2.2. Steady State

A system can reach a steady-state if its describing Hamiltonian is or eventually becomes time-invariant[XVI]. In this case the Green's function depends only on the time difference $t' := t_a - t_b$, i.e. $G(t_a, t_b) \to G(t_a - t_b)$ and a Fourier transform from time t' to energy[XVII] ω can be performed. The following sign convention is used and only the inverse transform carries a factor $(2\pi)^{-1}$:

$$G(\omega) = \int_{-\infty}^{\infty} \mathrm{d}t'\, G(t') \mathrm{e}^{i\omega t'} \tag{2.2.38}$$

With the integral representation of $\delta(t')$, a steady-state expectation value (equal-time correlation) is then obtained via integration:

$$\langle B(t)A(t)\rangle = \langle BA(0)\rangle = \frac{1}{i}\int_{-\infty}^{\infty} \mathrm{d}t'\, G^{<}_{AB}(t') \frac{1}{2\pi}\int_{-\infty}^{\infty} \mathrm{d}\omega\, \mathrm{e}^{i\omega t'} = \frac{1}{2\pi i}\int_{-\infty}^{\infty} \mathrm{d}\omega\, G^{<}_{AB}(\omega) \tag{2.2.39}$$

The steady state for contour-ordered Green's functions is in fact technically appealing as the occurring integrals can be transformed into convolution terms (denoted by an asterisk $*$) that reduce to simple multiplication according to the Fourier convolution theorem. The substitution $\tau = t - t_b$ and $\mathrm{d}\tau = \mathrm{d}t$ gives

$$\begin{aligned} \int_{-\infty}^{\infty} \mathrm{d}t\, g(t_a - t) G(t - t_b) &= \int_{-\infty}^{\infty} \mathrm{d}\tau\, g(t_a - t_b - \tau) G(\tau) \\ &=: (g * G)(t_a - t_b) \\ &= (g * G)(t') \end{aligned} \tag{2.2.40}$$

and its Fourier transform is simply the product of the individual transforms:

$$\int_{-\infty}^{\infty} \mathrm{d}t'\, (g * G)(t') \mathrm{e}^{i\omega t'} = g(\omega) G(\omega) \tag{2.2.41}$$

The first term in the equation of motion gives

$$\int_{-\infty}^{\infty} \mathrm{d}t'\, \mathrm{e}^{i\omega t'} g_a(t') \,\langle\{A(t_b), B(t_b)\}\rangle = \langle\{A(0), B(0)\}\rangle \int_{-\infty}^{\infty} \mathrm{d}t'\, \mathrm{e}^{i\omega t'} g_a(t') = \langle\{A, B\}\rangle\, g_a(\omega), \tag{2.2.42}$$

as the time difference in the anticommutator is zero. And so the equations of motion in ω become just algebraic equations:

$$\boxed{\begin{aligned} \langle\!\langle A; B\rangle\!\rangle^{\gtrless}_{\omega} &= g^{\gtrless}_a(\omega)\,\langle\{A, B\}\rangle \quad + g^{\mathrm{R}}_a(\omega) \langle\!\langle [A, H_1]; B\rangle\!\rangle^{\gtrless}_{\omega} + g^{\gtrless}_a(\omega) \langle\!\langle [A, H_1]; B\rangle\!\rangle^{\mathrm{A}}_{\omega} \\ \langle\!\langle A; B\rangle\!\rangle^{\mathrm{R/A}}_{\omega} &= g^{\mathrm{R/A}}_a(\omega)\,\langle\{A, B\}\rangle + g^{\mathrm{R/A}}_a(\omega) \langle\!\langle [A, H_1]; B\rangle\!\rangle^{\mathrm{R/A}}_{\omega} \end{aligned}} \tag{2.2.43}$$

Using the equation for $G^{\mathrm{R/A}}$ to express the higher advanced function in the equation for $G^{\gtrless}$, the expectation value can be eliminated and the following form is obtained:

$$\boxed{\langle\!\langle A; B\rangle\!\rangle^{\gtrless}_{\omega} = \frac{g^{\gtrless}_a(\omega)}{g^{\mathrm{A}}_a(\omega)} \langle\!\langle A; B\rangle\!\rangle^{\mathrm{A}}_{\omega} + g^{\mathrm{R}}_a(\omega) \langle\!\langle [A, H_1]; B\rangle\!\rangle^{\gtrless}_{\omega}} \tag{2.2.44}$$

[XVI] $\mathrm{e}^{\int \mathrm{d}t H} \to \mathrm{e}^{Ht} : \langle A(t_a)B(t_b)\rangle \to \langle A(t_a - t_b)B(0)\rangle$

[XVII] As $\hbar = 1$.

The Fourier transform of the retarded single-particle non-interacting Green's function $g_a^{\mathrm{R}}(t')$ leads to an integration over positive time differences t'

$$g_a^{\mathrm{R}}(\omega) = -i\int_0^\infty \mathrm{d}t'\, \mathrm{e}^{it'(\omega-\gamma_a)} = -\frac{\mathrm{e}^{it'(\omega-\gamma_a)}}{\omega-\gamma_a}\bigg|_0^\infty, \tag{2.2.45}$$

which has no well-defined solution due to the $\propto \exp(i\infty)$ term. However, this can be overcome by introducing an infinitesimally small imaginary part to the energy ω, i.e.

$$\omega \to \lim_{\eta\to 0^+} \omega + i\eta,$$

which leads to the solution

$$g_a^{\mathrm{R}}(\omega) = \lim_{\eta\to 0^+} \frac{1}{\omega-\gamma_a+i\eta}. \tag{2.2.46}$$

The advanced function leads to the similar problem, but with integration over negative time differences t'

$$g_a^{\mathrm{A}}(\omega) = i\int_{-\infty}^0 \mathrm{d}t'\, \mathrm{e}^{it'(\omega-\gamma_a)} = \frac{\mathrm{e}^{it'(\omega-\gamma_a)}}{\omega-\gamma_a}\bigg|_{-\infty}^0, \tag{2.2.47}$$

where the opposite sign for the imaginary part is needed, i.e.

$$\omega \to \lim_{\eta\to 0^+} \omega - i\eta,$$

and the solution is obtained as

$$g_a^{\mathrm{A}}(\omega) = \lim_{\eta\to 0^+} \frac{1}{\omega-\gamma_a-i\eta}. \tag{2.2.48}$$

Summarizing, a positive (negative) imaginary part $i\eta$ needs to be added to the transformation variable ω for positive (negative) time difference t', so the replacement

$$\omega \to \lim_{\eta\to 0^+} \omega + i\eta\,\mathrm{sgn}(t')$$

can be introduced for the entire real axis, which is needed for the lesser and greater functions:

$$\begin{aligned}
g_a^{\gtrless}(\omega) &= iP^{\gtrless}(\varphi_a)\int_{-\infty}^\infty \mathrm{d}t'\, \mathrm{e}^{it'(\omega-\gamma_a)} \\
&\to iP^{\gtrless}(\varphi_a)\lim_{\eta\to 0^+}\int_{-\infty}^\infty \mathrm{d}t'\, \mathrm{e}^{it'(\omega-\gamma_a+i\eta\,\mathrm{sgn}(t'))} \\
&= iP^{\gtrless}(\varphi_a)\lim_{\eta\to 0^+}\left[\int_{-\infty}^0 \mathrm{d}t'\, \mathrm{e}^{it'(\omega-\gamma_a)+\eta t'} + \int_0^\infty \mathrm{d}t'\, \mathrm{e}^{it'(\omega-\gamma_a)-\eta t'}\right] \\
&= iP^{\gtrless}(\varphi_a)\lim_{\eta\to 0^+}\left[\frac{\mathrm{e}^{it'(\omega-\gamma_a)}\mathrm{e}^{\eta t'}}{i(\omega-\gamma_a)+\eta}\bigg|_{-\infty}^0 + \frac{\mathrm{e}^{it'(\omega-\gamma_a)}\mathrm{e}^{-\eta t'}}{i(\omega-\gamma_a)-\eta}\bigg|_0^\infty\right] \\
&= iP^{\gtrless}(\varphi_a)\lim_{\eta\to 0^+}\left[\frac{1}{i(\omega-\gamma_a)+\eta} - \frac{1}{i(\omega-\gamma_a)-\eta}\right] \\
&= 2iP^{\gtrless}(\varphi_a)\lim_{\eta\to 0^+}\frac{\eta}{(\omega-\gamma_a)^2+\eta^2}
\end{aligned} \tag{2.2.49}$$

The limit can be interpreted as[XVIII]

$$2\pi i P^{\gtrless}(\varphi_a)\delta\left(\omega-\gamma_a\right),$$

which can also be obtained by transforming $g^{\gtrless}(t')$ directly with a purely real ω and exploiting the definition of how the Dirac delta distribution acts on a function $f(x)$, namely

$$f(y)=\int_{-\infty}^{\infty}\mathrm{d}x\, f(x)\delta(x-y).$$

This formal result can be understood as a placeholder that fulfils the invertibility property of the Fourier transform, namely that the inverse transform of a Fourier transform returns to the original function:

$$\begin{aligned}\frac{1}{2\pi}\int_{-\infty}^{\infty}\mathrm{d}\omega\, g^{\gtrless}(\omega)\mathrm{e}^{-i\omega t'} &= iP^{\gtrless}(\varphi)\int_{-\infty}^{\infty}\mathrm{d}\omega\,\delta\left(\omega-\gamma\right)\mathrm{e}^{-i\omega t'}\\ &= iP^{\gtrless}(\varphi)\mathrm{e}^{-i\gamma t'}\\ &= g^{\gtrless}(t')\end{aligned}\tag{2.2.50}$$

Keeping this in mind, another placeholder function can be found for the case $\beta_i=\beta$, i.e. no temperature gradient between the particle types the operator is acting on[XIX]. In that case, φ can be expressed as a function of γ

$$\varphi=\sum_i\lambda_i\beta_i(\varepsilon_i-\mu_i)\overset{\beta_i=\beta}{=}\beta\sum_i\lambda_i(\varepsilon_i-\mu_i)=\beta\left(\gamma-\sum_i\lambda_i\mu_i\right):=\varphi(\gamma)$$

and

$$g^{\gtrless}(\omega)=2\pi i P^{\gtrless}(\varphi(\omega))\delta\left(\omega-\gamma\right),\tag{2.2.51}$$

where $P^{\gtrless}$ is now a function of $\varphi(\omega)$. This returns the same function in time:

$$\begin{aligned}\frac{1}{2\pi}\int_{-\infty}^{\infty}\mathrm{d}\omega\, g^{\gtrless}(\omega)\mathrm{e}^{-i\omega t'} &= i\int_{-\infty}^{\infty}\mathrm{d}\omega\, P^{\gtrless}(\varphi(\omega))\delta\left(\omega-\gamma\right)\mathrm{e}^{-i\omega t'}\\ &= iP^{\gtrless}(\varphi(\gamma))\mathrm{e}^{-i\gamma t'}\\ &\overset{\beta_i=\beta}{=} iP^{\gtrless}(\varphi)\mathrm{e}^{-i\gamma t'}=g^{\gtrless}(t')\end{aligned}\tag{2.2.52}$$

As shown later on, this change in argument can be useful where integrals of type

$$\int\mathrm{d}\gamma\,\rho(\gamma)g(\omega;\gamma)$$

are needed, as $P(\omega)$ does not need to be integrated. This choice seems even more justified as it does not violate a certain form of the fluctuation-dissipation theorem in equilibrium, as shown as an example in section 4.1.1.

[XVIII] See section A.2.1 in the appendix for the normalizing constant of π.

[XIX] The result from (2.2.49) is valid for different values of β_i though.

2.3. Alternative Expression for the Equation of Motion

The equations of motion discussed above are mostly governed by the dynamics of the first operator $A(t_a)$. However, for some Green's functions it may be convenient to have an expression in the second operator $B(t_b)$, especially when treating correlations with non-interacting particles, as their time evolution relates only to other basic correlations and does not produce an infinite or non-trivial hierarchy of new Green's functions.

In equilibrium this can be achieved for retarded and advanced Green's functions by differentiation with respect to the second time and its Fourier transformed version reads

$$\omega \langle\langle A; B \rangle\rangle^{\mathrm{R/A}} = \left\langle \left\{ \hat{A}, \hat{B} \right\} \right\rangle + \langle\langle A; [H, B] \rangle\rangle^{\mathrm{R/A}}.$$

This form has been used before (e.g. in [12], [13] and [14]), but, to the author's knowledge, not yet in non-equilibrium situations for greater and lesser functions.

In order to find a non-equilibrium analogy to the above equation the following symmetry relation is found:

$$\begin{aligned} i\langle\langle A(t_a); B(t_b) \rangle\rangle &= \sum_{n=0}^{\infty} \frac{(-i)^n}{n!} \int_C \mathrm{d}t_1 \ldots \int_C \mathrm{d}t_n \, \mathrm{tr}\{\hat{\rho}_0 \mathcal{T}_C \left[A(t_a) B(t_b) H_1(t_1) \ldots H_1(t_n) \right]\} \\ &= -\sum_{n=0}^{\infty} \frac{(-i)^n}{n!} \int_C \mathrm{d}t_1 \ldots \int_C \mathrm{d}t_n \, \mathrm{tr}\{\hat{\rho}_0 \mathcal{T}_C \left[B(t_b) A(t_a) H_1(t_1) \ldots H_1(t_n) \right]\} \\ &= -i\langle\langle B(t_b); A(t_a) \rangle\rangle \end{aligned} \tag{2.3.1}$$

So the contour-ordered Green's function is antisymmetric under exchange of operator and time argument.

As used in Langreth's path-splitting, fixing the times t_a and t_b relative to each other makes it clear which Green's function describes correctly the physical situation. Choosing $t_a \prec t_b$ gives

$$\langle\langle A(t_a); B(t_b) \rangle\rangle^{<} \qquad \text{but} \qquad \langle\langle B(t_b); A(t_a) \rangle\rangle^{>}$$

and vice versa. So the following relations hold using equation (2.3.1)

$$\begin{aligned} \langle\langle A(t_a); B(t_b) \rangle\rangle^{<} &= -\langle\langle B(t_b); A(t_a) \rangle\rangle^{>} \\ \langle\langle A(t_a); B(t_b) \rangle\rangle^{>} &= -\langle\langle B(t_b); A(t_a) \rangle\rangle^{<}, \end{aligned} \tag{2.3.2}$$

and can be used to determine relations for retarded and advanced functions:

$$\begin{aligned} \langle\langle A(t_a); B(t_b) \rangle\rangle^{\mathrm{R}} &= \Theta(t_a - t_b) \left[\langle\langle A(t_a); B(t_b) \rangle\rangle^{>} - \langle\langle A(t_a); B(t_b) \rangle\rangle^{<} \right] \\ &= \Theta(t_a - t_b) \left[\langle\langle B(t_b); A(t_a) \rangle\rangle^{>} - \langle\langle B(t_b); A(t_a) \rangle\rangle^{<} \right] \\ &= -\langle\langle B(t_b); A(t_a) \rangle\rangle^{\mathrm{A}} \\ \langle\langle A(t_a); B(t_b) \rangle\rangle^{\mathrm{A}} &= -\Theta(t_b - t_a) \left[\langle\langle A(t_a); B(t_b) \rangle\rangle^{>} - \langle\langle A(t_a); B(t_b) \rangle\rangle^{<} \right] \\ &= -\langle\langle B(t_b); A(t_a) \rangle\rangle^{\mathrm{R}} \end{aligned} \tag{2.3.3}$$

According to equation (2.2.23) the equation of motion for switched operators is just

$$\langle\langle B(t_b); A(t_a) \rangle\rangle = g_b(t_b - t_a) \left\langle D_a^+ \right\rangle + \int_C \mathrm{d}t \, g_b(t_b - t) \langle\langle C_t; A_a \rangle\rangle,$$

where here

$$C_t = [B_t, H_t] = -[H_t, B_t] =: -\widetilde{C}_t$$

and so the higher Green's function can be written as

$$\langle\langle C_t; A_a \rangle\rangle = -\langle\langle A_a; C_t \rangle\rangle = \langle\langle A_a; \widetilde{C}_t \rangle\rangle.$$

Using the antisymmetric relation (2.3.1), the contour-ordered equation of motion in the second operator is just

$$\boxed{\langle\langle A(t_a); B(t_b) \rangle\rangle = -g_b(t_b - t_a) \langle \{A(t_a), B(t_a)\} \rangle - \int_C \mathrm{d}t\, g_b(t_b - t) \langle\langle A(t_a); [H_1(t), B(t)] \rangle\rangle} \tag{2.3.4}$$

The explicit Langreth splitting of equation (2.3.4) can be obtained analogously to section 2.2.1, but it seems more convenient to use the equations of motion (2.2.37) for $\langle\langle B(t_b); A(t_a) \rangle\rangle$ and replace the expressions according to the symmetry relations found in (2.3.2) and (2.3.3).

Lesser and greater Green's functions yield

$$\begin{aligned}
\langle\langle B(t_b); A(t_a) \rangle\rangle^{\lessgtr} &= g_b^{\lessgtr}(t_b - t_a) \langle \{B(t_a), A(t_a)\} \rangle \\
&\quad + \int_{-\infty}^{\infty} \mathrm{d}t\, g_b^{\mathrm{R}}(t_b - t) \langle\langle [B(t), H_1(t)]; A(t_a) \rangle\rangle^{\lessgtr} \\
&\quad + \int_{-\infty}^{\infty} \mathrm{d}t\, g_b^{\lessgtr}(t_b - t) \langle\langle [B(t), H_1(t)]; A(t_a) \rangle\rangle^{\mathrm{A}} \\
&= g_b^{\lessgtr}(t_b - t_a) \langle \{A(t_a), B(t_a)\} \rangle \\
&\quad + \int_{-\infty}^{\infty} \mathrm{d}t\, g_b^{\mathrm{R}}(t_b - t) \langle\langle A(t_a); [H_1(t), B(t)] \rangle\rangle^{\gtrless} \\
&\quad + \int_{-\infty}^{\infty} \mathrm{d}t\, g_b^{\lessgtr}(t_b - t) \langle\langle A(t_a); [H_1(t), B(t)] \rangle\rangle^{\mathrm{R}}
\end{aligned} \tag{2.3.5}$$

and retarded and advanced

$$\begin{aligned}
\langle\langle B(t_b); A(t_a) \rangle\rangle^{\mathrm{A/R}} &= g_b^{\mathrm{A/R}}(t_b - t_a) \langle \{B(t_b), A(t_b)\} \rangle \\
&\quad + \int_{-\infty}^{\infty} \mathrm{d}t\, g_b^{\mathrm{A/R}}(t_b - t) \langle\langle [B(t), H_1(t)]; A(t_a) \rangle\rangle^{\mathrm{A/R}} \\
&= g_b^{\mathrm{A/R}}(t_b - t_a) \langle \{A(t_b), B(t_b)\} \rangle \\
&\quad + \int_{-\infty}^{\infty} \mathrm{d}t\, g_b^{\mathrm{A/R}}(t_b - t) \langle\langle A(t_a); [H_1(t), B(t)] \rangle\rangle^{\mathrm{R/A}},
\end{aligned} \tag{2.3.6}$$

where the symmetry relations (2.3.2) and (2.3.2) were used only on the right-hand side of the above equations. Applying the relations to the left-hand side finally gives

$$\boxed{\begin{aligned}
\langle\langle A(t_a); B(t_b) \rangle\rangle^{\gtrless} &= -g_b^{\lessgtr}(t_b - t_a) \langle \{A(t_a), B(t_a)\} \rangle \\
&\quad - \int_{-\infty}^{\infty} \mathrm{d}t\, g_b^{\mathrm{R}}(t_b - t) \langle\langle A(t_a); [H_1(t), B(t)] \rangle\rangle^{\gtrless} \\
&\quad - \int_{-\infty}^{\infty} \mathrm{d}t\, g_b^{\lessgtr}(t_b - t) \langle\langle A(t_a); [H_1(t), B(t)] \rangle\rangle^{\mathrm{R}} \\
\langle\langle A(t_a); B(t_b) \rangle\rangle^{\mathrm{R/A}} &= -g_b^{\mathrm{A/R}}(t_b - t_a) \langle \{A(t_b), B(t_b)\} \rangle \\
&\quad - \int_{-\infty}^{\infty} \mathrm{d}t\, g_b^{\mathrm{A/R}}(t_b - t) \langle\langle A(t_a); [H_1(t), B(t)] \rangle\rangle^{\mathrm{R/A}}.
\end{aligned}} \tag{2.3.7}$$

Notice the use of the different superscripts $\gtrless$ and $\lessgtr$ as well as R/A and A/R whose positions, i.e. up/down or left/right, must be maintained when evaluating the equations for a specific superscript.

Since the equations shall be used together with the equations from the previous section, the Fourier transform must be done in the same time argument $t' = t_a - t_b$. The substitution $\tau = t - t_b$ and $\mathrm{d}\tau = \mathrm{d}t$ leads again to a convolution

$$\begin{aligned}\int_{-\infty}^{\infty} \mathrm{d}t\, g(t_b - t)G(t_a - t) &= \int_{-\infty}^{\infty} \mathrm{d}\tau \overbrace{g(-\tau)}^{=:\overline{g}(\tau)} G(t_a - t_b - \tau) \\ &= \int_{-\infty}^{\infty} \mathrm{d}\tau\, \overline{g}(\tau)G(t' - \tau) \\ &= (\overline{g} * G)(t')\end{aligned} \tag{2.3.8}$$

whose Fourier transform is just the product

$$\int_{-\infty}^{\infty} \mathrm{d}t'\, (\overline{g} * G)(t')\mathrm{e}^{i\omega t'} = \left[\int_{-\infty}^{\infty} \mathrm{d}t'\, \overline{g}(t')\mathrm{e}^{i\omega t'}\right]\left[\int_{-\infty}^{\infty} \mathrm{d}t'\, G(t')\mathrm{e}^{i\omega t'}\right] = \overline{g}(\omega)G(\omega). \tag{2.3.9}$$

Before rewriting the explicit equations of motion in terms of Fourier transforms, the transform of the function $\overline{g}(t')$ is examined. At first, it is clear that $\overline{g}(t')$ represents simply the non-interacting Green's functions as they occur in (2.3.7), as

$$\overline{g}_b(t') = g_b(-t') = g_b(t_b - t_a),$$

and it is therefore sufficient to calculate the transformations of $g_b(-t')$.

With analogous argumentation as in section 2.2.2 the transformation for the lesser and greater functions read[XX]

$$\overline{g}_b^{\lessgtr}(\omega) = \int_{-\infty}^{\infty} \mathrm{d}t'\, g_b^{\lessgtr}(-t')\mathrm{e}^{i\omega t'} = iP^{\lessgtr}(\varphi_b)\int_{-\infty}^{\infty} \mathrm{d}t'\, \mathrm{e}^{it'(\omega+\gamma_b)} = 2\pi i P^{\lessgtr}(\varphi_b)\delta(\omega + \gamma_b). \tag{2.3.10}$$

In order to achieve (formal) equivalence to the expressions for the first operator $A(t_a)$, where the argument in the delta distribution is $\omega - \gamma$ (cf. equation (2.2.49)), the following replacements are made

$$\gamma_b \to -\widetilde{\gamma}_b \qquad \text{and} \qquad \varphi_b \to -\widetilde{\varphi}_b,$$

where $\widetilde{\gamma}_b$ is obtained from $[H_0, B_{t_b}]$ instead of $[B_{t_b}, H_0]$, which accounts for the minus sign and is, in addition, consistent with $\widetilde{C} = [H, B]$. Using the symmetry shown in (2.2.24) and (2.2.25) the prefactor becomes

$$P^{\lessgtr}(\varphi_b) \to P^{\lessgtr}(-\widetilde{\varphi}_b) = -P^{\gtrless}(\widetilde{\varphi}_b),$$

where the superscripts changed, and so

$$\overline{g}_b^{\lessgtr}(\omega) = -2\pi i P^{\gtrless}(\widetilde{\varphi}_b)\delta(\omega - \widetilde{\gamma}_b).$$

[XX] The expression using a limit in η applies here as well; for convenience the transformation is shown without η.

The retarded and advanced functions read

$$\begin{aligned} \overline{g}_b^{\mathrm{R}}(t_b - t_a) &= \Theta(t_b - t_a)\left[g_b^{>}(t_b - t_a) - g_b^{<}(t_b - t_a)\right] = -i\Theta(-t')\mathrm{e}^{it'\gamma_b} \\ \overline{g}_b^{\mathrm{R}}(\omega) &= -i\int_{-\infty}^{0} \mathrm{d}t'\, \mathrm{e}^{it'(\omega+\gamma_b)} = \lim_{\eta\to 0^+} -\frac{1}{\omega + \gamma_b - i\eta} \end{aligned} \tag{2.3.11}$$

and

$$\begin{aligned} \overline{g}_b^{\mathrm{A}}(t_b - t_a) &= -\Theta(t_a - t_b)\left[g_b^{>}(t_b - t_a) - g_b^{<}(t_b - t_a)\right] = i\Theta(t')\mathrm{e}^{it'\gamma_b} \\ \overline{g}_b^{\mathrm{A}}(\omega) &= i\int_{0}^{\infty} \mathrm{d}t'\, \mathrm{e}^{it'(\omega+\gamma_b)} = \lim_{\eta\to 0^+} -\frac{1}{\omega + \gamma_b + i\eta}. \end{aligned} \tag{2.3.12}$$

Applying the replacements mentioned above, the transform of $\overline{g}_b$ can be related to newly defined transforms (in accordance with section 2.2.2):

$$\begin{aligned} \overline{g}_b^{\lessgtr}(\omega) &= -2\pi i P^{\gtrless}(\widetilde{\varphi}_b)\delta(\omega - \widetilde{\gamma}_b) =: -\widetilde{g}_b^{\gtrless}(\omega) \\ \overline{g}_b^{\mathrm{A/R}}(\omega) &= \lim_{\eta\to 0^+} -\frac{1}{\omega - \widetilde{\gamma}_b \pm i\eta} \qquad =: -\widetilde{g}_b^{\mathrm{R/A}}(\omega) \end{aligned} \tag{2.3.13}$$

And finally the equations

$$\boxed{\begin{aligned} \langle\!\langle A;B\rangle\!\rangle_\omega^{\gtrless} &= \widetilde{g}_b^{\gtrless}(\omega)\,\langle\{A,B\}\rangle \quad + \widetilde{g}_b^{\mathrm{A}}(\omega)\langle\!\langle A;[H_1,B]\rangle\!\rangle_\omega^{\gtrless} + \widetilde{g}_b^{\gtrless}(\omega)\langle\!\langle A;[H_1,B]\rangle\!\rangle_\omega^{\mathrm{R}} \\ \langle\!\langle A;B\rangle\!\rangle_\omega^{\mathrm{R/A}} &= \widetilde{g}_b^{\mathrm{R/A}}(\omega)\,\langle\{A,B\}\rangle + \widetilde{g}_b^{\mathrm{R/A}}(\omega)\langle\!\langle A;[H_1,B]\rangle\!\rangle_\omega^{\mathrm{R/A}} \end{aligned}} \tag{2.3.14}$$

are found, or alternatively for the lesser and greater functions

$$\boxed{\langle\!\langle A;B\rangle\!\rangle_\omega^{\gtrless} = \frac{\widetilde{g}_b^{\gtrless}(\omega)}{\widetilde{g}_b^{\mathrm{R}}(\omega)}\langle\!\langle A;B\rangle\!\rangle_\omega^{\mathrm{R}} + \widetilde{g}_a^{\mathrm{A}}(\omega)\langle\!\langle A;[H_1,B]\rangle\!\rangle_\omega^{\gtrless}.} \tag{2.3.15}$$

For the case where the second operator is a creation operator, i.e. $B = c^\dagger$, the relations

$$\begin{aligned} \widetilde{\gamma}_{c^\dagger} &= \gamma_c \\ \widetilde{\varphi}_{c^\dagger} &= \varphi_c \end{aligned} \tag{2.3.16}$$

are found and further

$$\widetilde{g}_{c^\dagger}(\omega) = g_c(\omega). \tag{2.3.17}$$

Thus, the alternative definitions are not necessarily needed and the quantities can be obtained from the regular definition by treating B as annihilation operator.

2.4. Summary and *Plug-and-Play* Equations

In the current chapter, the framework for the equation-of-motion technique was set up in non-equilibrium and certain aspects were discussed in more detail. In this last section of the current chapter, the equations and definitions used in the subsequent chapters shall be summarized as a quick reference for the application-oriented reader.

The steady-state equations of motion for Green's functions of arbitrary odd products of creation- and annihilation operators

$$A = \prod_{i=1}^{2m+1} \alpha_i \quad \text{and} \quad B = \prod_{i=1}^{2n+1} \beta_i$$

in a fermionic system whose Hamiltonian is split in a part H_0, containing only number operator terms, and the rest H_1, containing hopping and interaction terms, are given by

$$\boxed{\begin{aligned} \langle\langle A;B\rangle\rangle_\omega^{\gtrless} &= \frac{g_a^{\gtrless}(\omega)}{g_a^{\mathrm{A}}(\omega)} \langle\langle A;B\rangle\rangle_\omega^{\mathrm{A}} \quad + g_a^{\mathrm{R}}(\omega) \langle\langle [A,H_1];B\rangle\rangle_\omega^{\gtrless} \\ \langle\langle A;B\rangle\rangle_\omega^{\mathrm{R/A}} &= g_a^{\mathrm{R/A}}(\omega)\, \langle\{A,B\}\rangle + g_a^{\mathrm{R/A}}(\omega) \langle\langle [A,H_1];B\rangle\rangle_\omega^{\mathrm{R/A}}, \end{aligned}}$$

where

$$\begin{aligned} g_a^{\mathrm{R/A}}(\omega) &= \frac{1}{\omega - \gamma_a \pm i\eta} \\ g_a^{\gtrless}(\omega) &= \frac{2i\eta}{(\omega-\gamma_a)^2+\eta^2} \left(f\left(\frac{\omega-\mu_a}{T}\right) - \delta_{\gtrless,>} \right), \end{aligned}$$

the (curly) square brackets denote the usual (anti)commutator and f denotes the Fermi function. The constants are obtained from

$$[A, H_0] = \gamma_a A \quad \text{and} \quad \mu_a = \gamma_a \Big|_{\varepsilon_i = \mu_i}.$$

For correlations with a single creation operator an alternative formulation is found, treating $c^\dagger$ as annihilation operator when determining the constants:

$$\boxed{\begin{aligned} \langle\langle A;c^\dagger\rangle\rangle_\omega^{\gtrless} &= \frac{g_c^{\gtrless}(\omega)}{g_c^{\mathrm{R}}(\omega)} \langle\langle A;c^\dagger\rangle\rangle_\omega^{\mathrm{R}} \quad + g_c^{\mathrm{A}}(\omega) \langle\langle A;\left[H_1,c^\dagger\right]\rangle\rangle_\omega^{\gtrless} \\ \langle\langle A;c^\dagger\rangle\rangle_\omega^{\mathrm{R/A}} &= g_c^{\mathrm{R/A}}(\omega) \left\langle\left\{A,c^\dagger\right\}\right\rangle + g_c^{\mathrm{R/A}}(\omega) \langle\langle A;\left[H_1,c^\dagger\right]\rangle\rangle_\omega^{\mathrm{R/A}} \end{aligned}}$$

3. The Interacting Resonant Level Model

In this chapter, the Interacting Resonant Level Model (IRLM) is shortly introduced and serves as an explicit example throughout the rest of the thesis on how to apply the equation-of-motion technique. This involves modelling the *leads* or *baths*, i.e. the large surroundings to which the interacting system is coupled, and aims at the fundamental set of equations describing the non-equilibrium Green's function problem in the IRLM.

The IRLM is a linear lattice model for spinless fermions, i.e. it involves fermionic creation- and annihilation operators with the usual anticommutation relations, but no explicit spin degree of freedom appears. It is chosen as benchmark model, as an exact expression for the current-voltage characteristic is available for a special parameter set known as the *self-dual* point. The solution is obtained in [15] and formulated in closed form as a hypergeometric function in [16]. Furthermore, the model exhibits an interesting feature due to interaction, namely negative differential conductance, i.e. the current through the system decreases with increasing voltage in a certain range (see [17]).

In its simplest form it consists of three lattice sites[I] and two baths of non-interacting electrons. As depicted in figure 3.1, the left (right) site $a(b)$ couples to states $k \in \mathrm{L(R)}$ and the inner sites are linearly connected via nearest-neighbour hopping. The electron interaction is reduced to inner neighbouring sites. The system is at temperature T, and the non-equilibrium situation is only evoked by different chemical potentials μ_i in the leads, accounting for a voltage applied to the system.

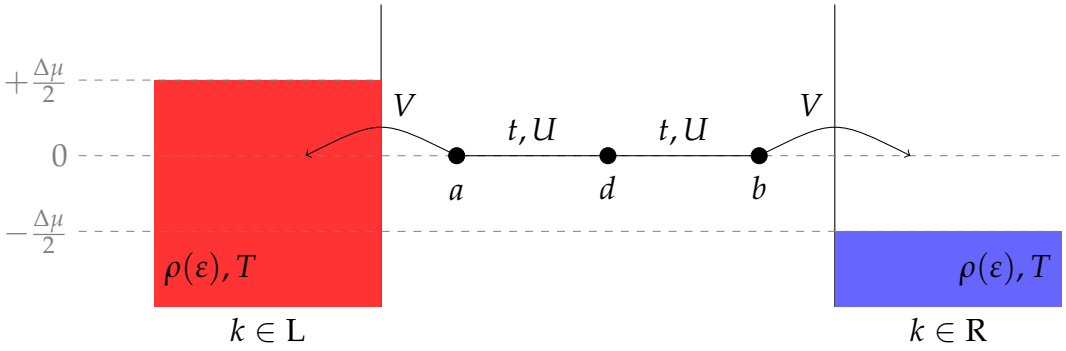

Figure 3.1.: Schematic representation of the IRLM and its system parameters.

The IRLM is described by a Hamiltonian $H = H_0 + H_1$, where

$$\begin{aligned} H_0 &= \varepsilon_d \hat{n} + \sum_{m=a,b} \varepsilon_m \hat{n}_m + \sum_{k\in \mathrm{L,R}} \varepsilon_k \hat{n}_k \\ H_1 &= \sum_{m=a,b} \left[-t \left(c_m^\dagger d + d^\dagger c_m \right) + U \hat{n}_m \hat{n} \right] - V \sum_{k\in \mathrm{L,R}} \left(c_{a,b}^\dagger c_k + c_k^\dagger c_{a,b} \right). \end{aligned} \tag{3.0.1}$$

[I] An extension to multiple inner sites d_i can be found in [18].

The operators $d^\dagger$ and d create and annihilate a particle on the central lattice site, the corresponding number operator is denoted simply by $\hat{n} = d^\dagger d$. The operators $c^\dagger_{a(b)}$, $c_{a(b)}$ and $\hat{n}_{a(b)}$ describe particles on the left (right) lattice site, and $c^\dagger_k$, c_k and $\hat{n}_k$ a particle in state k in the left (right) lead if $k \in \mathrm{L(R)}$. The on-site energies ε_k in the leads are defined via a certain density of states $\rho(\varepsilon)$ characterizing the type of lead, whereas $\varepsilon_d, \varepsilon_a$ and ε_b are parameters to choose. The other parameters t and V denote the so-called *hopping integrals*, describing the kinetic and potential energies related to a single-particle tunnelling from one site to another, where t connects the inner sites and V connects the system to the leads. And finally, U describes the electron-electron Coulomb repulsion between to neighbouring inner sites.

It can be shown[II] that this Hamiltonian is invariant under the particle-hole transformation

$$c_n \to (-1)^n c^\dagger_{-n}, \tag{3.0.2}$$

where c_n (and $c^\dagger_n$ respectively) maps to the the operators from above via

c_{-2}	c_{-1}	c_0	c_1	c_2
$c_{k\in\mathrm{L}}$	c_a	d	c_b	$c_{k\in\mathrm{R}}$

,

if the on-site energies fulfil the relations

$$\begin{aligned} 2\varepsilon_{a,b} = \varepsilon_d &= -U \\ \varepsilon_{k\in\mathrm{L}} &= \varepsilon_{k\in\mathrm{R}}. \end{aligned} \tag{3.0.3}$$

In fact, the exact solution is obtained for the particle-hole symmetric case, but for now the on-site energies remain general parameters in the following equations until particle-hole symmetry is applied explicitly.

3.1. Definition of the Current

The current through a system plays a major role in non-equilibrium physics and is usually calculated through the change in total particle number of a region x in the system. So, recalling equation (1.0.1) for electronic systems,

$$I_x = -e \left\langle \frac{\mathrm{d}\hat{N}_x}{\mathrm{d}t} \right\rangle = -ie \left\langle \left[H, \hat{N}_x\right] \right\rangle,$$

where e is the elementary charge and the commutator comes from the Heisenberg equation. In the IRLM, the current can be measured from the leads to the inner system or over the inner junctions. The two corresponding regions can be identified as simply left or right lead and a lead plus the neighbouring site a or b. As the current over the whole system must be conserved and the system is left-right symmetric, the currents sum up as

$$I_{i,\mathrm{L}} + I_{i,\mathrm{R}} = 0$$

[II] See section A.1.4 in the appendix for the proof.

and only one side needs to be considered. So, the two regions are characterized by the total number operators

$$\begin{aligned}\hat{N}_1 &= \sum_{k\in \mathrm{L}} \hat{n}_k \\ \hat{N}_2 &= \hat{n}_a + \sum_{k\in \mathrm{L}} \hat{n}_k.\end{aligned} \tag{3.1.1}$$

In order to obtain an expression for the current, the following commutators[III] with the Hamiltonian (3.0.1) are needed. The commutator from the left lead results in

$$\begin{aligned}\left[H, \sum_{k\in \mathrm{L}} \hat{n}_k\right] = \sum_{k\in \mathrm{L}} [H, \hat{n}_k] &= -V \sum_{k\in \mathrm{L}} \left[c_a^\dagger c_k + c_k^\dagger c_a, \hat{n}_k\right] \\ &= -V \sum_{k\in \mathrm{L}} \left(c_a^\dagger c_k - c_k^\dagger c_a\right)\end{aligned} \tag{3.1.2}$$

and for site a

$$\begin{aligned}[H, \hat{n}_a] &= \left[-t\left(c_a^\dagger d + d^\dagger c_a\right) - V \sum_{k\in \mathrm{L}} \left(c_a^\dagger c_k + c_k^\dagger c_a\right), \hat{n}_a\right] \\ &= +t\left(c_a^\dagger d - d^\dagger c_a\right) + V \sum_{k\in \mathrm{L}} \left(c_a^\dagger c_k - c_k^\dagger c_a\right) \\ &= +t\left(c_a^\dagger d - d^\dagger c_a\right) - \sum_{k\in \mathrm{L}} [H, \hat{n}_k],\end{aligned} \tag{3.1.3}$$

where the commutator (3.1.2) is used in the last step. And so, according to (1.0.1) the two currents are obtained as

$$\begin{aligned}I_1 &= -ie\left\langle\left[H, \hat{N}_1\right]\right\rangle = -ie \sum_{k\in \mathrm{L}} \langle [H, \hat{n}_k]\rangle = +ieV \sum_{k\in \mathrm{L}} \left(\left\langle c_a^\dagger c_k\right\rangle - \left\langle c_k^\dagger c_a\right\rangle\right) =: I_{\mathrm{L,lead}} \\ I_2 &= -ie\left\langle\left[H, \hat{N}_2\right]\right\rangle = -ie\left\langle [H, \hat{n}_a] + \sum_{k\in \mathrm{L}} [H, \hat{n}_k]\right\rangle = -iet\left(\left\langle c_a^\dagger d\right\rangle - \left\langle d^\dagger c_a\right\rangle\right) =: I_{\mathrm{L}},\end{aligned} \tag{3.1.4}$$

where the expectation values can be calculated by integrating over the corresponding lesser Green's function[IV].

3.2. Modelling of the Leads - Hybridization Strength

The IRLM includes two non-interacting leads that are coupled symmetrically to the system. As they appear as sums of operators creating and annihilating a particle with energy ε_k in the Hamiltonian, the resulting equations of motion naturally contain sums of some bath quantities $Q(\varepsilon_k; \omega)$.

[III] The equation-of-motion technique requires calculating a lot of commutators which can become quite cumbersome, and is further a popular source of (sign) errors. However, this tedious work can be avoided using some neat packages like the *Mathematica* package SNEG. See [19] for details and download information.

[IV] While I_2 is directly obtained from the expectation values needed for the later described self-consistency loop, I_1 is obtained from Green's functions as described in 5.5.

These energies ε_k, i.e. the inner structure of the leads, are not given explicitly, but encoded in a density of states $\rho(\varepsilon)$, so that the general procedure to calculate these terms is based on rewriting the sums as integrals over the given density:

$$\sum_k Q(\varepsilon_k;\omega) \to \int \mathrm{d}\varepsilon\, \rho(\varepsilon) Q(\varepsilon;\omega)$$

An important quantity connected to the single-particle Green's function is the so-called *hybridization function*

$$\Delta_{\mathrm{B}}^{\varkappa}(\omega) := V^2 \sum_{k\in\mathrm{B}} g_{c_k}^{\varkappa}(\omega) := V^2 \sum_{k\in\mathrm{B}} g_k^{\varkappa}(\omega),$$

where $\varkappa = <, >, \mathrm{R}, \mathrm{A}$ and $\mathrm{B} = \mathrm{L},\mathrm{R}$ stands for the left or right bath. The following commutator defines $\gamma_k := \gamma_{c_k}$, namely

$$[c_k, H_0] = \varepsilon_k c_k \to \gamma_k = \varepsilon_k,$$

and so according to (2.2.3) the retarded and advanced hybridization function read

$$\Delta_{\mathrm{B}}^{\mathrm{R/A}}(\omega) := \Delta_{\mathrm{B}}^{\pm}(\omega) := V^2 \sum_{k\in\mathrm{B}} g_k^{\mathrm{R/A}}(\omega) = \sum_{k\in\mathrm{B}} \frac{V^2}{\omega - \varepsilon_k \pm i\eta} = \left(\Delta_{\mathrm{B}}^{\mp}(\omega)\right)^*. \tag{3.2.1}$$

Assuming the system is at temperature $T = \beta^{-1}$ and the non-equilibrium is governed by the different chemical potentials of the leads μ_{B}, according to (2.2.24) and (2.2.51) the lesser and greater functions read

$$\Delta_{\mathrm{B}}^{\gtrless}(\omega) := V^2 \sum_{k\in\mathrm{B}} g_k^{\gtrless}(\omega) = V^2 \left(f_{\mathrm{B}}(\omega) - \delta_{\gtrless,>}\right) \sum_{k\in\mathrm{B}} \frac{2i\eta}{(\omega-\varepsilon_k)^2 + \eta^2}, \tag{3.2.2}$$

where

$$f_{\mathrm{B}}(\omega) = \frac{1}{1 + \mathrm{e}^{\beta(\omega-\mu_{\mathrm{B}})}}$$

is the Fermi function for the B (= L,R) bath. The imaginary parts[V] of $\Delta_{\mathrm{B}}^{\mathrm{R/A}}(\omega)$ and $\Delta_{\mathrm{B}}^{\gtrless}(\omega)$ are related to each other via

$$\begin{aligned} 2\left(f_{\mathrm{B}}(\omega) - \delta_{\gtrless,>}\right) \mathrm{Im}\left\{\Delta_{\mathrm{B}}^{\pm}(\omega)\right\} &= 2\left(f_{\mathrm{B}}(\omega) - \delta_{\gtrless,>}\right) \mathrm{Im}\left\{\sum_{k\in\mathrm{B}} \frac{V^2}{\omega - \varepsilon_k \pm i\eta}\right\} \\ &= \mp V^2 \left(f_{\mathrm{B}}(\omega) - \delta_{\gtrless,>}\right) \sum_{k\in\mathrm{B}} \frac{2\eta}{(\omega-\varepsilon_k)^2 + \eta^2} \\ &= \mp\, \mathrm{Im}\left\{\Delta_{\mathrm{B}}^{\gtrless}(\omega)\right\} \end{aligned} \tag{3.2.3}$$

and furthermore the relation

$$\Delta_{\mathrm{B}}^{-}(\omega) - \Delta_{\mathrm{B}}^{+}(\omega) = \Delta_{\mathrm{B}}^{<}(\omega) - \Delta_{\mathrm{B}}^{>}(\omega)$$

holds, as

$$\Delta_{\mathrm{B}}^{-}(\omega) - \Delta_{\mathrm{B}}^{+}(\omega) = V^2 \sum_{k\in\mathrm{B}} \left(\frac{1}{\omega - \varepsilon_k - i\eta} - \frac{1}{\omega - \varepsilon_k + i\eta}\right) = V^2 \sum_{k\in\mathrm{B}} \frac{2i\eta}{(\omega-\varepsilon_k)^2 + \eta^2}$$

[V] As $\Delta^{\gtrless}$ is purely imaginary, it is fully determined by $\mathrm{Im}\{\Delta^{\pm}\}$.

and

$$\Delta_{\mathrm{B}}^{<}(\omega) - \Delta_{\mathrm{B}}^{>}(\omega) = V^2 \left(f_{\mathrm{B}}(\omega) - f_{\mathrm{B}}(\omega) + 1\right) \sum_{k\in\mathrm{B}} \frac{2i\eta}{(\omega-\varepsilon_k)^2+\eta^2} = V^2 \sum_{k\in\mathrm{B}} \frac{2i\eta}{(\omega-\varepsilon_k)^2+\eta^2}.$$

With the help of the retarded or advanced part of $\Delta_{\mathrm{B}}^{\gtrless}(\omega)$ it is useful to define a unit of energy[VI] in which all parameters occurring in the Hamiltonian can be expressed. For symmetric leads the index B can be dropped as the sum is evaluated with the same density of states and so

$$\Delta_{\mathrm{L}}^{\pm}(\omega) = \Delta_{\mathrm{R}}^{\pm}(\omega) =: \Delta^{\pm}(\omega) = \sum_k \frac{V^2}{\omega - \varepsilon_k \pm i\eta}.$$

This unit is called hybridization strength Γ and is defined as follows:

$$\Gamma := \mp \operatorname{Im}\{\Delta^{\pm}(\omega = 0)\}$$

With the relation between the density of states and the non-interacting (and uncoupled) Green's functions,

$$\rho_{\mathrm{Lead}}(\omega) = \mp\frac{1}{\pi} \operatorname{Im}\left\{\sum_k g_k^{\mathrm{R/A}}(\omega)\right\},$$

the hybridization strength can be written as

$$\Gamma = \pi V^2 \rho(0)$$

which in turn defines the coupling to the leads V for a given density of states.

In the following the hybridization functions and strengths for the two types of leads, or densities of states respectively, used in this thesis are calculated explicitly keeping Γ in the equations. Yet, from section 3.3 on Γ is the designated energy scale and is therefore omitted in the equations.

3.2.1. Hybridization Function in the Wide-Band Limit

The simplest kind of lead is completely structureless and characterized by a density of states that is just a box, i.e. the lead energies are continuous within a certain range and evenly distributed. Expanding this range to infinity leads to a so-called flat-band bath in wide-band limit, which is defined through the density of states

$$\rho(\omega) = \lim_{D\to\infty} \frac{1}{2D} \Theta(D - |\omega|),$$

where $\Theta(x)$ denotes the Heaviside step function. The hybridization strength is then given by

$$\Gamma = \lim_{D\to\infty} \frac{\pi V^2}{2D}$$

[VI] Recalling the preliminary remarks on units, by choosing a certain unit of energy in the Hamiltonian parameters, the temperature T and the Fourier frequency ω become scaled as well, as they are both energies in the present unit system.

and so the hybridization V becomes

$$V = \lim_{D\to\infty} \sqrt{\frac{2D\Gamma}{\pi}}.$$

The limit in the density of states or in the hybridization must not be evaluated separately, but just when they occur together in a closed form (usually an evaluable explicit sum over k) like in the hybridization function:

$$\begin{aligned}\Delta^{\pm}(\omega) &= \sum_k \frac{V^2}{\omega - \varepsilon_k \pm i\eta} \\ &\to V^2 \int \mathrm{d}\varepsilon \, \frac{\rho(\varepsilon)}{\omega - \varepsilon \pm i\eta} \\ &= \lim_{D\to\infty} \frac{V^2}{2D} \int_{-D}^{D} \mathrm{d}\varepsilon \, \frac{1}{\omega - \varepsilon \pm i\eta} \\ &= \frac{\Gamma}{\pi} \lim_{D\to\infty} \left[\ln(\omega + D \pm i\eta) - \ln(\omega - D \pm i\eta)\right] = \mp i\Gamma\end{aligned} \tag{3.2.4}$$

The advantage of the wide-band limit becomes clear as the hybridization function loses its ω-dependence[VII] in the wide-band limit and results in a simple constant imaginary part.

3.2.2. Hybridization Function for a Semi-Infinite Tight-Binding Chain

A more complex lead can be introduced by a semi-infinite tight-binding chain described by the Hamiltonian

$$H_{\mathrm{TB}} = \varepsilon_{\mathrm{TB}} \sum_{i=0}^{N} \hat{n}_i - t_0 \sum_{i=0}^{N} \left(c_i^\dagger c_{i+1} + c_{i+1}^\dagger c_i\right) \quad \text{and } N \to \infty$$

and depicted in figure 3.2. The energy $\varepsilon_{\mathrm{TB}}$ is just an overall energy shift for the whole chain.

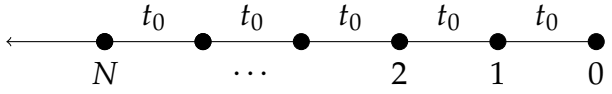

Figure 3.2.: Semi-infinite tight-binding chain

In this real-space representation, the system couples to the first site ($i = 0$) of the chain, whose density of states for $\varepsilon_{\mathrm{TB}} = 0$ is given by

$$\rho_{\mathrm{TB}}(\varepsilon) = \begin{cases} \frac{1}{2\pi t_0}\sqrt{4 - \left(\frac{\varepsilon}{t_0}\right)^2} & \text{if } |\varepsilon| \le 2t_0 \\ 0 & \text{otherwise.} \end{cases} \tag{3.2.5}$$

This leads to a hybridization strength of

$$\Gamma = \frac{\pi V^2 \sqrt{4}}{2\pi t_0}$$

[VII] See section A.1.5 in the appendix.

and further to

$$V = \sqrt{\Gamma t_0}.$$

With these definitions, the hybridization function reads

$$\begin{aligned}\Delta^{\pm}(\omega) &= \sum_k \frac{V^2}{\omega - \varepsilon_k \pm i\eta} \\ &\to V^2 \int \mathrm{d}\varepsilon' \, \frac{\rho_{\mathrm{TB}}(\varepsilon')}{\omega - \varepsilon' \pm i\eta} \\ &= \frac{\Gamma t_0}{2\pi t_0} \int_{-2t_0}^{2t_0} \frac{\mathrm{d}\varepsilon'}{\omega - \varepsilon' \pm i\eta} \sqrt{4 - \left(\frac{\varepsilon'}{t_0}\right)^2} \\ &= \frac{\Gamma}{2\pi} \int_{-2}^{2} \mathrm{d}\varepsilon \, \frac{\sqrt{4-\varepsilon^2}}{\omega_0^{\pm} - \varepsilon} =: \frac{\Gamma}{2\pi} I^{\pm}(\omega),\end{aligned} \tag{3.2.6}$$

where the in the last step the substitution $\varepsilon' = t_0\varepsilon$ is applied and $\omega_0^{\pm} = t_0^{-1}(\omega \pm i\eta)$. Within a ridiculously short calculation[VIII] the integral evaluates to

$$I^{\pm}(\omega) = \pi \left(\omega_0^{\pm} \mp i\sqrt{4 - \left(\omega_0^{\pm}\right)^2} \right) \tag{3.2.7}$$

and so for a chain with $t_0 = 1\Gamma$ the hybridization function becomes

$$\Delta^{\pm} = \frac{1}{2} \left(\omega^{\pm} \mp i\sqrt{4\Gamma^2 - \left(\omega^{\pm}\right)^2} \right) \tag{3.2.8}$$

which is the well-known result for the semi-infinite tight-binding chain (see, e.g., chapter 19 in [20]). The principal value is intended for the square roots in (3.2.7) and (3.2.8), i.e. $\mathrm{Re}\left\{\sqrt{\dots}\right\} \geq 0$ must be ensured in the numerical evaluation.

3.3. Equations of Motion and Sets of Equations

As shown in the previous chapter, the equations of motion for the different Green's functions can be expressed in two forms, one of which leads to a hierarchy in the first operator and the other one in the second. In this thesis, as well as in most literature, only the first form is used for setting up the sets of equations. This choice is arbitrary and should not change the result. The second form is only used where expectation values of operators containing a bath creation operator are needed, as this gives an exact and simple relation for the underlying Green's function.

Correlation functions, or greater/lesser Green's functions, are needed in order to calculate non-equilibrium expectation values directly. Their equations of motion (2.2.44) involve retarded and advanced Green's functions, which themselves need to be solved first[IX] via

[VIII] See section A.2.2 in the appendix. Besides the direct evaluation of the integral, an alternative derivation of the hybridization function is shown in A.1.7, where no explicit density of states is needed.

[IX] As seen in later chapters, the sets of equations differ only in the inhomogeneous term and formally have the same solution, assuming a general inhomogeneous term.

their equations of motion. In the following, the single-particle retarded and advanced Green's function do not appear explicitly, but are rewritten as

$$\widetilde{\omega}_A := \left(g_a^{\mathrm{R/A}}(\omega)\right)^{-1}$$

in order to emphasize the ω-dependence in the sets of equations. With this definition and according to (2.2.43), the equation of motion for the retarded and advanced Green's function is given by

$$\widetilde{\omega}_A \langle\langle A; B^\dagger \rangle\rangle = \left\langle \left\{ A, B^\dagger \right\} \right\rangle + \langle\langle [A, H_1]; B^\dagger \rangle\rangle, \tag{3.3.1}$$

where

$$\widetilde{\omega}_A \equiv \widetilde{\omega}_A^{\pm} = \omega - \gamma_A \pm i\eta$$

defines the retarded (upper sign) and advanced (lower sign) function, and γ_A is determined by

$$A\gamma_A = [A, H_0].$$

As the imaginary part of the Green's function is introduced only via $\pm i\eta$, it is assured that the advanced and retarded functions are connected through complex conjugation, i.e.

$$\left(\langle\langle A; B^\dagger \rangle\rangle^{\mathrm{R}}\right)^* = \langle\langle A; B^\dagger \rangle\rangle^{\mathrm{A}}.$$

In order to set up the equations of motion for the desired Green's functions, the commutators with H_1 and the anticommutators of all operator pairs need to be evaluated. Even when starting with a supposedly simple quantity like the occupation number on the central site $\langle \hat{n} \rangle = \langle d^\dagger d \rangle$, it becomes clear that the equations of motion for the relevant Green's functions, i.e. $\langle\langle d; d^\dagger \rangle\rangle^<$ and $\langle\langle d; d^\dagger \rangle\rangle^{\mathrm{R/A}}$, open up a minimal set of equations that needs to be considered for two-operator Green's functions. In the case for $\langle \hat{n} \rangle$ this system consists of all two-operator functions $\langle\langle x; d^\dagger \rangle\rangle^{\varkappa}$, where x stands for the system's annihilation operators c_a, c_b, c_k, d and $\varkappa$ for the lesser, greater, retarded and advanced part of the Green's function.

A similar set is needed for the occupation numbers on site a and b and for a complete description of the current through the system. These *fundamental* sets of equations are described by the commutators

$$\begin{aligned}
[d, H_1] &= \sum_{m=\{a,b\}} \left[d, -td^\dagger c_m + U\hat{n}_m \hat{n} \right] = -t(c_a + c_b) + Ud(\hat{n}_a + \hat{n}_b) \\
[c_{a,b}, H_1] &= \left[c_{a,b}, -tc_{a,b}^\dagger d + U\hat{n}_{a,b}\hat{n} - V \sum_{k\in \mathrm{L,R}} c_{a,b}^\dagger c_k \right] = -td + Uc_{a,b}\hat{n} - V \sum_{k\in \mathrm{L,R}} c_k \\
[c_k, H_1] &= -V\left[c_k, c_k^\dagger c_{a,b} \right] = -Vc_{a,b} \text{ for } k \in \mathrm{L,R} \\
\left[H_1, c_k^\dagger \right] &= -Vc_{a,b}^\dagger \text{ for } k \in \mathrm{L,R}
\end{aligned} \tag{3.3.2}$$

and the anticommutators

$$\begin{aligned}
\left\{ d, d^\dagger \right\} = \left\{ c_a, c_a^\dagger \right\} = \left\{ c_b, c_b^\dagger \right\} = 1 \\
\left\{ d, c_{a,b}^\dagger \right\} = \left\{ d, c_k^\dagger \right\} = \left\{ c_{a,b}, c_{b,a}^\dagger \right\} = \left\{ c_{a,b}, c_k^\dagger \right\} = 0.
\end{aligned} \tag{3.3.3}$$

The fundamental sets for the retarded and advanced Green's functions are in principle three independent sets of equations, namely one in $d^\dagger$,

$$\begin{aligned}
\widetilde{\omega}_d \langle\langle d; d^\dagger \rangle\rangle &= 1 - t\left(\langle\langle c_a; d^\dagger\rangle\rangle + \langle\langle c_b; d^\dagger\rangle\rangle\right) + U\left(\langle\langle d\hat{n}_a; d^\dagger\rangle\rangle + \langle\langle d\hat{n}_b; d^\dagger\rangle\rangle\right) \\
\left(\widetilde{\omega}_a - \sum_{k\in \mathrm{L}} \frac{V^2}{\widetilde{\omega}_k}\right)\langle\langle c_a; d^\dagger\rangle\rangle &= -t\langle\langle d; d^\dagger\rangle\rangle + U\langle\langle c_a\hat{n}; d^\dagger\rangle\rangle \\
\left(\widetilde{\omega}_b - \sum_{k\in \mathrm{R}} \frac{V^2}{\widetilde{\omega}_k}\right)\langle\langle c_b; d^\dagger\rangle\rangle &= -t\langle\langle d; d^\dagger\rangle\rangle + U\langle\langle c_b\hat{n}; d^\dagger\rangle\rangle
\end{aligned} \tag{3.3.4}$$

and one each in $c_a^\dagger$ and $c_b^\dagger$,

$$\begin{aligned}
\widetilde{\omega}_d \langle\langle d; c_{a,b}^\dagger \rangle\rangle &= -t\left(\langle\langle c_a; c_{a,b}^\dagger\rangle\rangle + \langle\langle c_b; c_{a,b}^\dagger\rangle\rangle\right) + U\left(\langle\langle d\hat{n}_a; c_{a,b}^\dagger\rangle\rangle + \langle\langle d\hat{n}_b; c_{a,b}^\dagger\rangle\rangle\right) \\
\left(\widetilde{\omega}_{a,b} - \sum_{k\in \mathrm{L,R}} \frac{V^2}{\widetilde{\omega}_k}\right)\langle\langle c_{a,b}; c_{a,b}^\dagger\rangle\rangle &= 1 - t\langle\langle d; c_{a,b}^\dagger\rangle\rangle + U\langle\langle c_{a,b}\hat{n}; c_{a,b}^\dagger\rangle\rangle \\
\left(\widetilde{\omega}_{b,a} - \sum_{k\in \mathrm{R,L}} \frac{V^2}{\widetilde{\omega}_k}\right)\langle\langle c_{b,a}; c_{a,b}^\dagger\rangle\rangle &= -t\langle\langle d; c_{a,b}^\dagger\rangle\rangle + U\langle\langle c_{b,a}\hat{n}; c_{a,b}^\dagger\rangle\rangle,
\end{aligned} \tag{3.3.5}$$

where γ turns out to be just the corresponding on-site energy and so $\widetilde{\omega}_i \equiv \widetilde{\omega}_i^\pm = \omega - \varepsilon_i \pm i\eta$ for the retarded (upper sign) and advanced (lower sign) Green's function. The simple equation of motion for a Green's function with one bath annihilation operator,

$$\langle\langle c_k; x^\dagger\rangle\rangle = -V\frac{\langle\langle c_{a,b}; x^\dagger\rangle\rangle}{\widetilde{\omega}_k} \text{ for } k \in \mathrm{L,R},$$

has already been inserted in the above equation sets. Following the form (3.3.1) of the equation of motion only the first operator changes, while the second[X] remains the same in the whole hierarchy of equations. However, the equations for higher Green's functions in a specific creation operator might contain expectation values whose underlying Green's functions are described in the set of another creation operator. This means that the three sets of equations can formally be solved independently, but not evaluated numerically, as the solutions still contain expectation values that are calculated in a self-consistency loop. Therefore, all Green's functions and occurring expectation values need to be calculated simultaneously, which increases, of course, the effort, but a converged calculation provides then access to all two-operator quantities.

With the definition of $\widetilde{\omega}$, the equations of motion for lesser and greater Green's functions can be written as (cf. (2.2.44))

$$\widetilde{\omega}_A^+ \langle\langle A; B^\dagger\rangle\rangle^{\gtrless} = g_A^{\gtrless}|\widetilde{\omega}_A|^2\langle\langle A; B^\dagger\rangle\rangle^{\mathrm{A}} + \langle\langle [A, H_1]; B^\dagger\rangle\rangle^{\gtrless},$$

where

$$\begin{aligned}
g_A^{\gtrless}|\widetilde{\omega}_A|^2 &= 2iP_A^{\gtrless}(\omega)\frac{\eta}{(\omega-\varepsilon_A)^2+\eta^2}\left[(\omega-\varepsilon_A)^2+\eta^2\right] \\
&= 2i\eta P_A^{\gtrless}(\omega) \\
&= 2i\eta\left(f_A(\omega) - \delta_{\gtrless,>}\right)
\end{aligned} \tag{3.3.6}$$

[X] The second operator is here always a creation operator as correlations between two annihilation (or two creation) operators are zero in a particle-conserving fermionic system.

and

$$f_A(\omega) := \left(1 + \mathrm{e}^{\beta(\omega-\mu_A)}\right)^{-1}$$

is the Fermi function at the inverse temperature β. Although it might seem appealing to simply set the factors $g_A^{\gtrless}|\widetilde{\omega}_A|^2$ to zero as they are of $\mathcal{O}(\eta)$, this may lead to inconsistencies and wrong results. These terms are still understood as limit $\eta \to 0^+$ which has to be taken in the end of a calculation for the whole Green's function. In practice, these terms will vanish in the limit if the product

$$\langle\langle A; B^\dagger\rangle\rangle^{\mathrm{R}} \langle\langle A; B^\dagger\rangle\rangle^{\mathrm{A}} = \left|\langle\langle A; B^\dagger\rangle\rangle\right|^2$$

has no poles, which is the case for situations where the system has no isolated states. If a system exhibits such behaviour, terms like

$$\mathcal{O}(\eta)\left|\langle\langle A; B^\dagger\rangle\rangle\right|^2 \propto \delta(\omega_{AB})$$

become delta peaks that do not vanish in the limit and give a finite contribution to the expectation values. This is shown explicitly for tight-binding leads in section 4.2, where states appear outside the bandwidth of the leads. Therefore, in the following calculations η is kept in each term it appears.

Applying the equations of motion to the lesser and greater Green's functions leads to equation sets similar to (3.3.4) and (3.3.5) that can be represented in a general form for $x = d, c_a, c_b$, namely

$$\begin{aligned}
\widetilde{\omega}_d^+ \langle\langle d; x^\dagger\rangle\rangle^{\gtrless} &= g_d^{\gtrless}|\widetilde{\omega}_d|^2 \langle\langle d; x^\dagger\rangle\rangle^{\mathrm{A}} - t\left(\langle\langle c_a; x^\dagger\rangle\rangle^{\gtrless} + \langle\langle c_b; x^\dagger\rangle\rangle^{\gtrless}\right) \\
&\quad + U\left(\langle\langle d\hat{n}_a; x^\dagger\rangle\rangle^{\gtrless} + \langle\langle d\hat{n}_b; x^\dagger\rangle\rangle^{\gtrless}\right) \\
\left(\widetilde{\omega}_a^+ - \sum_{k\in\mathrm{L}} \frac{V^2}{\widetilde{\omega}_k^+}\right) \langle\langle c_a; x^\dagger\rangle\rangle^{\gtrless} &= \left(g_a^{\gtrless}|\widetilde{\omega}_a|^2 + V^2 \sum_{k\in\mathrm{L}} g_k^{\gtrless}\right) \langle\langle c_a; x^\dagger\rangle\rangle^{\mathrm{A}} - t\langle\langle d; x^\dagger\rangle\rangle^{\gtrless} \\
&\quad + U\langle\langle c_a\hat{n}; x^\dagger\rangle\rangle^{\gtrless} \\
\left(\widetilde{\omega}_b^+ - \sum_{k\in\mathrm{R}} \frac{V^2}{\widetilde{\omega}_k^+}\right) \langle\langle c_b; x^\dagger\rangle\rangle^{\gtrless} &= \left(g_b^{\gtrless}|\widetilde{\omega}_b|^2 + V^2 \sum_{k\in\mathrm{R}} g_k^{\gtrless}\right) \langle\langle c_b; x^\dagger\rangle\rangle^{\mathrm{A}} - t\langle\langle d; x^\dagger\rangle\rangle^{\gtrless} \\
&\quad + U\langle\langle c_b\hat{n}; x^\dagger\rangle\rangle^{\gtrless},
\end{aligned} \tag{3.3.7}$$

where the lead part

$$\langle\langle c_{k_{\mathrm{L,R}}}; x^\dagger\rangle\rangle^{\gtrless} = -V\left(g_{k_{\mathrm{L,R}}}^{\gtrless}\langle\langle c_{a,b}; x^\dagger\rangle\rangle^{\mathrm{A}} + \frac{\langle\langle c_{a,b}; x^\dagger\rangle\rangle^{\gtrless}}{\widetilde{\omega}_{k_{\mathrm{L,R}}}^+}\right) \tag{3.3.8}$$

is already inserted.

The framework and the fundamental equations are now set up. Concrete calculations and results are shown in the following chapters for different types of baths and different treatments of the electron-electron interaction that shows up as the Green's functions

$$U\langle\langle d\hat{n}_{a,b}; x^\dagger\rangle\rangle^{\lessgtr} \text{ and } U\langle\langle c_{a,b}\hat{n}; x^\dagger\rangle\rangle^{\lessgtr}.$$

4. Interaction in First-Order Truncation – Hartree-Fock Approximation

The equation sets in section 3.3 contain higher Green's functions, i.e. they consist of more than two operators, that themselves are described by equations of motion that in turn generate new and even higher Green's functions. In fact, as the system is infinite and takes interactions into account, the equations of motion lead to an infinite hierarchy of equations. In order to find at least an approximate solution, this hierarchy needs to be truncated in some way.

A common truncation scheme in Green's function methods is a mean-field like approximation to higher products of operators in Green's functions (see [3], [21] or [22] for applications and [23] for technical details). This is done by replacing a higher product of operators by the sum of its lower products acting in the mean field of the rest and taking care of the signs due to fermionic commutation.

In first order, i.e. starting from the fundamental equation sets, two types of operators are approximated as[I]

$$\begin{aligned} d\hat{n}_{a,b} = dc^\dagger_{a,b}c_{a,b} &\to \left\langle \hat{n}_{a,b} \right\rangle d - \left\langle c^\dagger_{a,b} d \right\rangle c_{a,b} \\ c_{a,b}\hat{n} = c_{a,b}d^\dagger d &\to \left\langle \hat{n} \right\rangle c_{a,b} - \left\langle d^\dagger c_{a,b} \right\rangle d, \end{aligned} \tag{4.0.1}$$

which closes the sets of equations and requires a self-consistent solution for the expectation values that are calculated by integrating over the lesser Green's function according to (2.2.39).

Applying the approximations (4.0.1) to the fundamental equation sets (3.3.4) and (3.3.5) leads to

$$\begin{aligned} \left[\widetilde{\omega}_d - U\left(\langle \hat{n}_a \rangle + \langle \hat{n}_b \rangle\right)\right] \langle\langle d; d^\dagger \rangle\rangle &= 1 - \tau_a \langle\langle c_a; d^\dagger \rangle\rangle - \tau_b \langle\langle c_b; d^\dagger \rangle\rangle \\ \left(\widetilde{\omega}_a - U\langle \hat{n} \rangle - \sum_{k\in \mathrm{L}} \frac{V^2}{\widetilde{\omega}_k}\right) \langle\langle c_a; d^\dagger \rangle\rangle &= -\tau_a^* \langle\langle d; d^\dagger \rangle\rangle \\ \left(\widetilde{\omega}_b - U\langle \hat{n} \rangle - \sum_{k\in \mathrm{R}} \frac{V^2}{\widetilde{\omega}_k}\right) \langle\langle c_b; d^\dagger \rangle\rangle &= -\tau_b^* \langle\langle d; d^\dagger \rangle\rangle \end{aligned} \tag{4.0.2}$$

[I] Note that in comparable spin systems like the Anderson model the interaction takes place between opposite spins on the same site and therefore operators of that type are approximated only by the first term with $\langle \hat{n}_i \rangle$, as the second term with a hopping correlation involves a spin flip which is usually neglected, cf. [3].

and

$$\begin{aligned}
\left[\widetilde{\omega}_d - U\left(\langle\hat{n}_a\rangle + \langle\hat{n}_b\rangle\right)\right]\langle\langle d; c_a^\dagger\rangle\rangle &= -\tau_a\langle\langle c_a; c_a^\dagger\rangle\rangle - \tau_b\langle\langle c_b; c_a^\dagger\rangle\rangle \\
\left(\widetilde{\omega}_a - U\langle\hat{n}\rangle - \sum_{k\in\mathrm{L}}\frac{V^2}{\widetilde{\omega}_k}\right)\langle\langle c_a; c_a^\dagger\rangle\rangle &= 1 - \tau_a^*\langle\langle d; c_a^\dagger\rangle\rangle \\
\left(\widetilde{\omega}_b - U\langle\hat{n}\rangle - \sum_{k\in\mathrm{R}}\frac{V^2}{\widetilde{\omega}_k}\right)\langle\langle c_b; c_a^\dagger\rangle\rangle &= -\tau_b^*\langle\langle d; c_a^\dagger\rangle\rangle,
\end{aligned} \tag{4.0.3}$$

where

$$\begin{aligned}
\tau_m &= t + U\left\langle c_m^\dagger d\right\rangle \\
\tau_m^* &= t + U\left\langle d^\dagger c_m\right\rangle.
\end{aligned} \tag{4.0.4}$$

For the sake of clarity, the set (4.0.3) and the following solutions are only shown for the equations in $c_a^\dagger$. As the system is symmetric in a and b the solutions are obtained by simply replacing $a \to b$, $\mathrm{L} \to \mathrm{R}$ and vice versa. In comparison to a system with no interaction (obtained by setting $U = 0$ in the fundamental equation sets), the applied truncation introduces, in a sense, effective system parameters. The on-site energies feel the influence of the occupation numbers, namely

$$\begin{aligned}
\varepsilon_d &\to \varepsilon_d \quad + U\left(\langle\hat{n}_a\rangle + \langle\hat{n}_b\rangle\right) \\
\varepsilon_{a,b} &\to \varepsilon_{a,b} + U\langle\hat{n}\rangle
\end{aligned} \tag{4.0.5}$$

and the hopping t splits into four effective complex hoppings by the influence of the hopping correlations, i.e.

$$t \to \tau_m, \tau_m^*. \tag{4.0.6}$$

It is worth mentioning that this truncation is equivalent to a direct Hartree-Fock approximation in the Hamiltonian term $\hat{n}_m\hat{n}$, namely (cf. [18])

$$\begin{aligned}
\hat{n}_m\hat{n} \to{}& \langle\hat{n}_m\rangle\,\hat{n} + \langle\hat{n}\rangle\,\hat{n}_m - \langle\hat{n}_m\rangle\langle\hat{n}\rangle \\
&- \left\langle c_m^\dagger d\right\rangle d^\dagger c_m - \left\langle d^\dagger c_m\right\rangle c_m^\dagger d + \left\langle c_m^\dagger d\right\rangle\left\langle d^\dagger c_m\right\rangle.
\end{aligned} \tag{4.0.7}$$

The Hartree-Fock Hamiltonian reads then

$$\begin{aligned}
H_{\mathrm{HF}} = {}& \left[\varepsilon_d + U\left(\langle\hat{n}_a\rangle + \langle\hat{n}_b\rangle\right)\right]\hat{n} + \sum_{m=a,b}\left[\left(\varepsilon_m + U\langle\hat{n}\rangle\right)\hat{n}_m - U\langle\hat{n}_m\rangle\langle\hat{n}\rangle\right] + \sum_{k\in\mathrm{L,R}}\varepsilon_k\hat{n}_k \\
&- \sum_{m=a,b}\left[\tau_m^* c_m^\dagger d + \tau_m d^\dagger c_m - U\left\langle c_m^\dagger d\right\rangle\left\langle d^\dagger c_m\right\rangle\right] - V\sum_{k\in\mathrm{L,R}}\left(c_{a,b}^\dagger c_k + c_k^\dagger c_{a,b}\right),
\end{aligned} \tag{4.0.8}$$

where the same effective parameters appear. So apart from the constant terms this describes exactly a non-interacting system with effective parameters as in (4.0.2) and (4.0.3). The constant terms are irrelevant as they get completely lost in commutators with the Hamiltonian.

The solutions to the sets of linear equations are given by

$$\begin{aligned}
\langle\langle d; d^\dagger \rangle\rangle &= \left[\widetilde{\omega}_d - U\left(\langle \hat{n}_a \rangle + \langle \hat{n}_b \rangle\right) - \sum_{m=a,b} \frac{\tau_m \tau_m^*}{\widetilde{\omega}_m - U\langle \hat{n} \rangle - \sum_{k_m} \frac{V^2}{\widetilde{\omega}_k}} \right]^{-1} \\
\langle\langle c_a; c_a^\dagger \rangle\rangle &= \left[\widetilde{\omega}_a - U\langle \hat{n} \rangle - \sum_{k\in \mathrm{L}} \frac{V^2}{\widetilde{\omega}_k} - \frac{\tau_a \tau_a^*}{\widetilde{\omega}_d - U\left(\langle \hat{n}_a \rangle + \langle \hat{n}_b \rangle\right) - \dfrac{\tau_b \tau_b^*}{\widetilde{\omega}_b - U\langle \hat{n} \rangle - \sum_{k\in \mathrm{R}} \frac{V^2}{\widetilde{\omega}_k}}} \right]^{-1},
\end{aligned} \tag{4.0.9}$$

where

$$\begin{aligned}
k_a &= k \in \mathrm{L} \\
k_b &= k \in \mathrm{R}.
\end{aligned}$$

The solutions to the other fundamental retarded and advanced Green's functions are not shown explicitly as they can simply be obtained by inserting the above solutions in (4.0.2) and (4.0.3).

Analogous to the retarded and advanced sets of equations the approximated equations for the lesser and greater functions become

$$\begin{aligned}
\left[\widetilde{\omega}_d^+ - U\left(\langle \hat{n}_a \rangle + \langle \hat{n}_b \rangle\right)\right] \langle\langle d; x^\dagger \rangle\rangle^{\gtrless} &= g_d^{\gtrless} |\widetilde{\omega}_d|^2 \langle\langle d; x^\dagger \rangle\rangle^{\mathrm{A}} - \tau_a \langle\langle c_a; x^\dagger \rangle\rangle^{\gtrless} - \tau_b \langle\langle c_b; x^\dagger \rangle\rangle^{\gtrless} \\
\left(\widetilde{\omega}_a^+ - U\langle \hat{n} \rangle - \sum_{k\in \mathrm{L}} \frac{V^2}{\widetilde{\omega}_k^+}\right) \langle\langle c_a; x^\dagger \rangle\rangle^{\gtrless} &= \left(g_a^{\gtrless} |\widetilde{\omega}_a|^2 + V^2 \sum_{k\in \mathrm{L}} g_k^{\gtrless}\right) \langle\langle c_a; x^\dagger \rangle\rangle^{\mathrm{A}} - \tau_a^* \langle\langle d; x^\dagger \rangle\rangle^{\gtrless} \\
\left(\widetilde{\omega}_b^+ - U\langle \hat{n} \rangle - \sum_{k\in \mathrm{R}} \frac{V^2}{\widetilde{\omega}_k^+}\right) \langle\langle c_b; x^\dagger \rangle\rangle^{\gtrless} &= \left(g_b^{\gtrless} |\widetilde{\omega}_b|^2 + V^2 \sum_{k\in \mathrm{R}} g_k^{\gtrless}\right) \langle\langle c_b; x^\dagger \rangle\rangle^{\mathrm{A}} - \tau_b^* \langle\langle d; x^\dagger \rangle\rangle^{\gtrless}.
\end{aligned} \tag{4.0.10}$$

The solution to the central-site equations is given by

$$\begin{aligned}
&\left[\widetilde{\omega}_d^+ - U\left(\langle \hat{n}_a \rangle + \langle \hat{n}_b \rangle\right) - \sum_{m=a,b} \frac{\tau_m \tau_m^*}{\widetilde{\omega}_m^+ - U\langle \hat{n} \rangle - \sum_k \frac{V^2}{\widetilde{\omega}_k^+}} \right] \langle\langle d; d^\dagger \rangle\rangle^{\gtrless} \\
&= g_d^{\gtrless} |\widetilde{\omega}_d|^2 \langle\langle d; d^\dagger \rangle\rangle^{\mathrm{A}} - \sum_{m=a,b} \frac{\tau_m \left(g_m^{\gtrless} |\widetilde{\omega}_m|^2 + V^2 \sum_{k\in \mathrm{L}} g_k^{\gtrless}\right)}{\widetilde{\omega}_m^+ - U\langle \hat{n} \rangle - \sum_k \frac{V^2}{\widetilde{\omega}_k^+}} \langle\langle c_m; d^\dagger \rangle\rangle^{\mathrm{A}} \\
&= \langle\langle d; d^\dagger \rangle\rangle^{\mathrm{A}} \left[g_d^{\gtrless} |\widetilde{\omega}_d|^2 + \sum_{m=a,b} \frac{\tau_m \tau_m^* \left(g_m^{\gtrless} |\widetilde{\omega}_m|^2 + V^2 \sum_{k\in \mathrm{L}} g_k^{\gtrless}\right)}{\left|\widetilde{\omega}_m - U\langle \hat{n} \rangle - \sum_k \frac{V^2}{\widetilde{\omega}_k}\right|^2} \right],
\end{aligned} \tag{4.0.11}$$

where equations from (4.0.2) have been used in the last step. The prefactor of $\langle\langle d; d^\dagger \rangle\rangle^{\gtrless}$ can be identified as the inverse of the corresponding retarded Green's function $\langle\langle d; d^\dagger \rangle\rangle^{\mathrm{R}}$, so that the final result can be written as

$$\langle\langle d; d^\dagger \rangle\rangle^{\gtrless} = \left|\langle\langle d; d^\dagger \rangle\rangle\right|^2 \left[g_d^{\gtrless} |\widetilde{\omega}_d|^2 + \sum_{m=a,b} \frac{\tau_m \tau_m^* \left(g_m^{\gtrless} |\widetilde{\omega}_m|^2 + V^2 \sum_{k_m} g_k^{\gtrless}\right)}{\left|\widetilde{\omega}_m - U\langle \hat{n} \rangle - \sum_{k_m} \frac{V^2}{\widetilde{\omega}_k}\right|^2} \right]. \tag{4.0.12}$$

The solution to the left-site equations is given by

$$\begin{aligned}
&\left[\widetilde{\omega}_a^+ - U\langle\hat{n}\rangle - \sum_{k\in\mathrm{L}}\frac{V^2}{\widetilde{\omega}_k^+} - \frac{\tau_a\tau_a^*}{\widetilde{\omega}_d^+ - U\left(\langle\hat{n}_a\rangle + \langle\hat{n}_b\rangle\right) - \dfrac{\tau_b\tau_b^*}{\widetilde{\omega}_b^+ - U\langle\hat{n}\rangle - \sum_{k\in\mathrm{R}}\frac{V^2}{\widetilde{\omega}_k^+}}}\right]\langle\langle c_a; c_a^\dagger\rangle\rangle^{\gtrless} \\
&= \left(g_a^{\gtrless}|\widetilde{\omega}_a|^2 + V^2\sum_{k\in\mathrm{L}} g_k^{\gtrless}\right)\langle\langle c_a; c_a^\dagger\rangle\rangle^{\mathrm{A}} - \frac{\tau_a^* g_d^{\gtrless}|\widetilde{\omega}_d|^2}{\widetilde{\omega}_d^+ - U(\langle\hat{n}_a\rangle + \langle\hat{n}_b\rangle) - \frac{\tau_b\tau_b^*}{\widetilde{\omega}_b^+ - U\langle\hat{n}\rangle - \sum_{k\in\mathrm{R}}\frac{V^2}{\widetilde{\omega}_k^+}}}\langle\langle d; c_a^\dagger\rangle\rangle^{\mathrm{A}} \\
&+ \frac{\tau_b\tau_a^*\left(g_b^{\gtrless}|\widetilde{\omega}_b|^2 + V^2\sum_{k\in\mathrm{R}} g_k^{\gtrless}\right)}{\left[\widetilde{\omega}_d^+ - U\left(\langle\hat{n}_a\rangle + \langle\hat{n}_b\rangle\right)\right]\left(\widetilde{\omega}_b^+ - U\langle\hat{n}\rangle - \sum_{k\in\mathrm{R}}\frac{V^2}{\widetilde{\omega}_k^+}\right) - \tau_b\tau_b^*}\langle\langle c_b; c_a^\dagger\rangle\rangle^{\mathrm{A}}
\end{aligned}$$

$$\begin{aligned}
&= \langle\langle c_a; c_a^\dagger\rangle\rangle^{\mathrm{A}}\left\{g_a^{\gtrless}|\widetilde{\omega}_a|^2 + V^2\sum_{k\in\mathrm{L}} g_k^{\gtrless} + \frac{\tau_a\tau_a^* g_d^{\gtrless}|\widetilde{\omega}_d|^2}{\left|\widetilde{\omega}_d - U(\langle\hat{n}_a\rangle + \langle\hat{n}_b\rangle) - \frac{\tau_b\tau_b^*}{\widetilde{\omega}_b - U\langle\hat{n}\rangle - \sum_{k\in\mathrm{R}}\frac{V^2}{\widetilde{\omega}_k}}\right|^2}\right. \\
&\left. + \frac{\tau_a\tau_a^*\tau_b\tau_b^*\left(g_b^{\gtrless}|\widetilde{\omega}_b|^2 + V^2\sum_{k\in\mathrm{R}} g_k^{\gtrless}\right)}{\left|\left[\widetilde{\omega}_d - U\left(\langle\hat{n}_a\rangle + \langle\hat{n}_b\rangle\right)\right]\left(\widetilde{\omega}_b - U\langle\hat{n}\rangle - \sum_{k\in\mathrm{R}}\frac{V^2}{\widetilde{\omega}_k}\right) - \tau_b\tau_b^*\right|^2}\right\},
\end{aligned} \tag{4.0.13}$$

where equations from (4.0.3) have been used in the last step. Similar to the central-site solution, the prefactor of $\langle\langle c_a; c_a^\dagger\rangle\rangle^{\gtrless}$ is the inverse of its corresponding retarded Green's function and the result can be written as

$$\begin{aligned}
\langle\langle c_a; c_a^\dagger\rangle\rangle^{\gtrless} = \left|\langle\langle c_a; c_a^\dagger\rangle\rangle\right|^2 &\left\{g_a^{\gtrless}|\widetilde{\omega}_a|^2 + V^2\sum_{k\in\mathrm{L}} g_k^{\gtrless} + \frac{\tau_a\tau_a^* g_d^{\gtrless}|\widetilde{\omega}_d|^2}{\left|\widetilde{\omega}_d - U(\langle\hat{n}_a\rangle + \langle\hat{n}_b\rangle) - \frac{\tau_b\tau_b^*}{\widetilde{\omega}_b - U\langle\hat{n}\rangle - \sum_{k\in\mathrm{R}}\frac{V^2}{\widetilde{\omega}_k}}\right|^2}\right. \\
&\left. + \frac{\tau_a\tau_a^*\tau_b\tau_b^*\left(g_b^{\gtrless}|\widetilde{\omega}_b|^2 + V^2\sum_{k\in\mathrm{R}} g_k^{\gtrless}\right)}{\left|\left[\widetilde{\omega}_d - U\left(\langle\hat{n}_a\rangle + \langle\hat{n}_b\rangle\right)\right]\left(\widetilde{\omega}_b - U\langle\hat{n}\rangle - \sum_{k\in\mathrm{R}}\frac{V^2}{\widetilde{\omega}_k}\right) - \tau_b\tau_b^*\right|^2}\right\}.
\end{aligned} \tag{4.0.14}$$

As already mentioned, only the solution in the left site a is shown, as the solution in b can be obtained by simple replacements.

The solution for the hopping Green's function $\langle\langle c_a; d^\dagger \rangle\rangle^{\gtrless}$ is shown explicitly to emphasize its structure and relation to $\langle\langle d; c_a^\dagger \rangle\rangle^{\gtrless}$:

$$
\begin{aligned}
&\left[\widetilde{\omega}_a^+ - U\langle\hat{n}\rangle - \sum_{k\in\mathrm{L}} \frac{V^2}{\widetilde{\omega}_k^+} - \frac{\tau_a \tau_a^*}{\widetilde{\omega}_d^+ - U\left(\langle\hat{n}_a\rangle + \langle\hat{n}_b\rangle\right) - \dfrac{\tau_b \tau_b^*}{\widetilde{\omega}_b^+ - U\langle\hat{n}\rangle - \sum_{k\in\mathrm{R}} \frac{V^2}{\widetilde{\omega}_k^+}}} \right] \langle\langle c_a; d^\dagger \rangle\rangle^{\gtrless} \\
&= \left(g_a^{\gtrless} |\widetilde{\omega}_a|^2 + V^2 \sum_{k\in\mathrm{L}} g_k^{\gtrless} \right) \langle\langle c_a; d^\dagger \rangle\rangle^{\mathrm{A}} - \frac{\tau_a^* g_d^{\gtrless} |\widetilde{\omega}_d|^2}{\widetilde{\omega}_d^+ - U(\langle\hat{n}_a\rangle + \langle\hat{n}_b\rangle) - \frac{\tau_b \tau_b^*}{\widetilde{\omega}_b^+ - U\langle\hat{n}\rangle - \sum_{k\in\mathrm{R}} \frac{V^2}{\widetilde{\omega}_k^+}}} \langle\langle d; d^\dagger \rangle\rangle^{\mathrm{A}} \\
&+ \frac{\tau_a^* \tau_b \left(g_b^{\gtrless} |\widetilde{\omega}_b|^2 + V^2 \sum_{k\in\mathrm{R}} g_k^{\gtrless} \right)}{\left[\widetilde{\omega}_d^+ - U(\langle\hat{n}_a\rangle + \langle\hat{n}_b\rangle)\right] \left(\widetilde{\omega}_b^+ - U\langle\hat{n}\rangle - \sum_{k\in\mathrm{R}} \frac{V^2}{\widetilde{\omega}_k^+} \right) - \tau_b \tau_b^*} \langle\langle c_b; d^\dagger \rangle\rangle^{\mathrm{A}} \\
&= -\tau_a^* \langle\langle d; d^\dagger \rangle\rangle^{\mathrm{A}} \left\{ \frac{g_a^{\gtrless} |\widetilde{\omega}_a|^2 + V^2 \sum_{k\in\mathrm{L}} g_k^{\gtrless}}{\widetilde{\omega}_a^- - U\langle\hat{n}\rangle - \sum_{k\in\mathrm{L}} \frac{V^2}{\widetilde{\omega}_k^-}} + \frac{g_d^{\gtrless} |\widetilde{\omega}_d|^2}{\widetilde{\omega}_d^+ - U(\langle\hat{n}_a\rangle + \langle\hat{n}_b\rangle) - \frac{\tau_b \tau_b^*}{\widetilde{\omega}_b^+ - U\langle\hat{n}\rangle - \sum_{k\in\mathrm{R}} \frac{V^2}{\widetilde{\omega}_k^+}}} + \right. \\
&\left. \frac{\tau_b \tau_b^* \left(g_b^{\gtrless} |\widetilde{\omega}_b|^2 + V^2 \sum_{k\in\mathrm{R}} g_k^{\gtrless} \right)}{\left(\widetilde{\omega}_b^- - U\langle\hat{n}\rangle - \sum_{k\in\mathrm{R}} \frac{V^2}{\widetilde{\omega}_k^-} \right) \left\{ \left[\widetilde{\omega}_d^+ - U(\langle\hat{n}_a\rangle + \langle\hat{n}_b\rangle)\right] \left(\widetilde{\omega}_b^+ - U\langle\hat{n}\rangle - \sum_{k\in\mathrm{R}} \frac{V^2}{\widetilde{\omega}_k^+} \right) - \tau_b \tau_b^* \right\}} \right\}
\end{aligned}
\tag{4.0.15}
$$

Identifying the prefactor of $\langle\langle c_a; d^\dagger \rangle\rangle^{\gtrless}$ as $\langle\langle c_a; c_a^\dagger \rangle\rangle^{\mathrm{R}}$ leads to the expression

$$
\langle\langle c_a; d^\dagger \rangle\rangle^{\gtrless} = -\tau_a^* \langle\langle c_a; c_a^\dagger \rangle\rangle^{\mathrm{R}} \langle\langle d; d^\dagger \rangle\rangle^{\mathrm{A}} \{\ldots\}, \tag{4.0.16}
$$

where the dots indicate the same content in the curly brackets as in (4.0.15). Solving the equations for $\langle\langle d; c_a^\dagger \rangle\rangle^{\gtrless}$ gives a similar expression

$$
\langle\langle d; c_a^\dagger \rangle\rangle^{\gtrless} = \tau_a \langle\langle d; d^\dagger \rangle\rangle^{\mathrm{R}} \langle\langle c_a; c_a^\dagger \rangle\rangle^{\mathrm{A}} \{\ldots\}^*, \tag{4.0.17}
$$

where the complex conjugation (*) of all terms in the curly brackets is achieved by the substitutions $\widetilde{\omega}_i^{\pm} \to \widetilde{\omega}_i^{\mp}$ and $g_i^{\gtrless} \to -g_i^{\gtrless}$, as these are the only terms containing an imaginary part. The expression can be rewritten as

$$
\langle\langle d; c_a^\dagger \rangle\rangle^{\gtrless} = \left\{ \tau_a^* \langle\langle d; d^\dagger \rangle\rangle^{\mathrm{A}} \langle\langle c_a; c_a^\dagger \rangle\rangle^{\mathrm{R}} \{\ldots\} \right\}^*, \tag{4.0.18}
$$

which implies the relation

$$
-\langle\langle d; c_a^\dagger \rangle\rangle^{\gtrless} = \left(\langle\langle c_a; d^\dagger \rangle\rangle^{\gtrless} \right)^* \tag{4.0.19}
$$

and is consistent with the usual relation between such expectation values, i.e. $\left\langle c_a^\dagger d \right\rangle = \left\langle d^\dagger c_a \right\rangle^*$, as

$$
\left\langle c_a^\dagger d \right\rangle = \frac{1}{2\pi i} \int_{-\infty}^{\infty} \mathrm{d}\omega \, \langle\langle d; c_a^\dagger \rangle\rangle^{\gtrless} = \left(\frac{1}{2\pi i} \int_{-\infty}^{\infty} \mathrm{d}\omega \, \langle\langle c_a; d^\dagger \rangle\rangle^{\gtrless} \right)^* = \left\langle d^\dagger c_a \right\rangle^*. \tag{4.0.20}
$$

4.1. Explicit Particle-Hole Symmetry

Up to this point, all equations and their solutions are formulated for general model parameters and baths. The exact solution in [15] and numerical treatments in [18] and [17], however, are done on the particle-hole symmetric case, which implies some restrictions on the on-site energies and expectation values.

The system's symmetry combined with particle-hole symmetry (see (3.0.3) and section A.1.4 in the appendix) implies

$$\begin{aligned}
\langle n \rangle &= \frac{1}{2} \\
\langle \hat{n}_a \rangle &= 1 - \langle \hat{n}_b \rangle \\
\left\langle c_a^\dagger d \right\rangle &= \left\langle d^\dagger c_b \right\rangle \\
\left\langle d^\dagger c_a \right\rangle &= \left\langle c_b^\dagger d \right\rangle \\
\left\langle c_a^\dagger c_b \right\rangle &= -\left\langle c_a^\dagger c_b \right\rangle = 0 \\
\left\langle c_b^\dagger c_a \right\rangle &= -\left\langle c_b^\dagger c_a \right\rangle = 0,
\end{aligned} \tag{4.1.1}$$

which further simplifies the expressions

$$|\tau|^2 := \tau_a \tau_a^* = \left(t + U \left\langle c_a^\dagger d \right\rangle\right)\left(t + U \left\langle d^\dagger c_a \right\rangle\right) = \left(t + U \left\langle d^\dagger c_b \right\rangle\right)\left(t + U \left\langle c_b^\dagger d \right\rangle\right) = \tau_b^* \tau_b \tag{4.1.2}$$

and

$$\begin{aligned}
\widetilde{\omega}_m - U \langle \hat{n} \rangle &= \omega + U \left(\frac{1}{2} - \langle \hat{n} \rangle \right) \pm i\eta = \omega \pm i\eta =: \omega^\pm \\
\widetilde{\omega}_d - U \left(\langle \hat{n}_a \rangle + \langle \hat{n}_b \rangle \right) &= \omega + U \left(1 - \langle \hat{n}_a \rangle - \langle \hat{n}_b \rangle \right) \pm i\eta = \omega^\pm.
\end{aligned} \tag{4.1.3}$$

Furthermore, the non-equilibrium situation is only caused by a symmetric difference in the chemical potential, $\mu_{\mathrm{L,R}} = \pm \frac{\Delta\mu}{2}$, and the leads themselves have the same structure, i.e. the same density of states, and so the retarded and advanced hybridization functions are exactly the same for the left and right lead:

$$\Delta^\pm := \Delta^\pm(\omega) = \Delta_{\mathrm{L}}^\pm(\omega) = \Delta_{\mathrm{R}}^\pm(\omega) \tag{4.1.4}$$

As indicated above, the argument for left or right lead is dropped in the following. Applying (4.1.1)-(4.1.4), the particle-hole symmetric Green's functions in first-order truncation have the form

$$\begin{aligned}
\langle\langle d; d^\dagger \rangle\rangle^{\mathrm{R/A}} &= \left(\omega^\pm - \frac{2|\tau|^2}{\omega^\pm - \Delta^\pm} \right)^{-1} \\
\langle\langle c_a; c_a^\dagger \rangle\rangle^{\mathrm{R/A}} &= \left(\omega^\pm - \Delta^\pm - \frac{|\tau|^2}{\omega^\pm - \dfrac{|\tau|^2}{\omega^\pm - \Delta^\pm}} \right)^{-1}
\end{aligned} \tag{4.1.5}$$

and

$$\langle\langle d;d^\dagger\rangle\rangle^{\gtrless} = \left|\langle\langle d;d^\dagger\rangle\rangle\right|^2 \left[2i\eta P_d^{\gtrless}(\omega) + \frac{|\tau|^2}{|\omega^\pm - \Delta^\pm|^2}\sum_{m=a,b}\left(2i\eta P_m^{\gtrless}(\omega) + \Delta_{\mathrm{B}_m}^{\gtrless}\right)\right]$$

$$\langle\langle c_a;c_a^\dagger\rangle\rangle^{\gtrless} = \left|\langle\langle c_a;c_a^\dagger\rangle\rangle\right|^2 \left[2i\eta P_a^{\gtrless}(\omega) + \Delta_{\mathrm{L}}^{\gtrless} + \frac{2i\eta|\tau|^2 P_d^{\gtrless}(\omega)}{\left|\omega^\pm - \frac{|\tau|^2}{\omega^\pm - \Delta^\pm}\right|^2} + \frac{|\tau|^4\left(2i\eta P_b^{\gtrless}(\omega) + \Delta_{\mathrm{R}}^{\gtrless}\right)}{\left|\omega^\pm\left(\omega^\pm - \Delta^\pm\right) - |\tau|^2\right|^2}\right], \tag{4.1.6}$$

where

$$\mathrm{B}_{a,b} := \mathrm{B}_{\mathrm{L,R}}$$
$$P_{a,b}^{\gtrless}(\omega) := f_{c_a,c_b}(\omega) - \delta_{\gtrless,>}$$

and (3.3.6) is used for the terms including non-interacting lesser or greater Green's functions. For the hopping Green's function $\langle\langle c_a;d^\dagger\rangle\rangle^{\gtrless}$ the following is obtained:

$$\begin{aligned}\langle\langle c_a;d^\dagger\rangle\rangle^{\gtrless} = \frac{-\tau^*}{\left|\omega^\pm\left(\omega^\pm - \Delta^\pm\right) - 2|\tau|^2\right|^2}\Bigg\{&2i\eta P_d^{\gtrless}(\omega)\left(\omega^- - \Delta^{\mathrm{A}}\right) + |\tau|^2\frac{2i\eta P_b^{\gtrless}(\omega) + \Delta_{\mathrm{R}}^{<}}{\omega^+ - \Delta^{\mathrm{R}}} \\ &+ \frac{\left(2i\eta P_a^{\gtrless}(\omega) + \Delta_{\mathrm{L}}^{<}\right)\left[\omega^+\left(\omega^+ - \Delta^{\mathrm{R}}\right) - |\tau|^2\right]}{\omega^+ - \Delta^{\mathrm{R}}}\Bigg\}\end{aligned} \tag{4.1.7}$$

The Fermi functions connected to the sites a, b and d require their own chemical potentials μ_a, μ_b and μ_d. Considering the system's symmetry, the following values are assumed:

$$\begin{aligned}\mu_d &= 0 \\ \mu_{a,b} &= \mu_{\mathrm{L,R}}\end{aligned} \tag{4.1.8}$$

As can be seen in the above equations, the particle-hole symmetric Green's do not depend on the occupation numbers, but only on the hopping expectation values occurring in τ, which are obtained self-consistently.

4.1.1. Distribution Function and Symmetries

A few words on symmetry relations between Green's functions are mentioned in this subsection, as in later chapters symmetry violations occur. All aforementioned system symmetries are intended to be fulfilled.

Distribution Function

In equilibrium, the distribution function in a fermionic system is known and expectation values can be calculated from the spectral function $A(\omega)$ via the fluctuation-dissipation theorem (cf. (2.0.2)):

$$\begin{aligned}\left\langle B^\dagger A\right\rangle_{\mathrm{EQ}} &= \int_{-\infty}^{\infty} \mathrm{d}\omega\, f(\omega) A_{AB}(\omega) \\ &= \frac{1}{2\pi}\int_{-\infty}^{\infty} \mathrm{d}\omega\, f(\omega)\left(\langle\langle A; B^\dagger\rangle\rangle^{\mathrm{A}} - \langle\langle A; B^\dagger\rangle\rangle^{\mathrm{R}}\right) \\ &= \frac{1}{\pi}\int_{-\infty}^{\infty} \mathrm{d}\omega\, f(\omega)\,\mathrm{Im}\Big\{\langle\langle A; B^\dagger\rangle\rangle^{\mathrm{A}}\Big\}\end{aligned} \tag{4.1.9}$$

In a non-equilibrium situation, the distribution function may be more complicated and is generally not known. However, a formal equivalent can be constructed for local properties. The lesser components of local Green's functions, i.e. $A = B$, are completely imaginary and can therefore be written as

$$\langle\langle A; A^\dagger\rangle\rangle^{<} = i\,\mathrm{Im}\Big\{\langle\langle A; A^\dagger\rangle\rangle^{<}\Big\}.$$

Expectation values in non-equilibrium are directly related to lesser components via

$$\begin{aligned}\left\langle B^\dagger A\right\rangle_{\mathrm{NEQ}} &= \frac{1}{2\pi i}\int_{-\infty}^{\infty} \mathrm{d}\omega\, \langle\langle A; B^\dagger\rangle\rangle^{<} \\ \rightarrow \left\langle A^\dagger A\right\rangle_{\mathrm{NEQ}} &= \frac{1}{2\pi}\int_{-\infty}^{\infty} \mathrm{d}\omega\,\mathrm{Im}\Big\{\langle\langle A; A^\dagger\rangle\rangle^{<}\Big\}.\end{aligned} \tag{4.1.10}$$

Replacing the Fermi function by the non-equilibrium distribution function $S(\omega)$ the following relation needs to be satisfied:

$$\frac{1}{2\pi}\int_{-\infty}^{\infty} \mathrm{d}\omega\,\mathrm{Im}\Big\{\langle\langle A; A^\dagger\rangle\rangle^{<}\Big\} \stackrel{!}{=} \frac{1}{\pi}\int_{-\infty}^{\infty} \mathrm{d}\omega\, S_{AA}(\omega)\,\mathrm{Im}\Big\{\langle\langle A; A^\dagger\rangle\rangle^{\mathrm{A}}\Big\}$$

As the integration limits are the same on both sides, an expression for $S(\omega)$ can be obtained from the integrands, namely

$$\begin{aligned}\frac{1}{2\pi}\,\mathrm{Im}\Big\{\langle\langle A; A^\dagger\rangle\rangle^{<}\Big\} &\stackrel{!}{=} \frac{1}{\pi} S_{AA}(\omega)\,\mathrm{Im}\Big\{\langle\langle A; A^\dagger\rangle\rangle^{\mathrm{A}}\Big\} \\ \rightarrow S_{AA}(\omega) &= \frac{\mathrm{Im}\big\{\langle\langle A; A^\dagger\rangle\rangle^{<}\big\}}{2\,\mathrm{Im}\Big\{\langle\langle A; A^\dagger\rangle\rangle^{\mathrm{A}}\Big\}}.\end{aligned} \tag{4.1.11}$$

The explicit expressions for the imaginary parts then need to be obtained separately. The imaginary part of the advanced Green's functions for the central site evaluates to

$$\begin{aligned}\mathrm{Im}\Big\{\langle\langle d; d^\dagger\rangle\rangle^{\mathrm{A}}\Big\} &= \Big|\langle\langle d; d^\dagger\rangle\rangle\Big|^2\,\mathrm{Im}\left\{\frac{1}{\langle\langle d; d^\dagger\rangle\rangle^{\mathrm{R}}}\right\} \\ &= \Big|\langle\langle d; d^\dagger\rangle\rangle\Big|^2\,\mathrm{Im}\left\{\omega + i\eta - 2|\tau|^2\frac{1}{\omega + i\eta - \Delta^+}\right\} \\ &= \Big|\langle\langle d; d^\dagger\rangle\rangle\Big|^2\left[\eta + 2|\tau|^2\frac{\eta + \mathrm{Im}\{\Delta^-\}}{|\omega \pm i\eta - \Delta^\pm|^2}\right] \\ &= \Big|\langle\langle d; d^\dagger\rangle\rangle\Big|^2\left[\eta + 2\chi_\eta(\omega)\left(\eta + \mathrm{Im}\{\Delta^-\}\right)\right],\end{aligned} \tag{4.1.12}$$

where

$$\chi_\eta(\omega) := \frac{|\tau|^2}{|\omega \pm i\eta - \Delta^\pm|^2} = \frac{|\tau|^2}{|\omega^\pm - \Delta^\pm|^2}.$$

With (4.1.6) for the lesser function, the distribution function reads

$$\begin{aligned} S_{dd}(\omega) = \frac{\mathrm{Im}\{\langle\langle d; d^\dagger\rangle\rangle^<\}}{2\,\mathrm{Im}\left\{\langle\langle d; d^\dagger\rangle\rangle^\mathrm{A}\right\}} &= \frac{2\eta f_d(\omega) + \chi_\eta(\omega)\sum_{\mathrm{S=L,R}}\left(2\eta f_\mathrm{S}(\omega) + \mathrm{Im}\{\Delta_\mathrm{S}^<\}\right)}{2\eta + 2\chi_\eta(\omega)\left(2\eta + 2\,\mathrm{Im}\{\Delta^-\}\right)} \\ &= \frac{\eta f_d(\omega)}{\eta + 2\chi_\eta(\omega)\left(\eta + \mathrm{Im}\{\Delta^-\}\right)} \\ &\quad + \frac{\chi_\eta(\omega)\left(\eta + \mathrm{Im}\{\Delta^-\}\right)}{\eta + 2\chi_\eta(\omega)\left(\eta + \mathrm{Im}\{\Delta^-\}\right)}(f_\mathrm{L}(\omega) + f_\mathrm{R}(\omega)), \end{aligned} \tag{4.1.13}$$

where relation (3.2.3) is used in the last step. For regions where $\mathrm{Im}\{\Delta^-\} \neq 0$ and $\mathrm{Im}\{\Delta^-\} \not\approx \eta$ the limit $\eta \to 0^+$ can be carried out and the terms evaluate to

$$\begin{aligned} \lim_{\eta\to 0^+} \frac{\eta f_d(\omega)}{\eta + 2\chi_\eta(\omega)\left(\eta + \mathrm{Im}\{\Delta^-\}\right)} &= 0 \\ \lim_{\eta\to 0^+} \frac{\chi_\eta(\omega)\left(\eta + \mathrm{Im}\{\Delta^-\}\right)}{\eta + 2\chi_\eta(\omega)\left(\eta + \mathrm{Im}\{\Delta^-\}\right)} &= \frac{1}{2}. \end{aligned}$$

Note that for regions where $\mathrm{Im}\{\Delta^-\} \to 0$, i.e. outside the bandwidth of the leads, the limit does not result in a simple constant any more.

With the above-mentioned limitations the non-equilibrium distribution function $S_{dd}(\omega)$ becomes a double-Fermi function with chemical potentials $\mu_{L,R} = \pm\frac{\Delta\mu}{2}$, which merges to the regular Fermi function in equilibrium, where $f_\mathrm{L} = f_\mathrm{R}$:

$$S_{dd}(\omega) = \frac{1}{2}\left[f_\mathrm{L}(\omega) + f_\mathrm{R}(\omega)\right] \tag{4.1.14}$$

For the distribution function of the left site it is useful to define

$$\alpha_\eta(\omega) := \chi_\eta(\omega)\frac{|\tau|^2}{\left|\omega^\pm - \frac{|\tau|^2}{\omega^\pm - \Delta^\pm}\right|^2} = \left|\frac{|\tau|^2}{\omega^\pm\left(\omega^\pm - \Delta^\pm\right) - |\tau|^2}\right|^2 \tag{4.1.15}$$

and so the imaginary part of the advanced Green's function evaluates to

$$\begin{aligned}
\operatorname{Im}\left\{\langle\langle c_a; c_a^\dagger\rangle\rangle^{\mathrm{A}}\right\} &= \left|\langle\langle c_a; c_a^\dagger\rangle\rangle\right|^2 \operatorname{Im}\left\{\frac{1}{\langle\langle c_a; c_a^\dagger\rangle\rangle^{\mathrm{R}}}\right\} \\
&= \left|\langle\langle c_a; c_a^\dagger\rangle\rangle\right|^2 \operatorname{Im}\left\{\omega + i\eta - \Delta^+ - \frac{|\tau|^2}{\omega + i\eta - \frac{|\tau|^2}{\omega+i\eta-\Delta^+}}\right\} \\
&= \left|\langle\langle c_a; c_a^\dagger\rangle\rangle\right|^2 \left(\eta - \operatorname{Im}\{\Delta^+\} - |\tau|^2 \operatorname{Im}\left\{\frac{\omega + i\eta - \Delta^+}{(\omega+i\eta)(\omega+i\eta-\Delta^+) - |\tau|^2}\right\}\right) \\
&= \left|\langle\langle c_a; c_a^\dagger\rangle\rangle\right|^2 \left[\eta - \operatorname{Im}\{\Delta^+\} + \eta\frac{\alpha_\eta(\omega)}{\chi_\eta(\omega)} + \alpha_\eta(\omega)\left(\eta - \operatorname{Im}\{\Delta^+\}\right)\right] \\
&= \left|\langle\langle c_a; c_a^\dagger\rangle\rangle\right|^2 \left[\eta + \operatorname{Im}\{\Delta^-\} + \eta\frac{\alpha_\eta(\omega)}{\chi_\eta(\omega)} + \alpha_\eta(\omega)\left(\eta + \operatorname{Im}\{\Delta^-\}\right)\right],
\end{aligned} \tag{4.1.16}$$

where relation (3.2.1) is used in the last step.

With (4.1.6) for the lesser function, the distribution function reads

$$\begin{aligned}
S_{aa}(\omega) &= \frac{\operatorname{Im}\left\{\langle\langle c_a; c_a^\dagger\rangle\rangle^{<}\right\}}{2\operatorname{Im}\left\{\langle\langle c_a; c_a^\dagger\rangle\rangle^{\mathrm{A}}\right\}} \\
&= \frac{2\eta f_{\mathrm{L}}(\omega) + \operatorname{Im}\{\Delta_{\mathrm{L}}^<\} + 2\eta f_d(\omega)\frac{\alpha_\eta(\omega)}{\chi_\eta(\omega)} + \alpha_\eta(\omega)\left(2\eta f_{\mathrm{R}}(\omega) + \operatorname{Im}\{\Delta_{\mathrm{R}}^<\}\right)}{2\eta + 2\operatorname{Im}\{\Delta^-\} + 2\eta\frac{\alpha_\eta(\omega)}{\chi_\eta(\omega)} + \alpha_\eta(\omega)\left(2\eta + 2\operatorname{Im}\{\Delta^-\}\right)} \\
&= \frac{\eta f_d(\omega)\frac{\alpha_\eta(\omega)}{\chi_\eta(\omega)} + \left(f_{\mathrm{L}}(\omega) + f_{\mathrm{R}}(\omega)\alpha_\eta(\omega)\right)\left(\eta + \operatorname{Im}\{\Delta^-\}\right)}{\eta\frac{\alpha_\eta(\omega)}{\chi_\eta(\omega)} + \left(1 + \alpha_\eta(\omega)\right)\left(\eta + \operatorname{Im}\{\Delta^-\}\right)}.
\end{aligned} \tag{4.1.17}$$

Again, relation (3.2.3) is used in the last step. For regions where $\operatorname{Im}\{\Delta^-\} \neq 0$ and $\operatorname{Im}\{\Delta^-\} \not\approx \eta$ the limit $\eta \to 0^+$ can be done and evaluates to

$$\lim_{\eta\to 0^+} S_{aa}(\omega) = \frac{f_{\mathrm{L}}(\omega) + \alpha(\omega) f_{\mathrm{R}}(\omega)}{1 + \alpha(\omega)}, \tag{4.1.18}$$

where

$$\alpha(\omega) := \lim_{\eta\to 0^+} \alpha_\eta(\omega).$$

In equilibrium, S_{aa} merges to the regular Fermi function like S_{dd}, as

$$S_{aa}(\omega)|_{\Delta\mu=0} = \frac{f(\omega)\left(1 + \alpha(\omega)\right)}{1 + \alpha(\omega)} = f(\omega). \tag{4.1.19}$$

The fact that $\alpha(0) = 1$ causes $S_{aa}(0)$ to be fixed at a value that is independent from voltage and temperature:

$$S_{aa}(0) = \frac{f_{\mathrm{L}}(0) + \alpha(0) f_{\mathrm{R}}(0)}{1 + \alpha(0)} = \frac{1}{2}\left(f_{\mathrm{L}}(0) + f_{\mathrm{R}}(0)\right) = \frac{1}{2}\left[\left(1 + \mathrm{e}^{-\frac{\mu}{T}}\right)^{-1} + \left(1 + \mathrm{e}^{\frac{\mu}{T}}\right)^{-1}\right] = \frac{1}{2} \tag{4.1.20}$$

Symmetries

The definition of the non-equilibrium distribution function is taken in analogy to the fluctuation-dissipation theorem in equilibrium, where the distribution function is known, namely the Fermi function[II]. Thus, comparing (4.1.9) and (4.1.10), in equilibrium the following relation must hold (cf. (4.1.11)):

$$\mathrm{Im}\Big\{\langle\langle A;B^\dagger\rangle\rangle^<\Big\} \overset{\mathrm{EQ}}{=} 2f(\omega)\,\mathrm{Im}\Big\{\langle\langle A;B^\dagger\rangle\rangle^\mathrm{A}\Big\} \tag{4.1.21}$$

With the expressions obtained for the distribution function, this is checked by means of an example. Recalling the advanced part from (4.1.12),

$$\mathrm{Im}\Big\{\langle\langle d;d^\dagger\rangle\rangle^\mathrm{A}\Big\} = \Big|\langle\langle d;d^\dagger\rangle\rangle\Big|^2\left[\eta + 2\chi_\eta(\omega)\left(\eta + \mathrm{Im}\{\Delta^-\}\right)\right]$$

and the lesser from (4.1.6)

$$\begin{aligned}\mathrm{Im}\Big\{\langle\langle d;d^\dagger\rangle\rangle^<\Big\} &= \Big|\langle\langle d;d^\dagger\rangle\rangle\Big|^2\left[2\eta f_d(\omega) + \chi_\eta(\omega)\sum_{m=a,b}\left(2\eta f_m(\omega) + 2f_{\mathrm{B}_m}(\omega)\,\mathrm{Im}\{\Delta^-\}\right)\right]\\ &\overset{\mathrm{EQ}}{=} 2f(\omega)\Big|\langle\langle d;d^\dagger\rangle\rangle\Big|^2\left[\eta + \chi_\eta(\omega)\sum_{m=a,b}\left(\eta + \mathrm{Im}\{\Delta^-\}\right)\right]\\ &= 2f(\omega)\Big|\langle\langle d;d^\dagger\rangle\rangle\Big|^2\left[\eta + 2\chi_\eta(\omega)\left(\eta + \mathrm{Im}\{\Delta^-\}\right)\right],\end{aligned}$$

as all Fermi functions are per definition the same in equilibrium. The last line immediately shows that (4.1.21) is fulfilled. However, the Fermi functions are the crucial point: In section 2.2.2 an argument for a different form of $g^<(\omega)$ is brought that essentially changes the Fermi *factor* (in terms of ω) from $\sim f(\varepsilon_i - \mu_i)$ to a Fermi function $f(\omega - \mu_i)$. If this choice is not made, the Fermi factors do not coincide in equilibrium and, most importantly, the ω-dependence is completely lost, which is essential for the relation to be fulfilled.

Regardless of the choice for $g^<(\omega)$, however, the following relation should hold for general Green's functions:

$$G^\mathrm{A} - G^\mathrm{R} = 2i\,\mathrm{Im}\Big\{G^\mathrm{A}\Big\} = G^< - G^>$$

This can be seen, as lesser and greater Green's functions formally have the same structure and differ only in the Fermi-function terms, namely $f(\omega)$ for the lesser and $(f(\omega)-1)$ for the greater. Collecting the terms in $G^< - G^>$ leads to factors $\propto f(\omega) - (f(\omega)-1) = 1$, i.e. they cancel out. In the case of $\langle\langle d;d^\dagger\rangle\rangle$ this reduces to comparing the imaginary parts as above but without the Fermi function, which is obviously fulfilled.

For the sake of completeness, two more symmetry relations shown earlier are rementioned, namely

$$-G^\gtrless_{AB} = \left(G^\gtrless_{BA}\right)^*$$

shown in (4.0.19) and

$$G^\mathrm{A} = \left(G^\mathrm{R}\right)^*,$$

which is true by construction and mentioned in the beginning of section 3.3.

[II] Respectively the Bose function for bosons.

4.2. Results for Tight-Binding Leads

In this section an explicit choice is made for the type of leads, and hence for the hybridization function, and first quantitative results are obtained analytically and numerically. The leads are now assumed to be semi-infinite tight-binding chains, where, in real space, the system couples on both sides only to the first site of the chain. In terms of k states as used in the Hamiltonian (3.0.1), a density of states for the first site is needed. In order to compare the current to the results obtained in [18], a chain with $t_0 = 1\Gamma$ is used and so the density of states reads

$$\rho_{\mathrm{TB}}(\varepsilon) = \begin{cases} \frac{1}{2\pi\Gamma}\sqrt{4 - \left(\frac{\varepsilon}{\Gamma}\right)^2} & \text{if } |\varepsilon| \leq 2\Gamma \\ 0 & \text{otherwise,} \end{cases} \tag{4.2.1}$$

which further results in $V = 1\Gamma$, according to section 3.2. As introduced in section 3.2.2, the corresponding retarded and advanced hybridization function is given by

$$\Delta^{\pm} = \frac{1}{2}\left(\omega^{\pm} \mp i\sqrt{4\Gamma^2 - (\omega^{\pm})^2}\right), \tag{4.2.2}$$

where the advanced part is shown in figure 4.1 to explain the influence of η. The retarded function is just the complex conjugate and is not shown separately.

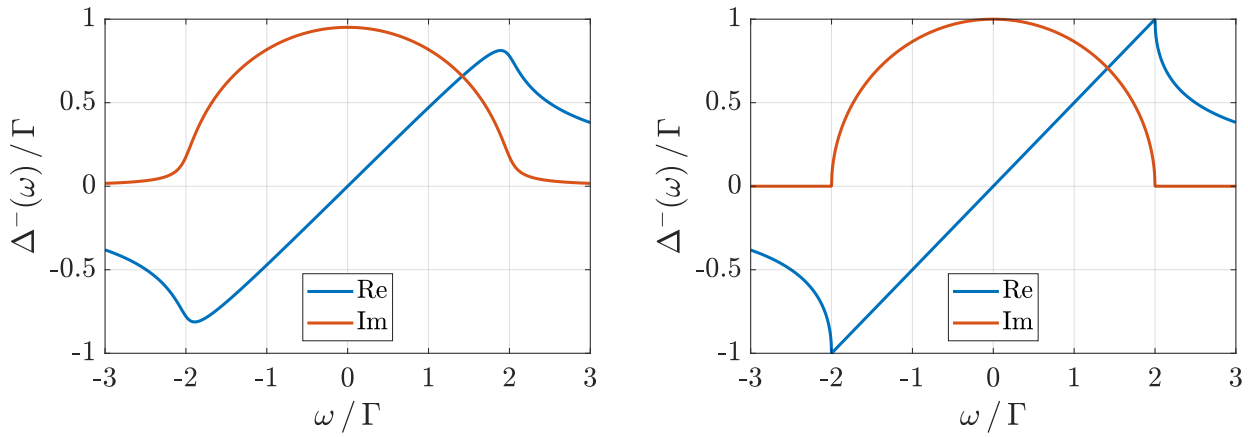

(a) Δ^- for a finite η

(b) Δ^- in the exact limit

Figure 4.1.: Advanced hybridization function Δ^- for the semi-infinite tight-binding chain with $t_0 = 1\Gamma$, shown with a finite $\eta = 0.1\Gamma$ and the exact limit $\eta \to 0^+$. The imaginary part follows the given density of states (4.2.1) and becomes equal to it in the limit, as described in section A.1.8 in the appendix. As shown in subfigure (a), a finite η causes the function to smear out and to extend the imaginary part outside the bandwidth boundary of 2Γ.

The lesser and greater part of the hybridization function is related only to the imaginary part of Δ^- (cf. (3.2.3)):

$$\Delta^{\gtrless}_{\mathrm{L,R}} = 2i\left(f(\omega)_{\mathrm{L,R}} - \delta_{\gtrless,>}\right)\mathrm{Im}\{\Delta^-\} \tag{4.2.3}$$

As shown in figure 4.1, the imaginary part of $\Delta^{\pm}$ becomes zero in the limit $\eta \to 0^+$, and so, as mentioned in section 3.3 and 4.1.1, the limit for the Green's functions can not easily be

taken for the whole ω range at once. In fact, there are some intricacies in the calculation that can be overcome for local Green's functions, but persist for the hopping correlation functions. However, the limit and the occurring integrals can be carried out numerically without further problems.

Though, as an example for the analytical behaviour outside the bandwidth, only the spectral function on the central site and the corresponding expectation value at $T = 0$ are analysed by splitting the expectation value in inner (bandwidth) and outer region,

$$\langle \hat{n} \rangle = \langle \hat{n} \rangle_{\text{inner}} + \langle \hat{n} \rangle_{\text{outer}}$$

Starting with the behaviour inside the bandwidth of the leads, i.e. $|\omega| \leq 2$, where $\operatorname{Im}\{\Delta^{\pm}\} \neq 0$ and $\operatorname{Im}\{\Delta^{\pm}\} \not\approx \eta$ and therefore the limit $\eta \to 0^+$ can be done. So the hybridization becomes simply[III]

$$\lim_{\eta \to 0^+} \Delta^{\pm} = \frac{1}{2}\left(\omega \mp i\sqrt{4-\omega^2}\right), \tag{4.2.4}$$

which corresponds directly to $\operatorname{Re} \mp i \operatorname{Im}$, as the square root is always real. And further, the limit of the lesser Green's function $\langle\langle d; d^{\dagger} \rangle\rangle^{<}$ (cf. (4.1.6)), accounting for $\langle \hat{n} \rangle_{\text{inner}}$ becomes

$$\begin{aligned}
&\lim_{\eta \to 0^+} \left| \langle\langle d; d^{\dagger} \rangle\rangle \right|^2 \left[2i\eta f_d(\omega) + \frac{|\tau|^2}{|\omega^{\pm} - \Delta^{\pm}|^2} \sum_{\mathrm{S=L,R}} \left(2i\eta f_{\mathrm{S}}(\omega) + \Delta_{\mathrm{S}}^{<} \right) \right] \\
=& \lim_{\eta \to 0^+} 2i \left| \frac{1}{\omega^{\pm} - \frac{2|\tau|^2}{\omega^{\pm} - \Delta^{\pm}}} \right|^2 \left[\eta f_d(\omega) + \frac{|\tau|^2}{|\omega^{\pm} - \Delta^{\pm}|^2} \left(\eta + \operatorname{Im}\{\Delta^{-}\} \right) \left(f_{\mathrm{L}}(\omega) + f_{\mathrm{R}}(\omega) \right) \right] \\
=& \frac{i|\tau|^2\sqrt{4-\omega^2}}{\left| \frac{\omega}{2}\left(\omega \mp i\sqrt{4-\omega^2}\right) - 2|\tau|^2 \right|^2} \left(f_{\mathrm{L}}(\omega) + f_{\mathrm{R}}(\omega) \right) \\
=& \frac{i|\tau|^2\sqrt{4-\omega^2}}{\omega^2\left(1-2|\tau|^2\right) + 4|\tau|^4} \left(f_{\mathrm{L}}(\omega) + f_{\mathrm{R}}(\omega) \right).
\end{aligned} \tag{4.2.5}$$

Hence, for the inner expectation value at $T = 0$[IV] the integral

$$\begin{aligned}
\langle \hat{n} \rangle_{\text{inner}} &= \frac{1}{2\pi i} \int_{-2}^{2} \mathrm{d}\omega \, \langle\langle d; d^{\dagger} \rangle\rangle^{<} \\
&= \frac{1}{2\pi} \left(\int_{-2}^{\mu} \mathrm{d}\omega \, \frac{|\tau|^2\sqrt{4-\omega^2}}{\omega^2\left(1-2|\tau|^2\right) + 4|\tau|^4} + \int_{-2}^{-\mu} \mathrm{d}\omega \, \frac{|\tau|^2\sqrt{4-\omega^2}}{\omega^2\left(1-2|\tau|^2\right) + 4|\tau|^4} \right)
\end{aligned} \tag{4.2.6}$$

needs to be evaluated, which is similar to the integral solved for the hybridization function. The details are shown in section A.2.3 in the appendix and the result is given by:

$$\langle \hat{n} \rangle_{\text{inner}} = \frac{|\tau|^2 - \left|1 - |\tau|^2\right|}{2\left(2|\tau|^2 - 1\right)} = \begin{cases} \frac{1}{2\left(2|\tau|^2-1\right)} & \text{if } |\tau|^2 > 1 \\ \frac{1}{2} & \text{if } |\tau|^2 \leq 1 \end{cases} \tag{4.2.7}$$

[III] Γ is omitted in the following equations.

[IV] The Fermi function turns into a step function for $T = 0$ and cuts therefore only the integration limits.

Inside the bandwidth the spectral function (cf. (4.1.12)) can be related to the above lesser function (cf. (4.2.5)) and its integral as

$$\begin{aligned} A_{dd}(\omega) = \frac{1}{\pi}\operatorname{Im}\left\{\langle\langle d;d^\dagger\rangle\rangle^{\mathrm{A}}\right\} &= \lim_{\eta\to 0^+}\frac{1}{\pi}\left|\langle\langle d;d^\dagger\rangle\rangle\right|^2\left[\eta+\frac{2|\tau|^2}{\left|\omega^\pm-\Delta^\pm\right|^2}\left(\eta+\operatorname{Im}\{\Delta^-\}\right)\right] \\ &= \frac{1}{\pi}\frac{|\tau|^2\sqrt{4-\omega^2}}{\omega^2\left(1-2|\tau|^2\right)+4|\tau|^4} \end{aligned} \tag{4.2.8}$$

and therefore

$$\int_{-2}^{2}\mathrm{d}\omega\, A_{dd}(\omega) = 2\left\langle\hat{n}\right\rangle_{\text{inner}}\Big|_{\mu=2}. \tag{4.2.9}$$

The inner expectation value does not explicitly[V] depend on μ and so the integration over the spectral function gives just

$$\int_{-2}^{2}\mathrm{d}\omega\, A_{dd}(\omega) = 2\left\langle\hat{n}\right\rangle_{\text{inner}} = \begin{cases}\frac{1}{2|\tau|^2-1} & \text{if } |\tau|^2>1\\ 1 & \text{if } |\tau|^2\le 1.\end{cases} \tag{4.2.10}$$

As the spectral function is normalized to one, i.e.

$$1 \overset{!}{=} \int_{-\infty}^{\infty}\mathrm{d}\omega\, A_{dd}(\omega) = \int_{-2}^{2}\mathrm{d}\omega\, A_{dd}(\omega) + \int_{|\omega|>2}\mathrm{d}\omega\, A_{dd}(\omega),$$

a critical behaviour outside the bandwidth arises for $|\tau|^2 > 1$, where the inner integral starts to give less than one. The examination of the outer region can be done due to the above normalizing condition. However, this requires a somewhat longer mathematical argumentation that is done in section A.1.9 in the appendix. In the end it turns out that the full spectral function in the exact limit can be written as

$$A_{dd}(\omega) = \frac{1}{\pi}\frac{|\tau|^2\operatorname{Re}\left\{\sqrt{4-\omega^2}\right\}}{\omega^2\left(1-2|\tau|^2\right)+4|\tau|^4} + \Theta\left(|\tau|^2-1\right)\frac{|\tau|^2-1}{2|\tau|^2-1}\left(\delta(\omega-\omega_1)+\delta(\omega-\omega_2)\right), \tag{4.2.11}$$

where

$$\omega_{1,2} = \pm\frac{2|\tau|^2}{\sqrt{2|\tau|^2-1}}.$$

The second term accounts for the missing states in the inner region when $|\tau|^2 > 1$. They can be identified as delta distributions whose integrals give a finite contribution to the occupation number, but relates to isolated states outside of the bandwidth of the leads. See figure 4.5 for a graphical representation.

As already mentioned above, the results presented in the following are obtained numerically in the simple self-consistency algorithm 4.1. Using the definitions discussed in previous chapters and assuming a finite value for η, i.e. omitting the limit, the integration routines can deal with the delta distributions terms without further problems.

[V] However, eventually it does depend on μ, as $|\tau|^2$ needs to be evaluated for each voltage.

Require: $\langle x_i \rangle_{\text{start}}, \omega, \eta, t, U, T, \Delta\mu, \epsilon_{\text{abs}}$

$\langle x_i \rangle \leftarrow \langle x_i \rangle_{\text{start}}$
$chk \leftarrow 1$
while $chk > \epsilon_{\text{abs}}$ **do**
  $\langle x_i \rangle_{\text{old}} \leftarrow \langle x_i \rangle$
  $G_j^{\lessgtr}(\omega) \leftarrow f(\langle x_i \rangle, \omega, \eta, t, U, T, \Delta\mu)$ according to eq. (4.1.5)-(4.1.8)
  $\langle x_i \rangle \leftarrow (2\pi i)^{-1} \int \mathrm{d}\omega \, G_i^{<}(\omega)$
  $chk \leftarrow \max_i |\langle x_i \rangle - \langle x_i \rangle_{\text{old}}|$
end while

Algorithm 4.1: Self-consistency non-equilibrium loop

The computations are done in MATLAB with the integration routine **trapz** using an ω-grid with

$$\Delta\omega = \begin{cases} \frac{\eta}{2} & \text{for } |\omega| \leq 5\Gamma \\ 0.1\Gamma & \text{for } 5\Gamma < |\omega| \leq 100\Gamma \end{cases}$$

and with the following start values and convergence parameters

$$\langle n_i \rangle_{\text{start}} = 0.5 \quad \text{and} \quad \left\langle c_i^\dagger c_j \right\rangle_{\text{start}} = 0,$$
$$\epsilon_{\text{abs}} = 10^{-6} \quad \text{and} \quad \eta = 10^{-3}\Gamma.$$

A converged loop gives access to all two-operator expectation values as well as to the underlying Green's functions. The calculations are done in a $\Delta\mu$ range that covers the system's behaviour and for different values of t and U at $T = 0\Gamma$. Algorithm 4.1 sketches the solution for a given voltage ($\Delta\mu$) point. It can either be parallelized using the same start values for the desired voltage points or simply looped with ascending voltage, where it is recommended to use the converged expectation values from the previous voltage as new start values.

As mention in section 4.1, only the hopping expectation values $\langle d^\dagger c_{a,b} \rangle$ and $\left\langle c_{a,b}^\dagger d \right\rangle$ need to be solved explicitly in the loop; the Green's functions are hereby determined for each voltage and the other quantities can be calculated from them.

The self-consistent solutions to the absolute square of the effective hopping $|\tau|^2$ are shown in figure 4.2. The qualitative behaviour is similar for different parameters, namely a decrease in the hopping over voltage, i.e. an effective decoupling of sites a and b, which in turn technically explains the negative differential conductance appearing in the current (see figure 4.3). Compared to the non-interacting case ($U = 0\Gamma$), where the hopping is just given by t (cf. the black dashed line in figure 4.2 for t^2), the sites a and b are very strongly coupled to the central site for low voltages, but looser than for $U = 0\Gamma$ for high voltages, where $|\tau|^2 < t^2$.

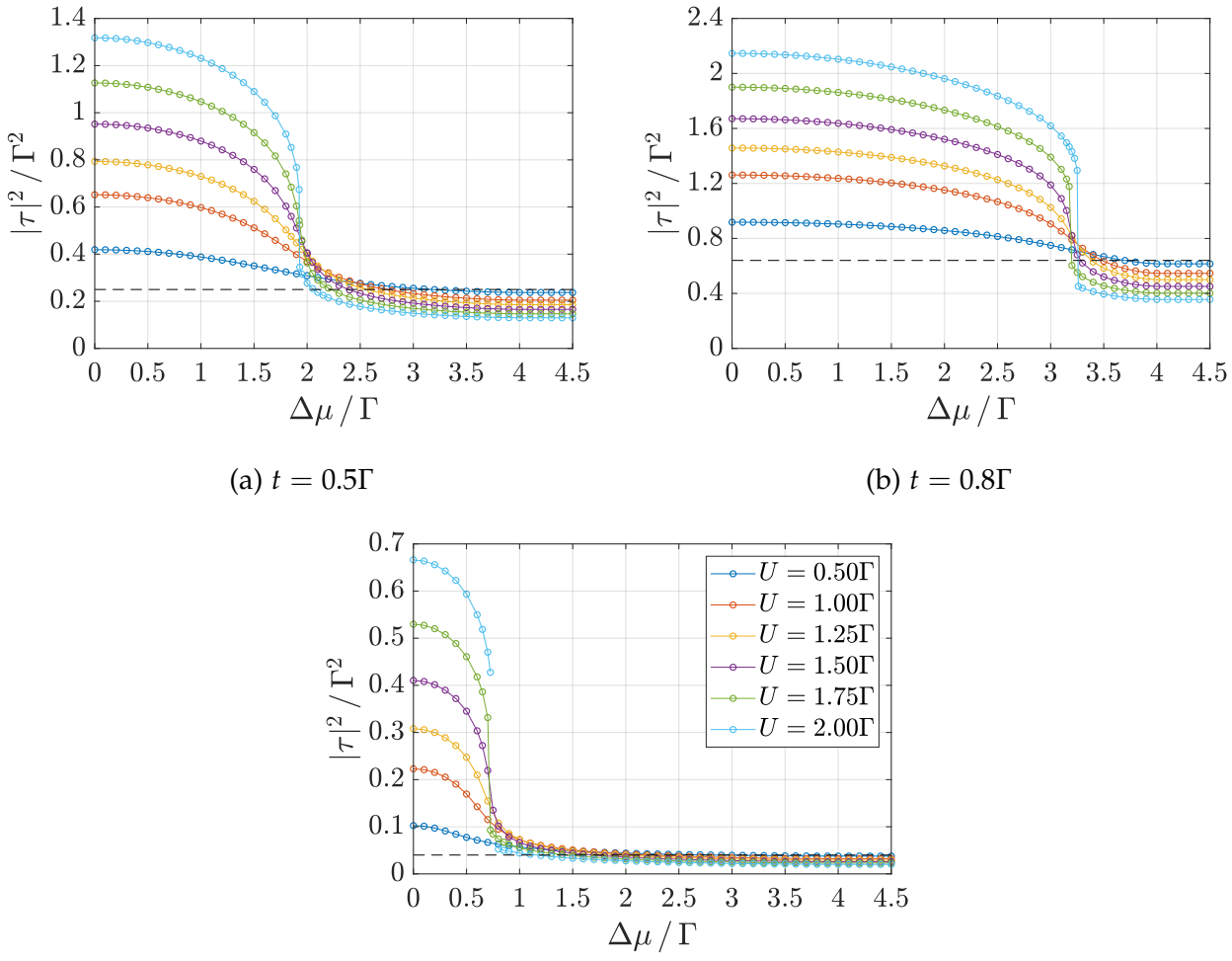

(a) $t = 0.5\Gamma$

(b) $t = 0.8\Gamma$

(c) $t = 0.2\Gamma$

Figure 4.2.: Self-consistent solutions for the effective hopping $|\tau|^2$ in the model with tight-binding leads for different values of U and t. The black dashed lines in each subfigure show the hopping t^2 at $U = 0\Gamma$. The legend in (c) refers to all subfigures. In (c), the line for $U = 2\Gamma$ is not connected for some values around $\Delta\mu = 0.75\Gamma$, where the self-consistent iteration does not converge within the demanded accuracy.

The self-consistency loop does not converge for certain parameters shown in figure 4.2c, but seems to oscillate between, at least, two solutions. A similar behaviour occurs for the calculations with leads in wide-band limit in the next section, where the problem is addressed in more detail.

The current and the Green's functions are directly determined by the self-consistent solutions for the hopping expectation values and $|\tau|^2$, and so subsequently the occupation numbers can be calculated. As expected, the currents over both possible junctions (cf. section 3.1), i.e. lead-system and intra-system, coincide in the range of η, as the current should be conserved. Further, left and right currents as well as with negative voltages are perfectly symmetric, and the calculated occupation numbers agree with the symmetry relations (4.1.1). Therefore, the non-trivial physical quantities obtained from expectation values reduce to one current and the occupation number on site a, which are shown in figure 4.3.

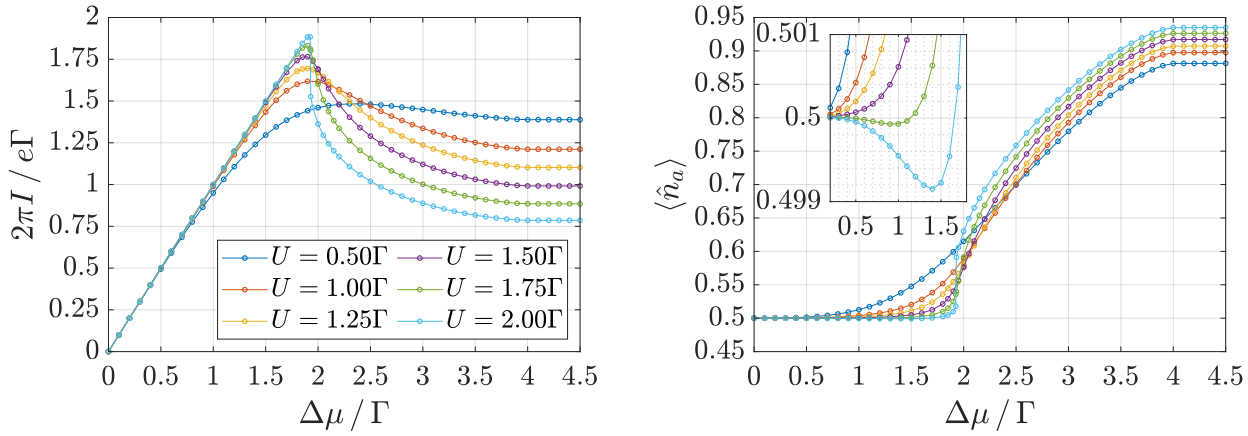

(a) Current

(b) Occupation number

Figure 4.3.: Current and occupation number for $t = 0.5\Gamma$ and different values of U. The legend in (a) refers to both subfigures. The current curves feature negative differential conductance in the region for $\Delta\mu \gtrsim 2\Gamma$ as well as a sharp drop for $U \gtrsim 2\Gamma$. The occupation number is somewhat constant for low voltages, with a small decrease for $U \gtrsim 1.75\Gamma$, before it rises to its maximum value reached at bandwidth of 4Γ. The decrease for $U = 2\Gamma$ of about 10^{-3} does not depend on the chosen η of $10^{-3}\Gamma$. This feature is more pronounced in the results for wide-band limit leads and occurs also in the non-interacting case, cf. the results in the next section.

Negative differential conductance appears in the current curves for all values of $U > 0\Gamma$ and t (only shown for $t = 0.5\Gamma$), which is also a prominent feature in the exact and numerical solutions in [15] and is discussed in more detail in [17]. Yet for higher voltages a qualitative description fails, as the current stays constant (in the range of η) for voltages beyond the lead bandwidth of 4Γ, where the exact solution continues to decrease (see figure 4.4).

The obtained current curves for the self-dual point, i.e. $U = 2\Gamma$, are now compared to the exact solution as well as to other numerical results obtained from a direct Hartree-Fock approximation to the Hamiltonian and time-evolution in [18], which are reproduced with a deviation in the range of η or less. The comparison is shown in figure 4.4:

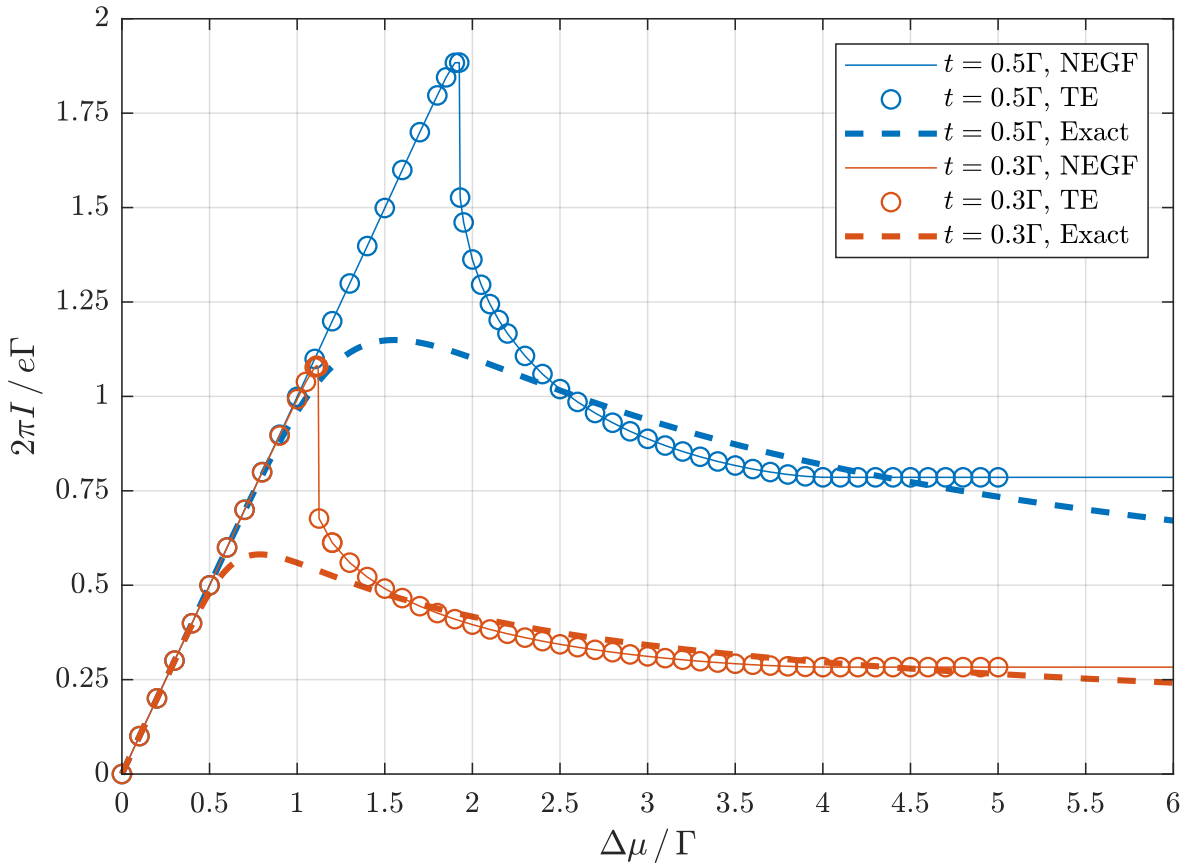

Figure 4.4.: Current comparison with numerical results from [18] and the exact solution from [16] for $t = 0.5\Gamma$ (blue lines) and $t = 0.3\Gamma$ (red lines). The solid lines represent the results obtained in this thesis (NEGF), the circles stand for the results from time-evolution (TE), and the dashed lines for the exact solution.

As mentioned in an earlier section and shown with equations (4.0.7) and (4.0.8), the approximated Hamiltonian used in [18] leads to the same equation set obtained in the beginning of this chapter, and it is therefore not surprising that both methods lead to the same result. However, this shows at least that the equation-of-motion method is suitable to produce proper steady-state solutions for (effectively) non-interacting systems out of equilibrium.

Compared to the exact solution, the Hartree-Fock approximation describes the current well in the linear regime for low voltages, but overestimates it in the region where a decrease sets in. The high-voltage limit cannot be described, as the HF current always saturates, but the deviation is smaller for smaller values of t.

The spectral function for site i is directly obtained from the Green's function via

$$A_{ii}(\omega) = \frac{1}{2\pi i}\left(G^{\mathrm{A}}_{ii}(\omega) - G^{\mathrm{R}}_{ii}(\omega)\right) = \pm\frac{1}{\pi}\,\mathrm{Im}\left\{G^{\mathrm{A/R}}_{ii}(\omega)\right\},$$

and is shown for site d and a in the self-dual point and for different voltages in figure 4.5 and 4.6. A prominent feature of the spectral function at the central site A_{dd} seems to

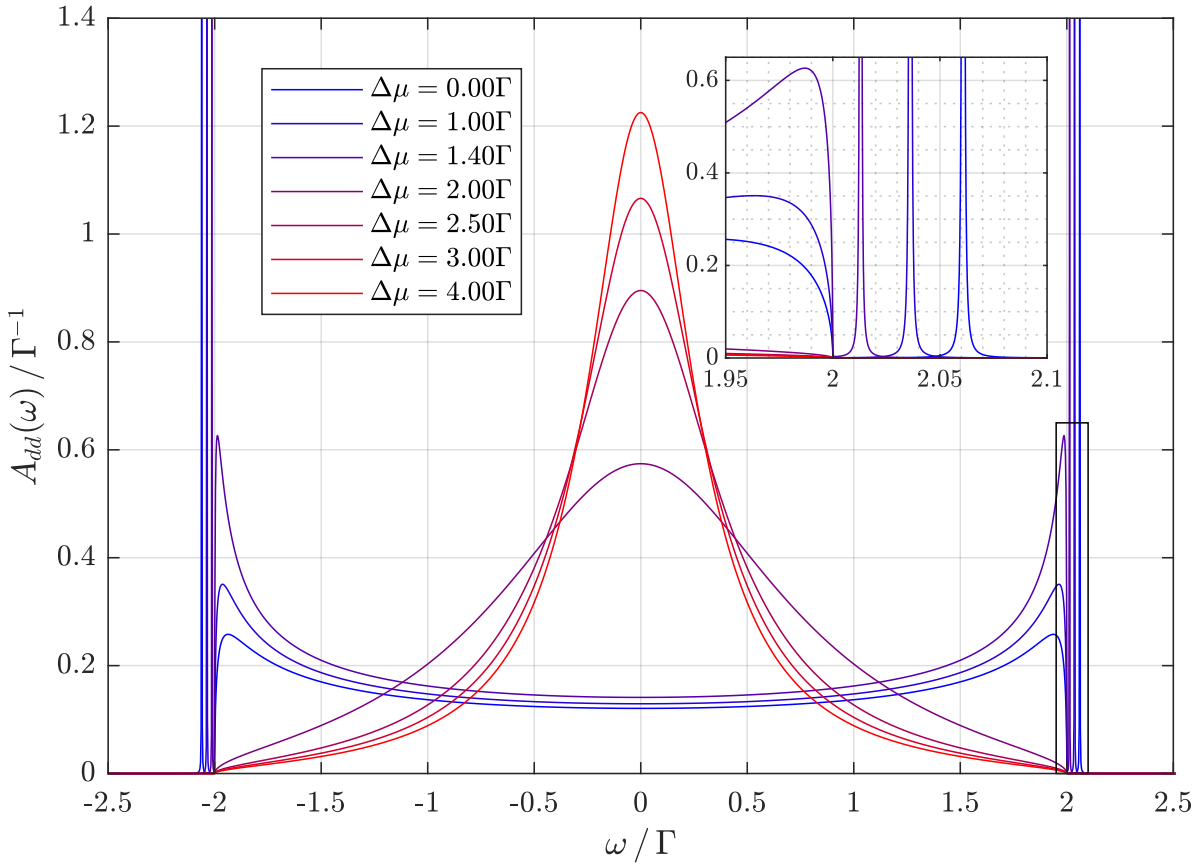

Figure 4.5.: Spectral function for the central site for $U = 2\Gamma$, $t = 0.5\Gamma$ and different voltages, featuring the two main shapes (see text). The delta peaks on the sides at $\omega = |\omega_{1,2}|$, cf. (4.2.11), represent the isolated states outside the bandwidth of the leads, and are shown for $\eta = 10^{-5}\Gamma$ and are emphasized in the inset. The curve for $\Delta\mu = 1.40\Gamma$ is only chosen for a better representation of the Lorentzians, but it is not the voltage where the spectral functions changes between the two qualitative shapes.

be that there are two qualitatively different states, one which is similar to the density of states of an infinite tight-binding chain, occurring at low voltages (and thus high hoppings), and another with a single peak concentrated around $\omega = 0\Gamma$ for higher voltages (lower hoppings). A qualitatively similar result, at least for the low and high-voltage regime, can be found in figure 3b in [17], but without the strict bandwidth cuts and hence without isolated states. Further, the central peak is split into two side-peaks that merge for high voltages and the peaks around $|\omega| \approx 2\Gamma$ decrease, but still persist in the high-voltage regime. The central-peak merging, however, can be observed in the results for wide-band-limit leads in the next section.

The spectral function on site a shows a similar two-state behaviour as well as the isolated states:

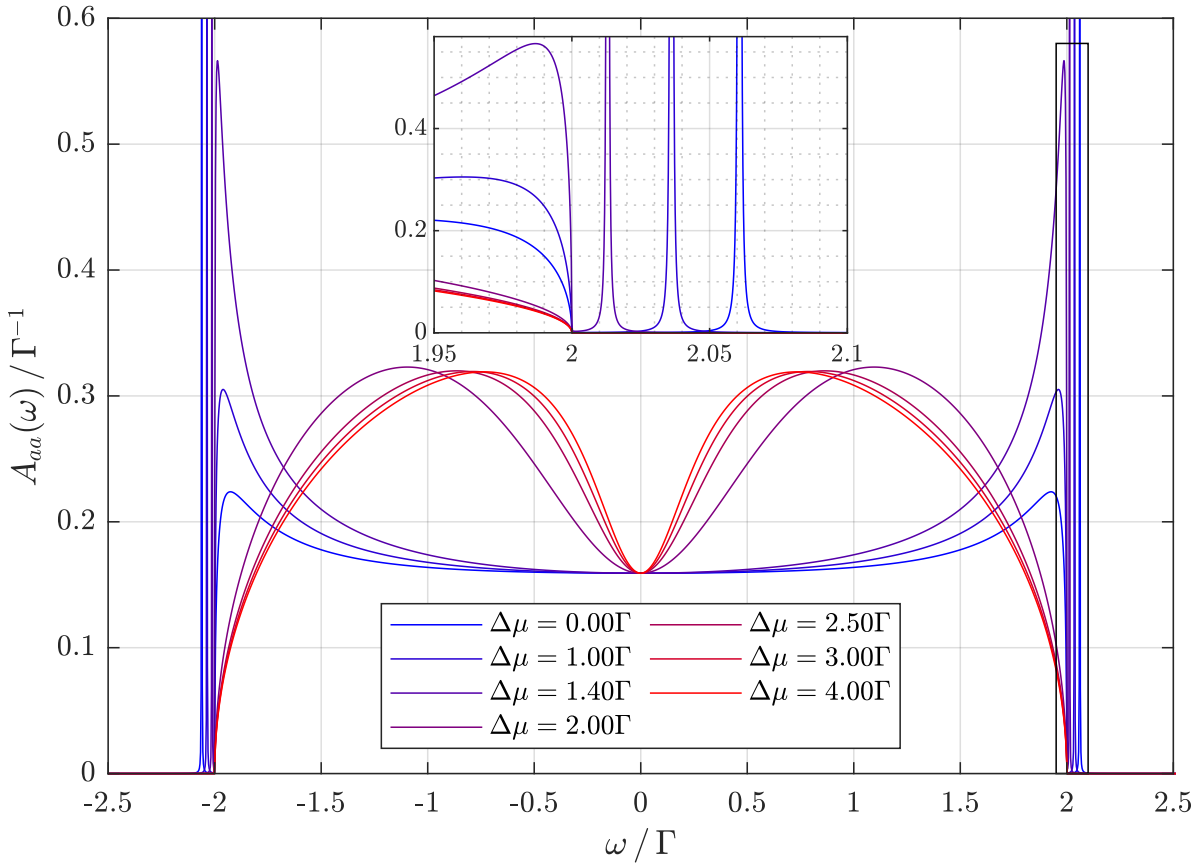

Figure 4.6.: Spectral function for site a for $U = 2\Gamma$, $t = 0.5\Gamma$ and different voltages. Again, two main shapes are present. The plotting details can be taken from the caption in figure 4.5.

Again, the low-voltage shapes are similar to the density of states of an infinite tight-binding chain, and therefore only slightly different from the central-site results (cf. the inner bandwidth peak heights in the insets). This can be explained by having a look at the values for the effective hopping from figure 4.2a, which are around $\sqrt{1.2\Gamma^2} \approx 1.1\Gamma$ for $\Delta\mu \lesssim 1.5\Gamma$, and recalling the hopping for the semi-infinite tight-binding chain of $t_0 = 1\Gamma$, i.e. the whole system behaves in fact approximately like an infinite tight-binding chain for low voltages.

In comparison to the results in figure 5 in [17], the low-voltage regime is in qualitative agreement, but there is no major change in the spectral function for high voltages besides an asymmetric height shift in the peaks around $|\omega| \approx 2\Gamma$, which is not present in figure 4.6.

Up to here, all results were calculated for $T = 0\Gamma$. As an example, some thermal calculations are shown for relatively high temperatures[VI] of $T = 0.1\Gamma$. However, the results in current and occupation number are almost the same as for zero temperature, they only differ in the high voltage regime, as the thermal curves show changes beyond the bandwidth of 4Γ, where the zero temperature results are constant (in the range of η).

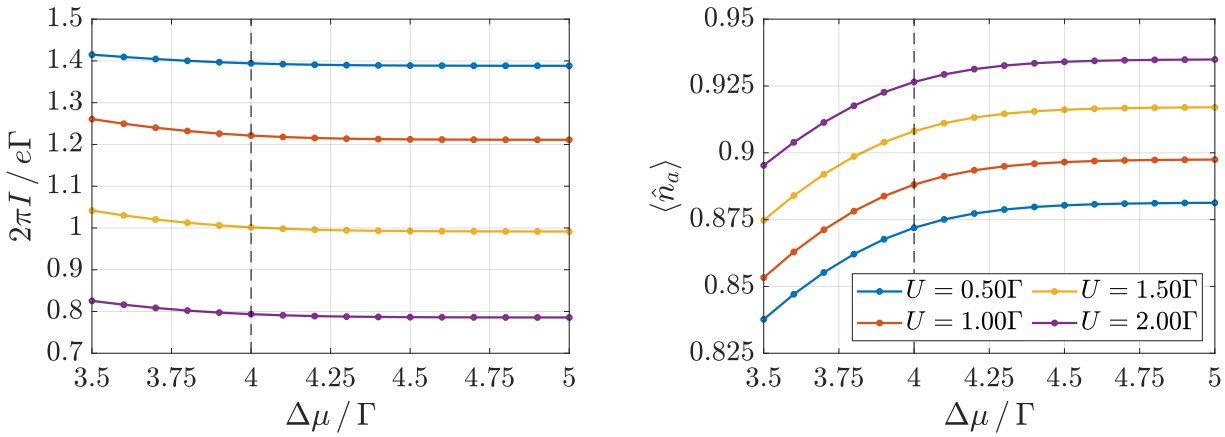

(a) Current

(b) Occupation

Figure 4.7.: Parts of current and occupation number beyond the bandwidth of 4Γ (dashed line) for $t = 0.5\Gamma$ and $T = 0.1\Gamma$. The legend in (b) refers to both subfigures.

4.3. Results for Wide-Band-Limit Leads

In this section, the system is coupled to another kind of lead introduced in section 3.2.1, namely leads in the wide-band limit. The advantage here is that the retarded and advanced hybridization functions are just an imaginary constant and the resulting Green's functions can be integrated exactly. The determining equations for the expectation values therefore do not have to be solved by iterative integration, however, the results are still transcendental equations whose solutions are found graphically/numerically by intersections.

As $\mathrm{Im}\{\Delta^{\pm}(\omega)\} \neq 0$ for $\forall\omega$, the limit $\eta \to 0^+$ should be feasible without further problems (cf. section 4.1.1). In fact, analysing the occurrence of the hybridization functions and η in the wide-band limit, so

$$\begin{aligned} \Delta^{\pm} = \mp i \qquad &\to \omega^{\pm} - \Delta^{\pm} \qquad = \omega \pm i(1+\eta) \\ \Delta^{<}_{\mathrm{L/R}} = 2if_{\mathrm{L/R}}(\omega) &\to g^{<}_{a,b}|\widetilde{\omega}_{a,b}|^2 + \Delta^{<}_{\mathrm{L/R}} = 2if_{\mathrm{L/R}}(\omega)(1+\eta), \end{aligned}$$

it turns out that η appears mostly in terms of $(1+\eta)$ and in $\omega^{\pm}+$ some non-zero term, where the limit can easily be taken by setting η to zero. Terms $\propto 2i\eta f_i(\omega)$ can also be set to zero as the absolute squares $\left|G^{\mathrm{R/A}}\right|^2$ show no poles. With these findings, the retarded

[VI] Assuming an energy scale of $\Gamma \sim 1\,\mathrm{eV}$, the corresponding temperature can be obtained from $k_{\mathrm{B}}T \sim 0.1\,\mathrm{eV}$ to be already about $T \sim 1160\,\mathrm{K}$.

and advanced Green's functions become just (complex) rational functions. The lesser and greater functions feature some additional Fermi functions.

In the wide-band limit the particle-hole symmetric functions from section 4.1 explicitly become

$$\langle\langle d; d^\dagger \rangle\rangle^{\mathrm{R/A}} = \left(\omega - \frac{2|\tau|^2}{\omega \pm i} \right)^{-1} = \frac{\omega \pm i}{\omega\left(\omega \pm i\right) - 2|\tau|^2} \tag{4.3.1}$$

$$\langle\langle c_a; c_a^\dagger \rangle\rangle^{\mathrm{R/A}} = \left(\omega \pm i - \frac{|\tau|^2}{\omega - \dfrac{|\tau|^2}{\omega \pm i}} \right)^{-1} = \frac{\omega\left(\omega \pm i\right) - |\tau|^2}{\left(\omega \pm i\right)\left[\omega\left(\omega \pm i\right) - 2|\tau|^2\right]} \tag{4.3.2}$$

and the product for the hopping correlations becomes

$$\langle\langle c_a; c_a^\dagger \rangle\rangle^{\mathrm{R}} \langle\langle d; d^\dagger \rangle\rangle^{\mathrm{A}} = \frac{\left[\omega\left(\omega + i\right) - |\tau|^2\right]\left(\omega - i\right)}{\left(\omega + i\right)\left|\omega\left(\omega \pm i\right) - 2|\tau|^2\right|^2}. \tag{4.3.3}$$

The lesser functions for the central and left site can the be written as

$$\langle\langle d; d^\dagger \rangle\rangle^{<} = \frac{2i|\tau|^2}{\left|\omega\left(\omega \pm i\right) - 2|\tau|^2\right|^2}\left(f_{\mathrm{L}}(\omega) + f_{\mathrm{R}}(\omega)\right) \tag{4.3.4}$$

and

$$\langle\langle c_a; c_a^\dagger \rangle\rangle^{<} = 2i\left|\frac{\omega\left(\omega \pm i\right) - |\tau|^2}{\left(\omega \pm i\right)\left[\omega\left(\omega \pm i\right) - 2|\tau|^2\right]}\right|^2 \left[f_{\mathrm{L}}(\omega) + \left|\frac{|\tau|^2}{\omega\left(\omega \pm i\right) - |\tau|^2}\right|^2 f_{\mathrm{R}}(\omega)\right], \tag{4.3.5}$$

and so the lesser hopping function as

$$\begin{aligned} \langle\langle c_a; d^\dagger \rangle\rangle^{<} &= \frac{-2i\tau^*}{\left|\omega\left(\omega \pm i\right) - 2|\tau|^2\right|^2}\left\{\frac{f_{\mathrm{L}}(\omega)\left[\omega\left(\omega + i\right) - |\tau|^2\right]}{\omega + i} + |\tau|^2 \frac{f_{\mathrm{R}}(\omega)}{\omega + i}\right\} \\ &= \frac{-2i\tau^*}{\left|\omega\left(\omega \pm i\right) - 2|\tau|^2\right|^2}\left[f_{\mathrm{L}}(\omega)\omega + \frac{|\tau|^2}{\omega + i}\left(f_{\mathrm{R}}(\omega) - f_{\mathrm{L}}(\omega)\right)\right]. \end{aligned} \tag{4.3.6}$$

The expectation values for current and occupation numbers are obtained by integrating over the corresponding lesser Green's functions, which can now be carried out exactly for $T = 0\Gamma$, as the Fermi-function becomes a simple Heaviside-step function that limits only the integration intervals.

The exact evaluation of the following integrals is described in section A.2.4 in the appendix and only their solutions are presented here. Besides the obvious dependences, coming from the system-describing parameters μ and $|\tau|^2$, the solutions contain the $|\tau|^2$-dependent terms

$$b = 1 - 4|\tau|^2 \qquad \text{and} \qquad c = \sqrt{1 - 8|\tau|^2}$$

that arise from the factorization

$$\left|\omega\left(\omega \pm i\right) - 2|\tau|^2\right|^2 = \omega^4 + \left(1 - 4|\tau|^2\right)\omega^2 + 4|\tau|^4 = \left[\omega^2 + \frac{1}{2}\left(b + c\right)\right]\left[\omega^2 + \frac{1}{2}\left(b - c\right)\right].$$

The integral for the occupation number on the central site d is given by

$$\begin{aligned}\langle \hat{n} \rangle &= \frac{1}{2\pi i}\int_{-\infty}^{\infty} \mathrm{d}\omega \, \langle\langle d; d^\dagger \rangle\rangle^< \\ &= \frac{|\tau|^2}{\pi}\left[\int_{-\infty}^{\mu} \frac{\mathrm{d}\omega}{\left|\omega\left(\omega \pm i\right) - 2|\tau|^2\right|^2} + \int_{-\infty}^{-\mu} \frac{\mathrm{d}\omega}{\left|\omega\left(\omega \pm i\right) - 2|\tau|^2\right|^2}\right].\end{aligned} \tag{4.3.7}$$

With the indefinite integral[VII]

$$\begin{aligned}I_1(\omega) :=& \int \mathrm{d}\omega \, \frac{1}{\left|\omega\left(\omega \pm i\right) - 2|\tau|^2\right|^2} \\ =& \frac{1}{c}\left[\frac{\sqrt{2}}{\sqrt{b-c}} \arctan\left(\frac{\omega\sqrt{2}}{\sqrt{b-c}}\right) - \frac{\sqrt{2}}{\sqrt{b+c}} \arctan\left(\frac{\omega\sqrt{2}}{\sqrt{b+c}}\right)\right]\end{aligned} \tag{4.3.8}$$

the occupation number becomes

$$\begin{aligned}\langle \hat{n} \rangle &= \frac{|\tau|^2}{\pi}\left(I_1(\mu) + I_1(-\mu) - 2I_1(-\infty)\right) \\ &= -\frac{2|\tau|^2}{\pi} I_1(-\infty) \\ &= \frac{2|\tau|^2}{\pi}\frac{\pi}{4|\tau|^2} = \frac{1}{2}\end{aligned} \tag{4.3.9}$$

as the inverse tangent is antisymmetric. This result is independent from the applied voltage $\Delta\mu$ and (renormalized) hopping τ and gives indeed the value stated in (4.1.1). However, the spectral function on the central site, $A_{dd}(\omega)$, changes with voltage, as it is still a function of $|\tau|^2$, which itself depends on $\Delta\mu$.

The integral for the occupation number on the left and right site is given by

$$\begin{aligned}\langle \hat{n}_a \rangle &= \frac{1}{2\pi i}\int_{-\infty}^{\infty} \mathrm{d}\omega \, \langle\langle c_a; c_a^\dagger \rangle\rangle^< \\ &= \frac{1}{\pi}\left[\int_{-\infty}^{\mu} \mathrm{d}\omega \, \frac{\left|\omega(\omega \pm i) - |\tau|^2\right|^2}{(\omega^2+1)\left|\omega\left(\omega \pm i\right) - 2|\tau|^2\right|^2} + \int_{-\infty}^{-\mu} \mathrm{d}\omega \, \frac{|\tau|^4}{(\omega^2+1)\left|\omega\left(\omega \pm i\right) - 2|\tau|^2\right|^2}\right].\end{aligned} \tag{4.3.10}$$

[VII] See appendix.

With the indefinite integrals

$$\begin{aligned} I_2(\omega) :=& \int \mathrm{d}\omega \, \frac{|\tau|^2}{(\omega^2+1)\left|\omega\,(\omega \pm i) - 2|\tau|^2\right|^2} \\ =& \frac{1}{4\left(1+|\tau|^2\right)} \Bigg\{ \arctan(\omega) \\ &+ \frac{1}{c\sqrt{2}} \left[\frac{b-c-2}{\sqrt{b+c}} \arctan\left(\frac{\omega\sqrt{2}}{\sqrt{b+c}}\right) - \frac{b+c-2}{\sqrt{b-c}} \arctan\left(\frac{\omega\sqrt{2}}{\sqrt{b-c}}\right) \right] \Bigg\} \end{aligned} \tag{4.3.11}$$

and

$$\begin{aligned} I_3(\omega) :=& \int \mathrm{d}\omega \, \frac{\left|\omega(\omega \pm i) - |\tau|^2\right|^2}{(\omega^2+1)\left|\omega\,(\omega \pm i) - 2|\tau|^2\right|^2} \\ =& \frac{1}{4\left(1+|\tau|^2\right)} \Bigg\{ \left(2+|\tau|^2\right) \arctan(\omega) \\ &+ \frac{1}{c\sqrt{2}} \left[\frac{(b+c)\left(2+3|\tau|^2\right)+8|\tau|^4}{\sqrt{b+c}} \arctan\left(\frac{\omega\sqrt{2}}{\sqrt{b+c}}\right) \right. \\ &\left. - \frac{(b-c)\left(2+3|\tau|^2\right)+8|\tau|^4}{\sqrt{b-c}} \arctan\left(\frac{\omega\sqrt{2}}{\sqrt{b-c}}\right) \right] \Bigg\} \end{aligned} \tag{4.3.12}$$

the occupation number becomes

$$\begin{aligned} \langle \hat{n}_a \rangle &= \frac{1}{\pi} \left(I_3(\mu) + |\tau|^2 I_2(-\mu) - I_3(-\infty) - |\tau|^2 I_2(-\infty) \right) \\ &= \frac{1}{\pi} \left(I_3(\mu) + |\tau|^2 I_2(-\mu) + \pi \frac{2+|\tau|^2}{4\left(1+|\tau|^2\right)} + \pi \frac{|\tau|^2}{4\left(1+|\tau|^2\right)} \right) \\ &= \frac{1}{2} + \frac{1}{\pi} \left(I_3(\mu) - |\tau|^2 I_2(\mu) \right), \end{aligned} \tag{4.3.13}$$

where again the antisymmetry of the inverse tangent is used in the last step. This result depends on voltage and hopping, but the equilibrium case, i.e. $\Delta\mu = \mu = 0$, is easily obtained as $I_{2,3}(0) = 0$ and so

$$\langle \hat{n}_a \rangle_{\mu=0} = \frac{1}{2}, \tag{4.3.14}$$

which does not depend on the hopping parameter. On the other hand, in the limit $\mu \to \infty$ the occupation number does not rise up to one, as one might expect, but still depends on

the hopping parameter:

$$\begin{aligned}\langle \hat{n}_a \rangle_{\mu\to\infty} &= \frac{1}{2} + \frac{1}{\pi}\left(I_3(\infty) - |\tau|^2 I_2(\infty)\right) \\ &= \frac{1}{2} + \frac{2+|\tau|^2}{4\left(1+|\tau|^2\right)} - \frac{|\tau|^2}{4\left(1+|\tau|^2\right)} \\ &= \frac{1}{2} + \frac{1}{2+2|\tau|^2}\end{aligned} \tag{4.3.15}$$

Further, as $\langle \hat{n}_b \rangle_\mu = \langle \hat{n}_a \rangle_{-\mu}$, summing the occupation numbers on the right and left site gives

$$\begin{aligned}\langle \hat{n}_a \rangle + \langle \hat{n}_b \rangle &= \frac{1}{2} + \frac{1}{\pi}\left(I_3(\mu) - |\tau|^2 I_2(\mu)\right) + \frac{1}{2} + \frac{1}{\pi}\left(I_3(-\mu) - |\tau|^2 I_2(-\mu)\right) \\ &= 1 + \frac{1}{\pi}\left(I_3(\mu) - |\tau|^2 I_2(\mu)\right) - \frac{1}{\pi}\left(I_3(\mu) - |\tau|^2 I_2(\mu)\right) \\ &= 1.\end{aligned} \tag{4.3.16}$$

This is indeed the relation obtained for particle-hole symmetry and is valid for any voltage and hopping.

The current is related to the expectation value

$$\begin{aligned}\left\langle d^\dagger c_a \right\rangle &= \frac{1}{2\pi i}\int_{-\infty}^{\infty} \mathrm{d}\omega \, \langle\langle c_a; d^\dagger \rangle\rangle^< \\ &= -\frac{\tau^*}{\pi}\left[\int_{-\infty}^{\mu} \mathrm{d}\omega \, \frac{\omega}{\left|\omega\left(\omega \pm i\right) - 2|\tau|^2\right|^2} - \int_{-\mu}^{\mu} \mathrm{d}\omega \, \frac{|\tau|^2}{(\omega+i)\left|\omega\left(\omega \pm i\right) - 2|\tau|^2\right|^2}\right],\end{aligned} \tag{4.3.17}$$

which is part of the renormalized hopping τ. The solutions to the integrals contain inverse-tangent terms and so, as $\left\langle d^\dagger c_a \right\rangle$ is a complex number depending explicitly on τ^* and $|\tau|^2$, the above equation gives a complex transcendental equation, which is not straightforward to solve directly for unique values. However, the terms can be rearranged so that $\left\langle d^\dagger c_a \right\rangle$ only depends on $|\tau|^2$ and the problem can thus be reduced to a real transcendental equation in $|\tau|^2$, that can easily be solved numerically by finding its real zeros.

For convenience, the two definite integrals (and their solutions) are defined as functions of $|\tau|^2$ with a parameter μ. The first one reads

$$\begin{aligned}f_1(|\tau|^2;\mu) &:= \int_{-\infty}^{\mu} \mathrm{d}\omega \, \frac{\omega}{\left|\omega\left(\omega \pm i\right) - 2|\tau|^2\right|^2} \\ &= \frac{1}{\sqrt{8|\tau|^2 - 1}}\left[\arctan\left(\frac{2\mu^2 - 4|\tau|^2 + 1}{\sqrt{8|\tau|^2 - 1}}\right) - \frac{\pi}{2}\right],\end{aligned} \tag{4.3.18}$$

where the solution is obtained by substitution[VIII]. The second integral can be split into real and imaginary part, namely

$$\begin{aligned} i f_2(|\tau|^2;\mu) &:= \int_{-\mu}^{\mu} \mathrm{d}\omega \, \frac{|\tau|^2}{(\omega+i)\left|\omega\,(\omega\pm i)-2|\tau|^2\right|^2} \\ &= \int_{-\mu}^{\mu} \mathrm{d}\omega \, \frac{\omega|\tau|^2}{(\omega^2+1)\left|\omega\,(\omega\pm i)-2|\tau|^2\right|^2} - \int_{-\mu}^{\mu} \mathrm{d}\omega \, \frac{i|\tau|^2}{(\omega^2+1)\left|\omega\,(\omega\pm i)-2|\tau|^2\right|^2}, \end{aligned} \tag{4.3.19}$$

where the integrand for the real part is antisymmetric in ω and so the integral vanishes due to the symmetric integration interval $[-\mu,\mu]$. Thus, the function f_2 is proportional to the indefinite integral I_2 defined[IX] above, as

$$\begin{aligned} i f_2(|\tau|^2;\mu) &= -\int_{-\mu}^{\mu} \mathrm{d}\omega \, \frac{i|\tau|^2}{(\omega^2+1)\left|\omega\,(\omega\pm i)-2|\tau|^2\right|^2} \\ &= -i\left(I_2(\mu)-I_2(-\mu)\right) \\ &= -2iI_2(\mu). \end{aligned} \tag{4.3.20}$$

The two functions f_1 and f_2 are plotted as function of $|\tau|^2$ for different voltages in figure 4.8.

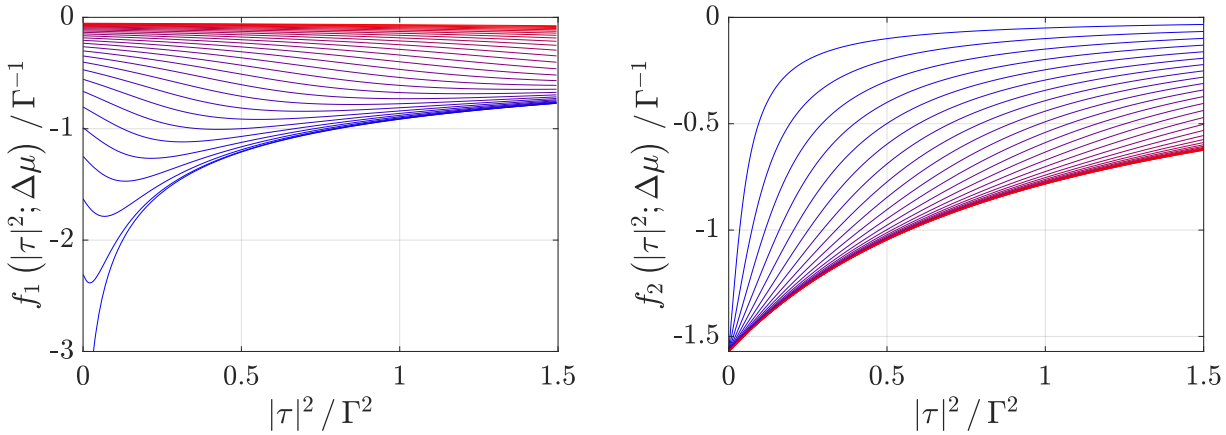

(a) $f_1(|\tau|^2;\mu)$ (b) $f_2(|\tau|^2;\mu)$

Figure 4.8.: f_1 and f_2 for $\Delta\mu = 0\ldots 6\Gamma$ (blue to red lines) with a $\Delta(\Delta\mu) = 0.2\Gamma$. In (b), f_2 is not shown for $\Delta\mu = 0\Gamma$, as it is zero.

[VIII] See section A.2.5 in the appendix.

[IX] The $|\tau|^2$-dependence of I_2 is not shown explicitly in order to be consistent with its definition in (4.3.11).

Equation (4.3.17) is formally solved for $\langle d^\dagger c_a \rangle$ and gives the expression in μ and $|\tau|^2$:

$$\begin{aligned}\left\langle d^\dagger c_a \right\rangle &= -\frac{\tau^*}{\pi}\left[f_1(|\tau|^2;\mu) - i f_2(|\tau|^2;\mu)\right] \\ &= -\frac{t + U\left\langle d^\dagger c_a \right\rangle}{\pi}\left[f_1(|\tau|^2;\mu) - i f_2(|\tau|^2;\mu)\right] \\ &= -t\frac{f_1(|\tau|^2;\mu) - i f_2(|\tau|^2;\mu)}{\pi + U\left[f_1(|\tau|^2;\mu) - i f_2(|\tau|^2;\mu)\right]}\end{aligned} \tag{4.3.21}$$

Using the definition of $\tau^{(*)}$ and the fact that $\langle d^\dagger c_a \rangle = \left\langle c_a^\dagger d \right\rangle^*$ (cf. (4.1.2) and (4.0.20)), the real transcendental equation

$$|\tau|^2 = \left(t + U\left\langle d^\dagger c_a \right\rangle\right)\left(t + U\left\langle d^\dagger c_a \right\rangle^*\right) = t^2 + 2tU\,\mathrm{Re}\left\{\left\langle d^\dagger c_a \right\rangle\right\} + U^2\left|\left\langle d^\dagger c_a \right\rangle\right|^2 \tag{4.3.22}$$

is found for $|\tau|^2$. The solution can be explained graphically, as each μ gives a curve for the

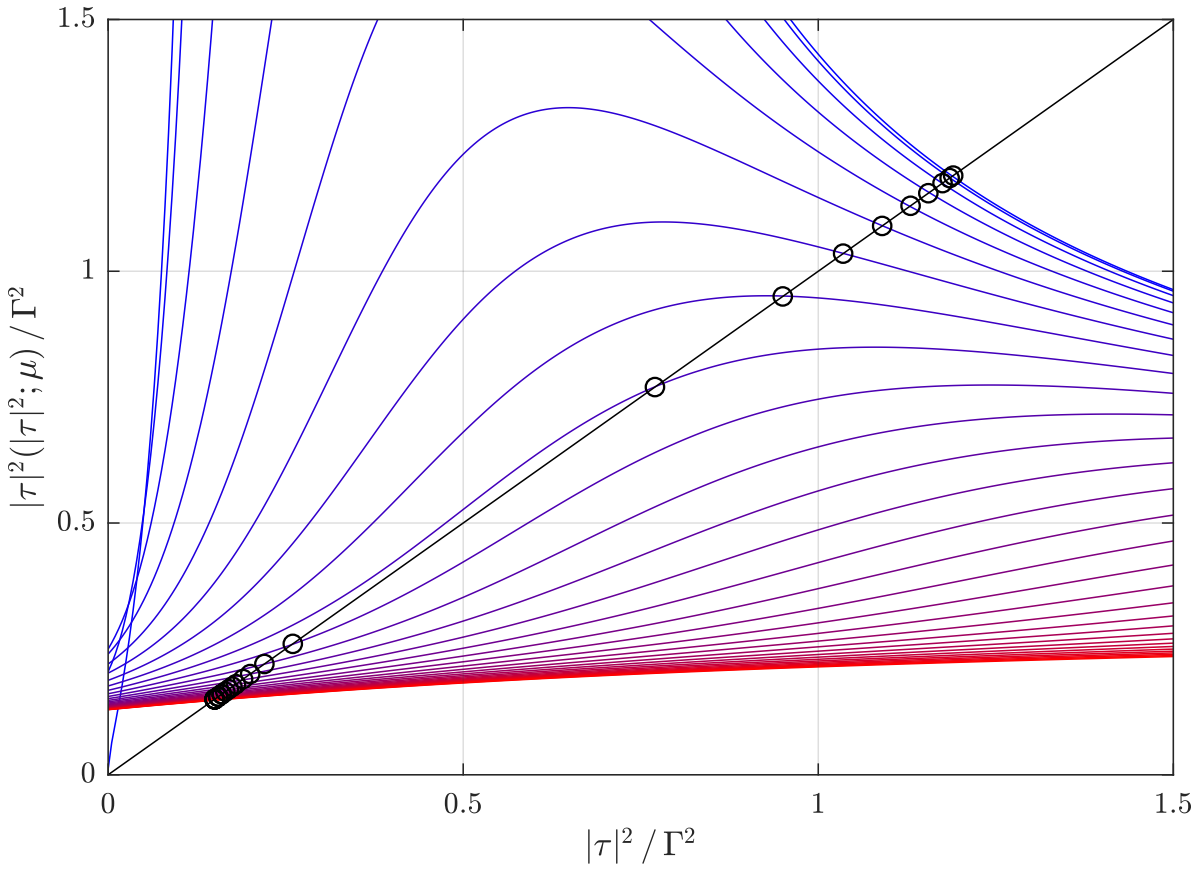

Figure 4.9.: Graphical representation of equation (4.3.22) for $t = 0.5\Gamma$, $U = 2\Gamma$ and voltages $\Delta\mu = 0 \ldots 6\Gamma$ (from blue to red) with a $\Delta(\Delta\mu) = 0.2\Gamma$. The curves represent the right-hand side, where the diagonal (black line) is for the left-hand side. Each intersection is marked with a circle and gives the solution for a specific voltage.

right-hand side, $F(|\tau|^2;\mu)$, and the solution lies in the intersection where $|\tau|^2 = F(|\tau|^2;\mu)$,

or alternatively in the zeros of $\widetilde{F} = F(|\tau|^2;\mu) - |\tau|^2 = 0$, which is easier from a numerical point of view. In fact, for a fixed μ and $|\tau|^2$-grid the solution is simply obtained by finding the location of the minimum value of $\widetilde{F}$ and using the $|\tau|^2$ value at that location. A graphical representation of the problem and its solutions is shown as an example in figure 4.9.

The explicit calculations are done for the same values of t and U as for the tight-binding leads and with

$$\Delta\left(|\tau|^2\right) = 5 \cdot 10^{-4}\Gamma^2$$

for the $|\tau|^2$-grid in the minimum search, and finally the solutions of equation (4.3.22) are shown in figure 4.10.

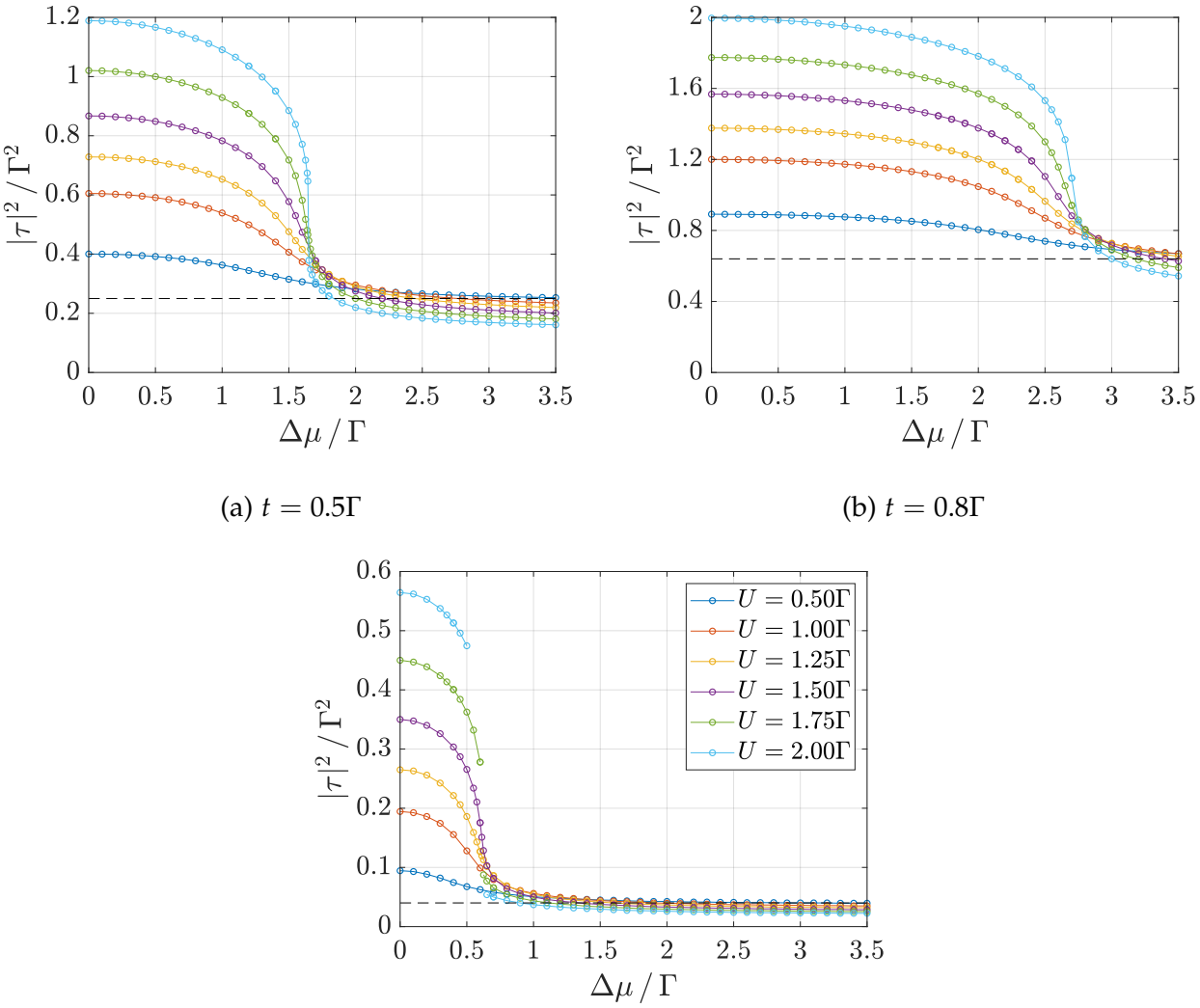

(a) $t = 0.5\Gamma$

(b) $t = 0.8\Gamma$

(c) $t = 0.2\Gamma$

Figure 4.10.: Solutions for the effective hopping from equation (4.3.22) in the model with wide-band-limit leads for different values of U and t. The black dashed lines in each subfigure show the hopping t^2 at $U = 0\Gamma$. The legend in (c) refers to all subfigures. For the chosen $\Delta\mu$-grid multiple solutions occur for $t = 0.2\Gamma$ and $U \geq 1.75\Gamma$ where the lines are not connected (cf. figure 4.19).

The solutions are similar to the tight-binding case, but overall the hoppings are a bit lower, the low-coupling regime is reached at lower voltages and the changes extend to very high voltages, as there is no limiting bandwidth of the leads. Though, the results in figure 4.10 are only shown up to $\Delta\mu = 3.5\Gamma$, as the changes in $|\tau|^2$ become small.

With the obtained solutions for $|\tau|^2$ and the previously presented integrals, the current and the occupation numbers are determined, as the current can be expressed via

$$I = iet\left(\left\langle d^\dagger c_a\right\rangle - \left\langle c_a^\dagger d\right\rangle\right) = -2et\,\mathrm{Im}\left\{\left\langle d^\dagger c_a\right\rangle\right\}$$

and the results for $t = 0.5\Gamma$ are plotted in figure 4.11.

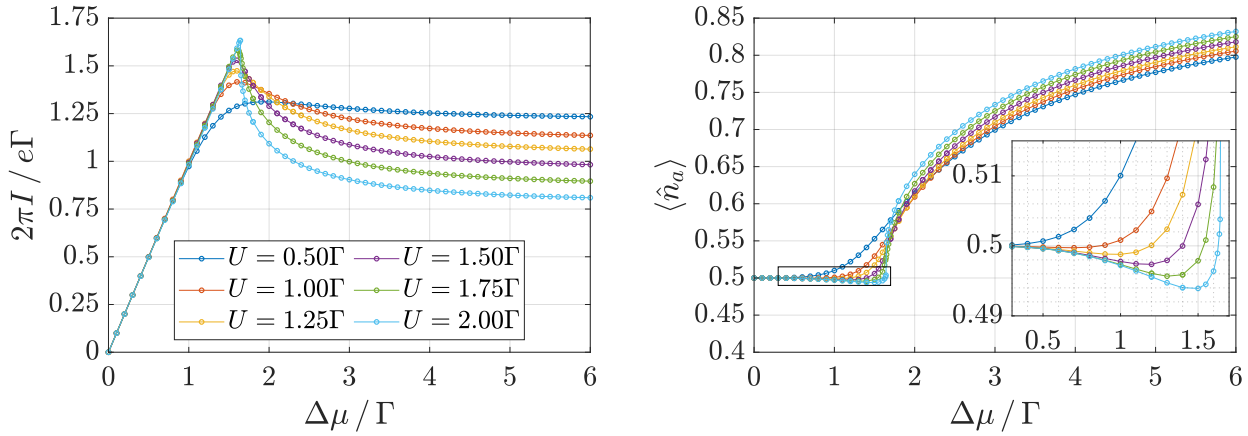

(a) Current

(b) Occupation

Figure 4.11.: Current and occupation number for $t = 0.5\Gamma$ and different values of U. The legend in (a) refers to both subfigures. The current curves feature negative differential conductance in the region for $\Delta\mu \gtrsim 1.5\Gamma$. The occupation numbers for $U \geq 1\Gamma$ show an initial decrease with increasing voltage, which is more pronounced than in the tight-binding results, and slowly saturate to the maximum value for high voltages, cf. equation (4.3.15).

In contrast to the solutions in figure 4.10, the curves in figure 4.11 are shown for voltages up to $\Delta\mu = 6\Gamma$ to depict, in particular, the course of the occupation numbers that saturate very slowly.

For $U = 2\Gamma$, the maximum decrease[X] in the occupation number with increasing voltage is about an order of magnitude higher than for the tight-binding leads. As shown later, the effect also occurs in the non-interacting case if $t^2 > \frac{1}{2}\Gamma^2$, which explains why the curve for $U = 0.5\Gamma$ shows no decrease at all in the above results: the solutions for $|\tau|^2$ stay $\lesssim 0.4\Gamma^2$, cf. figure 4.10a.

[X] Compared to the equilibrium value, i.e. $\langle \hat{n}_a \rangle_{\mu=0} - \min \langle \hat{n}_a \rangle_\mu$.

The obtained current curve for the self-dual point, i.e. $U = 2\Gamma$, and $t = 0.5\Gamma$ is compared to the tight-binding result in reference to the exact solution in figure 4.12:

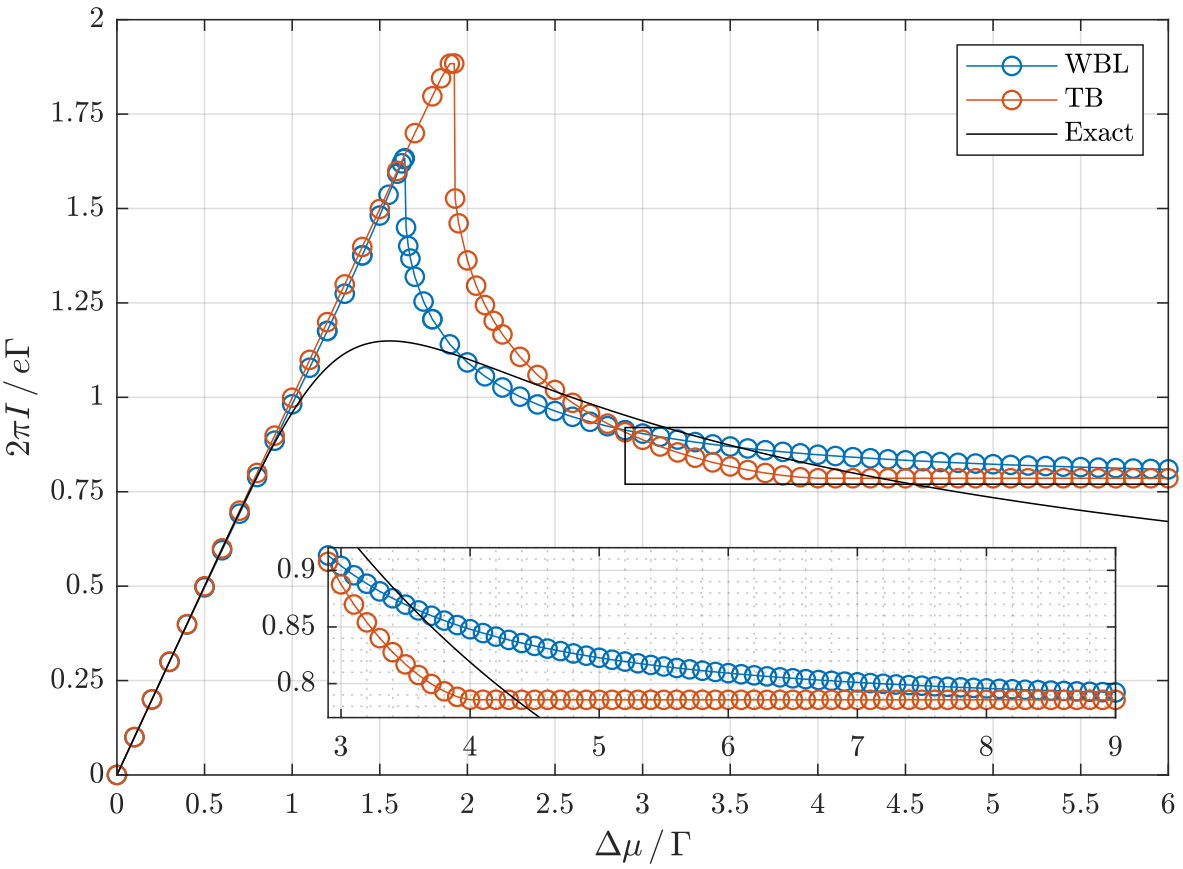

Figure 4.12.: Current comparison between wide-band (WBL, blue) and tight-binding (TB, red) leads for $t = 0.5\Gamma$ and $U = 2\Gamma$. The black solid line shows the exact solution from [16] as reference. The inset extends to and emphasizes on the high-voltage regime, where the TB solution is constant and the WBL solution eventually reaches the same plateau value.

As already stated for the previous results in this section, the main difference between the two leads, namely the behaviour beyond the tight-binding bandwidth of 4Γ, is here emphasized up to $\Delta\mu = 9\Gamma$ in the inset for the current. Another attribute becomes clear in figure 4.12: the WBL current describes the maximum location in the exact solution more accurately, as the exact maximum lies at $\Delta\mu \approx 1.5\Gamma$ and WBL and TB are at $\sim 1.6\Gamma$ and $\sim 1.9\Gamma$ respectively.

The spectral functions for central and left site are again obtained from the retarded or advanced Green's function and are shown in figure 4.13 and 4.14.

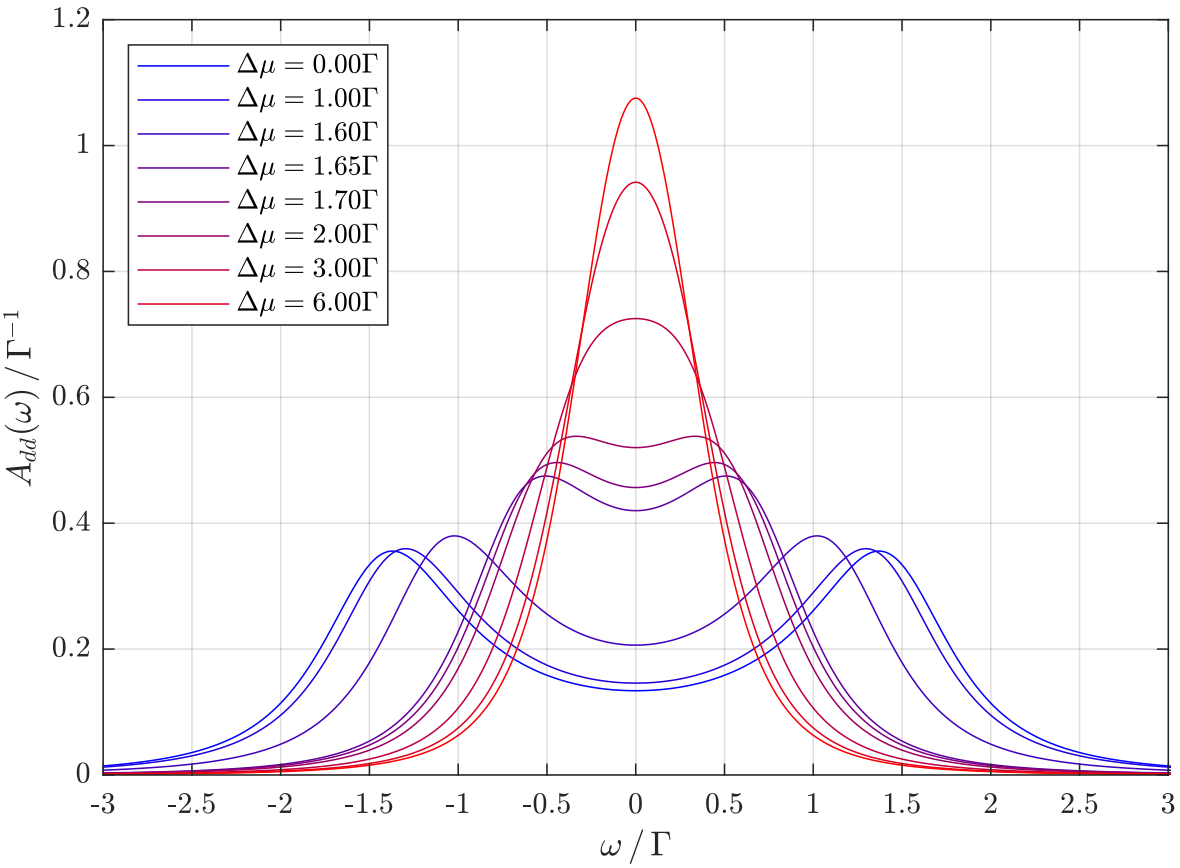

Figure 4.13.: Spectral function on the central site for $U = 2\Gamma$ and $t = 0.5\Gamma$ and different voltages.

The two distinct shapes described in the tight-binding results can be vaguely recognized as one with two symmetric peaks and one with a single central peak, but they rather smoothly merge into each other than show a quick transition.

The merging of the central peak can qualitatively be compared to the results in figure 3b in [17], with the difference that the persisting peaks at $|\omega| \approx 2\Gamma$ are not present in the WBL solution, as they stem from the tight-binding bandwidth limits.

The following figure shows the spectral function on the left site.

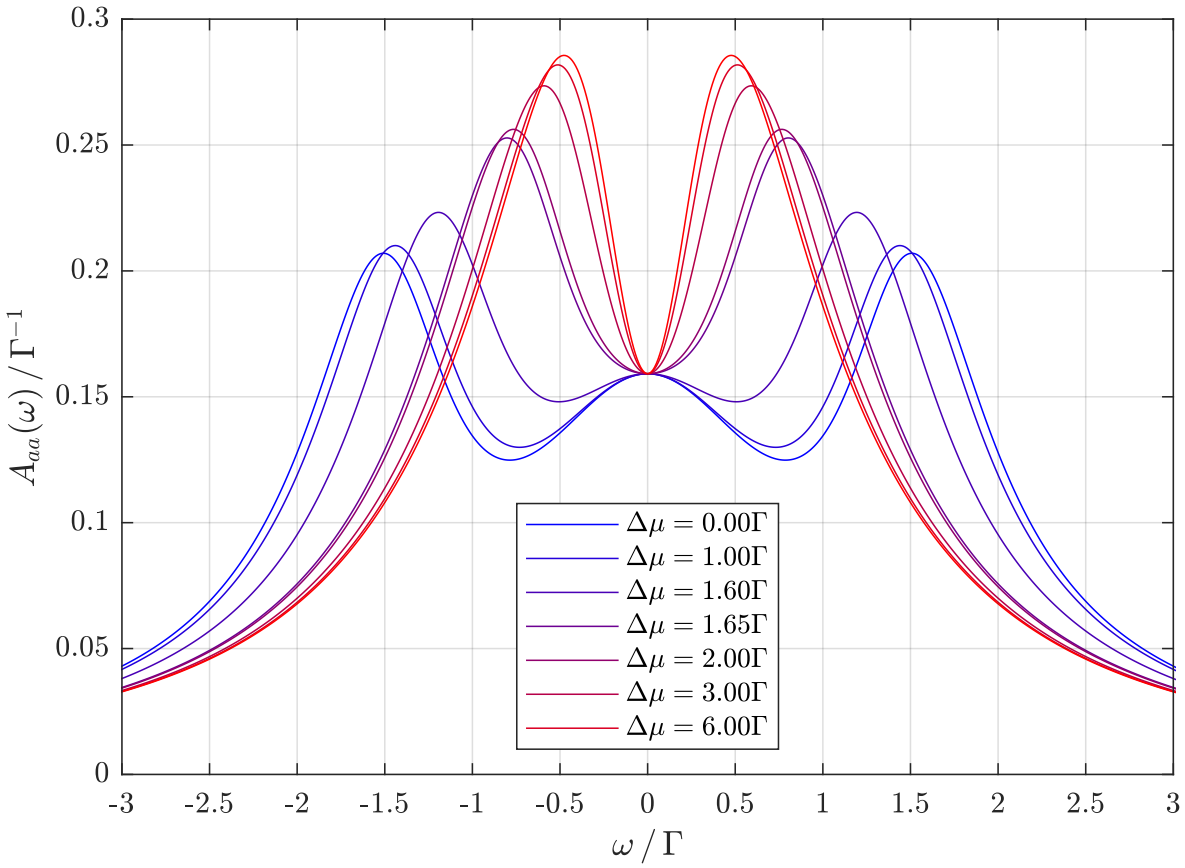

Figure 4.14.: Spectral function on the site a for $U = 2\Gamma$ and $t = 0.5\Gamma$ and different voltages.

Comparable to the central site, the side peaks move closer together and overcome the initial central peak, but do not merge eventually. As in the tight-binding case, the spectral function at $\omega = 0\Gamma$ is pinned to the same value for all voltages, cf. 4.6.

And again, the somewhat constant shape of the spectral function with a slight asymmetric peak weighting from [17] cannot be obtained.

As pointed out in the previous section, some information about the occurring effects can be gained by examining the non-interacting model, which is fully solved by the integrals defined in the course between (4.3.7) and (4.3.21). Current and occupation numbers are shown in figure 4.15 for values of $t > \frac{1}{\sqrt{2}}$ and higher voltages, where interesting effects occur. While the negative differential conductance is technically purely a feature of the

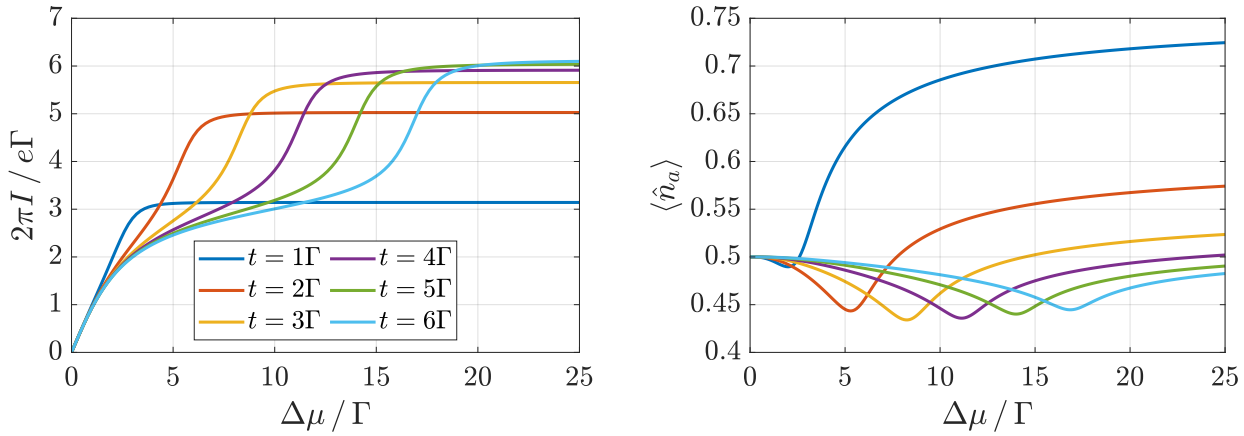

(a) Current

(b) Occupation number

Figure 4.15.: Current and occupation number on site a for $U = 0\Gamma$ and different values of t. All current curves have two inflection points that give rise to the double-plateau behaviour for high values of t (although they are very close for $t = 1\Gamma$), as well as all an initial decrease in the occupation number. The legend in (a) refers to both subfigures.

μ-dependent effective hopping and an effective decoupling of the leads (cf. figure 4.15a where the current curves are strictly increasing functions of voltage), the initial decrease in the occupation number can already be obtained in the non-interacting case for values $t > \frac{1}{\sqrt{2}}$ as shown in the following.

The decrease occurs if equation (4.3.10), as function of voltage, features a minimum that differs from the equilibrium value $\frac{1}{2}$ (cf. (4.3.14)). So a solution to

$$0 \stackrel{!}{=} \frac{\partial \langle \hat{n}_a \rangle}{\partial \mu} = \frac{\partial}{\partial \mu}\left[\frac{1}{2} + \frac{1}{\pi}\left(I_3(\mu) - |\tau|^2 I_2(\mu)\right)\right] = \frac{\partial}{\partial \mu}\left(I_3(\mu) - |\tau|^2 I_2(\mu)\right) \tag{4.3.23}$$

is needed for $|\tau|^2 = t^2$. As I_2 and I_3 are indefinite integrals the derivative gives just back the integrands, namely

$$\frac{\partial}{\partial \mu}\left(I_3(\mu) - |\tau|^2 I_2(\mu)\right)\Big|_{|\tau|^2 = t^2} = \frac{\left|\mu(\mu \pm i) - t^2\right|^2}{(\mu^2+1)\left|\mu\,(\mu \pm i) - 2t^2\right|^2} - \frac{t^4}{(\mu^2+1)\left|\mu\,(\mu \pm i) - 2t^2\right|^2}. \tag{4.3.24}$$

The denominators are the same and so the problem reduces to

$$\begin{aligned} 0 \stackrel{!}{=} &\left|\mu(\mu \pm i) - t^2\right|^2 - t^4 \\ = &\mu^4 + \left(1 - 2t^2\right)\mu^2 \end{aligned} \tag{4.3.25}$$

whose only non-zero (which corresponds to the equilibrium case where $\Delta\mu = 0\Gamma$) and positive solution is

$$\mu_{min} = \sqrt{2t^2 - 1},$$

which is real for

$$t^2 > \frac{1}{2}.$$

In the results from figure (4.10), the topic of multiple solutions is already raised, and shall be discussed in more detail in the following. The non-unique values for $|\tau|^2$ stem from multiple possible intersections occurring for certain pairs of U and t. An example plot is shown in figure 4.16:

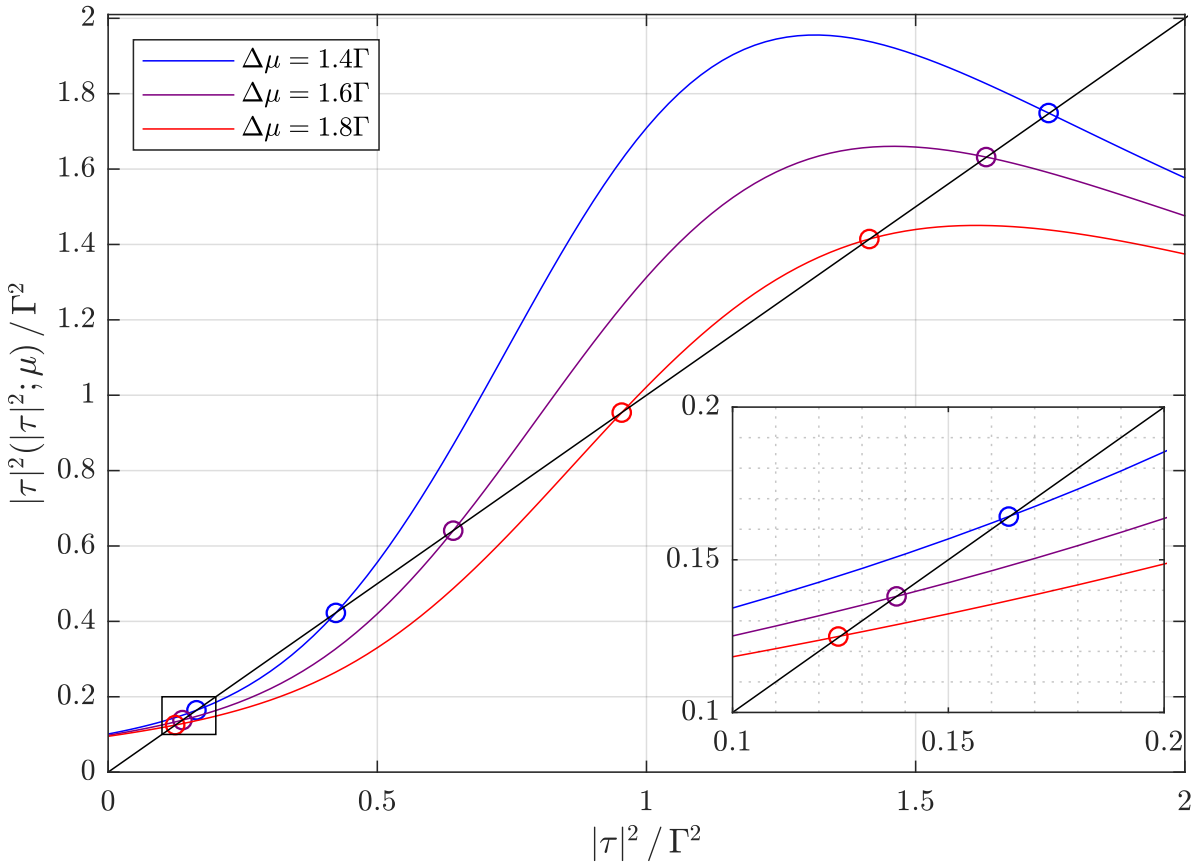

Figure 4.16.: Graphical representation of equation (4.3.22) for $t = 0.5\Gamma$, $U = 3\Gamma$ and selected voltages to explain the situation of non-unique solutions.

As the solutions are obtained for zero temperature, the minimal total energy determines the correct solution in equilibrium. In non-equilibrium, the total energy is not enough to determine the solution for the system, however, it can give more insight to the obtained solutions for $|\tau|^2$. The total energy $\langle H \rangle$ for each $|\tau|^2$ solution can be calculated from the

particle-hole symmetric HF Hamiltonian, which reads (cf. equation (4.0.7) and (4.1.1))

$$\begin{aligned} H_{\mathrm{HF}} = &-\frac{U}{2} + \sum_{k\in\mathrm{L}} \varepsilon_k \hat{n}_k + \sum_{k\in\mathrm{R}} \varepsilon_k \hat{n}_k \\ &- \sum_{m=a,b} \left[\tau_m^* c_m^\dagger d + \tau_m d^\dagger c_m - U \left\langle c_m^\dagger d \right\rangle \left\langle d^\dagger c_m \right\rangle \right] - V \sum_{k\in\mathrm{L,R}} \left(c_{a,b}^\dagger c_k + c_k^\dagger c_{a,b} \right), \end{aligned} \tag{4.3.26}$$

where the constant of $-\frac{U}{2}$ stems from the occupation numbers. In the expectation value, the sum of the two on-site lead terms vanishes (cf. section A.1.4 in the appendix) and so the total energy results in

$$\begin{aligned} \langle H_{\mathrm{HF}} \rangle &= -\frac{U}{2} - \sum_{m=a,b} \left(2t\,\mathrm{Re}\left\{ \left\langle d^\dagger c_m \right\rangle \right\} + U \left| \left\langle d^\dagger c_m \right\rangle \right|^2 \right) - 2V \sum_{k\in\mathrm{L,R}} \mathrm{Re}\left\{ \left\langle c_{a,b}^\dagger c_k \right\rangle \right\} \\ &= -\frac{U}{2} - 2\left(2t\,\mathrm{Re}\left\{ \left\langle d^\dagger c_a \right\rangle \right\} + U \left| \left\langle d^\dagger c_a \right\rangle \right|^2 \right) - 2V \sum_{k\in\mathrm{L,R}} \mathrm{Re}\left\{ \left\langle c_{a,b}^\dagger c_k \right\rangle \right\} \\ &= -\frac{U}{2} - 2\frac{|\tau|^2 - t^2}{U} - 2V \sum_{k\in\mathrm{L,R}} \mathrm{Re}\left\{ \left\langle c_{a,b}^\dagger c_k \right\rangle \right\} \end{aligned} \tag{4.3.27}$$

as $\langle d^\dagger c_a \rangle = \left\langle c_b^\dagger d \right\rangle$ and $\langle d^\dagger c_a \rangle^* = \left\langle c_a^\dagger d \right\rangle$ and with the use of equation (4.3.22) in the last step. The last term needs a little more work, but can be solved with the corresponding equation of motion and some exact integral solutions. From the equation of motion in (3.3.8), the following is obtained

$$\begin{aligned} V \sum_{k_{a,b}} \left\langle c_{a,b}^\dagger c_k \right\rangle &= \frac{V}{2\pi i} \sum_{k_{a,b}} \int_{-\infty}^{\infty} \mathrm{d}\omega \, \langle\langle c_{k_{a,b}}; c_{a,b}^\dagger \rangle\rangle^< \\ &= -\frac{1}{2\pi i} \int_{-\infty}^{\infty} \mathrm{d}\omega \left(\langle\langle c_{a,b}; c_{a,b}^\dagger \rangle\rangle^{\mathrm{A}} V^2 \sum_{k_{a,b}} g_{k_{a,b}}^< + \langle\langle c_{a,b}; c_{a,b}^\dagger \rangle\rangle^< V^2 \sum_{k_{a,b}} g_{k_{a,b}}^{\mathrm{R}} \right) \\ &= -\frac{1}{2\pi i} \int_{-\infty}^{\infty} \mathrm{d}\omega \left(\langle\langle c_{a,b}; c_{a,b}^\dagger \rangle\rangle^{\mathrm{A}} \Delta^< + \langle\langle c_{a,b}; c_{a,b}^\dagger \rangle\rangle^< \Delta^+ \right) \\ &= -\frac{1}{2\pi} \int_{-\infty}^{\infty} \mathrm{d}\omega \left(2 f_{\mathrm{L,R}}(\omega) \langle\langle c_{a,b}; c_{a,b}^\dagger \rangle\rangle^{\mathrm{A}} - \langle\langle c_{a,b}; c_{a,b}^\dagger \rangle\rangle^< \right), \end{aligned} \tag{4.3.28}$$

where the hybridization functions for the wide-band limit are used in the last step. As $G_{ii}^<$ is purely imaginary, the solution for the real part at $T = 0\Gamma$ is given by

$$\begin{aligned} V \sum_{k_{a,b}} \mathrm{Re}\left\{ \left\langle c_{\{a,b\}}^\dagger c_k \right\rangle \right\} &= -\frac{1}{\pi} \int_{-\infty}^{\infty} \mathrm{d}\omega \, f_{\mathrm{L,R}}(\omega) \, \mathrm{Re}\left\{ \langle\langle c_{a,b}; c_{a,b}^\dagger \rangle\rangle^{\mathrm{A}} \right\} \\ &= -\frac{1}{\pi} \int_{-\infty}^{\mu,-\mu} \mathrm{d}\omega \, \mathrm{Re}\left\{ \langle\langle c_{a,b}; c_{a,b}^\dagger \rangle\rangle^{\mathrm{A}} \right\}. \end{aligned} \tag{4.3.29}$$

The real part of the occurring Green's function is evaluated similarly to equation (4.1.16) and results in

$$\begin{aligned} \mathrm{Re}\left\{ \langle\langle c_a; c_a^\dagger \rangle\rangle^{\mathrm{A}} \right\} &= \left| \langle\langle c_a; c_a^\dagger \rangle\rangle \right|^2 \left[\omega + \mathrm{Re}\{\Delta^-\} - \omega \frac{\alpha(\omega)}{\chi(\omega)} + \alpha(\omega) \left(\omega + \mathrm{Re}\{\Delta^-\} \right) \right] \\ &= \left| \langle\langle c_a; c_a^\dagger \rangle\rangle \right|^2 \left(\omega - \omega \frac{\alpha(\omega)}{\chi(\omega)} + \omega\alpha(\omega) \right) \\ &= \omega \left| \langle\langle c_a; c_a^\dagger \rangle\rangle \right|^2 \left[1 + \alpha(\omega) \left(1 - \chi^{-1}(\omega) \right) \right], \end{aligned} \tag{4.3.30}$$

as $\Delta^{\pm}$ is purely imaginary in the wide-band limit. With equation (4.3.2) the prefactor becomes

$$\left|\langle\langle c_a; c_a^\dagger \rangle\rangle\right|^2 = \left| \frac{\omega\left(\omega \pm i\right) - |\tau|^2}{\left(\omega \pm i\right)\left[\omega\left(\omega \pm i\right) - 2|\tau|^2\right]} \right|^2 \tag{4.3.31}$$

and so the explicit form of the real part is given by

$$\begin{aligned} \mathrm{Re}\left\{ \langle\langle c_a; c_a^\dagger \rangle\rangle \right\} &= \omega \frac{\left|\omega\left(\omega \pm i\right) - |\tau|^2\right|^2 + |\tau|^4 - |\tau|^2|\omega \pm i|^2}{\left|\left(\omega \pm i\right)\left[\omega\left(\omega \pm i\right) - 2|\tau|^2\right]\right|^2} \\ &= \frac{\omega\left[\omega^4 + \left(1 - 3|\tau|^2\right)\omega^2 - |\tau|^2\left(1 - 2|\tau|^2\right)\right]}{\left(\omega^2 + 1\right)\left|\omega\left(\omega \pm i\right) - 2|\tau|^2\right|^2}. \end{aligned} \tag{4.3.32}$$

The integral is solved in section A.2.5 in the appendix and leads to the indefinite integral

$$\begin{aligned} I_4(\omega) := \int \mathrm{d}\omega\, \mathrm{Re}\left\{ \langle\langle c_a; c_a^\dagger \rangle\rangle^{\mathrm{A}} \right\} &= \frac{1}{4}\ln\left(\omega^2 + 1\right) + \frac{1}{8}\ln\left(\omega^4 + \left(1 - 4|\tau|^2\right)\omega^2 + 4|\tau|^4\right) \\ &\quad - \frac{1}{4\sqrt{8|\tau|^2 - 1}} \arctan\left(\frac{2\omega^2 - 4|\tau|^2 + 1}{\sqrt{8|\tau|^2 - 1}}\right). \end{aligned} \tag{4.3.33}$$

The complete lead contribution to the total energy is then obtained as

$$\begin{aligned} -2V \sum_{k \in \{\mathrm{L,R}\}} \mathrm{Re}\left\{ \left\langle c_{\{a,b\}}^\dagger c_k \right\rangle \right\} &= -2V \sum_{k \in \mathrm{L}} \mathrm{Re}\left\{ \left\langle c_a^\dagger c_k \right\rangle \right\} - 2V \sum_{k \in \mathrm{R}} \mathrm{Re}\left\{ \left\langle c_b^\dagger c_k \right\rangle \right\} \\ &= \frac{2}{\pi} \int_{-\infty}^{\mu} \mathrm{d}\omega\, \mathrm{Re}\left\{ \langle\langle c_a; c_a^\dagger \rangle\rangle^{\mathrm{A}} \right\} + \frac{2}{\pi} \int_{-\infty}^{-\mu} \mathrm{d}\omega\, \mathrm{Re}\left\{ \langle\langle c_b; c_b^\dagger \rangle\rangle^{\mathrm{A}} \right\} \\ &= \frac{2}{\pi}\left[I_4(\mu) + I_4(-\mu) - 2I_4(-\infty)\right] \\ &= \frac{4}{\pi}\left[I_4(\mu) - I_4(\infty)\right] \\ &= \frac{4}{\pi}\left[I_4(\mu) + \frac{\pi}{8\sqrt{8|\tau|^2 - 1}}\right] - \gamma_\infty, \end{aligned} \tag{4.3.34}$$

where

$$\gamma_\infty := \lim_{\omega \to \infty} \frac{1}{2\pi}\left(2\ln\left(\omega^2 + 1\right) + \ln\left(\omega^4 + \left(1 - 4|\tau|^2\right)\omega^2 + 4|\tau|^4\right)\right).$$

Although the total energy $\langle H_{\mathrm{HF}} \rangle$ corresponding to a certain solution $|\tau|^2$ is infinite, their difference is finite and $\langle H_{\mathrm{HF}} \rangle + \gamma_\infty$ can be considered, as

$$\gamma_\infty - \gamma'_\infty = \lim_{\omega \to -\infty} \frac{1}{2\pi} \ln\left(\frac{\omega^4 + \left(1 - 4|\tau|^2\right)\omega^2 + 4|\tau|^4}{\omega^4 + \left(1 - 4|\tau|'^2\right)\omega^2 + 4|\tau|'^4}\right) = 0.$$

For a given pair of U and t, multiple solutions may not occur over the whole voltage range. The extent of these multiple solutions can be seen in figure 4.17, where the solutions for $|\tau|^2$ and the corresponding total energies are shown as an example for $t = 0.5\Gamma$ and two higher values of U:

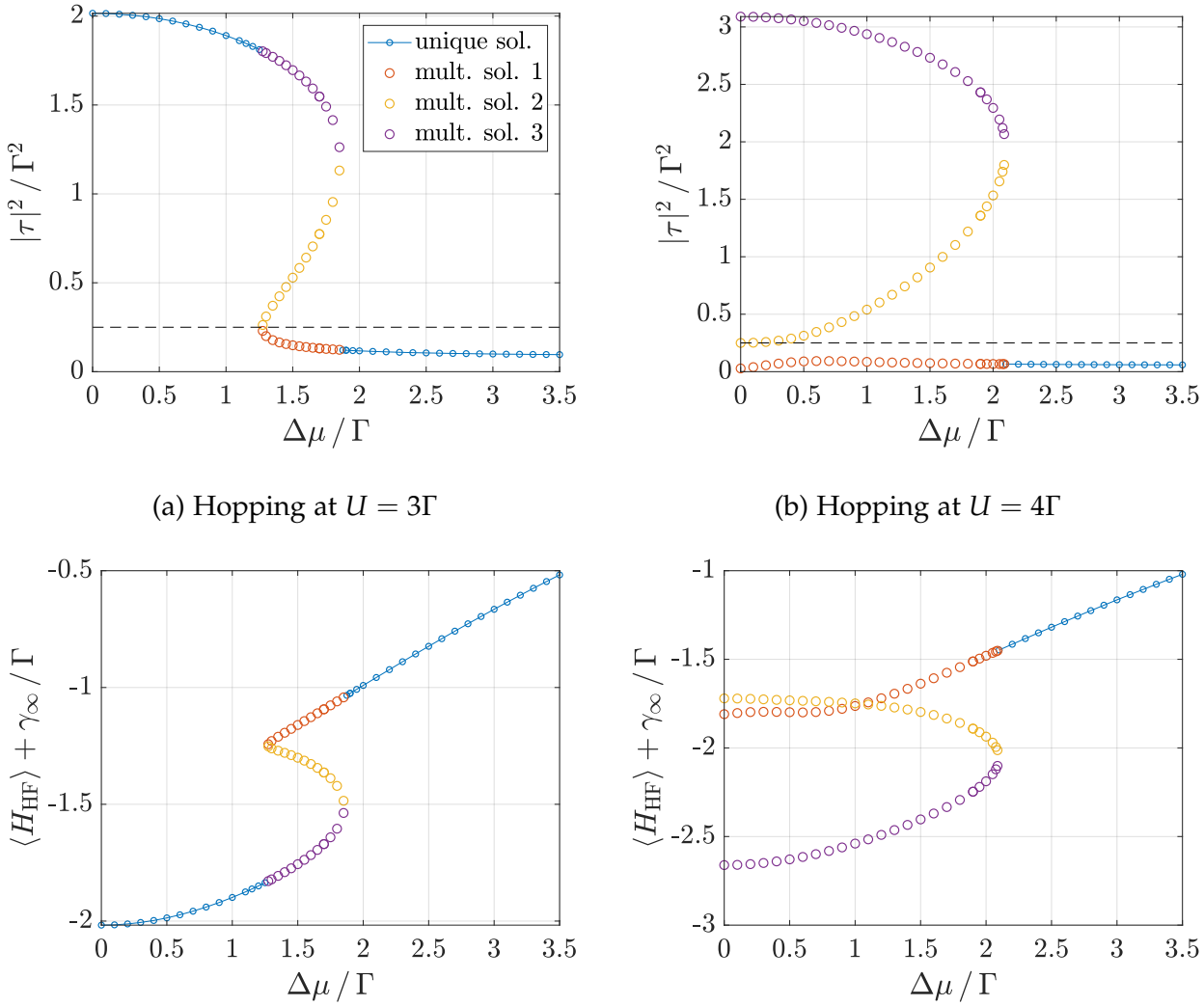

(a) Hopping at $U = 3\Gamma$

(b) Hopping at $U = 4\Gamma$

(c) Total energy at $U = 3\Gamma$

(d) Total energy at $U = 4\Gamma$

Figure 4.17.: Solutions for the effective hopping (upper row) and corresponding total energies (lower row) for parameter pairs $(t = 0.5\Gamma, U)$. Voltage points with unique solutions are connected and marked with small blue circles, multiple solutions are unconnected and marked with bigger circles. The black dashed line in the upper row represents t^2. The legend in (a) refers to all subfigures.

In figure 4.17 it can be seen that the multiple solutions for $U = 3\Gamma$ occur in the transition region from high to low coupling, but for $U = 4\Gamma$ they extend up to zero voltage and unique solutions are obtained only for high voltages. Furthermore, the solutions with the highest value for $|\tau|^2$ result in the lowest energy (solution 3 in the plots).

The current curves to the three solutions from figure 4.17 (and two more U-values in between) are shown in figure 4.18 with markers for the multiple-solution region (dashed lines). Figure 4.18b shows the curves with the lowest energies (solution 3).

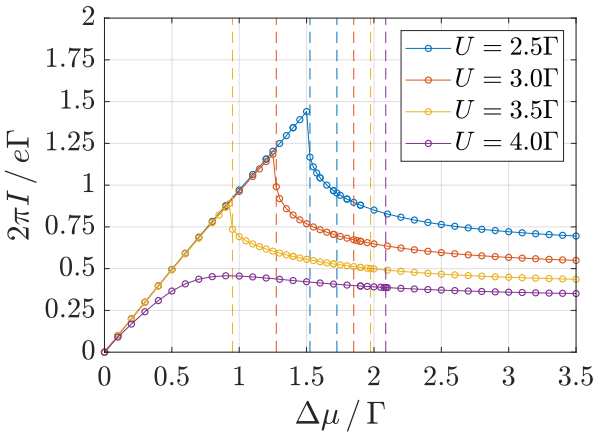

(a) Current following solution 1

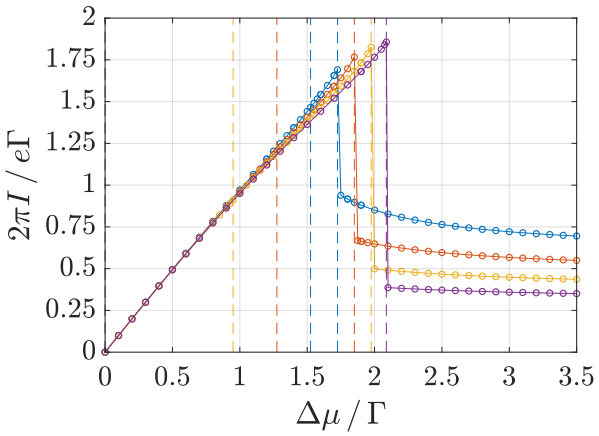

(b) Current following solution 3

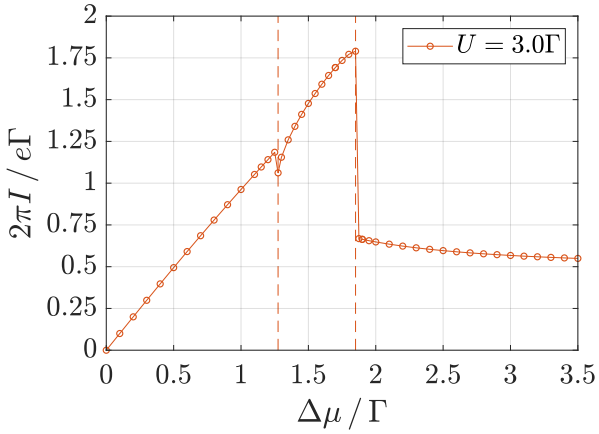

(c) Current following solution 2

Figure 4.18.: Current for $(t = 0.5\Gamma, U)$ pairs where multiple solutions occur. The vertical dashed lines indicate the region with multiple solutions for each U in the respective colour. The left dashed line for $U = 4\Gamma$ is at $\Delta\mu = 0\Gamma$ and is not shown. For solution 2 only one curve is shown, as in this case all curves in one plot seem too confusing. The legend in (a) refers also to (b).

Finally, the question arises for which parameter pairs the solutions are not unique. As this supposedly analytical task again leads to a transcendental equation, the question can only be answered numerically. For that purpose, something like a phase diagram in t and U is calculated in figure 4.19, showing parameter pairs with unique and multiple solutions.

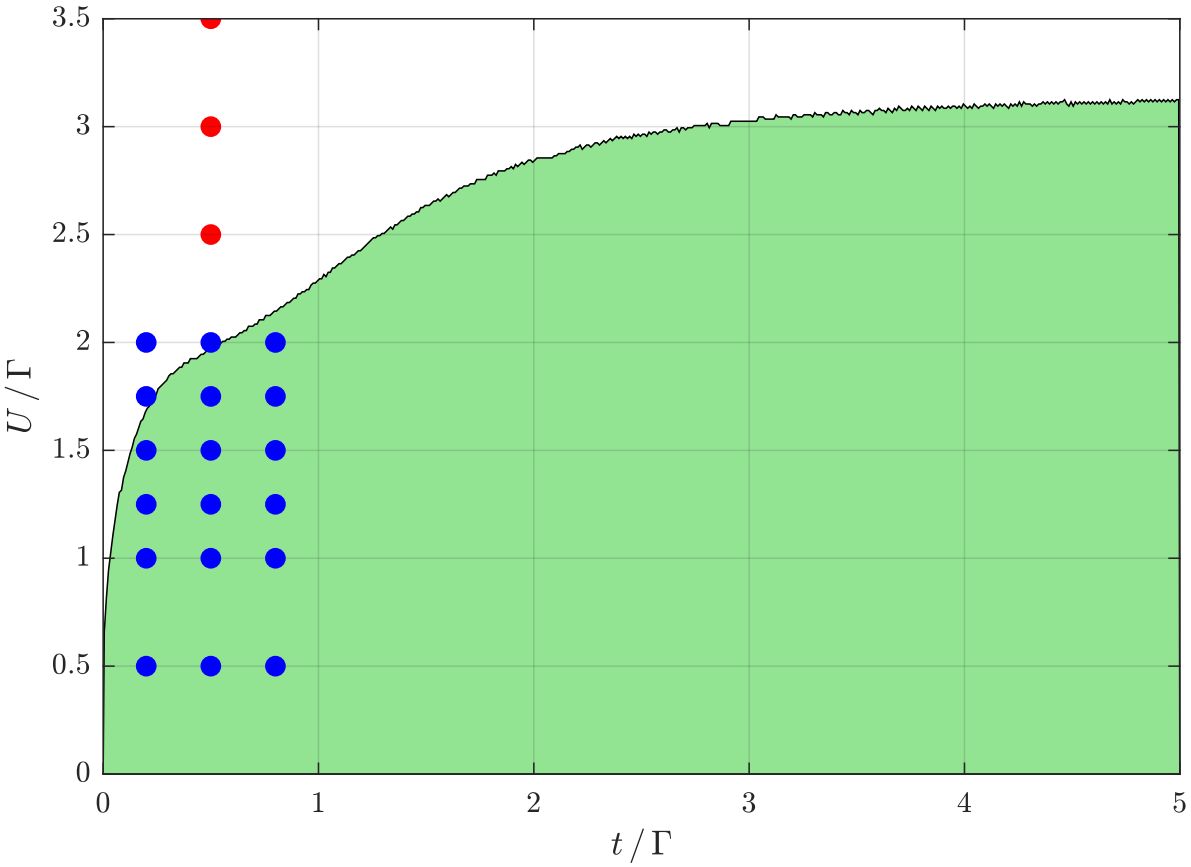

Figure 4.19.: Regions with unique (green area) and multiple (white area) solutions. The results are obtained as for fixed parameters, but for all combinations of t and U shown above with $\Delta t, \Delta U = 0.01\Gamma$ and $\Delta(\Delta\mu) = 10^{-3}\Gamma$, where the calculation for a given pair is stopped if multiple solutions are found. The blue dots indicate the solutions presented in figure 4.10 and the red dots indicate three of the four solutions presented in 4.18 and partially in 4.17.

In figure 4.19 it can be seen that, apart from the solutions that are intended as an example for multiple solutions (red dots), three of the solutions presented earlier (blue dots) lie in the white region and thus show multiple solutions for some voltage range. In the solutions for $t = 0.2\Gamma$ (closest column to the U axis) this behaviour is already pointed out in figure 4.10, where the multiple solutions for $t = 0.5\Gamma$ and $U = 2\Gamma$ are not yet detected, as the $\Delta\mu$-grid used in previous calculations has not sampling points in this small voltage region.

5. Interaction in Higher-Order Truncation

To go beyond a Hartree-Fock like approximation in the interaction terms, the equations of motion for higher Green's functions occurring on three different levels in the equation hierarchy are taken into account and new truncation schemes are introduced, each of them closing the set of equations at that very level. However, the sets of equations become quite large, their coefficient matrices can be dense, and so their symbolical solution by hand becomes quite cumbersome – therefore, it is done in Mathematica and the formulae are not shown explicitly.

Without further treatment, the approximations and truncations used in this chapter lead to results that break certain symmetries, some of which have already been addressed in the use of the equation-of-motion technique (cf. [24]). Additionally, a certain symmetry of the system is broken, namely particle-hole symmetry, which subsequently violates current conservation.

A note a this point: It seems natural – as the Hartree-Fock like approximation to the particle-hole symmetric model formally leads to the same Green's functions as the exact non-interacting model, but with a renormalized hopping amplitude – yet it is worth mentioning: the results in the previous chapter automatically conserve all symmetries mentioned above, including mathematical-structural symmetries in the Green's functions themselves as well as the intuitive physical symmetry of current conservation, i.e. $I_\mathrm{L} = -I_\mathrm{R}$ as well as $I_\mathrm{L} = I_\mathrm{L;lead}$.

As the so-called *scaling regime* is assumed for the exact solution in [15], where the actual shape of the leads should not matter (see [25]), the following calculations focus on leads in the wide-band limit for the sake of simplicity.

All numerical results in this chapter are obtained for $t = 0.5\Gamma$, $T = 0\Gamma$, and for different values of U. The integrations are done numerically using the same initial values and convergence parameters as in previous numerical calculations, but on an ω-grid with

$$\Delta\omega = \begin{cases} \frac{\eta}{2} & \text{for } |\omega| \leq 10\Gamma \\ 0.5\Gamma & \text{for } 10\Gamma < |\omega| \leq 1000\Gamma, \end{cases}$$

as the wide-band Green's functions formally extend to $|\omega| \to \infty$, in contrast to the tight-binding case in previous chapters, where the functions are either $\sim \eta$ or $\propto \delta(\omega - \omega_{1,2})$ outside the bandwidth.

5.1. Symmetry Breaking and Restoration

5.1.1. Green's Function Symmetry

General definitions of the different types of Green's functions imply the following relations in Fourier space:

$$\begin{aligned} G^{\mathrm{R}}_{AB}(\omega) &= \left(G^{\mathrm{A}}_{BA}(\omega)\right)^* \\ -G^{\gtrless}_{AB}(\omega) &= \left(G^{\gtrless}_{BA}(\omega)\right)^* \\ G^{\mathrm{A}}_{AB}(\omega) - G^{\mathrm{R}}_{AB}(\omega) &= G^{<}_{AB}(\omega) - G^{>}_{AB}(\omega) \end{aligned} \tag{5.1.1}$$

In [24] it is shown for two different models that common approximation schemes violate the relations above to some extent when used in an equation-of-motion technique. First higher-order calculations for the IRLM show similar symmetry breakings that lead to unphysical results and therefore need to be corrected.

To this end, a three-step restoration procedure that essentially restores the three relations above is suggested in [24]. This procedure is implemented for all occurring two-operator Green's functions with a slight variation: The authors of [24] suggest calculating the retarded and advanced Green's functions as a first step, then defining new functions that fulfil the first relation from above and calculating the greater and lesser functions with these new functions. However, this seems to rather introduce even higher asymmetries in the lesser and greater functions than no symmetrization at all, and therefore this step is dropped and all Green's functions are calculated simultaneously and symmetrized only afterwards and in each iteration step.

It is worth mentioning that the first and the last step of the suggested procedure, which redefine the retarded/advanced functions, are not needed if the self-consistency loop only requires expectation values that are obtained by integrating lesser functions.

5.1.2. Particle-Hole Symmetry (PHS) restoration

The symmetry restoration proposed in [24] fixes problems like a zero-voltage current and imaginary parts in the occupation number, but current conservation ($I_{\mathrm{L}} + I_{\mathrm{R}} = 0$) is not fulfilled in the first symmetrized calculations and tends to increase with increasing voltage. This is technically due to the results where

$$\left\langle d^\dagger c_a \right\rangle \neq \left\langle c_b^\dagger d \right\rangle$$

which should be assured through particle-hole symmetry and symmetric leads. So, obviously, the applied approximations do not only break general symmetry relations between Green's functions but also explicitly PHS. Thus, inspired by [24], in the following a PHS-restoration procedure is suggested. Applying the PHS transformations (3.0.2) to the single operators in the Green's functions leads, e.g., to

$$\begin{aligned} \langle\langle c_a; d^\dagger \rangle\rangle^{\varkappa}_{\omega} &\xrightarrow{\text{PHS}} -\langle\langle c_b^\dagger; d \rangle\rangle^{\varkappa}_{\omega} \\ \langle\langle c_a; c_a^\dagger \rangle\rangle^{\varkappa}_{\omega} &\xrightarrow{\text{PHS}} +\langle\langle c_b^\dagger; c_b \rangle\rangle^{\varkappa}_{\omega}. \end{aligned} \tag{5.1.2}$$

As the sets of equations are only calculated for Green's functions with a creation operator to the right, the functions on right-hand side of (5.1.2) need to be related to the calculated functions via the superscript-sensitive relations obtained in (2.3.2) and (2.3.3), which imply

$$\begin{aligned} G^{\gtrless}_{AB}(t) &= -G^{\lessgtr}_{BA}(-t) \\ G^{\mathrm{R/A}}_{AB}(t) &= -G^{\mathrm{A/R}}_{BA}(-t) \end{aligned} \tag{5.1.3}$$

for Green's functions in time $t = t_a - t_b$ or respectively in in ω as $F[f(-t)] = F(-\omega)$:

$$\begin{aligned} G^{\gtrless}_{AB}(\omega) &= -G^{\lessgtr}_{BA}(-\omega) \\ G^{\mathrm{R/A}}_{AB}(\omega) &= -G^{\mathrm{A/R}}_{BA}(-\omega) \end{aligned} \tag{5.1.4}$$

And so for the above examples the relations

$$\begin{aligned} \langle\!\langle c_a; d^\dagger \rangle\!\rangle^{\mathrm{R/A}}_{\omega} &\xrightarrow{\text{PHS}} -\langle\!\langle c_b^\dagger; d \rangle\!\rangle^{\mathrm{R/A}}_{\omega} &&= +\langle\!\langle d; c_b^\dagger \rangle\!\rangle^{\mathrm{A/R}}_{-\omega} \\ \langle\!\langle c_a; d^\dagger \rangle\!\rangle^{\gtrless}_{\omega} &\xrightarrow{\text{PHS}} -\langle\!\langle c_b^\dagger; d \rangle\!\rangle^{\gtrless}_{\omega} &&= +\langle\!\langle d; c_b^\dagger \rangle\!\rangle^{\lessgtr}_{-\omega} \\ \langle\!\langle c_a; c_a^\dagger \rangle\!\rangle^{\mathrm{R/A}}_{\omega} &\xrightarrow{\text{PHS}} +\langle\!\langle c_b^\dagger; c_b \rangle\!\rangle^{\mathrm{R/A}}_{\omega} &&= -\langle\!\langle c_b; c_b^\dagger \rangle\!\rangle^{\mathrm{A/R}}_{-\omega} \\ \langle\!\langle c_a; c_a^\dagger \rangle\!\rangle^{\gtrless}_{\omega} &\xrightarrow{\text{PHS}} +\langle\!\langle c_b^\dagger; c_b \rangle\!\rangle^{\gtrless}_{\omega} &&= -\langle\!\langle c_b; c_b^\dagger \rangle\!\rangle^{\lessgtr}_{-\omega} \end{aligned} \tag{5.1.5}$$

are obtained. And finally, the proposed PHS restoration for general operators reads

$$\begin{aligned} \widetilde{G}^{\mathrm{R/A}}_{AB}(\omega) &= \frac{1}{2}\left(G^{\mathrm{R/A}}_{AB}(\omega) - G^{\mathrm{A/R}}_{B^\bullet A^\bullet}(-\omega) \right) \\ \widetilde{G}^{\gtrless}_{AB}(\omega) &= \frac{1}{2}\left(G^{\gtrless}_{AB}(\omega) - G^{\lessgtr}_{B^\bullet A^\bullet}(-\omega) \right), \end{aligned} \tag{5.1.6}$$

where the bullet ($^\bullet$) denotes the PHS transformed operator and the negative argument can be obtained by simply flipping the numerical array, if the Green's functions are evaluated explicitly.

The explicit calculation procedure is described in algorithm 5.1 and occasionally a damping factor $0 \leq \alpha < 1$ is used for better convergence in the expectation values via

$$\langle x_i \rangle \leftarrow (1-\alpha)\langle x_i \rangle + \alpha \langle x_i \rangle_{\text{old}}. \tag{5.1.7}$$

5.2. Truncation Level 1: Strict Second Order

In the equation-of-motion literature, the truncation order is often labelled according to the number of commutations with the Hamiltonian H_1 considered at a certain level. In the previous chapters, only one commutator is considered for each two-operator Green's function and hence corresponds to a first-order truncation. In that sense, a strict second-order truncation requires the commutators

$$\begin{aligned} [d\hat{n}_a, H_1] &= -t\left(c_b\hat{n}_a + c_a\hat{n}\right) - V\sum_{k\in\mathrm{L}}\left(c_a^\dagger c_k d - c_k^\dagger c_a d\right) + U\left(d\hat{n}_a + d\hat{n}_a\hat{n}_b\right) \\ [d\hat{n}_b, H_1] &= -t\left(c_a\hat{n}_b + c_b\hat{n}\right) - V\sum_{k\in\mathrm{R}}\left(c_b^\dagger c_k d - c_k^\dagger c_b d\right) + U\left(d\hat{n}_b + d\hat{n}_a\hat{n}_b\right), \end{aligned} \tag{5.2.1}$$

Require: $\langle x_i \rangle_{\text{start}}, \omega, \eta, t, U, T, \Delta\mu, \epsilon_{\text{abs}}$

$\langle x_i \rangle \leftarrow \langle x_i \rangle_{\text{start}}$
$chk \leftarrow 1$
while $chk > \epsilon_{\text{abs}}$ **do**
  $\langle x_i \rangle_{\text{old}} \leftarrow \langle x_i \rangle$
  $G_j^{\varkappa}(\omega) \leftarrow f(\{\langle x_i \rangle\}, \omega, \eta, t, U, T, \Delta\mu)$ according to the respective results
  $\widetilde{G}_j^{\varkappa}(\omega) \leftarrow \text{PHS}(\{G_i^{\varkappa}(\omega)\})$ according to (5.1.6)
  $G_j^{\varkappa}(\omega) \leftarrow$ symmetrize $\{\widetilde{G}_i^{\varkappa}(\omega)\}$ according to [24] and subsection 5.1.1
  $\langle x_i \rangle \leftarrow (2\pi i)^{-1} \int \mathrm{d}\omega\, G_i^{<}(\omega)$
  $chk \leftarrow \max_i |\langle x_i \rangle - \langle x_i \rangle_{\text{old}}|$
  optional damping according to (5.1.7)
end while

Algorithm 5.1: Self-consistency non-equilibrium loop including symmetry restorations

and

$$\begin{aligned}
[c_a \hat{n}, H_1] &= -t\left(d\hat{n}_a + c_b^\dagger c_a d + d^\dagger c_b c_a\right) - V\sum_{k\in \mathrm{L}} c_k \hat{n} + U c_a \hat{n} \\
[c_b \hat{n}, H_1] &= -t\left(d\hat{n}_b + c_a^\dagger c_b d + d^\dagger c_a c_b\right) - V\sum_{k\in \mathrm{R}} c_k \hat{n} + U c_b \hat{n}.
\end{aligned} \tag{5.2.2}$$

For the sake of clarity, all four required commutators are shown explicitly, but as the system is symmetric in a and b, i.e. left (L) and right (R), from here on these sites are denoted by $\iota, \bar{\iota}$ and $k, \bar{k}$ respectively[I]. In this way, the non-zero anticommutators are

$$\begin{aligned}
\left\{d\hat{n}_\iota, d^\dagger\right\} &= \hat{n}_\iota \\
\left\{d\hat{n}_\iota, c_l^\dagger\right\} &= -c_l^\dagger d \\
\left\{c_\iota \hat{n}, d^\dagger\right\} &= -d^\dagger c_\iota \\
\left\{c_\iota \hat{n}, c_l^\dagger\right\} &= \hat{n}.
\end{aligned} \tag{5.2.3}$$

The equation sets for retarded/advanced and greater/lesser Green's functions have formally the same structure and differ only in the inhomogeneous term $\chi_{A,B}^{\varkappa}$, and so for $\varkappa = \mathrm{R,A,<,>}$ the additional equations of motion read

$$\begin{aligned}
(\widetilde{\omega}_d^{\varkappa} - U)\,\langle\langle d\hat{n}_\iota; x^\dagger\rangle\rangle^{\varkappa} &= \chi_{d\hat{n}_\iota,x}^{\varkappa} - t\left(\langle\langle c_{\bar{\iota}}\hat{n}_\iota; x^\dagger\rangle\rangle^{\varkappa} + \langle\langle c_\iota \hat{n}; x^\dagger\rangle\rangle^{\varkappa}\right) \\
&\quad + U\langle\langle d\hat{n}_\iota \hat{n}_{\bar{\iota}}; x^\dagger\rangle\rangle^{\varkappa} - V\sum_k\left[\langle\langle c_\iota^\dagger c_k d; x^\dagger\rangle\rangle^{\varkappa} - \langle\langle c_k^\dagger c_\iota d; x^\dagger\rangle\rangle^{\varkappa}\right] \\
(\widetilde{\omega}_\iota^{\varkappa} - U)\,\langle\langle c_\iota \hat{n}; x^\dagger\rangle\rangle^{\varkappa} &= \chi_{c_\iota\hat{n},x}^{\varkappa} - V\sum_k \langle\langle c_k \hat{n}; x^\dagger\rangle\rangle^{\varkappa} \\
&\quad - t\left[\langle\langle d\hat{n}_\iota; x^\dagger\rangle\rangle^{\varkappa} + \langle\langle c_{\bar{\iota}}^\dagger c_\iota d; x^\dagger\rangle\rangle^{\varkappa} + \langle\langle d^\dagger c_{\bar{\iota}} c_\iota; x^\dagger\rangle\rangle^{\varkappa}\right],
\end{aligned} \tag{5.2.4}$$

[I] So, e.g., if $\iota = a$, then $\bar{\iota} = b, k \in \mathrm{L}$ and $\bar{k} \in \mathrm{R}$ and vice versa.

where

$$\begin{aligned}
\chi^{\mathrm{R/A}}_{d\hat{n}_\iota,x} &= \langle \hat{n}_\iota \rangle \, \delta_{d,x} - \left\langle c_\iota^\dagger d \right\rangle \delta_{c_\iota,x} \\
\chi^{\mathrm{R/A}}_{c_\iota\hat{n},x} &= \langle \hat{n} \rangle \, \delta_{c_\iota,x} - \left\langle d^\dagger c_\iota \right\rangle \delta_{d,x} \\
\chi^{\gtrless}_{d\hat{n}_\iota,x} &= g_d^{\gtrless} \left|\widetilde{\omega}_d^{\pm}\right|^2 \langle\langle d\hat{n}_\iota; x^\dagger \rangle\rangle^{\mathrm{A}} \\
\chi^{\gtrless}_{c_\iota\hat{n},x} &= g_\iota^{\gtrless} \left|\widetilde{\omega}_\iota^{\pm}\right|^2 \langle\langle c_\iota\hat{n}; x^\dagger \rangle\rangle^{\mathrm{A}}
\end{aligned} \tag{5.2.5}$$

and

$$\begin{aligned}
\widetilde{\omega}_i^{\mathrm{R/A}} = \widetilde{\omega}_i^{\pm} &= \omega - \varepsilon_i \pm i\eta \\
\widetilde{\omega}_i^{\gtrless} = \widetilde{\omega}_i^{\mathrm{R}} &\qquad\qquad (i = \iota, d).
\end{aligned}$$

The complete equation set for this order of truncation consists of the fundamental equations of motion for the two-operator Green's functions, (3.3.5), (3.3.4), (3.3.7) and the higher equations in (5.2.4).

Analogous to the truncation scheme ("Scheme 1" in the following) used in first order, the new four-operator Green's functions are approximated as

$$\langle\langle a^\dagger bc; x^\dagger \rangle\rangle^{\kappa} \approx \left\langle a^\dagger b \right\rangle \langle\langle c; x^\dagger \rangle\rangle^{\kappa} - \left\langle a^\dagger c \right\rangle \langle\langle b; x^\dagger \rangle\rangle^{\kappa},$$

where a, b, c can be c_ι, c_k, d. This decomposition of Green's functions including a lead operator $c_k^{(\dagger)}$ gives rise to terms like

$$V \sum_k \left\langle x^\dagger c_k \right\rangle \text{ and } V \sum_k \left\langle c_k^\dagger x \right\rangle,$$

whose calculation is described in section 5.5. The procedure described in [23] can in principle be extended to the six-operator Green's functions which decompose to

$$\begin{aligned}
\langle\langle a^\dagger ab^\dagger bc; x^\dagger \rangle\rangle \approx{}& \left\langle a^\dagger a \right\rangle \langle\langle b^\dagger bc; x^\dagger \rangle\rangle + \left\langle b^\dagger b \right\rangle \langle\langle a^\dagger ac; x^\dagger \rangle\rangle \\
&- \left\langle a^\dagger c \right\rangle \langle\langle b^\dagger ba; x^\dagger \rangle\rangle - \left\langle b^\dagger c \right\rangle \langle\langle a^\dagger ab; x^\dagger \rangle\rangle \\
&- \left\langle a^\dagger b \right\rangle \langle\langle b^\dagger ac; x^\dagger \rangle\rangle - \left\langle b^\dagger a \right\rangle \langle\langle a^\dagger bc; x^\dagger \rangle\rangle \\
&+ \text{terms } \propto \text{four-operator expectation values},
\end{aligned} \tag{5.2.6}$$

but as seen later in the evaluation, the only approximation for the six-operator functions that does not violate PHS in the spectral functions already in equilibrium turns out to be

$$\langle\langle d\hat{n}_\iota \hat{n}_{\bar{\iota}}; x^\dagger \rangle\rangle^{\kappa} \approx \langle \hat{n}_\iota \rangle \langle\langle d\hat{n}_{\bar{\iota}}; x^\dagger \rangle\rangle^{\kappa} + \langle \hat{n}_{\bar{\iota}} \rangle \langle\langle d\hat{n}_\iota; x^\dagger \rangle\rangle^{\kappa}.$$

A first application of Scheme 1, where all symmetry restorations are applied, produces results that are governed by numerical artefacts, symmetry breakings and large discrepancies between the currents over different junctions. A closer look at the underlying equation set reveals that the sums of lead-operator expectation values, which are related to the current over the lead junction, appears only in the current-describing form

$$V \sum_k \left(\left\langle c_\iota^\dagger c_k \right\rangle - \left\langle c_k^\dagger c_\iota \right\rangle \right).$$

In an attempt to restore current conservation, the replacement

$$V \sum_k \left(\left\langle c_\iota^\dagger c_k \right\rangle - \left\langle c_k^\dagger c_\iota \right\rangle \right) \to t \left(\left\langle d^\dagger c_\iota \right\rangle - \left\langle c_\iota^\dagger d \right\rangle \right)$$

is proposed, as

$$I = iet \left(\left\langle d^\dagger c_\iota \right\rangle - \left\langle c_\iota^\dagger d \right\rangle \right) \stackrel{!}{=} ieV \sum_k \left(\left\langle c_\iota^\dagger c_k \right\rangle - \left\langle c_k^\dagger c_\iota \right\rangle \right) = I_{\text{lead}}.$$

The results obtained with the replacement are still not conserving the current over different junctions, but at least for some parameter sets all other symmetries are fulfilled. The results are shown in figure 5.1.

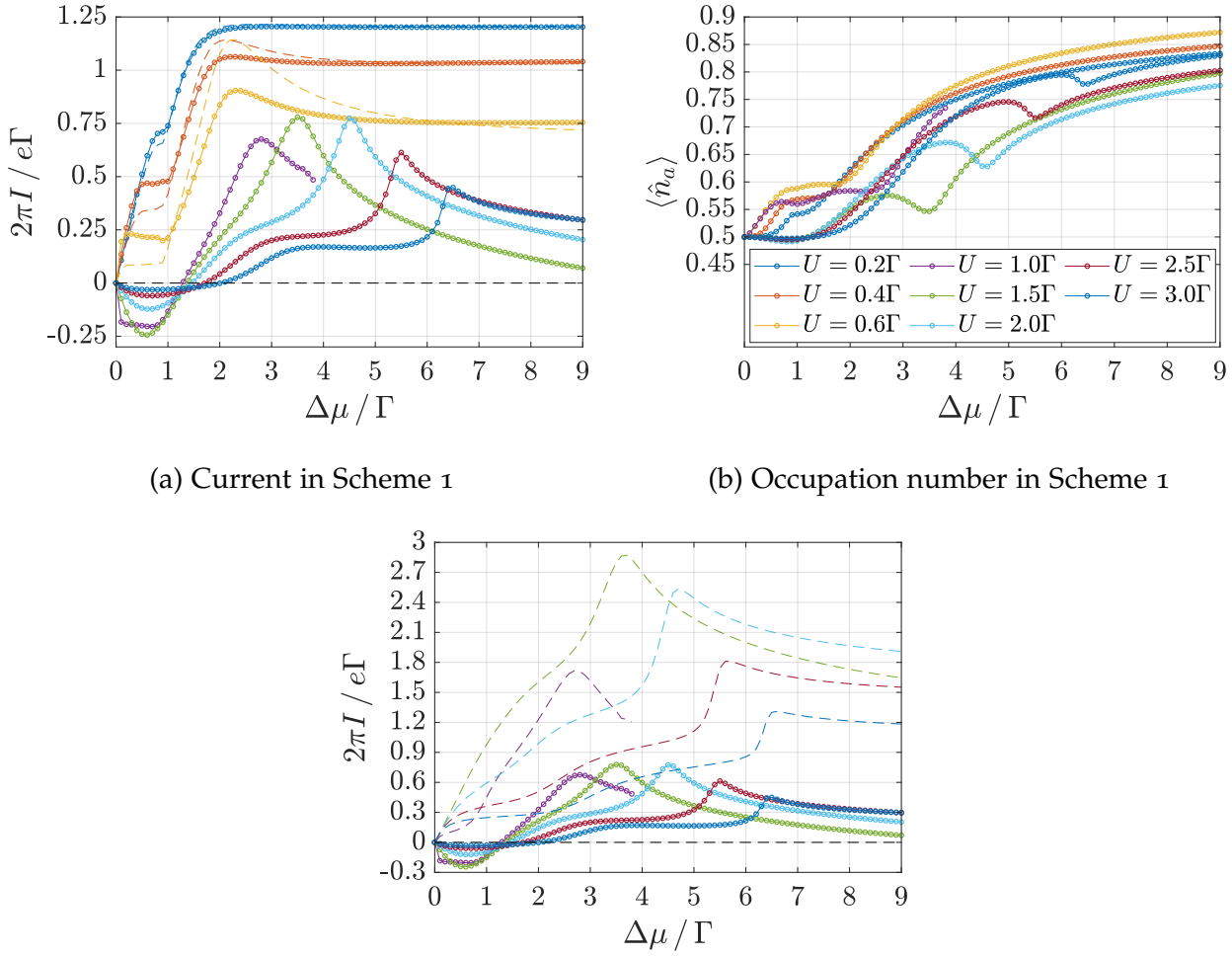

(a) Current in Scheme 1

(b) Occupation number in Scheme 1

(c) Lead-Current addition to (a)

Figure 5.1.: Current and occupation number on site a for Scheme 1, $t = 0.5\Gamma$ and different values of U. The lines with markers are for the intra-system current I and the dashed lines for I_{lead}. Especially for higher values of U in (c) the discrepancy between the two currents is very high. For values of U between 0.6Γ and 1.0Γ the other symmetries are already broken at low voltages and the results are not shown. The results for $U = 1.0\Gamma$ are shown only up to about $\Delta\mu \approx 4\Gamma$, as symmetries are broken for higher values. Refer to (b) for the legends.

As the results from figure 5.1 do not seem very promising compared to previously obtained results, features like negative current for values of $U \gtrsim 1\Gamma$ and the large discrepancy between the different currents, further results within that very approach are not shown.

However, staying at that truncation level, a different approximation scheme ("Scheme 2") can be found in the literature for Green's functions containing one non-interacting lead operator A_k, i.e. either c_k or $c_k^\dagger$. This scheme is applied to the full contour-ordered Green's function in time and can be obtained by treating the non-lead part B as a constant for the commutation, which results[II] in

$$\begin{aligned} [A_k B, H_0] &\approx [A_k, H_0]B \\ [A_k B, H_1] &\approx [A_k, H_1]B \\ \left\{A_k B, x^\dagger\right\} &\approx \left\{A_k, x^\dagger\right\}B = 0 \end{aligned} \tag{5.2.7}$$

for non-lead operators $x = d, c_a, c_b$. The approximation to the Green's function is then obtained via its equation of motion (cf. (2.2.23)):

$$\begin{aligned} \langle\langle (A_k B)_t \,; x_{t'}^\dagger \rangle\rangle &\approx 0 + \int_C \mathrm{d}\tau\, g_{A_k}(t-\tau) \langle\langle [A_k B, H_1]_\tau ; x_{t'}^\dagger \rangle\rangle \\ &\approx \int_C \mathrm{d}\tau\, g_{A_k}(t-\tau) \langle\langle ([A_k, H_1]B)_\tau \,; x_{t'}^\dagger \rangle\rangle \end{aligned} \tag{5.2.8}$$

With the commutators from (3.3.2) this yields

$$\langle\langle (A_k B)_t \,; x_{t'}^\dagger \rangle\rangle \approx \mp V \int_C \mathrm{d}\tau\, g_{A_k}(t-\tau) \langle\langle \left(c_\iota^{(\dagger)} B\right)_\tau ; x_{t'}^\dagger \rangle\rangle, \tag{5.2.9}$$

where the upper (lower) sign is for A_k being an annihilation (creation) operator. In order to get the expressions for the equation sets in ω, Langreth path-splitting and the Fourier transform are used as in the derivation in section 2.2.1 and 2.2.2. For the new functions generated in this order this gives explicitly

$$\begin{aligned} V\sum_k \langle\langle c_\iota^\dagger c_k d; x^\dagger \rangle\rangle^{\mathrm{R/A}} &\approx -V^2 \sum_k g_{c_k}^{\mathrm{R/A}} \langle\langle c_\iota^\dagger c_\iota d; x^\dagger \rangle\rangle^{\mathrm{R/A}} = -\Delta^{\mathrm{R/A}} \langle\langle d\hat{n}_\iota; x^\dagger \rangle\rangle^{\mathrm{R/A}} \\ V\sum_k \langle\langle c_k^\dagger c_\iota d; x^\dagger \rangle\rangle^{\mathrm{R/A}} &\approx +V^2 \sum_k g_{c_k^\dagger}^{\mathrm{R/A}} \langle\langle c_\iota^\dagger c_\iota d; x^\dagger \rangle\rangle^{\mathrm{R/A}} = +\Delta^{\mathrm{R/A}} \langle\langle d\hat{n}_\iota; x^\dagger \rangle\rangle^{\mathrm{R/A}} \\ V\sum_k \langle\langle c_k \hat{n}; x^\dagger \rangle\rangle^{\mathrm{R/A}} &\approx -V^2 \sum_k g_{c_k}^{\mathrm{R/A}} \langle\langle c_\iota \hat{n}; x^\dagger \rangle\rangle^{\mathrm{R/A}} = -\Delta^{\mathrm{R/A}} \langle\langle c_\iota \hat{n}; x^\dagger \rangle\rangle^{\mathrm{R/A}} \end{aligned} \tag{5.2.10}$$

and

$$\begin{aligned} V\sum_k \langle\langle c_\iota^\dagger c_k d; x^\dagger \rangle\rangle^{\gtrless} &\approx -\left(\Delta_k^{\gtrless} \langle\langle d\hat{n}_\iota; x^\dagger \rangle\rangle^{\mathrm{A}} + \Delta^{\mathrm{R}} \langle\langle d\hat{n}_\iota; x^\dagger \rangle\rangle^{\gtrless}\right) \\ V\sum_k \langle\langle c_k^\dagger c_\iota d; x^\dagger \rangle\rangle^{\gtrless} &\approx +\left(\Delta_k^{\gtrless} \langle\langle d\hat{n}_\iota; x^\dagger \rangle\rangle^{\mathrm{A}} + \Delta^{\mathrm{R}} \langle\langle d\hat{n}_\iota; x^\dagger \rangle\rangle^{\gtrless}\right) \\ V\sum_k \langle\langle c_k \hat{n}; x^\dagger \rangle\rangle^{\gtrless} &\approx -\left(\Delta_k^{\gtrless} \langle\langle c_\iota \hat{n}; x^\dagger \rangle\rangle^{\mathrm{A}} + \Delta^{\mathrm{R}} \langle\langle c_\iota \hat{n}; x^\dagger \rangle\rangle^{\gtrless}\right). \end{aligned} \tag{5.2.11}$$

[II] For the commutator the same can be obtained by ignoring the missing term $A_k[B, H]$.

The lesser part for the creation operator $c_k^\dagger$ results in $\Delta_{\bar{k}}^{\gtrless}$ (where $\bar{k}$ denotes the opposite bath) as

$$\begin{aligned} V^2 \sum_k g_{c_k}^{\gtrless} &\to 2i \left(f\left(\omega - \mu_k\right) - \delta_{\gtrless,>} \right) \\ V^2 \sum_k g_{c_k^\dagger}^{\gtrless} &\to 2i \left(f\left(\omega + \mu_k\right) - \delta_{\gtrless,>} \right) \end{aligned} \tag{5.2.12}$$

and the voltage is applied symmetrically, so

$$\mu_k = -\mu_{\bar{k}}.$$

The obtained approximations relate the lead Green's functions to system-operator functions whose equations of motion are already taken into account. Therefore, there is especially no need for approximations that lead to sums over lead expectation values and subsequently no replacement for current related terms is needed.

A first application of Scheme 2 in the equilibrium case, i.e. $\Delta\mu = 0\Gamma$, and without any symmetrization shows a strong asymmetry in the local spectral functions. Therefore an additional third scheme ("Scheme 3") is proposed, which seems to fix these asymmetries in the local spectral functions. It consists of setting differences between lead-operator Green's functions to zero, that can somewhat be interpreted as *hermitian counterparts* in a transport-related operator $\left(c_\iota^\dagger c_k - \text{h.c.}\right) \hat{O}$. In this order this means explicitly

$$\langle\langle c_\iota^\dagger c_k d; x^\dagger \rangle\rangle^{\nearrow} - \langle\langle c_k^\dagger c_\iota d; x^\dagger \rangle\rangle^{\nearrow} \approx 0.$$

However, other asymmetries in the Green's functions still persist, and so the symmetrization schemes have to be applied in order to obtain meaningful physical quantities, which seems to work even for Scheme 2 to some extent.

The results for current and occupation number in Scheme 2 and 3 are shown in figure 5.2 and the spectral functions on the central and left site are shown in figure 5.3.

A striking feature in all current curves is that the initial slope gets suppressed with higher values of U, which is not the case for the HF results. On the other hand, the sharp drop and problems with multiple solutions for higher values of U are missing in this order of truncation. A certain tendency to negative differential conductance is present in all curves, but is not so strongly pronounced; the curves rather tend to saturate straight beyond the maximum. The discrepancy between the two currents I and I_{lead} is higher for Scheme 2, but the current in Scheme 3 shows negative initial values.

Comparing the occupation numbers to the HF results, they start out linearly in contrast to the somewhat constant or even decreasing results from section 4.2 and 4.3.

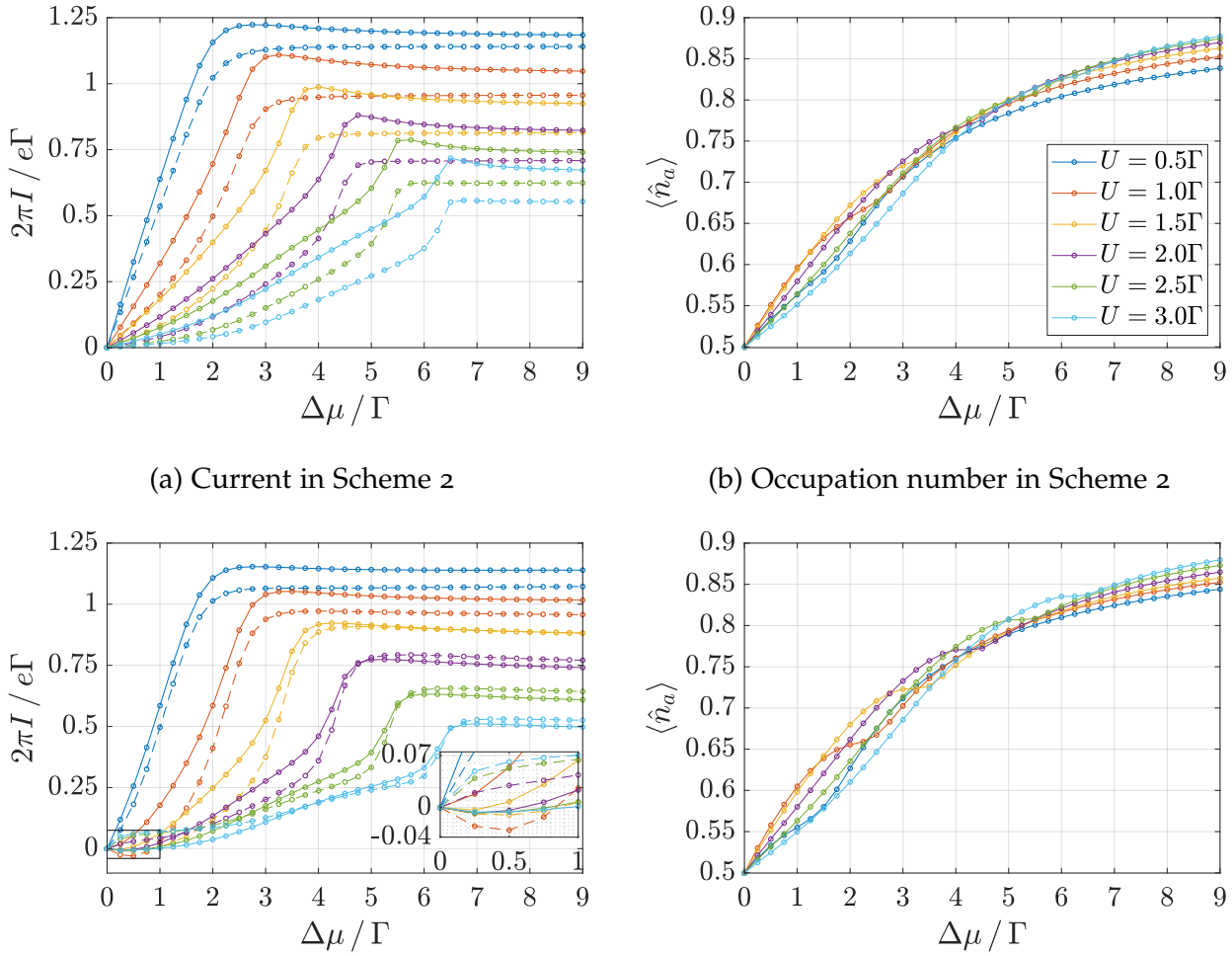

(a) Current in Scheme 2

(b) Occupation number in Scheme 2

(c) Current in Scheme 3

(d) Occupation number in Scheme 3

Figure 5.2.: Current and occupation number on site a for Scheme 2 and 3, $t = 0.5\Gamma$ and different values of U. The solid lines represent I and the dashed lines I_{lead}. The inset in (c) shows some negative current values. The legend in (b) refers to all subfigures.

The spectral functions on the left and central site for $U = 2\Gamma$ and Scheme 2 and 3 are shown in figure 5.3. On the central site, both results feature peaks slightly beyond $|\omega| = 2\Gamma$, that persist with higher voltage. Where it stays somewhat constant in Scheme 2, a prominent central peak arises in Scheme 3, which is comparable to the HF results, but especially to [17], as now side and central peaks are both present. Although it is previously mentioned that the spectral function on the central site is asymmetric in Scheme 2, the results are both symmetric, as the PHS restoration is applied. However, it is still unphysical in Scheme 2 as it shows negative values around $|\omega| \approx 2.5\Gamma$ for higher voltages.

For the left site, the overall shapes in both schemes are quite different than in [17], however the persisting side peaks with an asymmetric weighting are obtained, which is more pronounced for Scheme 3.

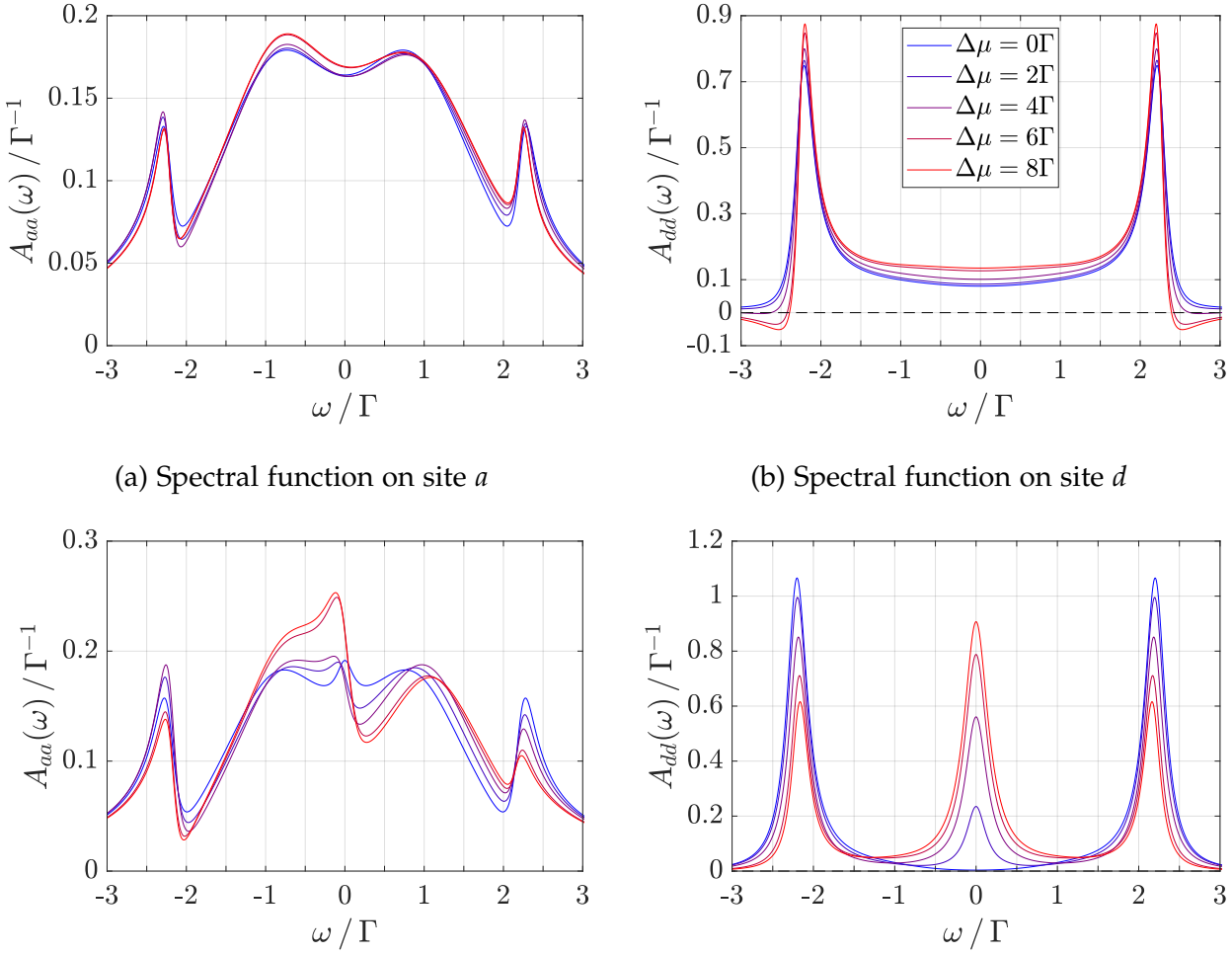

(a) Spectral function on site a

(b) Spectral function on site d

(c) Spectral function on site a

(d) Spectral function on site d

Figure 5.3.: Spectral functions for Scheme 2 (upper row) and 3 (lower row) on site a and d for $t = 0.5\Gamma$, $U = 2\Gamma$ and different voltages. The spectral function for the central site in Scheme 2 shows some negative values for $\Delta\mu \gtrsim 4\Gamma$. In Scheme 3 it is positive in the whole ω range. The legend in (b) refers to all subfigures.

5.3. Truncation Level 2: Four-Operator Terms in t

Following the strict systematic approach requires taking into account the equations of motion for the new Green's functions generated in (5.2.4). However, the Green's functions including a lead operator pose some problems that cannot be overcome in this order of truncation. They are explained using only one affected Green's function as an example, but are valid for the others as well. The equation of motion for a retarded or advanced lead-operator Green's function from (5.2.4) is given by[III]

$$\begin{aligned} V\sum_k \langle\langle c_k \hat{n}; x^\dagger \rangle\rangle = &-V\sum_k \frac{\langle d^\dagger c_k \rangle}{\widetilde{\omega}_k}\delta_{d,x} - \Delta^{\pm}\langle\langle c_\iota \hat{n}; x^\dagger\rangle\rangle \\ &- t\sum_k \frac{V}{\widetilde{\omega}_k}\left(\langle\langle d^\dagger c_\iota c_k; x^\dagger\rangle\rangle - \langle\langle c_\iota^\dagger d c_k; x^\dagger\rangle\rangle + \langle\langle d^\dagger c_{\bar{\iota}} c_k; x^\dagger\rangle\rangle - \langle\langle c_{\bar{\iota}}^\dagger d c_k; x^\dagger\rangle\rangle\right), \end{aligned} \tag{5.3.1}$$

[III]The corresponding commutators and other lead-operator Green's function are described in section A.1.10.

and is already written in the summation form as it appears in the hierarchy of equations. First of all, a potential symmetry issue catches the eye, arising in the terms

$$\langle\langle d^\dagger c_\iota c_k; x^\dagger\rangle\rangle - \langle\langle c_\iota^\dagger d c_k; x^\dagger\rangle\rangle$$

as the equation of motion for the second Green's functions is taken into account, because it already appears in the prior order of truncation, but the first, which can roughly be considered as its hermitian counterpart in a transport-related operator $\left(d^\dagger c_\iota - c_\iota^\dagger d\right) c_k$, has to be approximated[IV]. This is just mentioned as a presumption, though, the actual technical obstacle is the inhomogeneous term

$$V\sum_k \frac{\langle d^\dagger c_k\rangle}{\widetilde{\omega}_k}$$

and similar terms appearing in the other equations of motion as well as by application of approximation Scheme 1 to the new functions in this order, as

$$\begin{aligned}\sum_k \frac{V}{\widetilde{\omega}_k}\langle\langle d^\dagger c_{\bar\iota} c_k; x^\dagger\rangle\rangle &\approx -\left\langle d^\dagger c_{\bar\iota}\right\rangle \langle\langle c_\iota; x^\dagger\rangle\rangle \underbrace{\sum_k \frac{V^2}{\widetilde{\omega}_k^2}}_{=0} - V\sum_k \frac{\langle d^\dagger c_k\rangle}{\widetilde{\omega}_k}\langle\langle c_{\bar\iota}; x^\dagger\rangle\rangle \\ &= -\langle\langle c_{\bar\iota}; x^\dagger\rangle\rangle V\sum_k \frac{\langle d^\dagger c_k\rangle}{\widetilde{\omega}_k}.\end{aligned} \tag{5.3.2}$$

These terms result in ω-dependent functions that have to be evaluated numerically for each ω-point. As described later in section 5.5, in the wide-band limit they can be evaluated via

$$V\sum_k \frac{\langle d^\dagger c_k\rangle}{\omega - \varepsilon_k \pm i\eta} = -\frac{1}{\pi}\int_{-\infty}^{\infty} \mathrm{d}\omega' \left(\frac{f_{\mathrm{L,R}}(\omega')\langle\langle c_\iota; d^\dagger\rangle\rangle^{\mathrm{A}} - \langle\langle c_\iota; d^\dagger\rangle\rangle^{<}\delta_{\pm,-}}{\omega - \omega' \pm 2i\eta}\right), \tag{5.3.3}$$

which is done by numerical integration. Yet, for $T = 0\Gamma$ the integrand has a discontinuity at $\omega' = \mu$ and the integral seems to develop a logarithmic divergence at $\omega = \mu$ in the limit $\eta \to 0^+$.

Therefore, in this order of truncation the lead-operator Green's functions are just approximated as in the previous section. As another simplification the six-operator Green's function is also approximated as before, instead of taking its equation of motion. The equations of motion for the remaining new functions are obtained via the commutators

$$[c_{\bar\iota}\hat{n}_\iota, H_1] = -t\left(d\hat{n}_\iota + d^\dagger c_{\bar\iota} c_\iota - c_\iota^\dagger c_{\bar\iota} d\right) + U c_{\bar\iota}\hat{n}_\iota\hat{n} - V\left[\sum_{\bar k} c_{\bar k}\hat{n}_\iota + \sum_k \left(c_\iota^\dagger c_k c_{\bar\iota} - c_k^\dagger c_\iota c_{\bar\iota}\right)\right] \tag{5.3.4}$$

$$\left[c_{\bar\iota}^\dagger c_\iota d, H_1\right] = -t\left(c_\iota\hat{n} - c_\iota\hat{n}_{\bar\iota}\right) + U c_{\bar\iota}^\dagger c_\iota d - V\left(\sum_k c_{\bar\iota}^\dagger c_k d - \sum_{\bar k} c_{\bar k}^\dagger c_\iota d\right) \tag{5.3.5}$$

$$\left[d^\dagger c_{\bar\iota} c_\iota, H_1\right] = -t\left(c_{\bar\iota}\hat{n}_\iota - c_\iota\hat{n}_{\bar\iota} + c_\iota\hat{n} - c_{\bar\iota}\hat{n}\right) - V\left(\sum_k d^\dagger c_{\bar\iota} c_k + \sum_{\bar k} d^\dagger c_{\bar k} c_\iota\right) \tag{5.3.6}$$

[IV] Considering also the equation of motion for the first Green's function opens up similar symmetry issues that are addressed in section 6.

and the only non-zero anticommutators

$$\begin{aligned}
\left\{c_{\bar{\iota}}\hat{n}_{\iota}, c_{\bar{\iota}}^{\dagger}\right\} &= \hat{n}_{\iota} \\
\left\{c_{\bar{\iota}}\hat{n}_{\iota}, c_{l}^{\dagger}\right\} &= -c_{\iota}^{\dagger}c_{\bar{\iota}} \\
\left\{c_{\bar{\iota}}^{\dagger}c_{\iota}d, d^{\dagger}\right\} &= c_{\bar{\iota}}^{\dagger}c_{\iota} \\
\left\{c_{\bar{\iota}}^{\dagger}c_{\iota}d, c_{l}^{\dagger}\right\} &= -c_{\bar{\iota}}^{\dagger}d \\
\left\{d^{\dagger}c_{\bar{\iota}}c_{\iota}, c_{l}^{\dagger}\right\} &= d^{\dagger}c_{\bar{\iota}}.
\end{aligned} \tag{5.3.7}$$

With these operators all four-operator Green's functions generated by the hopping terms in the parameter t are taken into account.

The corresponding equations of motion read

$$\begin{aligned}
\widetilde{\omega}_{\bar{\iota}}^{\varkappa}\langle\langle c_{\bar{\iota}}\hat{n}_{\iota}; x^{\dagger}\rangle\rangle^{\varkappa} = \chi_{c_{\bar{\iota}}\hat{n}_{\iota},x}^{\varkappa} - t\left(\langle\langle d\hat{n}_{\iota}; x^{\dagger}\rangle\rangle^{\varkappa} + \langle\langle d^{\dagger}c_{\bar{\iota}}c_{\iota}; x^{\dagger}\rangle\rangle^{\varkappa} - \langle\langle c_{\iota}^{\dagger}c_{\bar{\iota}}d; x^{\dagger}\rangle\rangle^{\varkappa}\right) + U\langle\langle c_{\bar{\iota}}\hat{n}_{\iota}\hat{n}; x^{\dagger}\rangle\rangle^{\varkappa} \\
- V\left[\sum_{\bar{k}}\langle\langle c_{\bar{k}}\hat{n}_{\iota}; x^{\dagger}\rangle\rangle^{\varkappa} + \sum_{k}\left(\langle\langle c_{\iota}^{\dagger}c_{k}c_{\bar{\iota}}; x^{\dagger}\rangle\rangle^{\varkappa} - \langle\langle c_{k}^{\dagger}c_{\iota}c_{\bar{\iota}}; x^{\dagger}\rangle\rangle^{\varkappa}\right)\right]
\end{aligned} \tag{5.3.8}$$

$$\begin{aligned}
\left(\widetilde{\omega}^{\varkappa} + \varepsilon_{\bar{\iota}} - \varepsilon_{\iota} - \varepsilon_{d} - U\right)\langle\langle c_{\bar{\iota}}^{\dagger}c_{\iota}d; x^{\dagger}\rangle\rangle^{\varkappa} = \chi_{c_{\bar{\iota}}^{\dagger}c_{\iota}d,x}^{\varkappa} - V\left(\sum_{k}\langle\langle c_{\bar{\iota}}^{\dagger}c_{k}d; x^{\dagger}\rangle\rangle^{\varkappa} - \sum_{\bar{k}}\langle\langle c_{\bar{k}}^{\dagger}c_{\iota}d; x^{\dagger}\rangle\rangle^{\varkappa}\right) \\
- t\left(\langle\langle c_{\iota}\hat{n}; x^{\dagger}\rangle\rangle^{\varkappa} - \langle\langle c_{\iota}\hat{n}_{\bar{\iota}}; x^{\dagger}\rangle\rangle^{\varkappa}\right)
\end{aligned} \tag{5.3.9}$$

$$\begin{aligned}
\left(\widetilde{\omega}^{\varkappa} + \varepsilon_{d} - \varepsilon_{\iota} - \varepsilon_{\bar{\iota}}\right)\langle\langle d^{\dagger}c_{\bar{\iota}}c_{\iota}; x^{\dagger}\rangle\rangle^{\varkappa} = \chi_{d^{\dagger}c_{\bar{\iota}}c_{\iota},x}^{\varkappa} - V\left(\sum_{k}\langle\langle d^{\dagger}c_{\bar{\iota}}c_{k}; x^{\dagger}\rangle\rangle^{\varkappa} + \sum_{\bar{k}}\langle\langle d^{\dagger}c_{\bar{k}}c_{\iota}; x^{\dagger}\rangle\rangle^{\varkappa}\right) \\
- t\left(\langle\langle c_{\bar{\iota}}\hat{n}_{\iota}; x^{\dagger}\rangle\rangle^{\varkappa} - \langle\langle c_{\iota}\hat{n}_{\bar{\iota}}; x^{\dagger}\rangle\rangle^{\varkappa} + \langle\langle c_{\iota}\hat{n}; x^{\dagger}\rangle\rangle^{\varkappa} - \langle\langle c_{\bar{\iota}}\hat{n}; x^{\dagger}\rangle\rangle^{\varkappa}\right)
\end{aligned} \tag{5.3.10}$$

where

$$\begin{aligned}
\chi_{c_{\bar{\iota}}\hat{n}_{\iota},x}^{\mathrm{R/A}} &= \langle\hat{n}_{\iota}\rangle\,\delta_{c_{\bar{\iota}},x} - \left\langle c_{\iota}^{\dagger}c_{\bar{\iota}}\right\rangle\delta_{c_{\iota},x} \\
\chi_{c_{\bar{\iota}}^{\dagger}c_{\iota}d,x}^{\mathrm{R/A}} &= \left\langle c_{\bar{\iota}}^{\dagger}c_{\iota}\right\rangle\delta_{d,x} - \left\langle c_{\bar{\iota}}^{\dagger}d\right\rangle\delta_{c_{\iota},x} \\
\chi_{d^{\dagger}c_{\bar{\iota}}c_{\iota},x}^{\mathrm{R/A}} &= \left\langle d^{\dagger}c_{\bar{\iota}}\right\rangle\delta_{c_{\iota},x} - \left\langle d^{\dagger}c_{\iota}\right\rangle\delta_{c_{\bar{\iota}},x} \\
\chi_{c_{\bar{\iota}}\hat{n}_{\iota},x}^{\gtrless} &= g_{\bar{\iota}}^{\gtrless}\left|\widetilde{\omega}_{\bar{\iota}}^{\pm}\right|^{2}\langle\langle c_{\bar{\iota}}\hat{n}_{\iota}; x^{\dagger}\rangle\rangle^{\mathrm{A}} \\
\chi_{c_{\bar{\iota}}^{\dagger}c_{\iota}d,x}^{\gtrless} &= g_{c_{\bar{\iota}}^{\dagger}c_{\iota}d}^{\gtrless}\left|\widetilde{\omega}^{\pm} + \varepsilon_{\bar{\iota}} - \varepsilon_{\iota} - \varepsilon_{d}\right|^{2}\langle\langle c_{\bar{\iota}}^{\dagger}c_{\iota}d; x^{\dagger}\rangle\rangle^{\mathrm{A}} \\
\chi_{d^{\dagger}c_{\bar{\iota}}c_{\iota},x}^{\gtrless} &= g_{d^{\dagger}c_{\bar{\iota}}c_{\iota}}^{\gtrless}\left|\widetilde{\omega}^{\pm} + \varepsilon_{d} - \varepsilon_{\iota} - \varepsilon_{\bar{\iota}}\right|^{2}\langle\langle d^{\dagger}c_{\bar{\iota}}c_{\iota}; x^{\dagger}\rangle\rangle^{\mathrm{A}}.
\end{aligned} \tag{5.3.11}$$

The set of equations for this order of truncation consists of (3.3.5), (3.3.4), (3.3.7), (5.2.4) and (5.3.8)-(5.3.10).

The occurring six-operator Green's functions are approximated as

$$\begin{aligned}\langle\langle d\hat{n}_\iota\hat{n}_{\bar{\iota}}; x^\dagger\rangle\rangle^\kappa &\approx \langle\hat{n}_\iota\rangle\,\langle\langle d\hat{n}_{\bar{\iota}}; x^\dagger\rangle\rangle^\kappa + \langle\hat{n}_{\bar{\iota}}\rangle\,\langle\langle d\hat{n}_\iota; x^\dagger\rangle\rangle^\kappa \\ \langle\langle c_{\bar{\iota}}\hat{n}_\iota\hat{n}; x^\dagger\rangle\rangle^\varkappa &\approx \langle\hat{n}_\iota\rangle\,\langle\langle c_{\bar{\iota}}\hat{n}; x^\dagger\rangle\rangle^\kappa + \langle\hat{n}\rangle\,\langle\langle c_{\bar{\iota}}\hat{n}_\iota; x^\dagger\rangle\rangle^\kappa\end{aligned} \tag{5.3.12}$$

as a full decomposition[V] leads to similar asymmetries in the spectral functions as within the previous truncation order. The remaining four-operator Green's functions are approximated according to the three schemes presented in the previous order. For the new functions in Scheme 2 this gives explicitly

$$\begin{aligned}V\sum_{\bar{k}}\langle\langle c_{\bar{k}}\hat{n}_\iota; x^\dagger\rangle\rangle^{\mathrm{R/A}} &\approx -\Delta^{\mathrm{R/A}}\langle\langle c_{\bar{\iota}}\hat{n}_\iota; x^\dagger\rangle\rangle^{\mathrm{R/A}} \\ V\sum_{k}\langle\langle c_\iota^\dagger c_k c_{\bar{\iota}}; x^\dagger\rangle\rangle^{\mathrm{R/A}} &\approx -\Delta^{\mathrm{R/A}}\langle\langle c_{\bar{\iota}}\hat{n}_\iota; x^\dagger\rangle\rangle^{\mathrm{R/A}} \\ V\sum_{k}\langle\langle c_k^\dagger c_\iota c_{\bar{\iota}}; x^\dagger\rangle\rangle^{\mathrm{R/A}} &\approx +\Delta^{\mathrm{R/A}}\langle\langle c_{\bar{\iota}}\hat{n}_\iota; x^\dagger\rangle\rangle^{\mathrm{R/A}} \\ V\sum_{k}\langle\langle d^\dagger c_{\bar{\iota}} c_k; x^\dagger\rangle\rangle^{\mathrm{R/A}} &\approx -\Delta^{\mathrm{R/A}}\langle\langle d^\dagger c_{\bar{\iota}} c_\iota; x^\dagger\rangle\rangle^{\mathrm{R/A}}\end{aligned} \tag{5.3.13}$$

and

$$\begin{aligned}V\sum_{\bar{k}}\langle\langle c_{\bar{k}}\hat{n}_\iota; x^\dagger\rangle\rangle^{\gtrless} &\approx -\left(\Delta_{\bar{k}}^{\gtrless}\langle\langle c_{\bar{\iota}}\hat{n}_\iota; x^\dagger\rangle\rangle^{\mathrm{A}} + \Delta^{\mathrm{R}}\langle\langle c_{\bar{\iota}}\hat{n}_\iota; x^\dagger\rangle\rangle^{\gtrless}\right) \\ V\sum_{k}\langle\langle c_\iota^\dagger c_k c_{\bar{\iota}}; x^\dagger\rangle\rangle^{\gtrless} &\approx -\left(\Delta_{k}^{\gtrless}\langle\langle c_{\bar{\iota}}\hat{n}_\iota; x^\dagger\rangle\rangle^{\mathrm{A}} + \Delta^{\mathrm{R}}\langle\langle c_{\bar{\iota}}\hat{n}_\iota; x^\dagger\rangle\rangle^{\gtrless}\right) \\ V\sum_{k}\langle\langle c_k^\dagger c_\iota c_{\bar{\iota}}; x^\dagger\rangle\rangle^{\gtrless} &\approx +\left(\Delta_{\bar{k}}^{\gtrless}\langle\langle c_{\bar{\iota}}\hat{n}_\iota; x^\dagger\rangle\rangle^{\mathrm{A}} + \Delta^{\mathrm{R}}\langle\langle c_{\bar{\iota}}\hat{n}_\iota; x^\dagger\rangle\rangle^{\gtrless}\right) \\ V\sum_{k}\langle\langle d^\dagger c_{\bar{\iota}} c_k; x^\dagger\rangle\rangle^{\gtrless} &\approx -\left(\Delta_{k}^{\gtrless}\langle\langle d^\dagger c_{\bar{\iota}} c_\iota; x^\dagger\rangle\rangle^{\mathrm{A}} + \Delta^{\mathrm{R}}\langle\langle d^\dagger c_{\bar{\iota}} c_\iota; x^\dagger\rangle\rangle^{\gtrless}\right).\end{aligned} \tag{5.3.14}$$

Similar symmetry issues as within the previous truncation level occur in the local spectral functions, and so calculations are also done for Scheme 3, where

$$\langle\langle c_\iota^\dagger c_k c_{\bar{\iota}}; x^\dagger\rangle\rangle^\varkappa - \langle\langle c_k^\dagger c_\iota c_{\bar{\iota}}; x^\dagger\rangle\rangle^\varkappa \approx 0.$$

The self-consistency loop in the first approximation scheme produces reasonable results[VI] in the equilibrium case, i.e. $\Delta\mu = 0\Gamma$, or for very small voltages, but produces highly symmetry breaking results for higher voltages, if it converges at all. Therefore, no plots are shown for Scheme 1 and it is further discarded.

The results for Scheme 2 and 3 are shown in figure 5.4. The current curves are very similar to the previous truncation order. The main difference seems to be in the discrepancy between the currents, which is now higher in Scheme 3 (compared to Scheme 2 in the previous order).

[V] Keep in mind that all EoMs of the lower Green's functions generated in the decomposition are taken into account at this level of truncation, and none has to be further approximated as in the previous order.

[VI] I.e. $I = 0\,e\Gamma$ and $\langle\hat{n}_i\rangle = 0.5$.

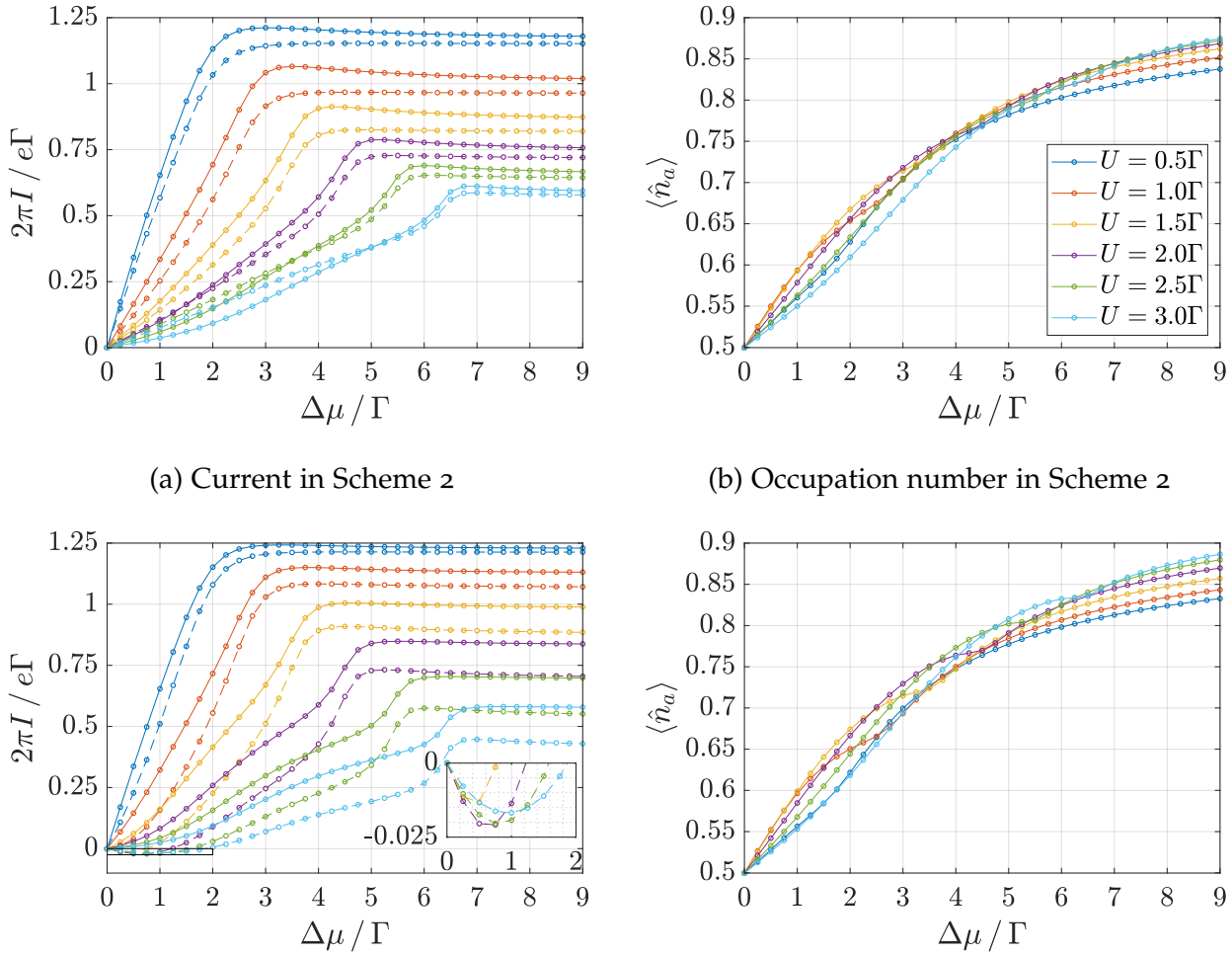

(a) Current in Scheme 2

(b) Occupation number in Scheme 2

(c) Current in Scheme 3

(d) Occupation number in Scheme 3

Figure 5.4.: Current and occupation number on site a for Scheme 2 and 3, $t = 0.5\Gamma$ and different values of U. The solid lines represent I and the dashed lines I_{lead}. The inset in (c) shows some negative current values. The legend in (b) refers to all subfigures.

The spectral functions for site a and d are shown in figure 5.5. Again, the spectral functions are quite similar to the results obtained in the previous section, the main difference can be spotted in the asymmetric weighting for site a, which is less prominent.

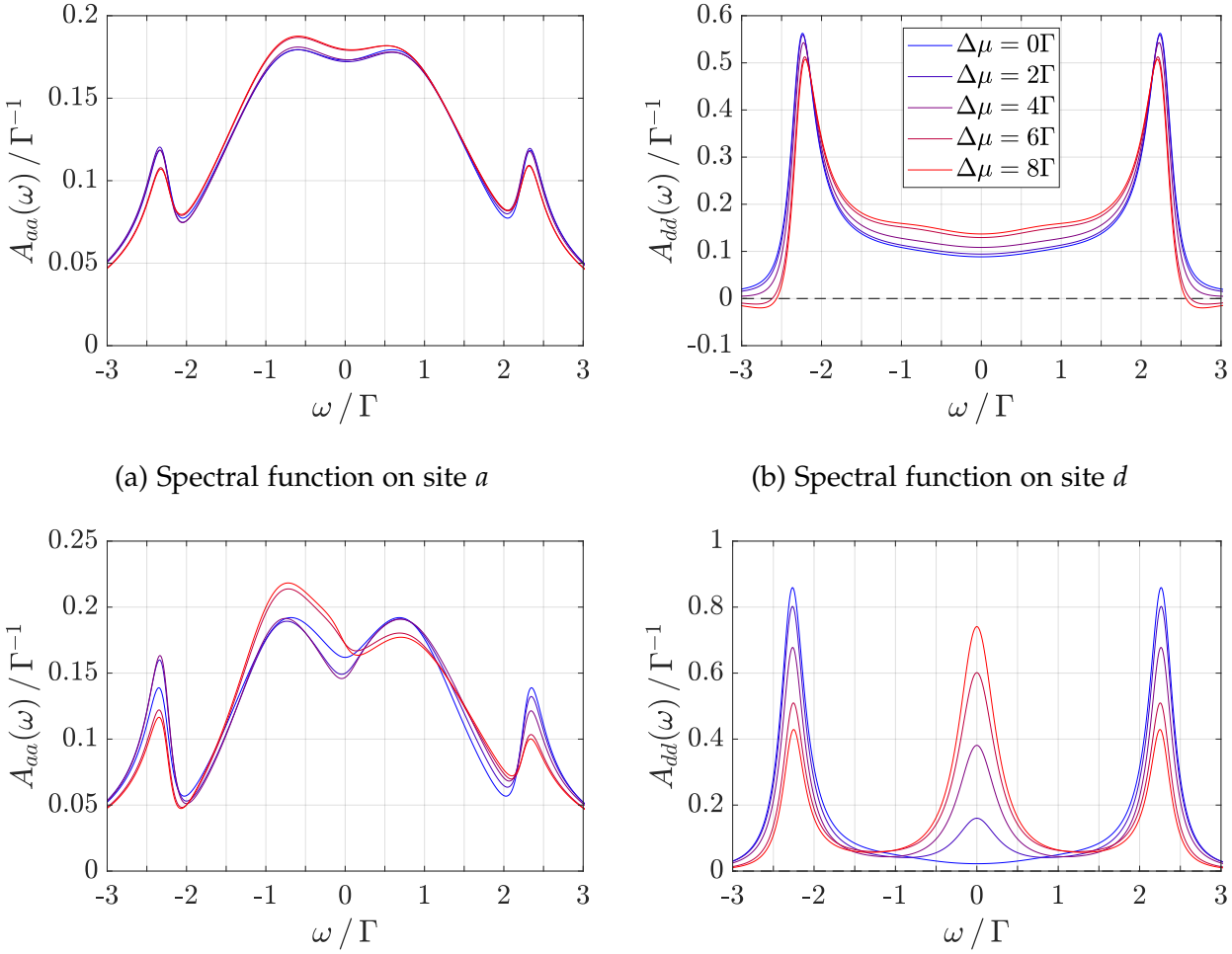

(a) Spectral function on site a

(b) Spectral function on site d

(c) Spectral function on site a

(d) Spectral function on site d

Figure 5.5.: Spectral functions for Scheme 2 (upper) and 3 (lower) on site a and d for $t = 0.5\Gamma$, $U = 2\Gamma$ and different voltages. Negative values can be seen for $\Delta\mu \geq 6\Gamma$ in the spectral function in (b). The legend in (b) refers to all subfigures.

5.4. Truncation Level 3: Six-Operator Terms in t and U

The last addition to the hierarchy of equations, whose results are treated in this thesis, are the equations of motion for the six-operator Green's functions, that are obtained with the commutators

$$\begin{aligned}[d\hat{n}_\iota\hat{n}_{\bar{\iota}}, H_1] = &-t\left(c_{\bar{\iota}}\hat{n}_\iota\hat{n} + c_\iota\hat{n}_{\bar{\iota}}\hat{n}\right) + 2Ud\hat{n}_\iota\hat{n}_{\bar{\iota}} \\ &- V\left[\sum_k\left(c_\iota^\dagger c_k d\hat{n}_{\bar{\iota}} - c_k^\dagger c_\iota d\hat{n}_{\bar{\iota}}\right) + \sum_{\bar{k}}\left(c_{\bar{\iota}}^\dagger c_{\bar{k}} d\hat{n}_\iota - c_{\bar{k}}^\dagger c_{\bar{\iota}} d\hat{n}_\iota\right)\right]\end{aligned} \tag{5.4.1}$$

$$\begin{aligned}[c_{\bar{\iota}}\hat{n}_\iota\hat{n}, H_1] = &-td\hat{n}_\iota\hat{n}_{\bar{\iota}} + Uc_{\bar{\iota}}\hat{n}_\iota\hat{n} \\ &- V\left[\sum_{\bar{k}} c_{\bar{k}}\hat{n}_\iota\hat{n} + \sum_k\left(c_\iota^\dagger c_k c_{\bar{\iota}}\hat{n} - c_k^\dagger c_\iota c_{\bar{\iota}}\hat{n}\right)\right]\end{aligned} \tag{5.4.2}$$

and the anticommutators

$$\begin{aligned}
\left\{d\hat{n}_\iota\hat{n}_{\bar{\iota}}, d^\dagger\right\} &= \hat{n}_\iota\hat{n}_{\bar{\iota}} \\
\left\{d\hat{n}_\iota\hat{n}_{\bar{\iota}}, c_l^\dagger\right\} &= -\hat{n}_{\bar{\iota}}c_l^\dagger d \\
\left\{c_{\bar{\iota}}\hat{n}_\iota\hat{n}, d^\dagger\right\} &= -\hat{n}_\iota d^\dagger c_{\bar{\iota}} \\
\left\{c_{\bar{\iota}}\hat{n}_\iota\hat{n}, c_l^\dagger\right\} &= -\hat{n}c_l^\dagger c_{\bar{\iota}} \\
\left\{c_{\bar{\iota}}\hat{n}_\iota\hat{n}, c_{\bar{\iota}}^\dagger\right\} &= \hat{n}_\iota\hat{n}.
\end{aligned} \tag{5.4.3}$$

And so the equations of motion read

$$\begin{aligned}
&(\widetilde{\omega}_d^{\gtrless} - 2U)\,\langle\langle d\hat{n}_\iota\hat{n}_{\bar{\iota}}; x^\dagger\rangle\rangle^{\gtrless} \\
&= \chi^{\gtrless}_{d\hat{n}_\iota\hat{n}_{\bar{\iota}},x} - t\left(\langle\langle c_{\bar{\iota}}\hat{n}_\iota\hat{n}; x^\dagger\rangle\rangle^{\gtrless} + \langle\langle c_\iota\hat{n}_{\bar{\iota}}\hat{n}; x^\dagger\rangle\rangle^{\gtrless}\right) \\
&- V\left[\sum_k\left(\langle\langle c_\iota^\dagger c_k d\hat{n}_{\bar{\iota}}; x^\dagger\rangle\rangle^{\gtrless} - \langle\langle c_k^\dagger c_\iota d\hat{n}_{\bar{\iota}}; x^\dagger\rangle\rangle^{\gtrless}\right) + \sum_{\bar{k}}\left(\langle\langle c_{\bar{\iota}}^\dagger c_{\bar{k}} d\hat{n}_\iota; x^\dagger\rangle\rangle^{\gtrless} - \langle\langle c_{\bar{k}}^\dagger c_{\bar{\iota}} d\hat{n}_\iota; x^\dagger\rangle\rangle^{\gtrless}\right)\right]
\end{aligned} \tag{5.4.4}$$

$$\begin{aligned}
(\widetilde{\omega}_{\bar{\iota}}^{\gtrless} - U)\,\langle\langle c_{\bar{\iota}}\hat{n}_\iota\hat{n}; x^\dagger\rangle\rangle^{\gtrless} &= \chi^{\gtrless}_{c_{\bar{\iota}}\hat{n}_\iota\hat{n},x} - t\langle\langle d\hat{n}_\iota\hat{n}_{\bar{\iota}}; x^\dagger\rangle\rangle^{\gtrless} \\
&- V\left[\sum_{\bar{k}}\langle\langle c_{\bar{k}}\hat{n}_\iota\hat{n}; x^\dagger\rangle\rangle^{\gtrless} + \sum_k\left(\langle\langle c_\iota^\dagger c_k c_{\bar{\iota}}\hat{n}; x^\dagger\rangle\rangle^{\gtrless} - \langle\langle c_k^\dagger c_\iota c_{\bar{\iota}}\hat{n}; x^\dagger\rangle\rangle^{\gtrless}\right)\right]
\end{aligned} \tag{5.4.5}$$

where

$$\begin{aligned}
\chi^{\mathrm{R/A}}_{d\hat{n}_\iota\hat{n}_{\bar{\iota}},x} &= \langle\hat{n}_\iota\hat{n}_{\bar{\iota}}\rangle\,\delta_{d,x} - \left\langle\hat{n}_{\bar{\iota}}c_l^\dagger d\right\rangle\delta_{c_\iota,x} - \left\langle\hat{n}_\iota c_{\bar{\iota}}^\dagger d\right\rangle\delta_{c_{\bar{\iota}},x} \\
\chi^{\mathrm{R/A}}_{c_{\bar{\iota}}\hat{n}_\iota\hat{n},x} &= \langle\hat{n}_\iota\hat{n}\rangle\,\delta_{c_{\bar{\iota}},x} - \left\langle\hat{n}c_l^\dagger c_{\bar{\iota}}\right\rangle\delta_{c_\iota,x} - \left\langle\hat{n}_\iota d^\dagger c_{\bar{\iota}}\right\rangle\delta_{d,x} \\
\chi^{\gtrless}_{d\hat{n}_\iota\hat{n}_{\bar{\iota}},x} &= g_d^{\gtrless}\left|\widetilde{\omega}_d^{\pm}\right|^2\langle\langle d\hat{n}_\iota\hat{n}_{\bar{\iota}}; x^\dagger\rangle\rangle^{\mathrm{A}} \\
\chi^{\gtrless}_{c_{\bar{\iota}}\hat{n}_\iota\hat{n},x} &= g_{c_{\bar{\iota}}}^{\gtrless}\left|\widetilde{\omega}_{\bar{\iota}}^{\pm}\right|^2\langle\langle c_{\bar{\iota}}\hat{n}_\iota\hat{n}_{\bar{\iota}}; x^\dagger\rangle\rangle^{\mathrm{A}}.
\end{aligned} \tag{5.4.6}$$

As the calculations are done for zero temperature, the four-operator expectation values can be decomposed exactly according to Wick's theorem:

$$\left\langle a^\dagger b c^\dagger d\right\rangle \overset{T=0}{=} \left\langle a^\dagger b\right\rangle\left\langle c^\dagger d\right\rangle - \left\langle a^\dagger d\right\rangle\left\langle c^\dagger b\right\rangle$$

For $T \neq 0\Gamma$ the procedure is analogous to the two-operator expectation values, i.e. integration over the corresponding lesser four-operator Green's function, where there are now two possibilities. For example, the following expectation value can be calculated as

$$-\frac{1}{2\pi i}\int_{-\infty}^{\infty}\mathrm{d}\omega\,\langle\langle c_l^\dagger c_{\bar{\iota}} d; c_{\bar{\iota}}^\dagger\rangle\rangle^{<} = \left\langle\hat{n}_{\bar{\iota}}c_l^\dagger d\right\rangle = \left\langle c_l^\dagger d\hat{n}_{\bar{\iota}}\right\rangle = \frac{1}{2\pi i}\int_{-\infty}^{\infty}\mathrm{d}\omega\,\langle\langle d\hat{n}_{\bar{\iota}}; c_l^\dagger\rangle\rangle^{<}. \tag{5.4.7}$$

Yet, in order to obtain results that do not violate the mentioned symmetry relations, the four-operator Green's functions need to be symmetrized as well. According to section 5.1

this requires Green's function counterparts where the second operator is evolved, which is not done in this thesis, as for this case the calculations are restricted to zero temperature.

At this point all functions generated by the hopping terms in the parameter t and by the interaction terms in U are taken into account, i.e. the hierarchy containing only system operators is closed and the approximations only affect the Green's functions containing one lead operator.

Approximation Scheme 1 is discarded for this order of truncation due to the bad results in the previous order. The additional approximations for Scheme 2 read

$$\begin{aligned}
V\sum_{\bar{k}}\langle\langle c_{\bar{k}}\hat{n}_\iota\hat{n};x^\dagger\rangle\rangle^{\mathrm{R/A}} &\approx -\Delta^{\mathrm{R/A}}\langle\langle c_{\bar{\iota}}\hat{n}_\iota\hat{n};x^\dagger\rangle\rangle^{\mathrm{R/A}}\\
V\sum_{k}\langle\langle c_\iota^\dagger c_k d\hat{n}_{\bar{\iota}};x^\dagger\rangle\rangle^{\mathrm{R/A}} &\approx -\Delta^{\mathrm{R/A}}\langle\langle d\hat{n}_\iota\hat{n}_{\bar{\iota}};x^\dagger\rangle\rangle^{\mathrm{R/A}}\\
V\sum_{k}\langle\langle c_k^\dagger c_\iota d\hat{n}_{\bar{\iota}};x^\dagger\rangle\rangle^{\mathrm{R/A}} &\approx +\Delta^{\mathrm{R/A}}\langle\langle d\hat{n}_\iota\hat{n}_{\bar{\iota}};x^\dagger\rangle\rangle^{\mathrm{R/A}}\\
V\sum_{k}\langle\langle c_\iota^\dagger c_k c_{\bar{\iota}}\hat{n};x^\dagger\rangle\rangle^{\mathrm{R/A}} &\approx -\Delta^{\mathrm{R/A}}\langle\langle c_{\bar{\iota}}\hat{n}_\iota\hat{n};x^\dagger\rangle\rangle^{\mathrm{R/A}}\\
V\sum_{k}\langle\langle c_k^\dagger c_\iota c_{\bar{\iota}}\hat{n};x^\dagger\rangle\rangle^{\mathrm{R/A}} &\approx +\Delta^{\mathrm{R/A}}\langle\langle c_{\bar{\iota}}\hat{n}_\iota\hat{n};x^\dagger\rangle\rangle^{\mathrm{R/A}}
\end{aligned} \tag{5.4.8}$$

and

$$\begin{aligned}
V\sum_{\bar{k}}\langle\langle c_{\bar{k}}\hat{n}_\iota\hat{n};x^\dagger\rangle\rangle^{\gtrless} &\approx -\left(\Delta_{\bar{k}}^{\gtrless}\langle\langle c_{\bar{\iota}}\hat{n}_\iota\hat{n};x^\dagger\rangle\rangle^{\mathrm{A}}+\Delta^{\mathrm{R}}\langle\langle c_{\bar{\iota}}\hat{n}_\iota\hat{n};x^\dagger\rangle\rangle^{\gtrless}\right)\\
V\sum_{k}\langle\langle c_\iota^\dagger c_k d\hat{n}_{\bar{\iota}};x^\dagger\rangle\rangle^{\gtrless} &\approx -\left(\Delta_{k}^{\gtrless}\langle\langle d\hat{n}_\iota\hat{n}_{\bar{\iota}};x^\dagger\rangle\rangle^{\mathrm{A}}+\Delta^{\mathrm{R}}\langle\langle d\hat{n}_\iota\hat{n}_{\bar{\iota}};x^\dagger\rangle\rangle^{\gtrless}\right)\\
V\sum_{k}\langle\langle c_k^\dagger c_\iota d\hat{n}_{\bar{\iota}};x^\dagger\rangle\rangle^{\gtrless} &\approx +\left(\Delta_{\bar{k}}^{\gtrless}\langle\langle d\hat{n}_\iota\hat{n}_{\bar{\iota}};x^\dagger\rangle\rangle^{\mathrm{A}}+\Delta^{\mathrm{R}}\langle\langle d\hat{n}_\iota\hat{n}_{\bar{\iota}};x^\dagger\rangle\rangle^{\gtrless}\right)\\
V\sum_{k}\langle\langle c_\iota^\dagger c_k c_{\bar{\iota}}\hat{n};x^\dagger\rangle\rangle^{\gtrless} &\approx -\left(\Delta_{k}^{\gtrless}\langle\langle c_{\bar{\iota}}\hat{n}_\iota\hat{n};x^\dagger\rangle\rangle^{\mathrm{A}}+\Delta^{\mathrm{R}}\langle\langle c_{\bar{\iota}}\hat{n}_\iota\hat{n};x^\dagger\rangle\rangle^{\gtrless}\right)\\
V\sum_{k}\langle\langle c_k^\dagger c_\iota c_{\bar{\iota}}\hat{n};x^\dagger\rangle\rangle^{\gtrless} &\approx +\left(\Delta_{\bar{k}}^{\gtrless}\langle\langle c_{\bar{\iota}}\hat{n}_\iota\hat{n};x^\dagger\rangle\rangle^{\mathrm{A}}+\Delta^{\mathrm{R}}\langle\langle c_{\bar{\iota}}\hat{n}_\iota\hat{n};x^\dagger\rangle\rangle^{\gtrless}\right),
\end{aligned} \tag{5.4.9}$$

where for Scheme 3 again differences in hermitian counterparts are set to zero:

$$\langle\langle c_\iota^\dagger c_k d\hat{n}_{\bar{\iota}};x^\dagger\rangle\rangle^{\varkappa}-\langle\langle c_k^\dagger c_\iota d\hat{n}_{\bar{\iota}};x^\dagger\rangle\rangle^{\varkappa}\approx\langle\langle c_\iota^\dagger c_k c_{\bar{\iota}}\hat{n};x^\dagger\rangle\rangle^{\varkappa}-\langle\langle c_k^\dagger c_\iota c_{\bar{\iota}}\hat{n};x^\dagger\rangle\rangle^{\varkappa}\approx 0$$

The results for the current and occupation number are shown in figure 5.6. The current and occupation curves from Scheme 2 are again quite similar to the previous order of truncation, but Scheme 3 gives notable changes: The occupation numbers do not rise linearly any more, but get suppressed for higher values of U. The discrepancy in the currents is predominant in the low-voltage regime and is more serious for higher values of U as the lead current seems to get suppressed. The intra-system current, on the contrary, starts out linearly for all values of U and with the same slope as obtained in the HF and exact results in the self-dual point. However, the negative differential conductance is still barely present and the current saturates. As can be seen from the inset in figure 5.6c, the curve for $U = 3\Gamma$ features two maxima and the other curves an inflection point before their maximum value.

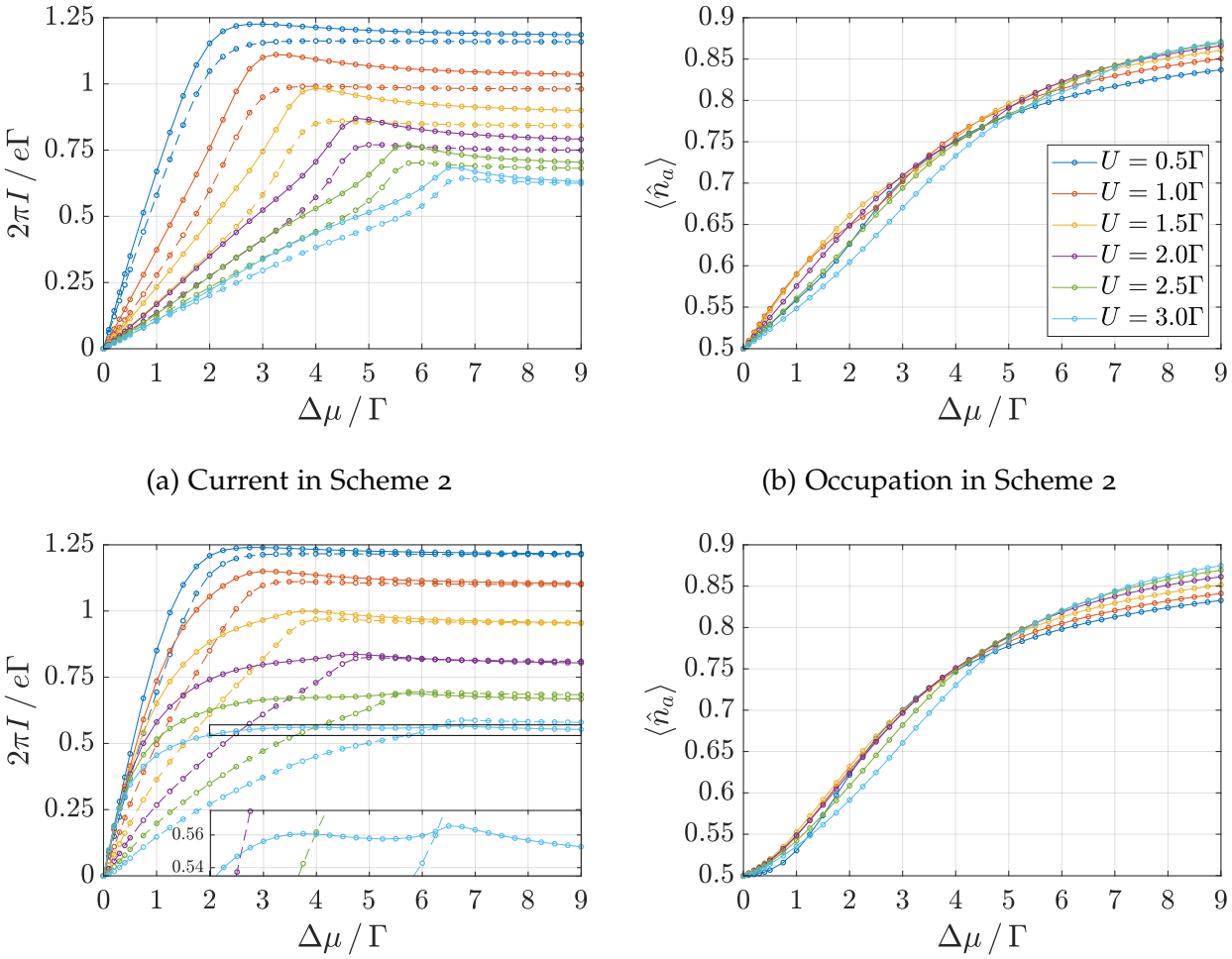

(a) Current in Scheme 2

(b) Occupation in Scheme 2

(c) Current in Scheme 3

(d) Occupation in Scheme 3

Figure 5.6.: Current and occupation number on site a for Scheme 2 and 3, $t = 0.5\Gamma$ and different values of U. The solid lines represent I and the dashed lines I_{lead}. The curve for $U = 3\Gamma$ in (c) is the only one to show two distinct maxima, which is highlighted in the inset. The curves for lower values of U show an inflection point before the maximum. The current curves in Scheme 3 show no negative values. The legend in (b) refers to all subfigures.

The spectral functions are shown in figure 5.7. The results for Scheme 2 are again quite similar to previous results, but the spectral function on the central site shows negative values already for the equilibrium. For Scheme 3, the arising central peak is more pronounced and reaches over the side peaks for higher voltages.

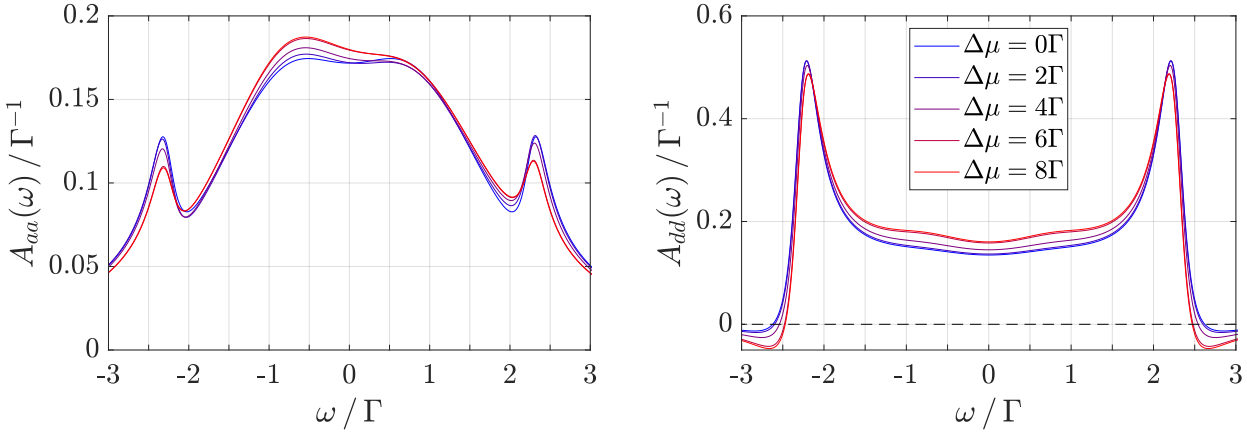

(a) Spectral function on site a

(b) Spectral function on site d

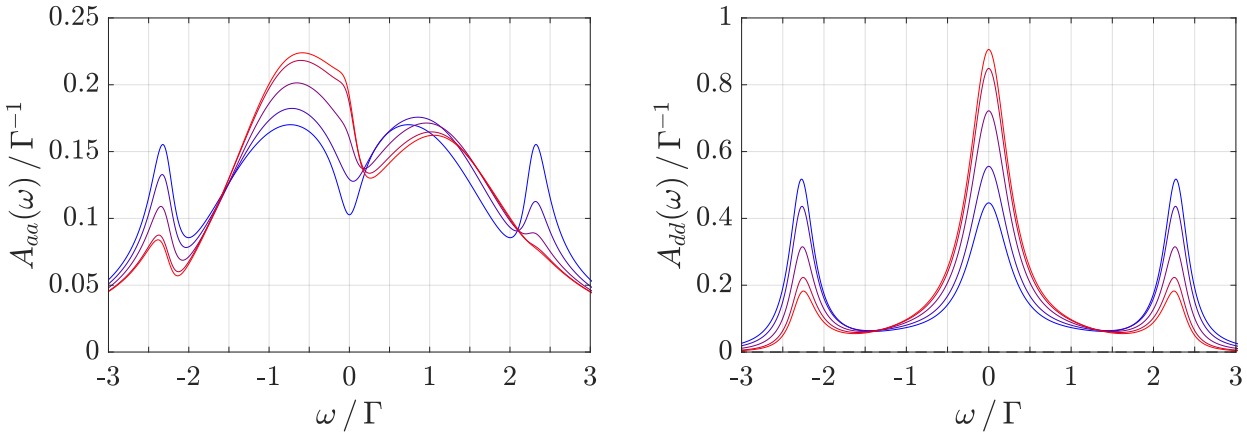

(c) Spectral function on site a

(d) Spectral function on site d

Figure 5.7.: Spectral functions for Scheme 2 (upper) and 3 (lower) on site a and d for $t = 0.5\Gamma$, $U = 2\Gamma$ and different voltages. Negative values are present for all voltages in the spectral function in (b). The legend in (b) refers to all subfigures.

Finally, the HF results from the previous chapter as well as the exact solution are compared to the current from the last order of truncation with Scheme 3, as this is the only solution that matches at least the low-voltage regime. The comparison plot is shown in figure 5.8.

The intra-system current I initially follows the linear behaviour of the exact solution, but already bends away for voltages around $\Delta\mu = 0.5\Gamma$. As can be seen in the inset in figure 5.8, it reaches its maximum just around the intersection with the HF solutions around $\Delta\mu = 5\Gamma$, where a small negative differential conductance sets in, but tends to saturate as previous solutions.

The lead current I_{lead} shows a similar behaviour, but it seems suppressed for lower voltages as the other lead-current solutions in this order.

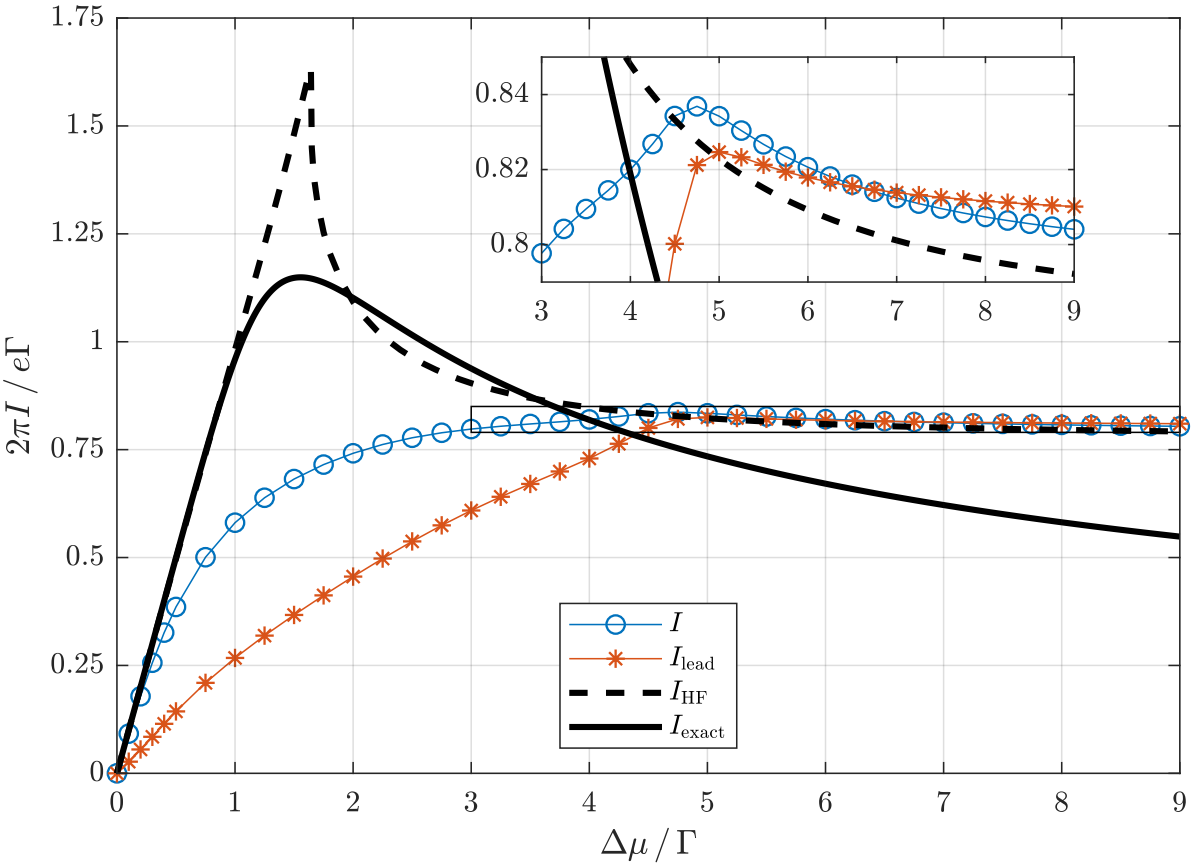

Figure 5.8.: Current comparison between HF results in wide-band limit (black dashed line), the intra-system (I, blue circles) and lead current I_{lead} (red asterisks) from the last order truncation with Scheme 3 for $t = 0.5\Gamma$ and $U = 2\Gamma$. The black solid line shows the exact solution from [16] as reference. The inset focuses on the high-voltage behaviour of I and I_{lead}.

5.5. Summing Over Bath Quantities

The lead current, some approximations presented in the previous section as well as orders of truncation that go beyond the presented solutions require the evaluation of bath related quantities. For the sake of completeness and for possible future investigations on the present topic some of these occurring terms shall be evaluated in this section for a flat-band bath in wide-band limit, which is defined through the density of states

$$\rho(\varepsilon) = \lim_{D\to\infty} \frac{1}{2D}\Theta(D - |\varepsilon|)$$

and the hybridization

$$V = \lim_{D\to\infty} \sqrt{\frac{2D}{\pi}}.$$

A simple result is obtained from summing over squared retarded or advanced single-particle Green's functions

$$\sum_k \frac{V^2}{\widetilde{\omega}_k^2} = \sum_k \frac{V^2}{(\omega - \varepsilon_k \pm i\eta)^2},$$

namely that they vanish[VII],

$$\to \lim_{D\to\infty} \frac{V^2}{2D} \int_{-D}^{D} \mathrm{d}\varepsilon \, \frac{1}{(\omega - \varepsilon \pm i\eta)^2} = \frac{1}{\pi} \lim_{D\to\infty} \left(\frac{1}{\omega - D \pm i\eta} - \frac{1}{\omega + D \pm i\eta} \right) = 0.$$

The same is true for shifted terms

$$\sum_k \frac{V^2}{(\omega - \varepsilon_k \pm i\eta)\,(\omega + c - \varepsilon_k \pm i\eta)}$$

as they can be split into

$$\frac{1}{(\omega - \varepsilon_k \pm i\eta)\,(\omega + c - \varepsilon_k \pm i\eta)} = \frac{1}{c} \left(\frac{1}{\omega - \varepsilon_k \pm i\eta} - \frac{1}{\omega + c - \varepsilon_k \pm i\eta} \right).$$

All other occurring bath sums contain expectation values of k-dependent operators, that can be calculated using the relation between expectation value and lesser Green's function,

$$\left\langle B^\dagger A \right\rangle = \frac{1}{2\pi i} \int_{-\infty}^{\infty} \mathrm{d}\omega \, \langle\langle A; B^\dagger \rangle\rangle^<,$$

and the corresponding exact equations of motion for $x \neq c_{k_{\mathrm{L,R}}}$

$$\begin{aligned}
\langle\langle c_{k_{\mathrm{L,R}}}; x^\dagger \rangle\rangle^{\mathrm{R/A}} &= -V \frac{\langle\langle c_{a,b}; x^\dagger \rangle\rangle^{\mathrm{R/A}}}{\widetilde{\omega}_k^\pm} \\
\langle\langle x; c_{k_{\mathrm{L,R}}}^\dagger \rangle\rangle^{\mathrm{R/A}} &= -V \frac{\langle\langle x; c_{a,b}^\dagger \rangle\rangle^{\mathrm{R/A}}}{\widetilde{\omega}_k^\pm} \\
\langle\langle c_{k_{\mathrm{L,R}}}; x^\dagger \rangle\rangle^{<} &= -V \left(g^<_{k_{\mathrm{L,R}}} \langle\langle c_{a,b}; x^\dagger \rangle\rangle^{\mathrm{A}} + \frac{\langle\langle c_{a,b}; x^\dagger \rangle\rangle^{<}}{\widetilde{\omega}^+_{k_{\mathrm{L,R}}}} \right) \\
\langle\langle x; c_{k_{\mathrm{L,R}}}^\dagger \rangle\rangle^{<} &= -V \left(g^<_{k_{\mathrm{L,R}}} \langle\langle x; c_{a,b}^\dagger \rangle\rangle^{\mathrm{R}} + \frac{\langle\langle x; c_{a,b}^\dagger \rangle\rangle^{<}}{\widetilde{\omega}^-_{k_{\mathrm{L,R}}}} \right)
\end{aligned} \tag{5.5.1}$$

and for occurring double sums in k, k'

$$\begin{aligned}
\langle\langle c_{k'}; c_k^\dagger \rangle\rangle^{\mathrm{R/A}} &= \frac{1}{\widetilde{\omega}_{k'}^\pm} \left(\delta_{k'k} - V \langle\langle c_{a',b'}; c_k^\dagger \rangle\rangle^{\mathrm{R/A}} \right) \\
&= \frac{\delta_{k'k}}{\widetilde{\omega}_{k'}^\pm} + V^2 \frac{\langle\langle c_{a',b'}; c_{a,b}^\dagger \rangle\rangle^{\mathrm{R/A}}}{\widetilde{\omega}_{k'}^\pm \widetilde{\omega}_k^\pm} \\
\langle\langle c_{k'}; c_k^\dagger \rangle\rangle^{<} &= g^<_{k'} \widetilde{\omega}^-_{k'} \langle\langle c_{k'}; c_k^\dagger \rangle\rangle^{\mathrm{A}} - V \frac{\langle\langle c_{a',b'}; c_k^\dagger \rangle\rangle^{<}}{\widetilde{\omega}^+_{k'}} \\
&= g^<_{k'} \left(\delta_{k'k} + V^2 \frac{\langle\langle c_{a',b'}; c_{a,b}^\dagger \rangle\rangle^{\mathrm{A}}}{\widetilde{\omega}^-_k} \right) + \frac{V^2}{\widetilde{\omega}^+_{k'}} \left(g^<_k \langle\langle c_{a',b'}; c_{a,b}^\dagger \rangle\rangle^{\mathrm{R}} + \frac{\langle\langle c_{a',b'}; c_{a,b}^\dagger \rangle\rangle^{<}}{\widetilde{\omega}^-_k} \right),
\end{aligned} \tag{5.5.2}$$

[VII] See section A.1.6 in the appendix.

which relate the bath Green's functions to the calculated system functions.

An important sum term, which is needed for the lead current, is the direct sum over expectation values containing only one bath operator,

$$\begin{aligned} V\sum_k \left\langle x^\dagger c_k \right\rangle &= V\sum_k \left(\frac{1}{2\pi i}\int_{-\infty}^{\infty} \mathrm{d}\omega \, \langle\!\langle c_k; x^\dagger \rangle\!\rangle^< \right) \\ &= -\frac{1}{2\pi i}\int_{-\infty}^{\infty} \mathrm{d}\omega \left(\langle\!\langle c_{a,b}; x^\dagger \rangle\!\rangle^{\mathrm{A}} V^2 \sum_k g_k^< + \langle\!\langle c_{a,b}; x^\dagger \rangle\!\rangle^< \sum_k \frac{V^2}{\widetilde{\omega}_k^+} \right) \\ &= -\frac{1}{2\pi i}\int_{-\infty}^{\infty} \mathrm{d}\omega \left(\Delta_{\mathrm{L,R}}^< \langle\!\langle c_{a,b}; x^\dagger \rangle\!\rangle^{\mathrm{A}} + \Delta^+ \langle\!\langle c_{a,b}; x^\dagger \rangle\!\rangle^< \right), \end{aligned} \tag{5.5.3}$$

where the sums over k include only the non-interacting Green's functions and thus give the hybridization function Δ, as defined in (3.2.1) and (3.2.2). In the wide-band limit Δ has a simple form, in particular its retarded and advanced part $\Delta^\pm = \mp i$ does not depend on ω and so the second part of the integral is proportional to the definition for expectation values used above, thus

$$V\sum_k \left\langle x^\dagger c_k \right\rangle = i \left\langle x^\dagger c_{a,b} \right\rangle - \frac{1}{\pi}\int_{-\infty}^{\infty} \mathrm{d}\omega \, f_{\mathrm{L,R}}(\omega) \langle\!\langle c_{a,b}; x^\dagger \rangle\!\rangle^{\mathrm{A}}. \tag{5.5.4}$$

The remaining integral needs to be evaluated numerically once in each iteration[VIII] during the self-consistency loop. The calculation for $\left\langle c_k^\dagger x \right\rangle$ is analogous and leads to

$$V\sum_k \left\langle c_k^\dagger x \right\rangle = -i \left\langle c_{a,b}^\dagger x \right\rangle - \frac{1}{\pi}\int_{-\infty}^{\infty} \mathrm{d}\omega \, f_{\mathrm{L,R}}(\omega) \langle\!\langle x; c_{a,b}^\dagger \rangle\!\rangle^{\mathrm{R}}. \tag{5.5.5}$$

With these two results the current over the lead junction is obtained as

$$\begin{aligned} I_{\mathrm{leads}} &= ieV \sum_{k\in \mathrm{L}} \left(\left\langle c_a^\dagger c_k \right\rangle - \left\langle c_k^\dagger c_a \right\rangle \right) \\ &= ie \left[2i \langle \hat{n}_a \rangle - \frac{1}{\pi}\int_{-\infty}^{\infty} \mathrm{d}\omega \, f_{\mathrm{L,R}}(\omega) \left(\langle\!\langle c_a; c_a^\dagger \rangle\!\rangle^{\mathrm{A}} - \langle\!\langle c_a; c_a^\dagger \rangle\!\rangle^{\mathrm{R}} \right) \right] \\ &= -2e \left[\langle \hat{n}_a \rangle - \frac{1}{\pi}\int_{-\infty}^{\infty} \mathrm{d}\omega \, f_{\mathrm{L,R}}(\omega) \, \mathrm{Im}\left\{ \langle\!\langle c_a; c_a^\dagger \rangle\!\rangle^{\mathrm{A}} \right\} \right]. \end{aligned} \tag{5.5.6}$$

A little more effort, analytically as well as numerically, has to be done for sums over products of non-interacting lead Green's functions $g_{a_k}^\varkappa$ and lead expectation values,

$$V\sum_k g_{a_k}^\varkappa(\omega) \left\langle x^\dagger c_k \right\rangle,$$

where $\varkappa = \mathrm{R,A,<,>}$ and a_k is a product of operators containing a lead operator. For retarded and advanced components, where $\omega_c = \omega + c$ depends on a_k ($c \in \mathbb{R}$), and assuming that the lead operator in a_k is an annihilation operator c_k, the function can be written as

$$g_{a_k}^{\mathrm{R/A}}(\omega) = g_k^{\mathrm{R/A}}(\omega_c)$$

[VIII] If needed in the approximations.

and so

$$
\begin{aligned}
V\sum_k g_k^{\mathrm{R/A}}(\omega_c)\left\langle x^\dagger c_k\right\rangle &= V\sum_k \frac{\left\langle x^\dagger c_k\right\rangle}{\omega_c-\varepsilon_k\pm i\eta}\\
&= -\frac{V^2}{2\pi i}\sum_k \frac{1}{\omega_c-\varepsilon_k\pm i\eta}\int_{-\infty}^{\infty}\mathrm{d}\omega'\left(g^{<}_{k_{\mathrm{L,R}}}\langle\!\langle c_{a,b};x^\dagger\rangle\!\rangle^{\mathrm{A}}+\frac{\langle\!\langle c_{a,b};x^\dagger\rangle\!\rangle^{<}}{\widetilde{\omega}^{+}_{k_{\mathrm{L,R}}}}\right)\\
&= -\frac{V^2}{2\pi i}\int_{-\infty}^{\infty}\mathrm{d}\omega'\left(2if_{\mathrm{L,R}}\langle\!\langle c_{a,b};x^\dagger\rangle\!\rangle^{\mathrm{A}}\sum_k\frac{\eta}{(\omega_c-\varepsilon_k\pm i\eta)\left[(\omega'-\varepsilon_k)^2+\eta^2\right]}\right.\\
&\qquad\left.+\langle\!\langle c_{a,b};x^\dagger\rangle\!\rangle^{<}\sum_k\frac{1}{(\omega_c-\varepsilon_k\pm i\eta)(\omega'-\varepsilon_k+i\eta)}\right)\\
&= -\frac{V^2}{2D}\frac{1}{2\pi i}\int_{-\infty}^{\infty}\mathrm{d}\omega'\left(2if_{\mathrm{L,R}}\langle\!\langle c_{a,b};x^\dagger\rangle\!\rangle^{\mathrm{A}}\int_{-D}^{D}\mathrm{d}\varepsilon\,\frac{\eta}{(\omega_c-\varepsilon\pm i\eta)\left[(\omega'-\varepsilon)^2+\eta^2\right]}\right.\\
&\qquad\left.+\langle\!\langle c_{a,b};x^\dagger\rangle\!\rangle^{<}\int_{-D}^{D}\mathrm{d}\varepsilon\,\frac{1}{(\omega_c-\varepsilon\pm i\eta)(\omega'-\varepsilon+i\eta)}\right).
\end{aligned}
\tag{5.5.7}
$$

The two ε-integrals have an exact solution[IX] for $D\to\infty$, namely

$$
\begin{aligned}
\int_{-\infty}^{\infty}\mathrm{d}\varepsilon\,\frac{\eta}{(\omega_c-\varepsilon\pm i\eta)\left[(\omega'-\varepsilon)^2+\eta^2\right]} &= \frac{\pi}{\omega_c-\omega'\pm 2i\eta}\\
\int_{-\infty}^{\infty}\mathrm{d}\varepsilon\,\frac{1}{(\omega_c-\varepsilon\pm i\eta)(\omega'-\varepsilon+i\eta)} &= -\frac{2\pi i}{\omega_c-\omega'-2i\eta}\delta_{\pm,-}
\end{aligned}
\tag{5.5.8}
$$

and so the evaluation reduces to

$$
V\sum_k\frac{\left\langle x^\dagger c_k\right\rangle}{\omega_c-\varepsilon_k\pm i\eta} = -\frac{1}{\pi}\int_{-\infty}^{\infty}\mathrm{d}\omega'\left(\frac{f_{\mathrm{L,R}}(\omega')\langle\!\langle c_{a,b};x^\dagger\rangle\!\rangle^{\mathrm{A}}-\langle\!\langle c_{a,b};x^\dagger\rangle\!\rangle^{<}\delta_{\pm,-}}{\omega_c-\omega'\pm 2i\eta}\right). \tag{5.5.9}
$$

In the same way, the sums for the hermitian conjugate expectation value lead to:

$$
V\sum_k\frac{\left\langle c_k^\dagger x\right\rangle}{\omega_c-\varepsilon_k\pm i\eta} = -\frac{1}{\pi}\int_{-\infty}^{\infty}\mathrm{d}\omega'\left(\frac{f_{\mathrm{L,R}}(\omega')\langle\!\langle c_{a,b};x^\dagger\rangle\!\rangle^{\mathrm{R}}+\langle\!\langle c_{a,b};x^\dagger\rangle\!\rangle^{<}\delta_{\pm,+}}{\omega_c-\omega'\pm 2i\eta}\right) \tag{5.5.10}
$$

Defining the result from (5.5.9) as function of ω_c, namely

$$
F^{\pm}(\omega_c) := V\sum_k\frac{\left\langle x^\dagger c_k\right\rangle}{\omega_c-\varepsilon_k\pm i\eta},
$$

sums in $+\varepsilon_k$, appearing in the equations of motion for Green's function containing a bath creation operator $c_k^\dagger$ in the first-operator position, give just

$$
V\sum_k\frac{\left\langle x^\dagger c_k\right\rangle}{\omega_c+\varepsilon_k\pm i\eta} = -V\sum_k\frac{\left\langle x^\dagger c_k\right\rangle}{-\omega_c-\varepsilon_k\mp i\eta} = -F^{\mp}(-\omega_c), \tag{5.5.11}
$$

[IX] See section A.2.6 in the appendix

where the superscript has changed from $\pm$ to $\mp$. So in general, as the numerical evaluation is expensive, the kind of integral is only evaluated once per iteration and involved Green's function for $\omega_c = \omega$ and is then flipped ($\omega \to -\omega$) and/or translated ($\omega \to \omega_c$) if possible.

The sums including lesser and greater functions $g^<(\omega)$ are obtained in the same way (here the $\pm$ sign stands for a creation (upper) or an annihilation (lower) operator in a_k):

$$\begin{aligned}
&V\sum_k g^{\gtrless}_{a_k}(\omega)\left\langle x^\dagger c_k\right\rangle = 2iP^{\gtrless}_{a_k}(\omega)V\sum_k \frac{\eta\left\langle x^\dagger c_k\right\rangle}{(\omega_c \pm \varepsilon_k)^2+\eta^2}\\
&= -\frac{P^{\gtrless}_{a_k}(\omega)}{\pi}\int_{-\infty}^{\infty}\mathrm{d}\omega'\,\frac{V^2}{2D}\int_{-D}^{D}\mathrm{d}\varepsilon\,\frac{\eta}{(\omega_c\pm\varepsilon)^2+\eta^2}\left(\frac{2i\eta f_{\mathrm{L,R}}(\omega')}{(\omega'-\varepsilon)+\eta^2}\langle\!\langle c_{a,b};x^\dagger\rangle\!\rangle^{\mathrm{A}}_{\omega'}+\frac{\langle\!\langle c_{a,b};x^\dagger\rangle\!\rangle^{<}_{\omega'}}{\omega'-\varepsilon+i\eta}\right)\\
&= -\frac{P^{\gtrless}_{a_k}(\omega)}{\pi}\int_{-\infty}^{\infty}\mathrm{d}\omega'\,\frac{1}{\pi}\left(2if_{\mathrm{L,R}}(\omega')\,\langle\!\langle c_{a,b};x^\dagger\rangle\!\rangle^{\mathrm{A}}_{\omega'}\int_{-D}^{D}\mathrm{d}\varepsilon\,\frac{\eta}{(\omega_c\pm\varepsilon)^2+\eta^2}\frac{\eta}{(\omega'-\varepsilon)^2+\eta^2}\right.\\
&\qquad\left.+\langle\!\langle c_{a,b};x^\dagger\rangle\!\rangle^{<}_{\omega'}\int_{-D}^{D}\mathrm{d}\varepsilon\,\frac{\eta}{(\omega'-\varepsilon+i\eta)\left[(\omega_c\pm\varepsilon)^2+\eta^2\right]}\right)
\end{aligned} \tag{5.5.12}$$

For clarity, the argument of the occurring Green's functions is indicated explicitly as subscript. Again, the two integrals have an exact solution for $D \to \infty$, namely[X]

$$\begin{aligned}
\int_{-\infty}^{\infty}\mathrm{d}\varepsilon\,\frac{\eta}{(\omega_c\pm\varepsilon)^2+\eta^2}\frac{\eta}{(\omega'-\varepsilon)^2+\eta^2} &= \frac{2\eta\pi}{(\mp\omega_c-\omega')^2+(2\eta)^2}\\
\int_{-\infty}^{\infty}\mathrm{d}\varepsilon\,\frac{\eta}{(\omega'-\varepsilon+i\eta)\left[(\omega_c\pm\varepsilon)^2+\eta^2\right]} &= -\frac{\pi}{\mp\omega_c-\omega'-2i\eta},
\end{aligned} \tag{5.5.13}$$

eventually leading to

$$\begin{aligned}
&V\sum_k g^{\gtrless}_{a_k}(\omega)\left\langle x^\dagger c_k\right\rangle\\
&= -\frac{P^{\gtrless}_{a_k}(\omega)}{\pi}\int_{-\infty}^{\infty}\mathrm{d}\omega'\left(2\pi i f_{\mathrm{L,R}}(\omega')\,\langle\!\langle c_{a,b};x^\dagger\rangle\!\rangle^{\mathrm{A}}_{\omega'}\frac{1}{\pi}\frac{2\eta}{(\mp\omega_c-\omega')^2+(2\eta)^2}-\frac{\langle\!\langle c_{a,b};x^\dagger\rangle\!\rangle^{<}_{\omega'}}{\mp\omega_c-\omega'-2i\eta}\right)\\
&= -2iP^{\gtrless}_{a_k}(\omega)f_{\mathrm{L,R}}(\mp\omega_c)\,\langle\!\langle c_{a,b};x^\dagger\rangle\!\rangle^{\mathrm{A}}_{\mp\omega_c}+\frac{P^{\gtrless}_{a_k}(\omega)}{\pi}\int_{-\infty}^{\infty}\mathrm{d}\omega'\,\frac{\langle\!\langle c_{a,b};x^\dagger\rangle\!\rangle^{<}_{\omega'}}{\mp\omega_c-\omega'-2i\eta},
\end{aligned} \tag{5.5.14}$$

where the property of the nascent delta distribution

$$\lim_{\eta\to0^+}\frac{1}{\pi}\frac{2\eta}{(\mp\omega_c-\omega')^2+(2\eta)^2}\overset{\widetilde{\eta}=2\eta}{=}\lim_{\widetilde{\eta}\to0^+}\frac{1}{\pi}\frac{\widetilde{\eta}}{(\mp\omega_c-\omega')^2+\widetilde{\eta}^2}\to\delta(\mp\omega_c-\omega')$$

is used in the last step[XI].

[X] See section A.2.6 in the appendix.

[XI] Note that the limit $\eta \to 0^+$ should actually be taken at the end of the calculation for all terms together. As shown in section 4.2 the limit can result in non-trivial solutions in regions where the retarded/advanced hybridization function tends to or is equal zero. In this case, as the calculation is done explicitly for the wide-band limit, i.e. $\forall\omega, \Delta^{\pm}(\omega) \neq 0$, it is assumed that it is legitimate to do this very limit separately and use the property of the delta distribution.

The sum with the hermitian conjugate gives

$$V\sum_k g^{\gtrless}_{a_k}(\omega)\left\langle c_k^\dagger x\right\rangle = -2iP^{\gtrless}_{a_k}(\omega)f_{\mathrm{L,R}}\left(\mp\omega_c\right)\left\langle\!\left\langle c_{a,b};x^\dagger\right\rangle\!\right\rangle^{\mathrm{R}}_{\mp\omega_c} + \frac{P^{\gtrless}_{a_k}(\omega)}{\pi}\int_{-\infty}^{\infty}\mathrm{d}\omega'\,\frac{\left\langle\!\left\langle c_{a,b};x^\dagger\right\rangle\!\right\rangle^{<}_{\omega'}}{\mp\omega_c-\omega'+2i\eta}. \tag{5.5.15}$$

Through approximations the following double sums may appear, where

$$G = \left\langle\!\left\langle c_{a',b'};c^\dagger_{a,b}\right\rangle\!\right\rangle$$

depending on the combination of $k\in\mathrm{B}$ and $k'\in\mathrm{B}'$, where $\mathrm{B}^{(\prime)}=\mathrm{L,R}$. Inserting the equation of motion (5.5.2)

$$\begin{aligned}&V^2\sum_{k,k'}\frac{\left\langle c_k^\dagger c_{k'}\right\rangle}{\omega_c-\varepsilon_{k'}\pm i\eta}\\&=\frac{1}{2\pi i}\int_{-\infty}^{\infty}\mathrm{d}\omega'\sum_{k'}\frac{V^2}{\omega_c-\varepsilon_{k'}\pm i\eta}\left[g^<_{k'}\left(\delta_{\mathrm{BB}'}+G^{\mathrm{A}}\Delta^-\right)+\frac{1}{\widetilde{\omega}^+_{k'}}\left(G^{\mathrm{R}}\Delta^<_{\mathrm{B}}+G^<\Delta^-\right)\right]\end{aligned} \tag{5.5.16}$$

the sum over k can be done, resulting in the hybridization functions, and $\delta_{kk'}$ becomes $\delta_{\mathrm{BB}'}$, which accounts for the anticommutator if k and k' are both in the same lead. The remaining sum over k' gives the same expressions as in (5.5.7), and so for the wide-band limit

$$\begin{aligned}&V^2\sum_{k,k'}\frac{\left\langle c_k^\dagger c_{k'}\right\rangle}{\omega_c-\varepsilon_{k'}\pm i\eta}\\&=\frac{1}{2\pi i}\int_{-\infty}^{\infty}\mathrm{d}\omega'\,\frac{1}{\pi}\left[2\pi i\frac{f_{\mathrm{B}'}\left(\omega'\right)\left(\delta_{\mathrm{BB}'}+iG^{\mathrm{A}}(\omega')\right)}{\omega_c-\omega'\pm 2i\eta}-2\pi i\frac{2if_{\mathrm{B}}\left(\omega'\right)G^{\mathrm{R}}\left(\omega'\right)+iG^<\left(\omega'\right)}{\omega_c-\omega'-2i\eta}\delta_{\pm,-}\right]\\&=\frac{1}{\pi}\int_{-\infty}^{\infty}\mathrm{d}\omega'\left[\frac{\left(\delta_{\mathrm{BB}'}+iG^{\mathrm{A}}(\omega')\right)f_{\mathrm{B}'}\left(\omega'\right)-\left(2if_{\mathrm{B}}\left(\omega'\right)G^{\mathrm{R}}\left(\omega'\right)+iG^<\left(\omega'\right)\right)\delta_{\pm,-}}{\omega_c-\omega'\pm 2i\eta}\right]\end{aligned} \tag{5.5.17}$$

With the same argumentation as for (5.5.11) and defining

$$\widetilde{F}^{\pm}\left(\omega_c\right) := V^2\sum_{k,k'}\frac{\left\langle c_k^\dagger c_{k'}\right\rangle}{\omega_c-\varepsilon_{k'}\pm i\eta}$$

the following is found for the sum with $+\varepsilon_k$:

$$V^2\sum_{k,k'}\frac{\left\langle c_k^\dagger c_{k'}\right\rangle}{\omega_c+\varepsilon_{k'}\pm i\eta} = -V^2\sum_{k,k'}\frac{\left\langle c_k^\dagger c_{k'}\right\rangle}{-\omega_c-\varepsilon_{k'}\mp i\eta} = -\widetilde{F}^{\mp}\left(-\omega_c\right)$$

In the sum above, the common index k' links the non-interacting Green's function to the annihilation operator; the calculation of a sum linking to the creation operator is similar, but there is a little caveat in the $\delta_{k'k}$ term. Where the first sum has

$$V^2 g^<_{k'}\sum_k\left(\delta_{k'k}+G^{\mathrm{A}}\frac{V^2}{\widetilde{\omega}^-_k}\right) = V^2 g^<_{k'}\left(\delta_{k'k'}\delta_{\mathrm{BB}'}+G^{\mathrm{A}}\Delta^-\right) = V^2 g^<_{k'}\left(\delta_{\mathrm{BB}'}+G^{\mathrm{A}}\Delta^-\right)$$

the term in the second has

$$V^2 \sum_k g_k^< \left(\delta_{k'k} + G^{\mathrm{A}} \frac{V^2}{\omega_{k'}^-} \right) = V^2 g_{k'}^< \delta_{\mathrm{BB}'} + G^{\mathrm{A}} \frac{V^2}{\omega_{k'}^-} \Delta_{\mathrm{B}}^<$$

the rest is analogous and leads to

$$\begin{aligned} & V^2 \sum_{k,k'} \frac{\left\langle c_{k'}^\dagger c_k \right\rangle}{\omega_c - \varepsilon_{k'} \pm i\eta} \\ & = \frac{1}{\pi} \int_{-\infty}^{\infty} \mathrm{d}\omega' \left[\frac{\left(\delta_{\mathrm{BB}'} - iG^{\mathrm{R}}(\omega') \right) f_{\mathrm{B}'}(\omega') - \left(2i f_{\mathrm{B}}(\omega') G^{\mathrm{A}}(\omega') - iG^<(\omega') \right) \delta_{\pm,-}}{\omega_c - \omega' \pm 2i\eta} \right]. \end{aligned} \tag{5.5.18}$$

The integral expression in this section are explicitly derived for leads in the wide-band limit. The procedure is analogous for different types of leads, yet, the k-sums (ε-integrals) may no longer be solvable exactly. In this case, the numerical effort increases, as the expressions result in double (ω and ε) or triple (ω, ε and ε') integrals that need to be evaluated in each iteration.

6. Outlook and Conclusion

Beyond Presented Orders

The four-operator Green's functions ${}_{4k}G_j$ involving one lead operator $c_k^{(\dagger)}$ are completely left out, which is mainly due to the two problems addressed in the beginning of section 5.3. As outlook, they shall be examined in more detail to suggest a possible solution.

The first is a potential symmetry problem, stemming from terms like

$$\langle\langle d^\dagger c_\iota c_k; x^\dagger \rangle\rangle - \langle\langle c_\iota^\dagger d c_k; x^\dagger \rangle\rangle,$$

where one Green's function is approximated and the other is considered through its equation of motion. Such terms can roughly be interpreted as *hermitian counterparts* of each other considering a transport-related operator $\left(d^\dagger c_\iota - c_\iota^\dagger d\right) c_k$, cf. equation (3.1.4), where the current operator $\hat{I} \propto \left(d^\dagger c_\iota - c_\iota^\dagger d\right)$. By trying to include the equations of motion for both, it turns out that they branch out very strongly, i.e. each new equation creates a similar situation, and the formal symmetry issues terminate only if the complete hierarchy of the ${}_{4k}G_j$ is taken into account. This leads to twenty-four equations of motion[I] that close in terms of those Green's functions. An approximation with scheme 2 or 3 to the remaining higher and two-lead-operator Green's functions leads then to

$${}_{4k}G_j \approx \chi(\varepsilon_k, \omega; \langle \ldots \rangle_k) + \sum_i R_i(\varepsilon_k, \omega)\, {}_4G_i,$$

where ${}_4G_i$ denotes four-operator Green's functions containing only operators on site a, b and d, R_i is an analytical rational function in ε_k and ω, and χ is the inhomogeneous term containing k-dependent expectation values. With the above expression, the equation sets for the two-operator Green's functions close as well and a solution can be obtained. As the ${}_{4k}G_j$ appear always in k-sums, terms like

$$\sum_k R_i(\varepsilon_k, \omega) \quad \text{and} \quad \sum_k \chi(\varepsilon_k, \omega; \langle \ldots \rangle_k)$$

need to be evaluated. The sums over the rational functions lead to exactly solvable integrals if the lead density of states is constant (like in the wide-band), yet the inhomogeneities are more complicated and need to be evaluated numerically in the self-consistency loop.

[I] Due to the system's left-right symmetry, the structure of the resulting equation set can be described by twelve commutators, which are shown in section A.1.10 in the appendix. For the explicit Green's functions, though, the inhomogeneities still need to be determined.

The second problem addressed earlier relates to the inhomogeneous terms like

$$V \sum_k \frac{\langle d^\dagger c_k \rangle}{\omega - \varepsilon_k \pm i\eta}$$

that seem to develop a logarithmic divergence for $\eta \to 0^+$ if evaluated at $T = 0\Gamma$. They converge for finite temperatures, but in this thesis no implementation for these direct sums is found that does not lead to severe symmetry violations that persist despite the restoration procedure.

However, these sums do not only converge for finite temperatures, but also if a non-vanishing imaginary part is added in the denominator. So, solving the first problem, i.e. taking into account all ${}_{4k}G_j$, may solve this divergence automatically, as this provides imaginary parts from the hybridization function.

Conclusion

The derivation of the equation of motion for non-equilibrium Green's functions was discussed in detail and extended by an alternative form. It was further shown that the original formulation leads to inconsistencies.

The resulting equations for steady-state solutions were then applied to the IRLM as a benchmark model, starting by discussing the modelling of the leads and setting up the fundamental equation sets for two-operator Green's functions in the IRLM. A first formal solution is found in a Hartree-Fock like approximation to higher Green's functions, which was used to discuss some symmetry properties.

Quantitative results for occupation number and spectral functions are obtained for tight-binding leads, where the possibility of isolated states and how to deal with them is shown. Further numerical results for the current are presented, which are in fairly good agreement with literature values obtained from other methods.

In the same approximation, some analytical expressions for leads in the wide-band limit were obtained and self-consistencies could be solved graphically. The non-interacting case contains no self-consistencies and could be solved exactly, which allowed for comparison with certain emerging effects in current and occupation numbers in the interacting self-consistent solutions.

It turned out that higher truncation levels lead to symmetry violations in the resulting Green's function and in turn to unphysical observables. A symmetry restoration was discussed and applied, and numerical results were presented for different levels of truncation and approximation.

In the course of adding more Green's functions to the equation sets, the spectral functions gained more features present in – although not exact – literature results and the current could be calculated for higher interactions strengths without convergence problems or ambiguities in the solutions. However, a clear convergence tendency towards the exact solution for the current could not be observed. In fact, the simple Hartree-Fock like approximation produced the best results for the current curve compared to the exact solution.

Nevertheless, the presented method is a proper and consistent non-equilibrium theory in first place, which is not based on assumptions like weak interaction or coupling in its derivation, and therefore does not restrict possible systems. The sets of equations for simple approximations offer analytical expressions that give insights into the system's behaviour and, finally, quantitative results from self-consistencies do not require high numerical or computational effort.

Appendix

Appendix A.

Mathematical Appendix

This appendix is mostly intended as a mathematical support for the main text and here and there as collection of additional aspects. Therefore, it is partially provided with less text and some notations may vary.

A.1. Derivations, Proofs and Auxiliary Calculations

A.1.1. Dyson Series of the Time Evolution Operator

Additional information about the time evolution operator can be found on pages 108ff. in [7] or pages 56ff. in [26].

The time evolution operator $\mathcal{U}(t, t_0)$ must satisfy the initial value problem consisting of Schrödinger equation and continuity relation, so

$$i\frac{\partial}{\partial t}\mathcal{U}(t, t_0) = H(t)\mathcal{U}(t, t_0) \quad \text{with} \quad \mathcal{U}(t_0, t_0) = \mathbb{1}.$$

Integration from t_0 to t gives the formal solution

$$\begin{aligned} \int_{t_0}^{t} \mathrm{d}t_1 \, \frac{\partial}{\partial t_1}\mathcal{U}(t_1, t_0) &= -i \int_{t_0}^{t} \mathrm{d}t_1 \, H(t_1)\mathcal{U}(t_1, t_0) \\ \mathcal{U}(t, t_0) - \mathcal{U}(t_0, t_0) &= -i \int_{t_0}^{t} \mathrm{d}t_1 \, H(t_1)\mathcal{U}(t_1, t_0) \\ \rightarrow \mathcal{U}(t, t_0) &= \mathbb{1} - i \int_{t_0}^{t} \mathrm{d}t_1 \, H(t_1)\mathcal{U}(t_1, t_0). \end{aligned} \tag{A.1.1}$$

Iterated reinsertion of the formal solution gives the following sum of iterated integrals

$$\begin{aligned} \mathcal{U}(t, t_0) &= \mathbb{1} - i \int_{t_0}^{t} \mathrm{d}t_1 \, H(t_1) \left[\mathbb{1} - i \int_{t_0}^{t_1} \mathrm{d}t_2 \, H(t_2)\mathcal{U}(t_2, t_0) \right] \\ &= \mathbb{1} - i \int_{t_0}^{t} \mathrm{d}t_1 \, H(t_1) + (-i)^2 \int_{t_0}^{t} \mathrm{d}t_1 \int_{t_0}^{t_1} \mathrm{d}t_2 \, H(t_1)H(t_2) + \dots \\ &+ (-i)^n \int_{t_0}^{t} \mathrm{d}t_1 \dots \int_{t_0}^{t_{n-1}} \mathrm{d}t_n \, H(t_1) \dots H(t_n) \\ &=: \sum_{n=0}^{\infty} (-i)^n \int_{t_0}^{t} \mathrm{d}t_1 \dots \int_{t_0}^{t_{n-1}} \mathrm{d}t_n \, H(t_1) \dots H(t_n), \end{aligned} \tag{A.1.2}$$

where the $n = 0$ term is defined to be $\mathbb{1}$.

The terms are now rewritten by reversing the order of integration in order to set each upper integration limit equal to t.

For the $n = 2$ term the integration is changed as follows

$$\int_{t_0}^{t} \mathrm{d}t_1 \int_{t_0}^{t_1} \mathrm{d}t_2 \ldots = \int_{t_0}^{t} \mathrm{d}t_2 \int_{t_2}^{t} \mathrm{d}t_1 \ldots,$$

which can be explained graphically as the equivalence of summing (integrating) slices of either $\mathrm{d}y$ or $\mathrm{d}x$ in a triangular plane, in order to calculate the area (see chapter 3 in [26]). So the double integral can be written as

$$\begin{aligned} \int_{t_0}^{t} \mathrm{d}t_1 \int_{t_0}^{t_1} \mathrm{d}t_2 \, H(t_1)H(t_2) &= \int_{t_0}^{t} \mathrm{d}t_2 \int_{t_2}^{t} \mathrm{d}t_1 \, H(t_1)H(t_2) \\ &= \int_{t_0}^{t} \mathrm{d}t_1 \int_{t_1}^{t} \mathrm{d}t_2 \, H(t_2)H(t_1), \end{aligned} \tag{A.1.3}$$

where the dummy variables t_1 and t_2 are interchanged in the last step. Further, the integration limits can be replaced by a step function

$$\int_{t_2}^{t} \mathrm{d}t_1 \ldots = \int_{t_0}^{t} \mathrm{d}t_1 \, \Theta(t_1 - t_2) \ldots.$$

And so another form for the double integral is

$$\begin{aligned} \int_{t_0}^{t} \mathrm{d}t_1 \int_{t_0}^{t_1} \mathrm{d}t_2 \, H(t_1)H(t_2) &= \frac{1}{2} \left[\int_{t_0}^{t} \mathrm{d}t_2 \int_{t_0}^{t} \mathrm{d}t_1 \, \Theta(t_1 - t_2)H(t_1)H(t_2) \right. \\ &\quad \left. + \int_{t_0}^{t} \mathrm{d}t_1 \int_{t_0}^{t} \mathrm{d}t_2 \, \Theta(t_2 - t_1)H(t_2)H(t_1) \right] \\ &= \frac{1}{2} \int_{t_0}^{t} \mathrm{d}t_1 \int_{t_0}^{t} \mathrm{d}t_2 \left[\Theta(t_1 - t_2)H(t_1)H(t_2) + \Theta(t_2 - t_1)H(t_2)H(t_1) \right] \\ &= \frac{1}{2} \int_{t_0}^{t} \mathrm{d}t_1 \int_{t_0}^{t} \mathrm{d}t_2 \, \mathcal{T} \left[H(t_1)H(t_2) \right], \end{aligned} \tag{A.1.4}$$

where $\mathcal{T}$ is the time-ordering operator and no additional sign for fermions is necessary, as the number of creation- and annihilation operators in the Hamiltonian is always even.

In principle, the same strategy can be pursued for the nth term, i.e. starting from the innermost time t_n and iteratively changing the order of integration with its left neighbours. This is rather cumbersome since it has to be done for each time $t_{i \leq n}$ in order to reach t as an overall upper integration limit. A shorter approach is to consider the absolute order of times that is implied by the integration limits in one iterated integral, namely

$$\int_{t_0}^{t} \mathrm{d}t_1 \ldots \int_{t_0}^{t_{n-1}} \mathrm{d}t_n \Rightarrow \begin{cases} & t_0 \leq t_n \leq t_{n-1} \\ & \vdots \\ \wedge & t_0 \leq t_{n-i} \leq t_{n-i-1} \\ & \vdots \\ \wedge & t_0 \leq t_1 \leq t \end{cases} \quad \Leftrightarrow \quad t_0 \leq t_n \leq \ldots \leq t_{n-i} \leq \ldots \leq t_1 \leq t. \tag{A.1.5}$$

The desired inversion can be obtained directly as

$$t_0 \leq t_n \leq \ldots \leq t_{n-i} \leq \ldots \leq t_1 \leq t \Leftrightarrow \begin{cases} & t_2 \leq t_1 \leq t \\ \wedge & t_3 \leq t_2 \leq t \\ & \vdots \\ \wedge & t_{i+1} \leq t_i \leq t \\ & \vdots \\ \wedge & t_n \leq t_{n-1} \leq t \\ \wedge & t_0 \leq t_n \leq t, \end{cases} \tag{A.1.6}$$

and the corresponding integral reads

$$\int_{t_0}^{t} \mathrm{d}t_n \int_{t_n}^{t} \mathrm{d}t_{n-1} \ldots \int_{t_{i+1}}^{t} \mathrm{d}t_i \ldots \int_{t_3}^{t} \mathrm{d}t_2 \int_{t_2}^{t} \mathrm{d}t_1 \,.$$

The lower integration limits are adjusted in each integral with appropriate step functions, so that

$$\int_{t_0}^{t} \mathrm{d}t_n \ldots \int_{t_{i+1}}^{t} \mathrm{d}t_i \ldots \int_{t_2}^{t} \mathrm{d}t_1 \to \int_{t_0}^{t} \mathrm{d}t_n \ldots \int_{t_0}^{t} \mathrm{d}t_i \,\Theta(t_i - t_{i+1}) \ldots \int_{t_0}^{t} \mathrm{d}t_1 \,\Theta(t_1 - t_2).$$

After reversing the order of integration in the nth term, so that each upper integration limit is equal to t, the equivalent of equation (A.1.3) can be considered for this term and there are $n!$ possibilities (permutations) to rename the dummy time labels, so

$$\begin{aligned} &\to (-i)^n \int_{t_0}^{t} \mathrm{d}t_n \ldots \int_{t_0}^{t} \mathrm{d}t_1 \,\Theta(t_n \leq \ldots \leq t_1) H(t_1) \ldots H(t_n) \\ &= \frac{(-i)^n}{n!} \int_{t_0}^{t} \mathrm{d}t_n \ldots \int_{t_0}^{t} \mathrm{d}t_1 \sum_{\text{perms.}} \Theta(t_n \leq \ldots \leq t_1) H(t_1) \ldots H(t_n) \\ &= \frac{(-i)^n}{n!} \int_{t_0}^{t} \mathrm{d}t_n \ldots \int_{t_0}^{t} \mathrm{d}t_1 \,\mathcal{T}\left[H(t_1) \ldots H(t_n)\right]. \end{aligned} \tag{A.1.7}$$

And finally the complete sum is written as

$$\begin{aligned} \mathcal{U}(t, t_0) &= \sum_{n=0}^{\infty} (-i)^n \int_{t_0}^{t} \mathrm{d}t_1 \ldots \int_{t_0}^{t_{n-1}} \mathrm{d}t_n \, H(t_1) \ldots H(t_n) \\ &= \sum_{n=0}^{\infty} \frac{(-i)^n}{n!} \int_{t_0}^{t} \mathrm{d}t_n \ldots \int_{t_0}^{t} \mathrm{d}t_1 \,\mathcal{T}\left[H(t_1) \ldots H(t_n)\right] \\ &=: \mathcal{T} \exp\left[-i \int_{t_0}^{t} \mathrm{d}t' \, H(t')\right]. \end{aligned} \tag{A.1.8}$$

A.1.2. Commutation of A with the Density Operator

Recalling the definition of the operator A_a in the Dirac picture,

$$A_a = f_a(t_a) A_0,$$

and defining

$$\hat{\mathcal{N}} := \sum_j \beta_j(\varepsilon_j - \mu_j)\hat{n}_j$$
$$\widetilde{\varphi} := \sum_i \widetilde{\lambda}_i \beta_i(\varepsilon_i - \mu_i),$$

where j runs over all particles and i only over the A related particles, the following is obtained,

$$\left[A_a, \hat{\mathcal{N}}\right] = f_a(t_a)\left[A_0, \hat{\mathcal{N}}\right] = f_a(t_a)\sum_i \beta_i(\varepsilon_i - \mu_i)\underbrace{\left[A_0, \hat{n}_i\right]}_{\widetilde{\lambda}_i A_0} = f_a(t_a)\widetilde{\varphi}A_0 = \widetilde{\varphi}A_a,$$

as the commutators with $\hat{n}_j$ that are not part of i are zero. The density operator ρ_0 can be written as

$$Z_0\rho_0 = \mathrm{e}^{-\hat{\mathcal{N}}} = \sum_{m=0}^{\infty} \frac{\left(-\hat{\mathcal{N}}\right)^m}{m!} \tag{A.1.9}$$

and so

$$A_a Z_0\rho_0 = \sum_{m=0}^{\infty} \frac{(-1)^m}{m!} A_a \hat{\mathcal{N}}^m. \tag{A.1.10}$$

Rewriting

$$\begin{aligned} A_a\hat{\mathcal{N}} &= \left[A_a, \hat{\mathcal{N}}\right] + \hat{\mathcal{N}}A_a = \left(\widetilde{\varphi} + \hat{\mathcal{N}}\right) A_a \\ A_a\hat{\mathcal{N}}^m = A_a\hat{\mathcal{N}}\hat{\mathcal{N}}^{m-1} &= \left(\widetilde{\varphi} + \hat{\mathcal{N}}\right) A_a\hat{\mathcal{N}}^{m-1} \\ &= \left(\widetilde{\varphi} + \hat{\mathcal{N}}\right)^2 A_a\hat{\mathcal{N}}^{m-2} \\ &\vdots \\ &= \left(\widetilde{\varphi} + \hat{\mathcal{N}}\right)^k A_a\hat{\mathcal{N}}^{m-k}, \end{aligned} \tag{A.1.11}$$

where for $m = k$

$$A_a\hat{\mathcal{N}}^m = \left(\widetilde{\varphi} + \hat{\mathcal{N}}\right)^m A_a.$$

And so the commutation results in

$$\begin{aligned} A_a Z_0\rho_0 &= \sum_{m=0}^{\infty} \frac{(-1)^m}{m!} A_a\hat{\mathcal{N}}^m \\ &= \sum_{m=0}^{\infty} \frac{(-1)^m}{m!} \left(\widetilde{\varphi} + \hat{\mathcal{N}}\right)^m A_a \\ &= \mathrm{e}^{-\left(\widetilde{\varphi}+\hat{\mathcal{N}}\right)} A_a \\ &= \mathrm{e}^{-\widetilde{\varphi}} Z_0\rho_0 A_a \end{aligned} \tag{A.1.12}$$

and thus

$$\rightarrow A_a\rho_0 = \mathrm{e}^{-\widetilde{\varphi}}\rho_0 A_a.$$

A.1.3. Heaviside Relation

The relation

$$\Theta(t_a - t_b) \int_{t_b}^{t_a} \mathrm{d}t \ldots = \int_{-\infty}^{\infty} \mathrm{d}t\, \Theta(t_a - t)\Theta(t - t_b) \ldots$$

can be explained by having a closer look at the left-hand side expression case-by-case:

$$\Theta(t_a - t_b) \int_{t_b}^{t_a} \mathrm{d}t \ldots = \begin{cases} \int_{t_b}^{t_a} \mathrm{d}t \ldots & \text{if } t_a > t_b \\ 0 & \text{otherwise} \end{cases} \tag{A.1.13}$$

The two step functions on the right-hand side restrict the integration to the region where they overlap to one, which is only given for $t_a > t_b$. This reproduces exactly the left-hand side for the cases $t_a > t_b$ and $t_a < t_b$, as can be seen in figure A.1.

(a) $t_a > t_b$ (b) $t_a < t_b$

Figure A.1.: Schematics of the two step functions $\Theta(t_a - t)$ (dotted line) and $\Theta(t - t_b)$ (dashed line).

In the case of $t_a = t_b$ both sides give zero as

$$\int_{t_a}^{t_a} \ldots = 0.$$

A.1.4. Particle-Hole Symmetry

The IRLM Hamiltonian is invariant under the particle-hole transformation

$$x_n \to (-1)^n x_{-n}^\dagger ,$$

that means explicitly

$$\begin{aligned} c_{a,b} &\to -c_{b,a}^\dagger \\ d &\to d^\dagger \\ c_{k\in \mathrm{L}} &\to c_{k\in \mathrm{R}}^\dagger \end{aligned} \tag{A.1.14}$$

and so

$$\begin{aligned} c_a^\dagger d &\to -c_b d^\dagger = d^\dagger c_b \\ c_a^\dagger c_{k\in \mathrm{L}} &\to -c_b c_{k\in \mathrm{R}}^\dagger = c_{k\in \mathrm{R}}^\dagger c_b \\ \hat{n}_a = c_a^\dagger c_a &\to (-c_b)(-c_b^\dagger) = c_b c_b^\dagger = 1 - \hat{n}_b. \end{aligned} \tag{A.1.15}$$

The hopping terms in t and V are directly reproduced, but the PHS transformed H_0 and interaction terms impose some restrictions on the on-site energies ε_i as

$$\begin{aligned} H_0 \to \varepsilon_d + \varepsilon_a + \varepsilon_b + \sum_{k\in\mathrm{L}} \varepsilon_k + \sum_{k\in\mathrm{R}} \varepsilon_k \\ - \left(\varepsilon_d \hat{n} + \varepsilon_a \hat{n}_b + \varepsilon_b \hat{n}_a + \sum_{k\in\mathrm{L}} \varepsilon_{k\in\mathrm{R}} \hat{n}_{k\in\mathrm{R}} + \sum_{k\in\mathrm{R}} \varepsilon_{k\in\mathrm{L}} \hat{n}_{k\in\mathrm{L}} \right) \end{aligned} \tag{A.1.16}$$

and

$$H_1 \to H_t + H_V + U\left(2 - \hat{n}_a - \hat{n}_b - 2\hat{n} + \hat{n}_a\hat{n} + \hat{n}_b\hat{n}\right). \tag{A.1.17}$$

If the density of states in the leads is symmetric around zero, the lead energy sum becomes a symmetric integral over an antisymmetric function, which is zero, and so:

$$\sum_{k\in\mathrm{L}} \varepsilon_k = \sum_{k\in\mathrm{R}} \varepsilon_k = 0$$

Equating coefficients with the original Hamiltonian for the rest leads to

$$\begin{aligned} \varepsilon_L &\stackrel{!}{=} \varepsilon_R \\ \varepsilon_d + \varepsilon_a + \varepsilon_b + 2U &\stackrel{!}{=} 0 \\ -\varepsilon_d - 2U &\stackrel{!}{=} \varepsilon_d \\ -\varepsilon_a - U &\stackrel{!}{=} \varepsilon_b \\ -\varepsilon_b - U &\stackrel{!}{=} \varepsilon_a \end{aligned} \tag{A.1.18}$$

which leads to (apart from the obvious)

$$\varepsilon_a + \varepsilon_b = -U$$

where the $\varepsilon_a = \varepsilon_b$ is chosen to keep the complete system symmetric.

The k-sums appearing in the HF Hamiltonian equal

$$\begin{aligned} \sum_{k\in\mathrm{L}} \varepsilon_k \langle \hat{n}_k \rangle &= \sum_{k\in\mathrm{R}} \varepsilon_k \left(1 - \langle \hat{n}_k \rangle\right) \\ &= \underbrace{\sum_{k\in\mathrm{R}} \varepsilon_k}_{=0} - \sum_{k\in\mathrm{R}} \varepsilon_k \langle \hat{n}_k \rangle \\ \to \sum_{k\in\mathrm{L}} \varepsilon_k \langle \hat{n}_k \rangle + \sum_{k\in\mathrm{R}} \varepsilon_k \langle \hat{n}_k \rangle &= 0. \end{aligned} \tag{A.1.19}$$

A.1.5. Bare Bath Sum

For the limit $D \to \infty$, the complex logarithm is rewritten as

$$\ln(z) = \ln(|z|) + i\left(\arg(z) + 2k\pi\right) \quad \text{for } k = 0,$$

where the argument function is defined as

$$\arg(z) = \begin{cases} +\arccos\left(\frac{\mathrm{Re}\{z\}}{|z|}\right) & \text{if } \mathrm{Im}\{z\} \geq 0 \\ -\arccos\left(\frac{\mathrm{Re}\{z\}}{|z|}\right) & \text{otherwise.} \end{cases}$$

And so

$$\ln(\omega + D \pm i\eta) = \ln(|\ldots|) \pm i \arccos\left(\frac{\omega + D}{\sqrt{(w+D)^2 + \eta^2}}\right), \tag{A.1.20}$$

where

$$\lim_{D\to\infty} \frac{\omega + D}{\sqrt{(w+D)^2 + \eta^2}} = 1 \quad \text{and} \quad \arccos(1) = 0$$

and therefore

$$\to \ln(\omega + D \pm i\eta) = \lim_{D\to\infty} \ln\left(\sqrt{(w+D)^2 + \eta^2}\right). \tag{A.1.21}$$

For the other term

$$\to \ln(\omega - D \pm i\eta) = \lim_{D\to\infty} \ln\left(\sqrt{(w-D)^2 + \eta^2}\right) \pm i\pi \tag{A.1.22}$$

is obtained as

$$\lim_{D\to\infty} \frac{\omega - D}{\sqrt{(w-D)^2 + \eta^2}} = -1 \quad \text{and} \quad \arccos(-1) = \pi.$$

The divergent terms cancel out in the limit and so

$$\ln(\omega + D \pm i\eta) - \ln(\omega - D \pm i\eta) = \mp i\pi + \lim_{D\to\infty} \left(\ln\left(\sqrt{\ldots}\right) - \ln\left(\sqrt{\ldots}\right)\right) = \mp i\pi. \tag{A.1.23}$$

A.1.6. Squared Bath Sum

The integral result from the squared bath sum is split into real and imaginary part, so

$$\begin{aligned} \frac{1}{\omega - D \pm i\eta} - \frac{1}{\omega + D \pm i\eta} = \frac{\omega - D}{(\omega - D)^2 + \eta^2} - \frac{\omega + D}{(\omega + D)^2 + \eta^2} \\ \mp i\eta \left(\frac{1}{(\omega - D)^2 + \eta^2} - \frac{1}{(\omega + D)^2 + \eta^2}\right), \end{aligned} \tag{A.1.24}$$

where it is clearer to see that the single summands give all zero in the limit $D \to \infty$.

A.1.7. TB Chain

Alternatively the hybridization function can be determined from the equation of motion for the uncoupled, semi-infinite tight-binding chain in position space. With the Hamiltonian

$$H_{\mathrm{TB}} = \varepsilon_{\mathrm{TB}} \sum_{i=0}^{N} \hat{n}_i - t_0 \sum_{i=0}^{N} \left(c_i^\dagger c_{i+1} + c_{i+1}^\dagger c_i \right) \quad \text{and } N \to \infty$$

the equations of motion form the equation set

$$\begin{aligned} \langle\langle c_0; c_0^\dagger \rangle\rangle &= g_0 \left(1 - t_0 \langle\langle c_1; c_0^\dagger \rangle\rangle \right) \\ \langle\langle c_i; c_0^\dagger \rangle\rangle &= -t_0 g_i \left(\langle\langle c_{i-1}; c_0^\dagger \rangle\rangle + \langle\langle c_{i+1}; c_0^\dagger \rangle\rangle \right) \\ \langle\langle c_N; c_0^\dagger \rangle\rangle &= -t_0 g_N \langle\langle c_{N-1}; c_0^\dagger \rangle\rangle \end{aligned} \tag{A.1.25}$$

resulting in a continued fraction for the Green's function on site $i = 0$, so

$$\to \langle\langle c_0; c_0^\dagger \rangle\rangle = \cfrac{1}{z_0 - \cfrac{1}{z_1 - \cfrac{1}{z_2 - \cfrac{1}{\ddots - \cfrac{1}{z_N}}}}} \tag{A.1.26}$$

where

$$z_i := \frac{1}{t_0 g_i} = \frac{1}{t_0} \left(\omega - \varepsilon_{\mathrm{TB}} \pm i\eta \right) = \frac{\widetilde{\omega}^{\pm}}{t_0}.$$

This continued fraction can be expressed in a closed form for $N \to \infty$ and any complex number $z_i = z_{i+1} =: z \in \mathbb{C} \setminus \{0\}$, as it becomes self-similar and can be solved algebraically:

$$\langle\langle c_0; c_0^\dagger \rangle\rangle \overset{N \to \infty}{=} \cfrac{1}{z - \cfrac{1}{z - \cfrac{1}{z - \cfrac{1}{z - \cfrac{1}{\ddots}}}}} \tag{A.1.27}$$

Assuming convergence[I] of the infinite continued fraction, it can be assigned a finite (complex) value G, which leads to a quadratic equation that can be solved in a closed form.

$$\begin{aligned} G &= \frac{1}{z - G} \\ &\to G^2 - zG + 1 = 0 \\ G_{1,2} &= \frac{1}{2} \left(z \pm \sqrt{z^2 - 4} \right) \end{aligned} \tag{A.1.28}$$

[I] An infinite continued fraction converges if its convergents, i.e. the resulting finite fraction, when the recursion stops at n, tends to a finite limit. This is obviously the case for any $z \in \mathbb{C} \setminus \{0\}$.

Reinserting all definitions and choosing the convergent ($\omega \to \infty$) solution G_1 leads eventually to:

$$\begin{aligned}\langle\langle c_0; c_0^\dagger \rangle\rangle &= \frac{1}{2}\left(z + \sqrt{z^2 - 4}\right) \\ &= \frac{1}{2t_0}\left(\widetilde{\omega}^{\pm} + \sqrt{(\widetilde{\omega}^{\pm})^2 - 4t_0^2}\right) \\ &= \frac{1}{2t_0}\left(\widetilde{\omega}^{\pm} \mp i\sqrt{4t_0^2 - (\widetilde{\omega}^{\pm})^2}\right)\end{aligned} \tag{A.1.29}$$

A.1.8. Imaginary Part of the Hybridization Function

The exact limit $\eta \to 0^+$ for a single hybridization function, i.e. not appearing in a Green's function, can be related to the density of states. This derivation is valid for general baths, as the density of states $\rho(\varepsilon)$ is always a real-valued function.

$$\begin{aligned}\mathrm{Im}\left\{\sum_k \frac{V^2}{\omega - \varepsilon_k \pm i\eta}\right\} &= \mathrm{Im}\left\{V^2 \int_{-\infty}^{\infty} \mathrm{d}\varepsilon\, \frac{\rho(\varepsilon)}{\omega - \varepsilon \pm i\eta}\right\} = V^2 \int_{-\infty}^{\infty} \mathrm{d}\varepsilon\, \rho(\varepsilon)\, \mathrm{Im}\left\{\frac{1}{\omega - \varepsilon \pm i\eta}\right\} \\ &= V^2 \int_{-\infty}^{\infty} \mathrm{d}\varepsilon\, \rho(\varepsilon) \frac{\mp\eta}{(\omega - \varepsilon)^2 + \eta^2} \overset{\eta \to 0^+}{=} \mp V^2 \pi \rho(\omega)\end{aligned} \tag{A.1.30}$$

The result is obtained as the fraction acts like a delta distribution.

A.1.9. Outer Solution to the Occupation Number n

In order to analyse the spectral function in the outer region, the relation

$$\Delta_{\mathrm{TB}}^{\pm} = \frac{1}{\omega^{\pm} - \Delta_{\mathrm{TB}}^{\pm}}$$

for the tight-binding[II] hybridization function is used and the advanced and retarded Green's function becomes

$$\langle\langle d; d^\dagger \rangle\rangle = \left(\omega^{\pm} - \frac{2|\tau|^2}{\omega^{\pm} - \Delta^{\pm}}\right)^{-1} = \left(\omega^{\pm} - 2|\tau|^2 \Delta^{\pm}\right)^{-1}.$$

So for the spectral function $A_{dd}(\omega)$

$$\begin{aligned}\pi A_{dd}(\omega) = \mathrm{Im}\left\{\langle\langle d; d^\dagger \rangle\rangle^{\mathrm{A}}\right\} &= \left|\langle\langle d; d^\dagger \rangle\rangle\right|^2 \mathrm{Im}\left\{\frac{1}{\langle\langle d; d^\dagger \rangle\rangle^{\mathrm{R}}}\right\} \\ &= \frac{\eta - 2|\tau|^2\, \mathrm{Im}\{\Delta^+\}}{\left|\omega^{\pm} - 2|\tau|^2 \Delta^{\pm}\right|^2} \\ &= \frac{\eta + 2|\tau|^2\, \mathrm{Im}\{\Delta^-\}}{\left|\omega^{\pm} - 2|\tau|^2 \Delta^{\pm}\right|^2}\end{aligned} \tag{A.1.31}$$

[II] This relation results from the continued fraction arising in the alternative derivation in section A.1.7 in the appendix.

is obtained, where the numerator becomes

$$\eta + 2|\tau|^2 \operatorname{Im}\{\Delta^-\} \to \left(1 + 2|\tau|^2\right) \mathcal{O}(\eta) \qquad \text{for } |\omega| > 2.$$

The denominator becomes

$$\begin{aligned}
\left|\omega^\pm - 2|\tau|^2\Delta^\pm\right|^2 &= \left|\left(1-|\tau|^2\right)\omega^\pm \pm i|\tau|^2\sqrt{4-(\omega^\pm)^2}\right|^2 \\
&= \left(1-|\tau|^2\right)^2\left(\omega^2+\eta^2\right) + |\tau|^4\left|4-(\omega^\pm)^2\right| \\
&\quad - i|\tau|^2\left(1-|\tau|^2\right)\left(\omega^+\sqrt{4-(\omega^-)^2} - \omega^-\sqrt{4-(\omega^+)^2}\right) \qquad \text{(A.1.32)} \\
&= \left(1-|\tau|^2\right)^2\left(\omega^2+\eta^2\right) + |\tau|^4\left|(\omega^\pm)^2-4\right| \\
&\quad + \operatorname{sgn}(\omega) 2|\tau|^2\left(1-|\tau|^2\right)\operatorname{Re}\left\{\omega^+\sqrt{(\omega^-)^2-4}\right\}
\end{aligned}$$

and can further be written as

$$= \left(1-|\tau|^2\right)^2\left(\eta^2 + f_\eta(\omega)\right), \qquad \text{(A.1.33)}$$

where

$$f_\eta(\omega) = \omega^2 + \frac{|\tau|^4}{\left(1-|\tau|^2\right)^2}\left|(\omega^\pm)^2-4\right| + \operatorname{sgn}(\omega)\frac{2|\tau|^2}{1-|\tau|^2}\operatorname{Re}\left\{\omega^+\sqrt{(\omega^-)^2-4}\right\}.$$

This function can be expressed as the following square in the limit

$$\lim_{\eta\to 0^+} f_\eta(\omega) = \left(|\omega| + \frac{|\tau|^2}{1-|\tau|^2}\sqrt{\omega^2-4}\right)^2 =: \widetilde{f}^2(\omega) \qquad \text{if } |\omega| > 2$$

and develops the roots

$$\omega_{1,2} = \pm\frac{2|\tau|^2}{\sqrt{2|\tau|^2-1}}$$

that are outside the bandwidth, i.e. $|\omega_{1,2}| > 2$, for $|\tau|^2 > 1$. So in total the spectral function $A_{dd}(\omega)$ outside the bandwidth is proportional to

$$\pi A_{dd}(\omega) \propto \frac{1}{\left(1-|\tau|^2\right)^2}\lim_{\eta\to 0^+}\frac{\left(1+2|\tau|^2\right)\mathcal{O}(\eta)}{f_\eta(\omega)+\eta^2}.$$

As mentioned above, in the limit $\eta \to 0^+$ the function $f_\eta(\omega)$ becomes the real-valued square of a function $\widetilde{f}(\omega)$ with roots at $\omega_{1,2}$ and the function values of the ratio become

$$\frac{\mathcal{O}(\eta)}{f_\eta(\omega)+\eta^2} = \begin{cases} \mathcal{O}\left(\frac{1}{\eta}\right) \to \infty & \text{if } \omega = \omega_{1,2} \wedge |\omega| > 2 \\ \mathcal{O}(\eta) \to 0 & \text{otherwise.} \end{cases} \qquad \text{(A.1.34)}$$

The rational function acts hence like a sum of delta distributions,

$$\lim_{\eta\to 0^+} \frac{\left(1+2|\tau|^2\right)\mathcal{O}(\eta)}{f_\eta(\omega)+\eta^2} \propto Z\left(|\tau|^2\right)\frac{\delta\left(\omega-\omega_1\right)+\delta\left(\omega-\omega_2\right)}{2},$$

where the normalizing constant is given by the definite integral

$$Z\left(|\tau|^2\right) = \lim_{\eta\to 0^+}\int_{|\omega|>2} \mathrm{d}\omega\, \frac{\eta+2|\tau|^2\,\mathrm{Im}\{\Delta^-\}}{f_\eta(\omega)+\eta^2}$$

which has no exact solution[III]. However, it can be determined via

$$1 = \int_{-\infty}^{\infty}\mathrm{d}\omega\, A_{dd}(\omega) = \int_{-2}^{2}\mathrm{d}\omega\, A_{dd}(\omega) + \int_{|\omega|>2}\mathrm{d}\omega\, A_{dd}(\omega)$$

as the inner solution is known. For $|\tau|^2 \leq 1$ the outer integral must vanish, as

$$\int_{|\omega|>2}\mathrm{d}\omega\, A_{dd}(\omega)\Big|_{|\tau|^2\leq 1} = 1 - \int_{-2}^{2}\mathrm{d}\omega\, A_{dd}(\omega)\Big|_{|\tau|^2\leq 1} = 1-1 = 0.$$

As shown above, $|\omega_{1,2}| > 2$ for $|\tau|^2 > 1$ and therefore the integration over each delta distribution gives just one and the normalizing constant can be determined via

$$\begin{aligned} 1 &= \int_{-2}^{2}\mathrm{d}\omega\, A_{dd}(\omega)\Big|_{|\tau|^2>1} + \int_{|\omega|>2}\mathrm{d}\omega\, A_{dd}(\omega)\Big|_{|\tau|^2>1} \\ &= \frac{1}{2|\tau|^2-1} + \frac{Z\left(|\tau|^2\right)}{\pi\left(1-|\tau|^2\right)^2}\int_{|\omega|>2}\mathrm{d}\omega\,\frac{\delta(\omega-\omega_1)+\delta(\omega-\omega_2)}{2} \\ &= \frac{1}{2|\tau|^2-1} + \frac{Z\left(|\tau|^2\right)}{\pi\left(1-|\tau|^2\right)^2} \end{aligned} \tag{A.1.35}$$

and so in total

$$\to Z\left(|\tau|^2\right) = \begin{cases} \frac{2\pi\left(|\tau|^2-1\right)\left(1-|\tau|^2\right)^2}{2|\tau|^2-1} & \text{if } |\tau|^2 > 1 \\ 0 & \text{otherwise.} \end{cases} \tag{A.1.36}$$

With (4.2.8) the exact limit for the spectral function $A_{dd}(\omega)$ can be written as

$$\begin{aligned} A_{dd}(\omega) &= \frac{1}{\pi}\frac{|\tau|^2\,\mathrm{Re}\left\{\sqrt{4-\omega^2}\right\}}{\omega^2\left(1-2|\tau|^2\right)+4|\tau|^4} + \frac{Z\left(|\tau|^2\right)}{2\pi\left(1-|\tau|^2\right)^2}\left(\delta(\omega-\omega_1)+\delta(\omega-\omega_2)\right) \\ &\overset{|\tau|^2>1}{=} \frac{1}{\pi}\frac{|\tau|^2\,\mathrm{Re}\left\{\sqrt{4-\omega^2}\right\}}{\omega^2\left(1-2|\tau|^2\right)+4|\tau|^4} + \frac{|\tau|^2-1}{2|\tau|^2-1}\left(\delta(\omega-\omega_1)+\delta(\omega-\omega_2)\right). \end{aligned} \tag{A.1.37}$$

[III] At least to the knowledge of the author with his humble skills in the art of integration.

A.1.10. Commutators for Four-Operator Terms Containing a Lead Operator

For the sake of completeness, the corresponding commutators are listed here. The appearing combinations containing a number operator are

$$\begin{aligned}
[c_k\hat{n}, H_1] &= -t\left(d^\dagger c_\iota c_k - c_\iota^\dagger d c_k + d^\dagger c_{\bar{\iota}} c_k - c_{\bar{\iota}}^\dagger d c_k\right) - V c_\iota \hat{n} \\
[c_{\bar{k}}\hat{n}_\iota, H_1] &= -t\left(c_\iota^\dagger d c_{\bar{k}} - d^\dagger c_\iota c_{\bar{k}}\right) - V\left[c_{\bar{\iota}}\hat{n}_\iota + \sum_k\left(c_\iota^\dagger c_k c_{\bar{k}} - c_k^\dagger c_\iota c_{\bar{k}}\right)\right] \\
[c_k\hat{n}_\iota, H_1] &= -t\left(c_\iota^\dagger d c_k - d^\dagger c_\iota c_k\right) - V\sum_{k'}\left(c_\iota^\dagger c_{k'} c_k - c_{k'}^\dagger c_\iota c_k\right).
\end{aligned} \tag{A.1.38}$$

The combinations with central-site hoppings are

$$\begin{aligned}
\left[d^\dagger c_{\bar{\iota}} c_k, H_1\right] &= -t\left(c_k\hat{n} - c_k\hat{n}_{\bar{\iota}} - c_\iota^\dagger c_{\bar{\iota}} c_k\right) + U d^\dagger c_k c_{\bar{\iota}}\hat{n}_\iota - V\left(d^\dagger c_{\bar{\iota}} c_\iota + \sum_{\bar{k}} d^\dagger c_{\bar{k}} c_k\right) \\
\left[d^\dagger c_\iota c_{k'}, H_1\right] &= -t\left(c_k\hat{n} - c_k\hat{n}_\iota - c_{\bar{\iota}}^\dagger c_\iota c_k\right) + U d^\dagger c_k c_\iota\hat{n}_{\bar{\iota}} - V\sum_{k'} d^\dagger c_{k'} c_k \\
\left[c_\iota^\dagger c_k d, H_1\right] &= -t\left(c_k\hat{n} - c_k\hat{n}_\iota - c_\iota^\dagger c_{\bar{\iota}} c_k\right) + U c_\iota^\dagger c_k d\hat{n}_{\bar{\iota}} - V\left(d\hat{n}_\iota + \sum_{k'} c_{k'}^\dagger d c_k\right) \\
\left[c_\iota^\dagger c_{\bar{k}} d, H_1\right] &= -t\left(c_{\bar{k}}\hat{n} - c_{\bar{k}}\hat{n}_\iota - c_\iota^\dagger c_{\bar{\iota}} c_{\bar{k}}\right) + U c_\iota^\dagger c_{\bar{k}} d\hat{n}_{\bar{\iota}} - V\left(c_\iota^\dagger c_{\bar{\iota}} d + \sum_k c_k^\dagger d c_{\bar{k}}\right).
\end{aligned} \tag{A.1.39}$$

Combinations in left and right site are

$$\begin{aligned}
\left[c_\iota^\dagger c_k c_{\bar{\iota}}, H_1\right] &= -t\left(d^\dagger c_{\bar{\iota}} c_k - c_\iota^\dagger d c_k\right) - V\left(c_{\bar{\iota}}\hat{n}_\iota + \sum_{k'} c_{k'}^\dagger c_{\bar{\iota}} c_k + \sum_{\bar{k}} c_\iota^\dagger c_k c_{\bar{k}}\right) \\
\left[c_\iota^\dagger c_{\bar{k}} c_{\bar{\iota}}, H_1\right] &= -t\left(d^\dagger c_{\bar{\iota}} c_{\bar{k}} - c_\iota^\dagger d c_{\bar{k}}\right) - V\left(\sum_{\bar{k}'} c_\iota^\dagger c_{\bar{k}} c_{\bar{k}'} + \sum_k c_k^\dagger c_{\bar{\iota}} c_{\bar{k}}\right) \\
\left[c_k^\dagger c_\iota c_{\bar{\iota}}, H_1\right] &= -t\left(c_k^\dagger d c_{\bar{\iota}} - c_k^\dagger d c_\iota\right) - V\left(-c_{\bar{\iota}}\hat{n}_\iota + \sum_{k'} c_k^\dagger c_{k'} c_{\bar{\iota}} + \sum_{\bar{k}} c_k^\dagger c_\iota c_{\bar{k}}\right) + 2U c_k^\dagger c_\iota c_{\bar{\iota}}\hat{n}.
\end{aligned} \tag{A.1.40}$$

And two more connecting central, left/right site and lead:

$$\begin{aligned}
\left[c_k^\dagger d c_\iota, H_1\right] &= -t c_k^\dagger c_{\bar{\iota}} c_\iota + U\left(c_k^\dagger d c_\iota + c_k^\dagger d c_\iota\hat{n}_{\bar{\iota}}\right) - V\left(d\hat{n}_\iota + \sum_{k'} c_k^\dagger d c_{k'}\right) \\
\left[c_k^\dagger d c_{\bar{\iota}}, H_1\right] &= -t c_k^\dagger c_\iota c_{\bar{\iota}} + U\left(c_k^\dagger d c_{\bar{\iota}} + c_k^\dagger d c_{\bar{\iota}}\hat{n}_\iota\right) - V\left(c_\iota^\dagger c_{\bar{\iota}} d + \sum_{\bar{k}} c_k^\dagger d c_{\bar{k}}\right)
\end{aligned} \tag{A.1.41}$$

A.2. Exact Integral Solutions

A.2.1. Lorentz Curve

The integral over a Lorentz curve (= Lorentzian) is needed for the correct normalizing constant for $g^<$ functions in terms of delta distributions. So rewriting

$$\int_{-\infty}^{\infty} \mathrm{d}\varepsilon \, \frac{\eta}{(\omega-\varepsilon)^2+\eta^2} = \frac{1}{\eta}\int_{-\infty}^{\infty} \mathrm{d}\varepsilon \, \frac{1}{\left(\frac{\omega-\varepsilon}{\eta}\right)^2+1}$$

and using the substitution

$$u = \frac{\omega-\varepsilon}{\eta} \quad \text{and} \quad \eta\,\mathrm{d}u = -\,\mathrm{d}\varepsilon$$

the integral reduces to the inverse-tangent solution

$$\to -\int \mathrm{d}u \, \frac{1}{u^2+1} = -\arctan(u)$$

and so the area of Lorentzian is always

$$\to \int_{-\infty}^{\infty} \mathrm{d}\varepsilon \, \frac{\eta}{(\omega-\varepsilon)^2+\eta^2} = -\arctan\left(\frac{\omega-\varepsilon}{\eta}\right)\Bigg|_{-\infty}^{\infty} = \pi.$$

A.2.2. Evaluation of the Tight-Binding Integral

For the tight-binding hybridization the following integral is needed

$$I^{\pm}(\omega^{\pm},\mu) = \int_{-2}^{\mu} \mathrm{d}\varepsilon \, \frac{\sqrt{4-\varepsilon^2}}{\omega^{\pm}-\varepsilon} = \int_{-2}^{\mu} \mathrm{d}\varepsilon \, \frac{\sqrt{4-\varepsilon^2}}{\omega-\varepsilon\pm i\eta}, \tag{A.2.1}$$

where $-2 < \mu \leq 2$. The substitution $\varepsilon = 2\sin(u)$ and $\mathrm{d}\varepsilon = 2\cos(u)\,\mathrm{d}u$ gives

$$\begin{aligned} &= 2\int_{-\frac{\pi}{2}}^{u'} \mathrm{d}u \cos(u) \frac{\sqrt{4-4\sin^2(u)}}{\omega^{\pm}-2\sin(u)} \\ &= 4\int_{-\frac{\pi}{2}}^{u'} \mathrm{d}u \, \frac{\cos^2(u)}{\omega^{\pm}-2\sin(u)}, \end{aligned} \tag{A.2.2}$$

where $u' = \arcsin\left(\frac{\mu}{2}\right) \leq \frac{\pi}{2}$. A further substitution $v = \tan\left(\frac{u}{2}\right)$, $2\,\mathrm{d}v = \sec^2\left(\frac{u}{2}\right)$ and the relations

$$\sin(u) = \frac{2v}{v^2+1}, \quad \cos(u) = \frac{1-v^2}{v^2+1}, \quad \mathrm{d}u = \frac{2\,\mathrm{d}v}{v^2+1} \tag{A.2.3}$$

lead to

$$\begin{aligned} &= 4\int_{-1}^{v'} \frac{2\,\mathrm{d}v}{v^2+1} \frac{\left(\frac{1-v^2}{v^2+1}\right)^2}{\omega^{\pm} - \frac{4v}{1+v^2}} \\ &= 8\int_{-1}^{v'} \mathrm{d}v\, \frac{\left(1-v^2\right)^2}{\left(1+v^2\right)^3 \left(\omega^{\pm} - \frac{4v}{1+v^2}\right)}, \end{aligned} \tag{A.2.4}$$

where $v' = \tan\left(\frac{u'}{2}\right) \leq 1$. The integrand in v is split into its partial fractions

$$\begin{aligned} &\frac{\left(1-v^2\right)^2}{\left(1+v^2\right)^3 \left(\omega^{\pm} - \frac{4v}{1+v^2}\right)} \\ &= \frac{i\omega^{\pm}}{8}\left(\frac{1}{v+i} - \frac{1}{v-i}\right) + \frac{i}{4}\left[\frac{1}{(v+i)^2} - \frac{1}{(v-i)^2}\right] + \frac{4-\left(\omega^{\pm}\right)^2}{4\left(v^2\omega^{\pm} - 4v + \omega^{\pm}\right)}. \end{aligned} \tag{A.2.5}$$

The integration of the first two terms is straightforward and the main integral is reduced to

$$\begin{aligned} 8\int \mathrm{d}v\, \frac{\left(1-v^2\right)^2}{\left(1+v^2\right)^3 \left(\omega^{\pm} - \frac{4v}{1+v^2}\right)} &= i\omega^{\pm}\left[\ln\left(v+i\right) - \ln\left(v-i\right)\right] + 2i\left(\frac{1}{v-i} - \frac{1}{v+i}\right) \\ &\quad + 2\left[4 - \left(\omega^{\pm}\right)^2\right]\int \mathrm{d}v\, \frac{1}{v^2\omega^{\pm} - 4v + \omega^{\pm}}. \end{aligned} \tag{A.2.6}$$

By completing the square in the last denominator the remaining integral can be written as

$$\int \mathrm{d}v\, \frac{1}{v^2\omega^{\pm} - 4v + \omega^{\pm}} = \int \mathrm{d}v\, \frac{1}{\left(v\sqrt{\omega^{\pm}} - \frac{2}{\sqrt{\omega^{\pm}}}\right)^2 + \frac{(\omega^{\pm})^2 - 4}{\omega^{\pm}}} \tag{A.2.7}$$

and further solved by the substitution $z = v\sqrt{\omega^{\pm}} - \frac{2}{\sqrt{\omega^{\pm}}}$ and $\mathrm{d}z = \sqrt{\omega^{\pm}}\,\mathrm{d}v$:

$$\to \frac{1}{a\sqrt{\omega^{\pm}}}\int \mathrm{d}z\, \frac{1}{1+\frac{z^2}{a}} = \frac{\sqrt{a}}{a\sqrt{\omega^{\pm}}} \arctan\left(\frac{z}{\sqrt{a}}\right), \tag{A.2.8}$$

where

$$a = \frac{\left(\omega^{\pm}\right)^2 - 4}{\omega^{\pm}}.$$

Simplifying the complex square roots gives for the prefactor

$$\frac{\sqrt{a}}{a\sqrt{\omega^{\pm}}} = \frac{\mp i}{\sqrt{4-\left(\omega^{\pm}\right)^2}}$$

and for the argument

$$\frac{z}{\sqrt{a}} = \frac{v\sqrt{\omega^{\pm}} - \frac{2}{\sqrt{\omega^{\pm}}}}{\sqrt{a}} = \mp i\frac{v\omega^{\pm} - 2}{\sqrt{4-\left(\omega^{\pm}\right)^2}}.$$

The complete solution in v reads then

$$\begin{aligned} 8\int \mathrm{d}v \, \frac{\left(1-v^2\right)^2}{\left(1+v^2\right)^3\left(\omega^{\pm}-\frac{4v}{1+v^2}\right)} &= i\omega^{\pm}\left[\ln\left(v+i\right)-\ln\left(v-i\right)\right]+2i\left(\frac{1}{v-i}+\frac{1}{v+i}\right) \\ &\quad \mp 2i\frac{4-\left(\omega^{\pm}\right)^2}{\sqrt{4-\left(\omega^{\pm}\right)^2}}\arctan\left(\mp i\frac{v\omega^{\pm}-2}{\sqrt{4-\left(\omega^{\pm}\right)^2}}\right) \\ &= 2\omega^{\pm}\left(\arctan(v)-\frac{\pi}{2}\right)-\frac{4}{v^2+1} \\ &\quad +2i\sqrt{4-\left(\omega^{\pm}\right)^2}\arctan\left(i\frac{v\omega^{\pm}-2}{\sqrt{4-\left(\omega^{\pm}\right)^2}}\right), \end{aligned} \tag{A.2.9}$$

where the logarithmic relation for the inverse tangent is used in the last step.

Transforming back from $v=\tan\left(\frac{u}{2}\right)$ to u, with

$$-\frac{4}{v^2+1}\to-\frac{4}{\tan^2\left(\frac{u}{2}\right)+1}=-4\cos^2\left(\frac{u}{2}\right)=-2-2\cos(u),$$

gives

$$\omega^{\pm}\left(u-\pi\right)-2-2\cos(u)+2i\sqrt{4-\left(\omega^{\pm}\right)^2}\arctan\left(i\frac{\omega^{\pm}\tan\left(\frac{u}{2}\right)-2}{\sqrt{4-\left(\omega^{\pm}\right)^2}}\right), \tag{A.2.10}$$

and back from $u=\arcsin\left(\frac{\varepsilon}{2}\right)$ to ε, using the relations

$$\cos\left(\arcsin\left(\frac{\varepsilon}{2}\right)\right)=\sqrt{1-\frac{\varepsilon^2}{4}},\ \tan\left(\frac{u}{2}\right)=\frac{1-\cos(u)}{\sin(u)},$$

gives

$$c+\omega^{\pm}\arcsin\left(\frac{\varepsilon}{2}\right)-\sqrt{4-\varepsilon^2}+2i\sqrt{4-\left(\omega^{\pm}\right)^2}\arctan\left(i\frac{2\left(\omega^{\pm}-\varepsilon\right)-\omega^{\pm}\sqrt{4-\varepsilon^2}}{\varepsilon\sqrt{4-\left(\omega^{\pm}\right)^2}}\right), \tag{A.2.11}$$

where

$$c=-\pi\omega^{\pm}-2.$$

Finally the definite integral can be evaluated and gives

$$\begin{aligned}
&\int_{-2}^{\mu} \mathrm{d}\varepsilon \, \frac{\sqrt{4-\varepsilon^2}}{\omega - \varepsilon \pm i\eta} = \\
&\omega^{\pm} \arcsin\left(\frac{\mu}{2}\right) - \sqrt{4-\mu^2} + 2i\sqrt{4-(\omega^{\pm})^2} \arctan\left(i\frac{2\,(\omega^{\pm}-\mu) - \omega^{\pm}\sqrt{4-\mu^2}}{\mu\sqrt{4-(\omega^{\pm})^2}}\right) \\
&- \left[-\frac{\pi\omega^{\pm}}{2} + 2i\sqrt{4-(\omega^{\pm})^2} \arctan\left(-i\frac{\omega^{\pm}+2}{\sqrt{4-(\omega^{\pm})^2}}\right)\right] \\
&= \frac{\pi\omega^{\pm}}{2} + \omega^{\pm} \arcsin\left(\frac{\mu}{2}\right) - \sqrt{4-\mu^2} \\
&+ 2i\sqrt{4-(\omega^{\pm})^2}\left[\arctan\left(i\frac{2\,(\omega^{\pm}-\mu) - \omega^{\pm}\sqrt{4-\mu^2}}{\mu\sqrt{4-(\omega^{\pm})^2}}\right) + \arctan\left(i\frac{\omega^{\pm}+2}{\sqrt{4-(\omega^{\pm})^2}}\right)\right].
\end{aligned} \tag{A.2.12}$$

By rewriting the inverse tangent via $\arctan(z) = \frac{i}{2}\ln\left(\frac{1-iz}{1+iz}\right)$ the last term in the square brackets can be expressed as

$$\frac{i}{2}\ln\left(\frac{\sqrt{4-(\omega^{\pm})^2}+(\omega^{\pm}+2)}{\sqrt{4-(\omega^{\pm})^2}-(\omega^{\pm}+2)}\frac{\mu\sqrt{4-(\omega^{\pm})^2}+\left[2\,(\omega^{\pm}-\mu)-\omega^{\pm}\sqrt{4-\mu^2}\right]}{\mu\sqrt{4-(\omega^{\pm})^2}-\left[2\,(\omega^{\pm}-\mu)-\omega^{\pm}\sqrt{4-\mu^2}\right]}\right),$$

and with

$$\begin{aligned}
a + \frac{b}{-a+\sqrt{a^2-b}} &= -\sqrt{a^2-b} \\
\rightarrow \frac{i}{2}\ln\left(\frac{4-\mu\omega^{\pm}-\sqrt{4-\mu^2}\sqrt{4-(\omega^{\pm})^2}}{2\,(\omega^{\pm}-\mu)}\right).
\end{aligned}$$

And finally

$$\begin{aligned}
I^{\pm}(\omega^{\pm},\mu) = \frac{\pi\omega^{\pm}}{2} &+ \omega^{\pm}\arcsin\left(\frac{\mu}{2}\right) - \sqrt{4-\mu^2} \\
&- \sqrt{4-(\omega^{\pm})^2}\ln\left(\frac{4-\mu\omega^{\pm}-\sqrt{4-\mu^2}\sqrt{4-(\omega^{\pm})^2}}{2\,(\omega^{\pm}-\mu)}\right),
\end{aligned} \tag{A.2.13}$$

where for $\mu = 2$

$$\begin{aligned}
\frac{1}{2\pi} I^{\pm}(\omega, 2) &= \frac{\pi\omega^{\pm}}{2} + \frac{\pi\omega^{\pm}}{2} - \sqrt{4 - (\omega^{\pm})^2} \ln\left(\frac{4 - 2\omega^{\pm}}{2\omega^{\pm} - 4}\right) \\
&= \frac{1}{2\pi}\left(\pi\omega^{\pm} - \sqrt{4 - (\omega^{\pm})^2}(\pm i\pi)\right) \\
&= \frac{1}{2}\left(\omega^{\pm} \mp i\sqrt{4 - (\omega^{\pm})^2}\right) \\
&= \frac{1}{2}\left(\omega^{\pm} \mp i\sqrt{-(\omega^{\pm})^2\left(1 - \frac{4}{(\omega^{\pm})^2}\right)}\right) \\
&= \frac{1}{2}\left(\omega^{\pm} + (\mp i)^2\omega^{\pm}\sqrt{1 - \frac{4}{(\omega^{\pm})^2}}\right) \\
&= \frac{\omega^{\pm}}{2}\left(1 - \sqrt{1 - \frac{4}{(\omega^{\pm})^2}}\right).
\end{aligned} \tag{A.2.14}$$

A.2.3. Inner Solution to the Occupation Number *n*

The integrand for the inner expectation value is split into partial fractions that can be related to $I^{\pm}$ by

$$\frac{|\tau|^2\sqrt{4 - \omega^2}}{\omega^2\left(1 - 2|\tau|^2\right) + 4|\tau|^4} = \frac{i\sqrt{1 - 2|\tau|^2}}{4\left(1 - 2|\tau|^2\right)}\left(\frac{\sqrt{4 - \omega^2}}{\widetilde{a} - \omega} - \frac{\sqrt{4 - \omega^2}}{-\widetilde{a} - \omega}\right), \tag{A.2.15}$$

where

$$\widetilde{a} = i\frac{2|\tau|^2}{\sqrt{1 - 2|\tau|^2}}$$

and the integral reads then

$$\int_{-2}^{\mu} \mathrm{d}\omega \, \frac{|\tau|^2\sqrt{4 - \omega^2}}{\omega^2\left(1 - 2|\tau|^2\right) + 4|\tau|^4} = \frac{i\sqrt{1 - 2|\tau|^2}}{4\left(1 - 2|\tau|^2\right)}\left(I^{\pm}(\widetilde{a}, \mu) - I^{\pm}(-\widetilde{a}, \mu)\right). \tag{A.2.16}$$

The complete inner expectation value becomes hereby

$$\begin{aligned}
\langle\hat{n}\rangle_{\text{inner}} &= \frac{1}{2\pi}\frac{i\sqrt{1 - 2|\tau|^2}}{4\left(1 - 2|\tau|^2\right)}\left(I^{\pm}(\widetilde{a}, \mu) - I^{\pm}(-\widetilde{a}, \mu) + I^{\pm}(\widetilde{a}, -\mu) - I^{\pm}(-\widetilde{a}, -\mu)\right) \\
&= \frac{1}{2\pi}\frac{i\sqrt{1 - 2|\tau|^2}}{4\left(1 - 2|\tau|^2\right)}\left(2\pi\widetilde{a} + 2\widetilde{a}\arcsin\left(\frac{\mu}{2}\right) + 2\widetilde{a}\arcsin\left(\frac{-\mu}{2}\right) + f(z)\right) \\
&= \frac{1}{2\pi}\frac{i\sqrt{1 - 2|\tau|^2}}{4\left(1 - 2|\tau|^2\right)}\left(2\pi\widetilde{a} + f(z)\right),
\end{aligned} \tag{A.2.17}$$

where $f(z)$ is the sum of the four combinations in $z(\pm\widetilde{a}, \pm\mu)$ from the above integrals and evaluates to

$$f(z) = -2i\pi\sqrt{4-\widetilde{a}^2}\,\mathrm{sgn}\left(1-2|\tau|^2\right).$$

So the expectation value becomes

$$\begin{aligned}
\langle\hat{n}\rangle_{\text{inner}} &= -\frac{\sqrt{1-2|\tau|^2}}{4\left(1-2|\tau|^2\right)}\left(\frac{2|\tau|^2}{\sqrt{1-2|\tau|^2}} - \mathrm{sgn}\left(1-2|\tau|^2\right)\sqrt{4+\frac{4|\tau|^4}{1-2|\tau|^2}}\right)\\
&= -\frac{|\tau|^2}{2\left(1-2|\tau|^2\right)} + \frac{\left|1-|\tau|^2\right|}{2\left(1-2|\tau|^2\right)}\mathrm{sgn}\left(1-2|\tau|^2\right)\sqrt{1-2|\tau|^2}\sqrt{\frac{1}{1-2|\tau|^2}}\\
&= -\frac{|\tau|^2}{2\left(1-2|\tau|^2\right)} + \frac{\left|1-|\tau|^2\right|}{2\left(1-2|\tau|^2\right)}\mathrm{sgn}\left(1-2|\tau|^2\right)\mathrm{sgn}\left(1-2|\tau|^2\right) \qquad \text{(A.2.18)}\\
&= -\frac{|\tau|^2}{2\left(1-2|\tau|^2\right)} + \frac{\left|1-|\tau|^2\right|}{2\left(1-2|\tau|^2\right)}\\
&= \frac{|\tau|^2 - \left|1-|\tau|^2\right|}{2\left(2|\tau|^2-1\right)}.
\end{aligned}$$

A.2.4. WBL Integrals in HF with partial fractions

The integrals occurring in section 4.3 have similar integrands for which a decomposition in partial fractions is needed and based on the factorization

$$\left|\omega\left(\omega\pm i\right) - 2|\tau|^2\right|^2 = \left[\omega^2 + \frac{1}{2}\left(b+c\right)\right]\left[\omega^2 + \frac{1}{2}\left(b-c\right)\right].$$

Following relations are useful and hold for b and c:

$$(b+c)(b-c) = b^2 - c^2 = 1 - 8|\tau|^2 + 16|\tau|^4 - (1-8|\tau|^2) = 16|\tau|^4 \qquad \text{(A.2.19)}$$

and

$$(b+c-2)(b-c-2) = b^2 - c^2 + 4(1-b) = 16|\tau|^2\left(1+|\tau|^2\right) \qquad \text{(A.2.20)}$$

So the decompositions

$$\frac{1}{\left|\omega\left(\omega\pm i\right) - 2|\tau|^2\right|^2} = \frac{1}{c}\left[\frac{1}{\omega^2 + \frac{1}{2}\left(b-c\right)} - \frac{1}{\omega^2 + \frac{1}{2}\left(b+c\right)}\right] \qquad \text{(A.2.21)}$$

and

$$\begin{aligned}
\frac{\omega^2}{\left|\omega\left(\omega\pm i\right) - 2|\tau|^2\right|^2} &= \frac{\omega^2}{c}\left[\frac{1}{\omega^2 + \frac{1}{2}\left(b-c\right)} - \frac{1}{\omega^2 + \frac{1}{2}\left(b+c\right)}\right]\\
&= \frac{1}{2c}\left[-\frac{b-c}{\omega^2 + \frac{1}{2}\left(b-c\right)} + \frac{b+c}{\omega^2 + \frac{1}{2}\left(b+c\right)}\right]
\end{aligned} \qquad \text{(A.2.22)}$$

are easily found. The somewhat larger terms need a little more work, but eventually

$$\begin{aligned}
&\frac{|\tau|^2}{(\omega^2+1)\left[\omega^2+\frac{1}{2}(b+c)\right]\left[\omega^2+\frac{1}{2}(b-c)\right]} \\
&= \frac{1}{4\left(1+|\tau|^2\right)(\omega^2+1)} - \frac{2|\tau|^2}{c(b-c-2)\left[\omega^2+\frac{1}{2}(b-c)\right]} + \frac{2|\tau|^2}{c(b+c-2)\left[\omega^2+\frac{1}{2}(b+c)\right]} \\
&= \frac{1}{4\left(1+|\tau|^2\right)}\left\{\frac{1}{\omega^2+1} + \frac{1}{2c}\left[\frac{b-c-2}{\omega^2+\frac{1}{2}(b+c)} - \frac{b+c-2}{\omega^2+\frac{1}{2}(b-c)}\right]\right\}
\end{aligned} \tag{A.2.23}$$

and

$$\begin{aligned}
&\frac{\left|\omega(\omega\pm i)-|\tau|^2\right|^2}{(\omega^2+1)\left|\omega(\omega\pm i)-2|\tau|^2\right|^2} = \frac{\omega^4+\omega^2\left(1-2|\tau|^2\right)+|\tau|^4}{(\omega^2+1)\left[\omega+\frac{1}{2}(b+c)\right]\left[\omega+\frac{1}{2}(b-c)\right]} \\
&= \frac{1}{4\left(1+|\tau|^2\right)}\left\{\frac{2+|\tau|^2}{\omega^2+1}\right. \\
&\left.+\frac{1}{2c}\left[\frac{(b+c)\left(2+3|\tau|^2\right)+8|\tau|^4}{\omega^2+\frac{1}{2}(b+c)} - \frac{(b-c)\left(2+3|\tau|^2\right)+8|\tau|^4}{\omega^2+\frac{1}{2}(b-c)}\right]\right\}
\end{aligned} \tag{A.2.24}$$

is found. All these integrands are now split into sums of terms $\propto (\omega^2+\text{const.})^{-1}$ whose indefinite integrals are proportional to the inverse tangent as

$$\int \mathrm{d}\omega\, \frac{1}{\omega^2+a} = \frac{1}{\sqrt{a}} \arctan\left(\frac{\omega}{\sqrt{a}}\right). \tag{A.2.25}$$

And so the following integrals can be easily evaluated:

Integral no. 1

$$\begin{aligned}
I_1(\omega) :=& \int \mathrm{d}\omega\, \frac{1}{\left|\omega(\omega\pm i)-2|\tau|^2\right|^2} \\
=& \frac{1}{c}\left[\frac{\sqrt{2}}{\sqrt{b-c}} \arctan\left(\frac{\omega\sqrt{2}}{\sqrt{b-c}}\right) - \frac{\sqrt{2}}{\sqrt{b+c}} \arctan\left(\frac{\omega\sqrt{2}}{\sqrt{b+c}}\right)\right]
\end{aligned} \tag{A.2.26}$$

with the value

$$I_1(-\infty) = -\frac{\pi}{c\sqrt{2}}\left(\frac{1}{\sqrt{b-c}} - \frac{1}{\sqrt{b+c}}\right) = -\frac{\pi}{4c|\tau|^2\sqrt{2}}\left(\sqrt{b+c}-\sqrt{b-c}\right) = -\frac{\pi}{4|\tau|^2} \tag{A.2.27}$$

as

$$\left(\sqrt{b+c}-\sqrt{b-c}\right)^2 = b+c+b-c-8|\tau|^2 = 2-16|\tau|^2 = 2c^2.$$

Integral no. 2

$$\begin{aligned} I_2(\omega) :=& \int \mathrm{d}\omega \, \frac{|\tau|^2}{(\omega^2+1)\left|\omega\left(\omega \pm i\right) - 2|\tau|^2\right|^2} \\ =& \frac{1}{4\left(1+|\tau|^2\right)} \left\{ \arctan(\omega) \right. \\ & \left. + \frac{1}{c\sqrt{2}} \left[\frac{b-c-2}{\sqrt{b+c}} \arctan\left(\frac{\omega\sqrt{2}}{\sqrt{b+c}}\right) - \frac{b+c-2}{\sqrt{b-c}} \arctan\left(\frac{\omega\sqrt{2}}{\sqrt{b-c}}\right) \right] \right\} \end{aligned} \tag{A.2.28}$$

with the value

$$I_2(-\infty) = -\frac{1}{4\left(1+|\tau|^2\right)} \left\{ \frac{\pi}{2} + \frac{\pi}{2c\sqrt{2}} \left[\frac{b-c-2}{\sqrt{b+c}} - \frac{b+c-2}{\sqrt{b-c}} \right] \right\} \tag{A.2.29}$$

Defining the last two terms as

$$\begin{aligned} x :=& \frac{b-c-2}{\sqrt{b+c}} - \frac{b+c-2}{\sqrt{b-c}} \\ =& \frac{1}{4|\tau|^2} \left[(b-c-2)\sqrt{b-c} - (b+c-2)\sqrt{b+c} \right] \end{aligned} \tag{A.2.30}$$

and solving the square, it evaluates to

$$\begin{aligned} x^2 &= \frac{1}{16|\tau|^4} 32|\tau|^4 c^2 = 2c^2 \\ \rightarrow x &= c\sqrt{2}. \end{aligned} \tag{A.2.31}$$

And so

$$\begin{aligned} I_2(-\infty) &= -\frac{1}{4\left(1+|\tau|^2\right)} \left(\frac{\pi}{2} + \frac{\pi}{2c\sqrt{2}} c\sqrt{2} \right) \\ &= -\frac{\pi}{4\left(1+|\tau|^2\right)}. \end{aligned} \tag{A.2.32}$$

Integral no. 3

$$\begin{aligned} I_3(\omega) :=& \int \mathrm{d}\omega \frac{\left|\omega(\omega \pm i) - |\tau|^2\right|^2}{(\omega^2+1)\left|\omega\left(\omega \pm i\right) - 2|\tau|^2\right|^2} \\ =& \frac{1}{4\left(1+|\tau|^2\right)} \left\{ \left(2+|\tau|^2\right) \arctan(\omega) \right. \\ &+ \frac{1}{c\sqrt{2}} \left[\frac{(b+c)\left(2+3|\tau|^2\right)+8|\tau|^4}{\sqrt{b+c}} \arctan\left(\frac{\omega\sqrt{2}}{\sqrt{b+c}}\right) \right. \\ &\left. \left. - \frac{(b-c)\left(2+3|\tau|^2\right)+8|\tau|^4}{\sqrt{b-c}} \arctan\left(\frac{\omega\sqrt{2}}{\sqrt{b-c}}\right) \right] \right\} \end{aligned} \tag{A.2.33}$$

with the value

$$\begin{aligned} I_3(-\infty) = \frac{1}{4\left(1+|\tau|^2\right)} & \left\{ -\left(2+|\tau|^2\right)\frac{\pi}{2} \right. \\ & \left. - \frac{\pi}{4c} \left[\frac{(b+c)\left(2+3|\tau|^2\right)+8|\tau|^4}{\sqrt{\frac{1}{2}(b+c)}} - \frac{(b-c)\left(2+3|\tau|^2\right)+8|\tau|^4}{\sqrt{\frac{1}{2}(b-c)}} \right] \right\} \end{aligned} \tag{A.2.34}$$

Again, defining the last two terms as

$$\begin{aligned} x :=& \frac{(b+c)\left(2+3|\tau|^2\right)+8|\tau|^4}{\sqrt{\frac{1}{2}(b+c)}} - \frac{(b-c)\left(2+3|\tau|^2\right)+8|\tau|^4}{\sqrt{\frac{1}{2}(b-c)}} \\ =& \frac{\sqrt{2}}{4|\tau|^2} \left\{ \left[(b+c)\left(2+3|\tau|^2\right)+8|\tau|^4\right]\sqrt{b-c} - \left[(b-c)\left(2+3|\tau|^2\right)+8|\tau|^4\right]\sqrt{b+c} \right\} \end{aligned} \tag{A.2.35}$$

and arranging the terms in the square, results in

$$\begin{aligned} x^2 &= \frac{2}{16|\tau|^4} 32|\tau|^4 \left(2+|\tau|^2\right)^2 c^2 \\ &= 4c^2\left(2+|\tau|^2\right)^2 \\ \rightarrow x &= 2c\left(2+|\tau|^2\right). \end{aligned} \tag{A.2.36}$$

And so

$$\begin{aligned} I_3(-\infty) &= -\frac{1}{4\left(1+|\tau|^2\right)} \left[\left(2+|\tau|^2\right)\frac{\pi}{2} + \frac{\pi}{4c} 2c \left(2+|\tau|^2\right) \right] \\ &= -\frac{\pi\left(2+|\tau|^2\right)}{4\left(1+|\tau|^2\right)}. \end{aligned} \tag{A.2.37}$$

A.2.5. WBL Integrals in HF with substitutions

Some of the integrals require suitable substitutions, which are found in the following.

Integral with substitution for f_1

$$\int \mathrm{d}\omega \, \frac{\omega}{\left|\omega\left(\omega \pm i\right) - 2|\tau|^2\right|^2} = \int \mathrm{d}\omega \, \frac{\omega}{\omega^4 + \left(1 - 4|\tau|^2\right)\omega^2 + 4|\tau|^4}$$

The substitution $u = \omega^2$ and $\mathrm{d}u = 2\omega \, \mathrm{d}\omega$ in the integrand leads to

$$\rightarrow \frac{1}{2} \int \mathrm{d}u \left[u^2 + \left(1 - 4|\tau|^2\right) u + 4|\tau|^4\right]^{-1}$$

and completing the square in the denominator yields

$$u^2 + \left(1 - 4|\tau|^2\right) u + 4|\tau|^4 = \left(u - 2|\tau|^2 + \frac{1}{2}\right)^2 + \frac{1}{4}\left(8|\tau|^2 - 1\right).$$

A further substitution $v = u - 2|\tau|^2 + \frac{1}{2}$, $\mathrm{d}v = \mathrm{d}u$ and definition $a = \frac{1}{4}\left(8|\tau|^2 - 1\right)$ reduces the integral again to an inverse tangent term.

$$\rightarrow \frac{1}{2} \int \mathrm{d}v \, \frac{1}{v^2 + a} = \frac{1}{2\sqrt{a}} \arctan\left(\frac{v}{\sqrt{a}}\right) = \frac{1}{\sqrt{8|\tau|^2 - 1}} \arctan\left(\frac{2u - 4|\tau|^2 + 1}{\sqrt{8|\tau|^2 - 1}}\right)$$

And so, the definite integral is obtained as

$$\begin{aligned} &\rightarrow \frac{1}{\sqrt{8|\tau|^2 - 1}} \arctan\left(\frac{2\omega^2 - 4|\tau|^2 + 1}{\sqrt{8|\tau|^2 - 1}}\right)\Bigg|_{-\infty}^{\mu} \\ &= \frac{1}{\sqrt{8|\tau|^2 - 1}} \left[\arctan\left(\frac{2\mu^2 - 4|\tau|^2 + 1}{\sqrt{8|\tau|^2 - 1}}\right) - \frac{\pi}{2}\right]. \end{aligned} \tag{A.2.38}$$

Integral for Real Part in Total Energy

For the integral in the HF energy calculation

$$I_4(\omega) := \int \mathrm{d}\omega \, \mathrm{Re}\left\{\langle\langle c_a; c_a^\dagger \rangle\rangle\right\}$$

again, the partial fractions for the integrand are needed:

$$\begin{aligned}
\mathrm{Re}\Big\{\langle\!\langle c_a; c_a^\dagger\rangle\!\rangle\Big\} &= \frac{\omega\left[\omega^4+\left(1-3|\tau|^2\right)\omega^2-|\tau|^2\left(1-2|\tau|^2\right)\right]}{\left(\omega^2+1\right)\left|\omega\left(\omega\pm i\right)-2|\tau|^2\right|^2} \\
&= \frac{\omega\left[\omega^4+\left(1-3|\tau|^2\right)\omega^2-|\tau|^2\left(1-2|\tau|^2\right)\right]}{\left(\omega^2+1\right)\left[\omega^2+\frac{1}{2}(b+c)\right]\left[\omega^2+\frac{1}{2}(b-c)\right]} \\
&= \frac{\omega}{2\left(\omega^2+1\right)}+\frac{1}{4c}\left[\frac{\left(b+c+4|\tau|^2\right)\omega}{\omega^2+\frac{1}{2}(b+c)}-\frac{\left(b-c+4|\tau|^2\right)\omega}{\omega^2+\frac{1}{2}(b-c)}\right] \\
&= \frac{\omega}{2\left(\omega^2+1\right)}+\frac{1}{4c}\left[\frac{(1+c)\omega}{\omega^2+\frac{1}{2}(b+c)}-\frac{(1-c)\omega}{\omega^2+\frac{1}{2}(b-c)}\right]
\end{aligned} \tag{A.2.39}$$

Now the integrand consists only of terms $\propto \omega/(\omega^2+a)$, which can be solved via the substitution $u = a+\omega^2$ and $\mathrm{d}u = 2\omega\,\mathrm{d}\omega$ yielding

$$\int \mathrm{d}\omega\,\frac{\omega}{\omega^2+a} = \frac{1}{2}\int \mathrm{d}u\,\frac{1}{u} = \frac{1}{2}\ln\left(\omega^2+a\right).$$

So in total the integral reads

$$\begin{aligned}
I_4(\omega) &= \frac{1}{4}\ln\left(\omega^2+1\right)+\frac{1}{8c}\left[(1+c)\ln\left(\omega^2+\frac{1}{2}(b+c)\right)-(1-c)\ln\left(\omega^2+\frac{1}{2}(b-c)\right)\right] \\
&= \frac{1}{4}\ln\left(\omega^2+1\right)+\frac{1}{8c}\left[c\ln\left(\omega^4+\left(1-4|\tau|^2\right)\omega^2+4|\tau|^2\right)+\ln\left(\frac{\omega^2+\frac{1}{2}(b+c)}{\omega^2+\frac{1}{2}(b-c)}\right)\right] \\
&= \frac{1}{4}\ln\left(\omega^2+1\right)+\frac{1}{8}\ln\left(\omega^4+\left(1-4|\tau|^2\right)\omega^2+4|\tau|^4\right)+\frac{1}{8c}\ln\left(\frac{\omega^2+\frac{1}{2}(b+c)}{\omega^2+\frac{1}{2}(b-c)}\right).
\end{aligned} \tag{A.2.40}$$

The last term can be rewritten via the relation $\arctan(z) = \frac{i}{2}\ln\left(\frac{i+z}{i-z}\right)$, namely

$$\begin{aligned}
\frac{1}{8c}\ln\left(\frac{\omega^2+\frac{1}{2}(b+c)}{\omega^2+\frac{1}{2}(b-c)}\right) &= \frac{1}{8c}\ln\left(\frac{2\omega^2+b+\sqrt{1-8|\tau|^2}}{2\omega^2+b-\sqrt{1-8|\tau|^2}}\right) \\
&= \frac{1}{8c}\ln\left(\frac{2\omega^2+b+i\sqrt{8|\tau|^2-1}}{2\omega^2+b-i\sqrt{8|\tau|^2-1}}\right) \\
&= \frac{1}{8c}\ln\left(\frac{z+i}{z-i}\right),
\end{aligned} \tag{A.2.41}$$

where

$$z = \frac{2\omega^2+b}{\sqrt{8|\tau|^2-1}}.$$

Using $\ln(-x) = \ln(x) + \ln(-1) = \ln(x) + i\pi$

$$\begin{aligned}\frac{1}{8c}\ln\left(\frac{z+i}{z-i}\right) &= \frac{1}{8c}\ln\left(-\frac{i+z}{i-z}\right)\\ &= \frac{1}{8c}\left(\ln\left(\frac{i+z}{i-z}\right)+i\pi\right)\\ &= \frac{i}{8c}\left(-2\arctan(z)+\pi\right)\\ &= \frac{1}{8\sqrt{8|\tau|^2-1}}\left(-2\arctan\left(\frac{2\omega^2+b}{\sqrt{8|\tau|^2-1}}\right)+\pi\right)\end{aligned} \tag{A.2.42}$$

And finally, ignoring the constant term,

$$\begin{aligned}I_4(\omega) = \frac{1}{4}\ln\left(\omega^2+1\right) + \frac{1}{8}\ln\left(\omega^4+\left(1-4|\tau|^2\right)\omega^2+4|\tau|^4\right)\\ -\frac{1}{4\sqrt{8|\tau|^2-1}}\arctan\left(\frac{2\omega^2+b}{\sqrt{8|\tau|^2-1}}\right).\end{aligned} \tag{A.2.43}$$

A.2.6. Epsilon Integrals in Bath Sums

Occurring in R/A Sums

Partial fraction decomposition of the first integrand gives

$$\begin{aligned}\frac{\eta}{(\omega_c-\varepsilon\pm i\eta)\left[(\omega'-\varepsilon)^2+\eta^2\right]} &= \pm\frac{i}{2(\omega_c-\omega')}\frac{1}{\omega'-\varepsilon\pm i\eta}\\ &\quad\mp\frac{i}{2\left(\omega_c-\omega'\pm 2i\eta\right)}\frac{1}{\omega'-\varepsilon\mp i\eta}\\ &\quad+\frac{\eta}{(\omega_c-\omega')\left(\omega_c-\omega'\pm 2i\eta\right)}\frac{1}{\omega_c-\varepsilon\pm i\eta}\end{aligned} \tag{A.2.44}$$

and for the second integrand

$$\frac{1}{(\omega_c-\varepsilon\pm i\eta)(\omega'-\varepsilon+i\eta)} = \begin{cases}\frac{1}{\omega_c-\omega'}\left(\frac{1}{\omega'-\varepsilon+i\eta}-\frac{1}{\omega_c-\varepsilon+i\eta}\right) & \text{if } +i\eta\\ \frac{1}{\omega_c-\omega'-2i\eta}\left(\frac{1}{\omega'-\varepsilon+i\eta}-\frac{1}{\omega_c-\varepsilon-i\eta}\right) & \text{if } -i\eta.\end{cases} \tag{A.2.45}$$

The separate terms in ε are all of the same kind as the bare bath sum and the integral for $D\to\infty$ gives only $\pm i\pi$, independent of ω_c or ω'. So the second integral becomes zero for $+i\eta$. And summarizing, the results are

$$\begin{aligned}\int_{-\infty}^{\infty}\mathrm{d}\varepsilon\,\frac{\eta}{(\omega_c-\varepsilon\pm i\eta)\left[(\omega'-\varepsilon)^2+\eta^2\right]} &= \frac{\pi}{\omega_c-\omega'\pm 2i\eta}\\ \int_{-\infty}^{\infty}\mathrm{d}\varepsilon\,\frac{1}{(\omega_c-\varepsilon\pm i\eta)(\omega'-\varepsilon+i\eta)} &= -\frac{2i\pi}{\omega_c-\omega'-2i\eta}\delta_{\pm,-}.\end{aligned} \tag{A.2.46}$$

Occurring in Lesser Sums

Again, partial fraction decomposition leads to

$$\begin{aligned}\frac{\eta}{(\omega'-\varepsilon+i\eta)\left[(\omega_c\pm\varepsilon)^2+\eta^2\right]} &= \frac{\eta}{(\omega'-\varepsilon+i\eta)\left[(\mp\omega_c-\varepsilon)^2+\eta^2\right]}\\ &= -\frac{i}{2\left(\mp\omega_c-\omega'\right)}\frac{1}{\mp\omega_c-\varepsilon+i\eta}\\ &\quad+\frac{i}{2\left(\mp\omega_c-\omega'-2i\eta\right)}\frac{1}{\mp\omega_c-\varepsilon-i\eta}\\ &\quad+\frac{\eta}{\left(\mp\omega_c-\omega'\right)\left(\mp\omega_c-\omega'-2i\eta\right)}\frac{1}{\omega'-\varepsilon+i\eta}\end{aligned} \tag{A.2.47}$$

and

$$\begin{aligned}\frac{\eta}{(\omega_c\pm\varepsilon)^2+\eta^2}\frac{\eta}{(\omega'-\varepsilon)^2+\eta^2} &= \frac{\eta}{(\mp\omega_c-\varepsilon)^2+\eta^2}\frac{\eta}{(\omega'-\varepsilon)^2+\eta^2}\\ &= \frac{i\eta}{2\left(\mp\omega_c-\omega'\right)}\\ &\quad\times\left[\frac{1}{\mp\omega_c-\omega'+2i\eta}\left(\frac{1}{\mp\omega_c-\varepsilon+i\eta}-\frac{1}{\omega'-\varepsilon-i\eta}\right)\right.\\ &\quad\left.-\frac{1}{\mp\omega_c-\omega'-2i\eta}\left(\frac{1}{\mp\omega_c-\varepsilon-i\eta}-\frac{1}{\omega'-\varepsilon+i\eta}\right)\right].\end{aligned} \tag{A.2.48}$$

With the same argumentation as before, the results read

$$\begin{aligned}\int_{-\infty}^{\infty}\mathrm{d}\varepsilon\,\frac{\eta}{(\omega_c\pm\varepsilon)^2+\eta^2}\frac{\eta}{(\omega'-\varepsilon)^2+\eta^2} &= \frac{2\eta\pi}{(\mp\omega_c-\omega')^2+(2\eta)^2}\\ \int_{-\infty}^{\infty}\mathrm{d}\varepsilon\,\frac{\eta}{(\omega'-\varepsilon+i\eta)\left[(\omega_c\pm\varepsilon)^2+\eta^2\right]} &= -\frac{\pi}{\mp\omega_c-\omega'-2i\eta}.\end{aligned} \tag{A.2.49}$$

Bibliography

[1] Hartmut Haug and Antti-Pekka Jauho. *Quantum Kinetics in Transport and Optics of Semiconductors*. Springer Series in Solid-State Sciences, Volume 123. Springer-Verlag Berlin Heidelberg, 2008. DOI: 10.1007/978-3-540-73564-9.

[2] Gernot Schaller. Open Quantum Systems Far from Equilibrium. volume 881 of *Lecture Notes in Physics*. Springer, Cham, 2014. DOI: 10.1007/978-3-319-03877-3.

[3] C. Lacroix. Density of states for the Anderson model. *Journal of Physics F: Metal Physics*, 11(11):2389–2397, 1981. DOI: 10.1088/0305-4608/11/11/020.

[4] Hong-Gang Luo, Zu-Jian Ying, and Shun-Jin Wang. Equation of motion approach to the solution of the Anderson model. *Physical Review B*, 59, 1999. DOI: 10.1103/PhysRevB.59.9710.

[5] Mircea Crisan, Ioan Grosu, and Ionel Ţifrea. An equation of motion analysis of the two stage Kondo effect in T-shaped double-quantum-dot systems. *Physica E: Low-dimensional Systems and Nanostructures*, 66:245–251, 2015. DOI: 10.1016/j.physe.2014.10.017.

[6] Daisuke Yamamoto, Synge Todo, and Susumu Kurihara. Green's function theory for spin-$\frac{1}{2}$ ferromagnets with an easy-plane exchange anisotropy. *Physical Review B*, 78:024440, 2008. DOI: 10.1103/PhysRevB.78.024440.

[7] Wolfgang Nolting. *Grundkurs Theoretische Physik 7: Viel-Teilchen-Theorie*. Springer-Verlag Berlin Heidelberg, 2015. DOI: 10.1007/978-3-642-25808-4.

[8] C. Niu, D. L. Lin, and T.-H. Lin. Equation of motion for nonequilibrium Green functions. *Journal of Physics: Condensed Matter*, 11(6):1511–1521, 1999. DOI: 10.1088/0953-8984/11/6/015.

[9] Jørgen Rammer. *Quantum Field Theory of Non-equilibrium States*. Cambridge University Press, 2007. DOI: 10.1017/CBO9780511618956.

[10] Huzihiro Araki. On the Kubo-Martin-Schwinger Boundary Condition. *Progress of Theoretical Physics Supplement*, 64:12–20, 1978. DOI: 10.1143/PTPS.64.12.

[11] David C. Langreth. *Linear and Nonlinear Response Theory with Applications*, pages 3–32 in *Linear and Nonlinear Electron Transport in Solids*. Springer US, Boston, MA, 1976. DOI: 10.1007/978-1-4757-0875-2_1.

[12] Alexander L. Kuzemsky. Irreducible Green Functions Method and Many-Particle Interacting Systems on a Lattice. *Rivista Nuovo Cimento*, 25:1–91, 2002. arXiv:cond-mat/0208219.

[13] Alexander L. Kuzemsky. Statistical Mechanics and the Physics of the Many-Particle Model Systems. *Physics of Particles and Nuclei*, 40(7):949, 2009. DOI: 10.1134/S1063779609070016.

[14] G. Górski, J. Mizia, and K. Kucab. Alternative Equation of Motion Approach to the Single-Impurity Anderson Model. *Acta Physica Polonica A*, 126:A–97, 2014. DOI: 10.12693/APhysPolA.126.A-97.

[15] E. Boulat, H. Saleur, and P. Schmitteckert. Twofold Advance in the Theoretical Understanding of Far-From-Equilibrium Properties of Interacting Nanostructures. *Physical Review Letters*, 101:140601, 2008. DOI: 10.1103/PhysRevLett.101.140601.

[16] Sam T. Carr, Dmitry A. Bagrets, and Peter Schmitteckert. Full Counting Statistics in the Self-Dual Interacting Resonant Level Model. *Physical Review Letters*, 107:206801, 2011. DOI: 10.1103/PhysRevLett.107.206801.

[17] Max E. Sorantin, Wolfgang von der Linden, Roman Lucrezi, and Enrico Arrigoni. Nonequilibrium Green's functions and their relation to the negative differential conductance in the interacting resonant level model. *Physical Review B*, 99:075139, 2019. DOI: 10.1103/PhysRevB.99.075139.

[18] Christian Schiegg, Michael Dzierzawa, and Ulrich Eckern. Non-equilibrium transport through a model quantum dot: Hartree–Fock approximation and beyond. *New Journal of Physics*, 17(8):083060, 2015. DOI: 10.1088/1367-2630/17/8/083060.

[19] Rok Žitko. SNEG - Mathematica package for symbolic calculations with second-quantization-operator expressions. *Computer Physics Communications*, 182(10):2259–2264, 2011. DOI: 10.1016/j.cpc.2011.05.013.

[20] Roger Haydock. The Recursive Solution of the Schrödinger Equation. volume 35 of *Solid State Physics*, pages 215–294. Academic Press, 1980. DOI: 10.1016/S0081-1947(08)60505-6.

[21] Tal J. Levy and Eran Rabani. Steady state conductance in a double quantum dot array: The nonequilibrium equation-of-motion Green function approach. *The Journal of Chemical Physics*, 138(16):164125, 2013. DOI: 10.1063/1.4802752.

[22] R. Świrkowicz, J. Barnaś, and M. Wilczyński. Nonequilibrium Kondo effect in quantum dots. *Physical Review B*, 68:195318, 2003. DOI: 10.1103/PhysRevB.68.195318.

[23] Nicolas Teeny and Manfred Fähnle. General decoupling procedure for expectation values of four-operator products in electron–phonon quantum kinetics. *Journal of Physics A: Mathematical and Theoretical*, 46(38):385302, 2013. DOI: 10.1088/1751-8113/46/38/385302.

[24] Tal J. Levy and Eran Rabani. Symmetry breaking and restoration using the equation-of-motion technique for nonequilibrium quantum impurity models. *Journal of Physics: Condensed Matter*, 25(11):115302, 2013. DOI: 10.1088/0953-8984/25/11/115302.

[25] Kemal Bidzhiev and Grégoire Misguich. Out-of-equilibrium dynamics in a quantum impurity model: Numerics for particle transport and entanglement entropy. *Physical Review B*, 96:195117, 2017. DOI: 10.1103/PhysRevB.96.195117.

[26] Alexander L. Fetter and John Dirk Walecka. *Quantum Theory of Many-Particle Systems*. Dover Books on Physics. Dover Publications, 2003. ISBN: 978-0-486-42827-7.